ABSORPTION IN COCURRENT GAS-LIQUID FLOW

IN HORIZONTAL TUBES

by

WALTER HAYDUK

B.A.Sc., University of British Columbia, 1954

M.A.Sc., University of British Columbia, 1956

A THESIS SUBMITTED IN PARTIAL FULFILMENT OF

THE REQUIREMENTS FOR THE DEGREE OF

DOCTOR OF PHILOSOPHY

in the Department of

CHEMICAL ENGINEERING

We accept this thesis as conforming to the

required standard

THE UNIVERSITY OF BRITISH COLUMBIA

July, 1964

In presenting this thesis in partial fulfilment of

the requirements for an advanced degree at the University of

British Columbia, I agree that the Library shall make it freely

available for reference and study. I further agree that per-

mission for extensive copying of this thesis for scholarly

purposes may be granted by the Head of my Department or by

his representatives. It is understood that copying or publi-

cation of this thesis for financial gain shall not be allowed

without my written permission.

Department of _____*Chemical Engineering*_____

The University of British Columbia,
Vancouver 8, Canada

Date _____*Sept. 17, 1964*_____

The University of British Columbia

FACULTY OF GRADUATE STUDIES

PROGRAMME OF THE

FINAL ORAL EXAMINATION

FOR THE   DEGREE OF

DOCTOR OF PHILOSOPHY

of

WALTER HAYDUK

B.A.Sc.,   The University of British Columbia, 1954

M.A.Sc.,   The University of British Columbia, 1956

IN ROOM 207, CHEMICAL ENGINEERING BUILDING

THURSDAY, JULY 9, 1964, at 1:30 P.M.

COMMITTEE IN CHARGE

Chairman: W. H. Gage

S.D. Cavers   E. Peters
J.S. Forsyth   K.L. Pinder
J. Lielmezs   I.T. Warren

External Examiner: G. Govier

Deputy Chairman, Oil and
Gas Conservation Board
Calgary

ABSORPTION IN GAS-LIQUID HORIZONTAL FLOW

ABSTRACT

Gas absorption rates were experimentally determined
for a number of two-phase gas-liquid systems in co-
current horizontal flow through circular tubes.
Sparingly soluble gases were used in order to determine
the liquid phase resistance to mass transfer. A series
of experiments was designed to separate the effects of
gas density, liquid-phase diffusivity, viscosity, sur-
face tension, and tube diameter, on the mass transfer
rates. The gas-liquid systems employed, in a single
tube 1.757 cm. in diameter, were CO_2-water, He-water,
CO_2-ethanol, and CO_2-ethylene glycol. Two additional
tube sizes, 1.228 and 2.504 cm. in diameter were em-
ployed with the CO_2-water system to determine the effect
of tube diameter. The gas and liquid flow rates used
produced four different flow regions, bubble, plug,
slug, and annular flow. The gas, and liquid, super-
ficial velocities ranged from 0.1 to 40 fps, and 0.5 to
3.6 fps, respectively.

Two correlations were developed for predicting mass
transfer rates in two-phase flow. The first, based on
a theory that each bubble represents a "mixing stage",
is applicable to the bubble and plug regions of flow,
and correlates the experimental data for a wide range
of liquid physical properties, as well as gas and
liquid flow rates, with a probable error of approxi-
mately 15%. The second correlation, applicable to slug
flow, empirically correlates the data for this region,
over the same wide range of physical properties and
flow rates, with a probable error of approximately 10%.

The surface renewal or "penetration theory"
mechanism of transfer is shown to be consistent with
the experimental results obtained in the bubble and
plug regions. In the slug region, on the other hand,
evidence is available to indicate that another
mechanism (probably that proposed by Kishinevskii),
becomes increasingly important as the degree of
turbulence increases.

GRADUATE STUDIES

Field of Study: Chemical Engineering

Industrial Chemical Reactions	D.S. Scott
Engineering Calculations	N. Epstein
Fluid Flow	N. Epstein
Heat Transfer	L.W. Shemilt
Chemical Engineering Thermodynamics	L.W. Shemilt
Advanced Chemical Reactor Design	D.S. Scott
Momentum, Heat and Mass Transfer	S.D. Cavers

Related Studies:

Topics in Organic Chemistry	A. Rosenthal
Production Techniques	H.C. Wilkinson
Theory of Measurements	A.M. Crooker
Computer Programming	C. Froese
Mathematical Statistics	L. Schwartz
Heat Transfer	W. Wolfe

ABSTRACT

Gas absorption rates were experimentally determined for a number of two-phase gas-liquid systems in cocurrent horizontal flow through circular tubes. Sparingly soluble gases were used in order to determine the liquid phase resistance to mass transfer. A series of experiments was designed to separate the effects of gas density, liquid-phase diffusivity, viscosity, surface tension, and tube diameter, on the mass transfer rates. The gas-liquid systems employed, in a single tube 1.757 cm in diameter, were CO_2-water, He-water, CO_2-ethanol, and CO_2-ethylene glycol. Two additional tube sizes, 1.228 and 2.504 cm in diameter were employed with the CO_2-water system to determine the effect of tube diameter. The gas and liquid flow rates used produced four different flow regions, bubble, plug, slug, and annular flow. The gas and liquid superficial velocities ranged from 0.1 to 40 fps, and 0.5 to 3.6 fps, respectively.

Two correlations were developed for predicting mass transfer rates in two-phase flow. The first, based on a theory that each bubble represents a "mixing stage", is applicable to the bubble and plug regions of flow, and correlates with experimental data for a wide range of liquid physical properties, as well as gas and liquid flow rates, with a probable error of

approximately 15%. The second correlation, applicable to slug flow, empirically correlates the data for this region, over the same wide range of physical properties and flow rates, with a probable error of approximately 10%.

The surface renewal or "penetration theory" mechanism of transfer is shown to be consistent with the experimental results obtained in the bubble and plug regions. In the slug region, on the other hand, evidence is available to indicate that another mechanism (probably that proposed by Kishinevskii), becomes increasingly important as the degree of turbulence increases.

TABLE OF CONTENTS

LIST OF FIGURES

LIST OF TABLES

ACKNOWLEDGEMENT

The author wishes to express his acknowledgement to

Dr. D. S. Scott, under whose supervision this work was under-

taken, for his assistance and guidance.

Appreciation is also extended to Drs. N. Epstein, and

J. S. Forsyth for their helpful suggestions and encouragement

which expedited the completion of this project, in Dr. Scott's

absence.

A particular indebtedness is expressed to Mr. E. Rudischer

for his willing assistance in the construction and assembling

of equipment.

Financial support for this research was contributed by the

Standard Oil Company of British Columbia in the form of their

Postgraduate Fellowship for two consecutive years (1961-2 and

1962-3). Additional financial support was provided by the

National Research Council of Canada from grants made available

to the Chemical Engineering Department at this university.

INTRODUCTION

A study of gas absorption in two-phase cocurrent flow will

include at least two major areas of chemical engineering

enquiry: the mechanism of inter-phase mass transfer, and the

hydrodynamic processes which produce the interfacial areas

involved. An adequate explanation of the mechanism of mass

transfer is dependent on a realistic picture of the fluid

dynamics. The fluid behaviour of one type of bubble flow in

vertical tubes has been explained in some detail (1), and con-

siderable effort has been expended on the analysis of the flow

characteristics of upward annular gas-liquid flow (2,3). For

many of the two-phase flow regions in both vertical and hori-

zontal tubes, however, studies of the fluid dynamics have not

yet been particularly successful. Reports in the literature

of the rates of mass transfer in two-phase cocurrent flow

(horizontal and vertical) have been extremely sparse (4,5,6)

and in none of these articles has the actual mechanism of mass

transfer been brought to light.

In this research experiments designed to improve present

knowledge about mass transfer processes in horizontal two-phase

gas-liquid flow, have been performed. For the bubble and plug

flow regions an attempt was made to postulate from the observed

shape and behaviour of the gas-liquid interface, which of several possible mechanisms might be operative in the flowing fluids. For these regions, therefore, it was possible to put forward an explanation for the observed variations in rates of mass transfer. For the slug and annular regions of flow, however, a more empirical approach was necessary.

Some characteristics peculiar to horizontal gas-liquid tubular flow set it apart from single-phase flow. A knowledge of the volumetric rates of input for both the gas and liquid does not directly afford a knowledge of the actual average velocities of either of the phases in the tube. The volume fraction of each of the flowing phases usually differs from that at the inlet. For horizontal two-phase flow, therefore, a number of correlations are to be found in the literature (7,8,9) which predict the volume fraction of one of the phases in the tube. The lack of more success with these correlations has been ascribed, in part, to an apparent disregard of the method of bringing the two phases together at the tube entrance. For single-phases flow, the mass or heat transfer coefficients nearly always depend on the fluid velocity to a power less than unity. For mass transfer in two-phase slug, however, this does not seem to be the case.

Occurrences of two-phase flow are relatively frequent;

these include transporting of petroleum products in gas-oil
pipelines, processing equipment such as condensers and reboilers,
and also steam generating units. In these situations, the
occurrence of two-phase flow is usually a consequence of the
processing operation rather than of a purposeful application.
The application of two-phase flow to vertical tube vaporizers,
utilizing the gas-lift effect for increasing the turbulence
at the heat transfer surfaces, is becoming more prevalent
because of the resulting unusually high heat transfer coeffi-
cients.

Cocurrent gas-liquid tubular contactors have a number of
possible applications as mass transfer devices. Because the
gas and liquid flow in the same direction, however, they have
the potential disadvantages of any cocurrent contacting scheme.
For some particular applications such as the absorption of a
pure gas by a liquid, or the absorption of a gas which reacts
irreversibly with the liquid, cocurrent contacting is essen-
tially equivalent to countercurrent contacting. For these
situations two-phase cocurrent contactors have a potential
advantage when compared to more common contacting equipment
such as packed towers. Application of tubular contactors to gas-
liquid heterogeneous systems, such as the oxidation of slurries,
appears possible. The presence of the solid particles in the

liquid prohibits the use of packed towers, but would not

affect the performance of tubular contactors. A specific

application in the pulp and paper industry which has been

recently patented, employs a pipeline contactor for the

oxidation of black liquor (10).

Reported mass transfer studies with two-phase flow contac-

tors are very limited indeed. Varlamov (4,5) utilized the gas-

lift principle in vertical tubes for absorption and reaction of

gas in the liquid phase. The calculation of overall mass

transfer coefficients was based on the internal wetted area of

the tube. Mass transfer controlled by diffusion in the gas

phase (ammonia, air, and water) has been studied by Anderson

(6) for horizontal annular flow. Overall mass transfer co-

efficients were also based on the tube internal wetted area.

It was shown that the amount of transfer could be correlated by

the same relationships as those used for wetted wall columns

provided that an additional contributing factor directly pro-

portional to the liquid superficial Reynolds number was included.

The specific objective of this research was to investigate

the liquid phase resistance to mass transfer for two-phase gas-

liquid flow in horizontal tubes. The range of the investiga-

tion was to include a sufficient number of gas-liquid systems,

and several flow regions, to permit the development of generalized

correlations which would allow the prediction of absorption rates for most gas-liquid systems. An experimental program was designed to permit the separate evaluation of the molecular effects of liquid phase diffusivity, interfacial tension and viscosity, as well as geometric effects such as tube diameter, and inlet arrangements. No guidance was available from previous research to indicate the relative importance on the absorption rates of the host of variables associated with two-phase flow. As a result some variables appreciably affecting the absorption rate may have been altogether omitted from this study (such as liquid density), some variables which probably should have been studied more thoroughly (such as type of entrance) were only superficially investigated, while other variables (such as the liquid flow rate) perhaps need not have been investigated so completely. This research must be considered somewhat exploratory, therefore, defining areas of interest which in the future will undoubtedly be more intensively investigated, and consequently better understood.

SCOPE OF RESEARCH

The selection of gases and liquids to be used in the absorption tests was based on a choice of experimentally desirable conditions. To permit the determination of the liquid phase resistance to mass transfer only, the use of pure gases was desirable to eliminate any gas phase resistance. So that the properties of the liquid would remain essentially unchanged by the absorption of the gas, the use of only sparingly soluble gases was indicated. In addition, for the sake of safety, the gases as well as the vapours of the liquids, needed to be non-toxic, and non-explosive with air, because large quantities were to be used and contamination of the work area with the gases and vapours appeared unavoidable. The gases chosen were carbon dioxide (CO_2) and helium (He), and the liquids, water, ethanol, and ethylene glycol. Ethanol was used because of its low surface tension when compared with that for water. Ethylene glycol was chosen because of its relatively high viscosity. For the pure liquids and gases, solubility and diffusivity data were available from the literature, except for the CO_2 solubility in ethylene glycol which was experimentally obtained.

The absorption tubes were constructed of glass to permit

the visual inspection of the two-phase flow patterns. The
glass walls of the tubes were wetted by the liquids used.
The wetting characteristics of the tubes were, therefore,
comparable to those for most metallic surfaces such as iron
and copper, but unlike those for many plastic materials such as
tygon and polyethylene. A typical absorption tube installation
consisted of an entrance tee, an entrance section, a test sec-
tion, a short exit section, and a cyclone separator. The gas
and liquid, initially brought together in the entrance tee,
formed a consistent flow pattern in the entrance section which
was then maintained along the rest of the tube. Liquid phase
concentration measurements were made at the inlet and outlet
of that section of the tube designated as the test section.
The two phases were separated in the outlet cyclone. Three
tube sizes were used for the absorption experiments, 1.228,
1.757 and 2.504 cm in internal diameter. Each tube was fitted
with the same type of entrance tee, for which geometric simi-
larity was maintained in scaling up from one tube size to the
next. The entrance tee was mounted so that the liquid flowed
upward and the gas downward, and then on mixing the two phases
flowed horizontally into the absorption tube.

The test method consisted of contacting the gas and liquid
isothermally in one of the absorption tubes. Liquid phase

concentrations were measured at both ends of the test section by withdrawing and analyzing liquid samples. The liquid was continuously circulated through the absorption tube and a desorption apparatus. This process permitted the repeated use of the same liquid for many absorption experiments. The gas, on the other hand, supplied from high pressure cylinders, was discarded after a single pass through the absorption tube. The range of liquid flow rates was more limited than the much wider range of gas flow rates investigated. The approximate liquid superficial velocities ranged between 0.5 and 3.6 fps, and the approximate gas superficial velocities between 0.1 and 40 fps. This combination of gas and liquid flow rates and tube sizes produced four different types of flow: bubble, plug, slug and annular. It should be noted that the classification of two-phase flow patterns is somewhat arbitrary, and that the transition between flow patterns is usually indistinct. The flow regions as listed above conform to a classification introduced by Alves (11) for horizontal two-phase flow. The flow regions can be generally described as follows:

(a) <u>Bubble flow</u>: In this flow region discrete gas bubbles move along the upper surface of the tube at roughly the same average velocity as the average liquid velocity.

(b) <u>Plug flow</u>: The difference between bubble and plug flow

is largely concerned with the length of the "bubbles" with respect to their depth. When the length exceeds the depth by a factor of between 10 and 15, then the flow is considered to be plug flow.

(c) <u>Slug flow</u>: In this flow region the average velocity of the gas which flows along the top portion of the tube is much higher than the average liquid velocity. Intermittent waves of highly agitated liquid frequently rise to seal the tube as they are carried by the rapidly moving gas.

(d) <u>Annular flow</u>: The gas moves at a high velocity in the core of the tube carrying with it some of the liquid as a spray. Most of the liquid is distributed as a film around the tube wall with the greatest film thickness occurring at the bottom of the tube. The rapidly moving gas produces many waves and ripples on the liquid surface making the gas-liquid interface extremely irregular.

In analyzing mass transfer in horizontal two-phase flow it will be useful to separate all the pertinent variables into logical categories. All the variables can first be separated into two categories, one consisting of the primary variables and the other of the secondary variables. The primary variables would include those which are fundamental properties such as density and viscosity. The secondary variables would include

those which are some function of one or more of the primary variables. Secondary variables would include pressure drop, interfacial area, and the actual average liquid or gas velocities. The primary variables are listed under subheadings as follows:

(a) Gas phase: density, viscosity, volumetric flow rate, and concentration (in this research, pure gas).

(b) Liquid phase: density, viscosity, volumetric flow rate, and concentration of dissolved gas.

(c) Both gas and liquid phases: solubility, interfacial tension, and liquid phase diffusivity.

(d) Tube geometry: tube diameter, tube length, and entrance type.

The primary variables for the gas and liquid phases are commonly used properties and are usually readily available, measureable, or predictable. The tube dimensions and entrance type are variables which would be logically considered from experience with single-phase flow. The secondary variables, on the other hand, are often difficult if not impossible to evaluate because of the present lack of knowledge of the processes involved. Some of the more common secondary variables are listed below:

(a)   Fraction of the tube volume filled with liquid (or gas).

(b)   The actual average velocity in the tube of the liquid

    (or gas).

(c)   Two-phase pressure drop over an interval of tube length.

(d)   Number of transfer units, length of transfer unit, or

    some other measure of the mass transfer characteristics.

(e)   Interfacial area for an interval of tube length.

(f)   Surface conditions such as surface tension, and surface

    viscosity.

The intent of this research was to determine if the primary

variables could be used to express the mass transfer rates in

horizontal two-phase flow by relatively simple, and logical

relationships. The absorption rate expressed as the number of

transfer units (NTU) was considered a useful concept for the

tubular type of contactor, particularly because this variable

was independent of the liquid phase concentration which was

expected to vary in a wide range between essentially zero and

the saturated value. The effects on the mass transfer rates of

most of the primary variables listed above were investigated.

It was desirable to carefully choose only those variables which

on investigation were most likely to give useful information.

For example, the study of the effect of gas-phase concentration

on two-phase mass transfer would involve the gas-phase

coefficient combined with that in the liquid phase. It appeared

prudent to limit the investigations to the behaviour of the

liquid phase. Further, as discussed in some detail in a subse-

quent chapter, the shear forces in the gas phase, except perhaps

in the annular flow region, were most probably small with respect

to the shear forces in the liquid phase. Consequently, the gas

phase viscosity was considered to have a relatively small

effect on the mass transfer rates and was omitted from this

study. The effect of the liquid phase density was also omitted

from this study. Unless the effect of density on the absorption

rate is very pronounced, its omission should not seriously

affect the results of this investigation. The densities of

most liquids that are likely to be used for the absorption of

gases lie in a relatively narrow range. The specific gravities

of the liquids used in this research varied between 0.8 (for

ethanol) and 1.1 (for ethylene glycol), and the assumption was

made that provided the superficial velocities of the liquids

were the same all other effects of density could be ignored.

Partial justification for this assumption is outlined in a

following chapter. The primary variables, the liquid phase con-

centration and the gas solubility, were both involved in the

calculation for the number of transfer units. A number of

experiments with different entrance types were included to show

whether or not the absorption rate was independent of the type
of entrance. All the remaining experiments, however, were con-
ducted with only one type of entrance.

In summary, the primary variables which were investigated,
and the maximum ranges encountered in this research, are as
follows:

(a) Q_G, gas volumetric flow rate, 1.4 to 220 cfh.

(b) Q_L, liquid volumetric flow rate, 0.6 to 4.2 gpm.

(c) ρ_G, gas density, 0.18 to 2.6 gm l^{-1}.

(d) $\mathscr{D}_L$, liquid phase diffusivity, o.14 (10^{-5}) to 3.69 (10^{-5})
       cm^2 sec^{-1}.

(e) σ, interfacial tension, 22 to 74 dynes cm^{-1}.

(f) μ_L, liquid phase viscosity, 0.4 to 26 cp.

(g) D_T, tube diameter, 1.23 to 2.50 cm.

DESIGN OF EXPERIMENTS

In studying the rates of absorption in horizontal two-phase flow no prior knowledge was assumed about the system. It appeared advisable to measure the effects, on the absorption rates, of variations in the primary variables such as surface tension and viscosity rather than of changes in such dimension-less groups as the Schmidt number, Weber number, Froude number, and Reynolds number. Each of these dimensionless numbers could be legitimately expected to play a role in mass transfer processes in horizontal two-phase flow because the viscous, inertial, surface tension, and buoyancy forces were all involved; however, at the present state of knowledge, the correct definition for the terms which comprise each of the dimension-less groups was difficult, if not impossible, to ascertain for the two-phase system. For example, a number of different definitions of Reynolds number applying to two-phase flow have been proposed, as discussed by Govier (12), none of which can be unequivocally supported. The reasons for the difficulty in defining a Reynolds number can be readily appreciated. They are associated with the determination of the true velocities of the two phases, and also of the mixing effects resulting from the fact that the flow channel for each phase has an effectively

variable cross-section. The difficulty in defining a true Reynolds number for each phase was appreciated in this work, but since this project was not directed toward the study of the hydrodynamics of horizontal two-phase flow, no enlightened method is proposed. Somewhat similar problems of definition and application exist for the other three dimensionless groups. The use of the Schmidt number for mass transfer situations where the penetration theory is applicable has been questioned (13). The surface tension and buoyancy forces might well play two different roles in two different locations, first at the entrance tee, and next in the tube during flow. For these reasons, it appeared necessary to investigate the overall effects of the primary variables in a contacting apparatus which included a particular type of entrance section. In this way, correlations for the mass transfer rates by meaningless dimensionless groups were avoided, but, of necessity, a certain amount of empiricism was introduced by considering only the overall effects of the various primary variables.

The determination of the effects of a number of variables could be theoretically resolved to a statistical experiment but for one consideration. The primary variables could not be independently varied. Because of the nature of chemical compounds some properties such as viscosity and diffusivity

are closely related, preventing the variation of one without affecting the other. The choice of gas-liquid systems suitable for investigating the effects of the variables was, therefore, limited to those which permitted the separation of the various effects.

The general method for determining the effects of the different primary variables was to choose one system, the CO_2-water system, and to establish the relationship between the absorption rate (expressed as NTU) and the gas and liquid superficial velocities (V_G^O and V_L^O). The method then consisted of changing one variable while keeping all the others constant and observing the effect on the NTU, V_G^O, and V_L^O relationships. The change in the absorption rates was assumed to be caused by the intentional change of the particular variable. When two primary variables were simultaneously changed and the effect of one had already been determined, the total effect on the absorption rate was adjusted to compensate for the known effect of the first variable. The net effect was then attributed to the second variable. It is apparent that the investigation of a combination of three variables and the adjustment of the overall effect on the absorption rate for two of them to obtain the net effect of the third, could introduce a large error in the measurement of the third effect. The particular gas-liquid systems were chosen

to minimize the possible error in the measurement of the
"third order" effects. The primary variable whose effect was
to be measured, was changed as much as possible when compared
with that for the CO_2-water system, while the other two primary
variables for which adjustments were required, were changed as
little as possible. The actual gas-liquid system and experi-
mental conditions used to measure the effect of each of the
primary variables will be described in detail in subsequent
paragraphs.

The effect of gas density was determined by using the same
system (CO_2-water) at the same temperature ($15^{o}C$), the same
absorption tube (1.757 cm in internal diameter), and the same
entrance section, and by measuring the absorption rates at
two different pressures in the absorption tube. Because the
absorption temperature was the same, the liquid phase viscosity,
the liquid phase (CO_2) diffusivity, and the interfacial tension
were assumed to be the same regardless of pressure. Absorption
rate measurements were obtained at approximately 10 and 20 psia,
thereby varying the gas density by an approximate factor of two
without changing any of the other variables. The calculation of
NTU involved the gas solubility which did change with pressure,
but was assumed to depend on pressure according to Henry's law.
The effect of gas density was, therefore, obtained by comparing

the absorption rates at the two pressures. The absorption rate

was found to be a function of the gas volumetric flow rate and

that, for a particular liquid flow, the curves of NTU vs the

gas flow rate were coincident for the two pressures provided

that the gas flow rate was expressed in volumetric units (or

as the gas superficial velocity). The coincident curves of NTU

and gas superficial velocity at a constant liquid flow rate for

the two pressures, 10 and 20 psia, are shown on a log-log

plot in Figure 1.

In order to permit the use of the low density gas, He, a

knowledge of the effect of gas density over a much wider range

than that obtained by changing the pressure of absorption with

the CO_2-water system was required. The absorption curve for the

He-water system was obtained at the same liquid temperature and

superficial velocity as for the CO_2-water system. It is also

shown in Figure 1. The fact that the inflections in the NTU

vs V_G^o curves for the He-water and CO_2-water systems occurred at

essentially the same values of V_G^o, was taken as a partial con-

firmation that the effect of gas density was largely compensated

for by the use of the gas superficial velocity, V_G^o. Referring

again to Figure 1, the displacement of the NTU vs V_G^o curve

for the He-water system when compared with that of the CO_2-

water system was, therefore, attributed to the difference
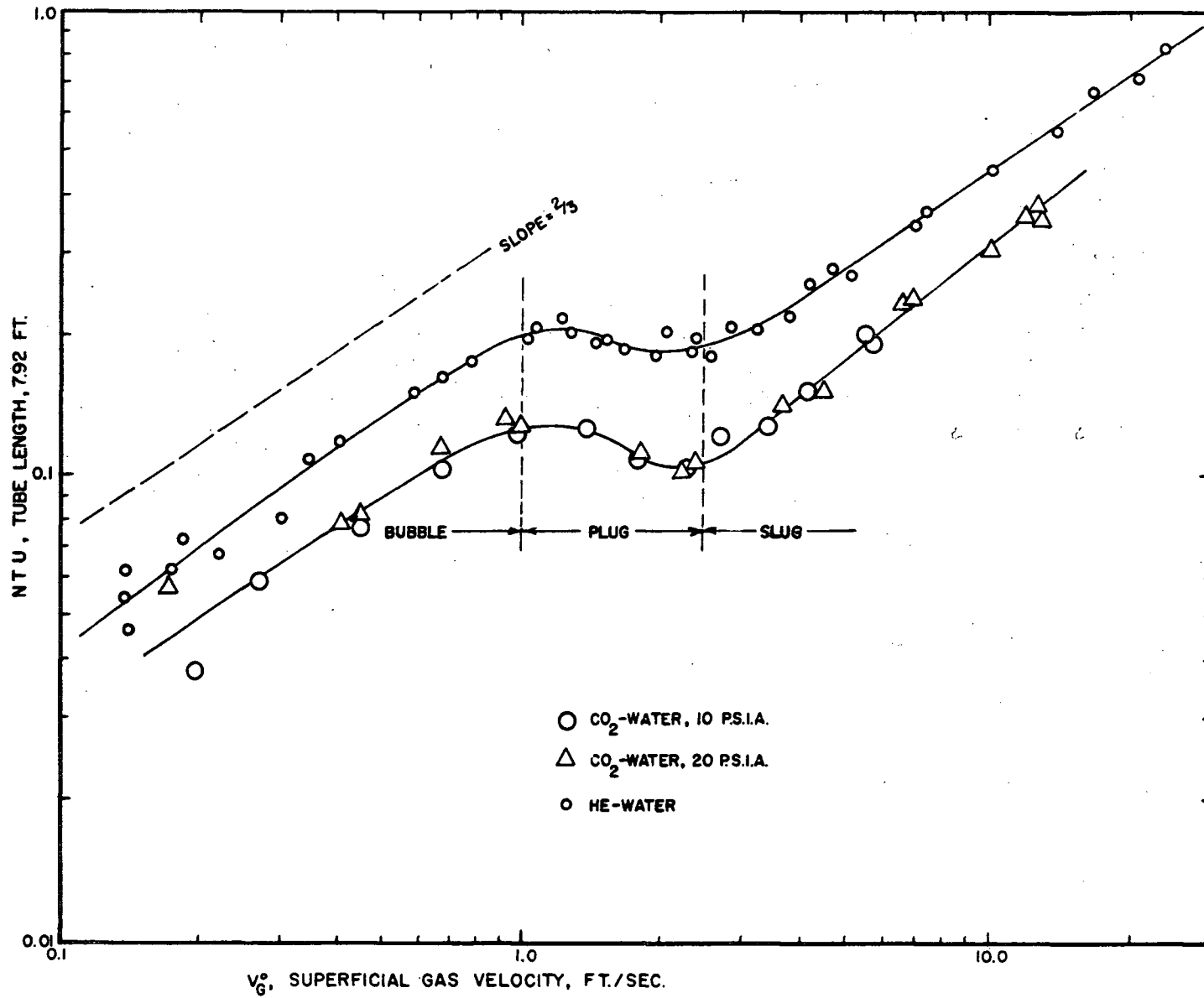
Figure 1. Effect of Gas Pressure and Liquid Phase Diffusivity on Absorption Rate

in the liquid phase diffusivity.

When changing from the CO_2-water system to the CO_2-ethanol and CO_2-ethylene glycol systems a problem arose as to the basis for obtaining an equivalent liquid flow rate for the three systems. Was a mass flow rate of ethanol equivalent to the same mass flow rate of water or ethylene glycol in its effect on the absorption rate? Or would the same Reynolds number, using the superficial velocity in its calculation, yield an equivalent flow for the three liquids? It was necessary to make a decision on the method for obtaining comparable liquid flow rates before any effects of such variables as liquid viscosity, or interfacial tension, could be ascertained. It was finally assumed that comparable liquid flow rates would be obtained for the three liquids, provided that the superficial velocities were kept the same. There were three reasons why this basis for comparison was adopted. First, in spite of the big density difference of He compared to that of CO_2, the shape of the absorption curves (NTU vs V_G^o) remained the same for the two gases at the same superficial velocities. This suggested that the volumetric throughput was of more consequence in two-phase flow than the mass throughput. The shape of the absorption curves (NTU vs V_G^o) for the same volumetric flow rates of the three liquids were nearly the same, and also the inflection

points corresponded roughly to the same gas superficial velocities, even for ethylene glycol, many times as viscous as water or ethanol. Finally, the appearance of the bubbles, plugs, and slugs (as well as regions of transition) was approximately the same at equal gas superficial velocities, for the same liquid superficial velocities. For these reasons identical liquid superficial velocities were considered to produce identical types of flow. Any change in the absorption rates when compared with the CO_2-water system was attributed, therefore, to changes of the other variables involved.

As indicated earlier, the effect of diffusivity was obtained by comparing the absorption rate curves for the He-water system with that for the CO_2-water system at the same liquid superficial velocities. During the experiments with both of these systems the liquid temperature and hence viscosity and density were identical. The interfacial tension was also considered to remain essentially the same for the two gas-liquid systems. The influence of the gas composition on the interfacial tension is discussed in more detail in the chapter on Specifications and Properties of the Test Fluids. The same tube and entrance tee were likewise used for the He-water and CO_2-water systems. The effect of the liquid phase diffusivity was, therefore, directly observable from the absorption

curves of NTU vs V_G^o for the two systems. The liquid phase

diffusivity was increased by a factor of 2.5 by changing

from the CO_2-water to the He-water system.

The effect of interfacial tension was investigated by using

the CO_2-ethanol system and comparing the absorption rate

curves with those of the CO_2-water system at the same super-

ficial velocities. Ethanol was chosen for this study because

of its unusually low interfacial tension compared with water.

It is less than one third that for water, and represents a value

somewhat lower than that for most common industrial solvents.

The intention in using ethanol had been to pick an absorption

temperature for which the viscosity of ethanol would be iden-

tical to that of water at 15^oC. Due to an oversight the

temperature finally chosen, 13.5^oC, corresponded to a viscosity

of ethanol slightly greater than that for water at 15^oC. At

this temperature the specific gravity of ethanol was very nearly

0.8. The diffusivity of CO_2 in ethanol at 13.5^oC was between

that of CO_2 in water and He in water. Although the variables,

density, diffusivity, and viscosity, were not held constant

when determining the effect of interfacial tension, the changes

in these variables with ethanol as the liquid were relatively

small when compared to the change in the interfacial tension.

The effect of viscosity was investigated by using the

CO_2-ethylene glycol system. To obtain the effect of viscosity at two different values, the absorption experiments were performed at two different temperatures, $30^{\circ}C$ and $15^{\circ}C$. At these temperatures the viscosity of ethylene glycol was a factor of 12.2, and 23.2, times as great, respectively, as that of water at $15^{\circ}C$. The absorption experiments were performed with the identical tube and entrance tee that were used for the CO_2-water, He-water, and CO_2-ethanol experiments, and at the same liquid superficial velocities. The specific gravity of the ethylene glycol was 1.1. The interfacial tension was only slightly lower than that for water. The CO_2 diffusivity was much lower in ethylene glycol than that of CO_2 in water at $15^{\circ}C$, however. The CO_2 diffusivity in ethylene glycol at $30^{\circ}C$ and $15^{\circ}C$ was approximately one fifth, and one tenth, respectively, of that in water at $15^{\circ}C$. It is apparent that the diffusivity effects as measured by the He-water system had to be extrapolated considerably for application to the CO_2-ethylene glycol system. However, no way of avoiding such an extrapolation could be devised since all viscous liquids exhibit a low diffusivity. Even though the change in diffusivity was large, the change in viscosity for the CO_2-ethylene glycol system was even greater, so that a reasonably good measure of the effect of viscosity should have resulted from the use of this system.

The effect of tube diameter was investigated using the CO_2-water system, by conducting absorption experiments with two tube sizes, one larger and one smaller than the one used for all the previous experiments. The internal diameters of the tubes were 2.504 cm and 1.228 cm compared with 1.757 cm for the most frequently used tube. The entrance tees were all geometrically similar. Absorption experiments were conducted at similar values of liquid superficial velocity for all the tube sizes. The conditions for absorption were likewise the same, 15°C, and essentially atmospheric pressure. The effect of tube diameter was very pronounced, so that the concentrations of CO_2 in the water were very low at some gas flow rates for the largest tube size, and approached saturated values for some gas flow rates for the smallest tube size. All the primary variables were identical for the experiments with the three tube sizes, and the changes in absorption rate could only be ascribed to the effect of the size of the absorption tube (and entrance tee).

The following summary lists the type and number of experiments that were employed in attempting to separate the effects of the various primary variables.

(a) The effect of <u>gas and liquid flow rates</u> was obtained with

the CO_2-water system at 15^oC and the 1.757-cm tube. Six

liquid flow rates corresponding to superficial velocities

of 0.5, 0.9, 1.3, 1.8, 2.6 and 3.6 fps were used in con-

junction with a range of corresponding gas superficial

velocities from 0.1 to 20 fps for each liquid rate.

(b) The effect of <u>gas density</u> was obtained with the CO_2-water

system at 15^oC and the 1.757-cm tube using absorption

pressures of 10 and 20 psia. One liquid flow rate corres-

ponding to 0.9 fps, and gas superficial velocities from

0.2 to 10 fps were used at each pressure.

(c) The effect of <u>liquid phase diffusivity</u> was obtained with

the He-water system at 15^oC and the 1.757-cm tube. Three

liquid flow rates were investigated corresponding to super-

ficial velocities of 0.5, 0.9, and 1.8 fps. Gas super-

ficial velocities for each liquid rate ranged from

0.1 to 20 fps.

(d) The effect of <u>interfacial tension</u> was obtained with the

CO_2-ethanol system at 13.5^oC using the 1.757-cm tube.

Liquid superficial velocities were 0.5, and 0.9, and 1.8

fps, while the gas superficial velocities ranged from

0.1 to 20 fps for each liquid rate.

(e) The effect of <u>liquid viscosity</u> was obtained using the

CO_2-ethylene glycol system at two temperatures, $15^{\circ}C$ and $30^{\circ}C$, and the 1.757-cm tube. For both temperatures three liquid flow rates corresponding to superficial velocities of 0.5, 0.9, and 1.8 fps were used. The gas superficial velocities ranged from 0.1 to 20 fps for each liquid rate.

(f) The effect of <u>tube diameter</u> was obtained by using two additional tube sizes, 2.504 and 1.228 cm, with the CO_2-water system at $15^{\circ}C$. Three liquid superficial velocities were investigated in each tube, again approximately 0.5, 0.9, and 1.8 fps. Gas superficial velocities ranged from 0.1 to 10 fps in the large tube and from 0.2 to 40 fps in the small tube.

(g) The effect of <u>absorption temperature</u> was investigated with the CO_2-water system using the 1.757-cm tube. Two additional temperatures were used, $30^{\circ}C$ and $45^{\circ}C$. The same liquid superficial velocity was used at both temperatures, 0.9 fps, while the gas superficial velocities ranged from 0.1 to 20 fps for each liquid rate.

THEORETICAL ASPECTS

In this chapter, the theoretical aspects of gas absorption in horizontal gas-liquid flow are discussed in three sections. In the first section, the general considerations which affect all absorption processes are discussed. In the second section, a postulated mechanism for mass transfer in the bubble flow region is developed, and, in the third section, the problems of developing a theoretical model for the slug region of flow are considered.

Factors Affecting Absorption Rate

The rate at which a pure gas will dissolve in a liquid in a particular contacting apparatus will depend on the gas solubility, the interfacial area, the concentration of the gas in the liquid, the condition of the interface, and finally the degree of mixing in the liquid phase. The degree to which the above mentioned variables influence the rate of absorption, comprises the study of absorption in general.

The gas solubility represents the maximum quantity of gas that will dissolve in a certain quantity of liquid at any given temperature and pressure. The solubility can also be considered to represent the maximum driving force for absorption. It is

usually highly dependent on temperature, and in this respect, is

not unlike the vapour pressure of liquids. The solubility is

also influenced by pressure, the effect of which is given by

Henry's law for sparingly soluble gases.

The determination of the interfacial area is usually diffi-

cult for most gas-liquid transfer processes. It is essential

to know the interfacial area if the effects of the interfacial

area and the liquid phase resistance to mass transfer are to be

separated. Except for a few specially designed systems such as

laminar jets (14), and short wetted-wall columns (15), indirect

methods for measuring the interfacial area are required. It is

sometimes possible to determine the interfacial area by the use

of a combination of experiments for the same contacting system,

which entails first, the measurement of the simple rates of

absorption and next, the measurement of the rates of absorp-

tion with chemical reaction of the absorbed gas. Provided

that the liquid properties are not significantly affected by

the chemical reaction, and that the reaction kinetics have

been established for the conditions of the experiment, the

interfacial area can be calculated. A knowledge of the true

interfacial area for absorption does not necessarily afford a

knowledge of the transport mechanism in the liquid phase,

although it does permit the calculation of an average liquid

phase coefficient. Whether the mechanism of transport is by
diffusion through a thin film at the interface, by unsteady-
state diffusion into "packets" of liquid brought to the inter-
face and rapidly carried away, or by agitation sufficiently
great to cause a velocity component away from the interface,
can only be postulated. These mechanisms, and combinations
of them, have been put forward for essentially all absorption
systems (16).

The influence on the absorption rate of the concentration
of absorbed gas in the liquid phase is largely due to its
effect on the concentration driving force. If the liquid is
saturated no additional transfer will take place, and if the
liquid contains no gas, the rate of solution will be the maxi-
mum for any particular method of contacting. It is generally
considered that the rate of absorption of a pure gas by a
liquid is directly proportional to the concentration driving
force for any one particular contacting system and set of
absorption conditions. This latter statement is true only if
the properties of the liquid remain the same for all the gas
concentrations obtained in the liquid. For slightly soluble
gases the assumption is frequently made that the liquid pro-
perties remain unchanged by the presence of the gas. For
highly soluble gases the change in properties of the absorbing

liquid cannot be neglected.

It is usually assumed that the resistance to mass transfer of the gas-liquid interface itself (perhaps 10 $\overset{o}{A}$ thick) is negligible (17). Impurities which concentrate at the interface affecting the conditions at the interface, are generally known as surface active agents. A layer of a surface active agent as little as one molecule in thickness at the interface can have an appreciable resistance and hence reduce the rate of mass transfer (18,19). The presence of a monolayer can also have a calming effect on the interface by virtue of its surface vis- cosity and resistance to local compression, reducing the extent of surface agitation and rippling (20). The condition of the interface, therefore, can influence the rate of absorption in two ways, by introducing an additional interfacial resistance, and by decreasing the agitation of the interface.

The discussion of the degree of mixing will be limited to its effect on absorption. If a pure gas is absorbed by a completely stagnant liquid, infinite in extent, the rate will be a decreasing function of time because the distance in the liquid phase across which the gas molecules diffuse, is increasing. The solution of the appropriate differential equation (21) indicates that for this situation the dependence of the mass transfer rate on the liquid phase diffusion

coefficient is to the 0.5 power. If turbulent stirring main-
tains the concentration of the bulk of the liquid during the
absorption of a pure gas at a constant value, it has been pro-
posed by Lewis and Whitman (22) that a certain thickness of
liquid at the interface is in laminar flow and that the direc-
tion of this flow is parallel to the interface. Through this
"laminar film" mass transfer occurs at a constant rate, as if
the layer were stagnant. For this situation, the rate of
transfer depends on the liquid phase diffusion coefficient to
the first power. It is perhaps significant that few absorption
studies have, in fact, shown a dependence of the mass transfer
rate on the liquid phase diffusivity to a power greater than
0.7. If a pure gas is absorbed by contact with a turbulent
liquid in which the average times of contact for portions of
liquid continually brought to the interface are short, the
steady-state theory of Lewis and Whitman cannot be valid.
Instead, as proposed by Higbie (23), the rate of mass transfer
would be of an unsteady-state type, depending inversely on the
square root of the average exposure time and directly on the
square root of the liquid phase diffusivity. In this mass
transfer model, it is assumed that the penetration of the
absorbed molecules at each exposure does not exceed the depth
of liquid for which the velocity is essentially the same as

that at the interface, and hence this development is known as the "penetration theory". It has been proposed as an explanation for the absorption in packed columns. The flow of liquid over the individual pieces of packing may be laminar, exposing the liquid for only short periods of time, while at the junction of one piece of packing and the next complete mixing may occur. The dependence of the rate of transfer on diffusivity and exposure times according to the Higbie model has in fact been observed in packed towers (24). In the limit of extreme turbulence when eddies of liquid are swept in and out of the interface with extreme rapidity, neither a laminar surface film, nor a momentarily stationary interface can be physically realistic, according to Kishinevskii (25). For this situation it is proposed that the rate of transfer is completely independent of liquid phase diffusivity and depends instead on the mean velocity of the liquid normal to the interface. This limit of extreme turbulence is seldom reached in any absorption operations. Kishinevskii was able to show by actual experiments (25) for the absorption of H_2, N_2, and O_2 into water stirred at an extremely high rate, that the rate of transfer for this high degree of turbulence was indeed independent of the liquid phase diffusivity. For intermediate stirring speeds however, the influence of diffusivity was

again significant.

In reviewing the proposed mechanisms for mass transfer for different situations, several observations can be made. Except for unsteady-state absorption into an infinite stagnant liquid, which is not a practical situation, all the proposed mechanisms suggest a certain type of dependence between the transfer rate, the degree of mixing, and the liquid phase diffusion coefficient. As the turbulence increases the dependence of the transfer rate on the liquid diffusivity decreases. Further, it appears likely that the mechanisms as proposed are suitable for specific situations only, and that combinations of these mechanisms perhaps most accurately describe many other practical absorption processes. The absorption rate could then depend directly on the liquid phase diffusivity to a power anywhere between zero and one, depending on the degree of turbulence and method of transfer.

A closer inspection of the "penetration theory" as a transport mechanism, and its application to real processes will perhaps be useful. There are at least two types of mass transfer processes (27) for which the "penetration theory" has been used as a model. One is the absorption of gas into a stirred liquid, for which one of the assumptions normally made is that complete mixing occurs in the bulk of the liquid due to

turbulence. Another assumption is that portions of the inter-
face and adjacent liquid are frequently, and randomly, replaced
by means of turbulent eddies. The other type of transfer
process occurs in packed columns. The assumptions made for
this latter situation include that the liquid is in laminar
flow while passing over a particular piece of packing, and that
complete mixing occurs at the junctions of flow between pieces
of packing. It is perhaps important to emphasize the dif-
ference between these two very similar transfer processes.
In the first instance the bulk of the liquid is turbulent, and
in the second, the flow is essentially laminar with mixing
occurring only at fixed positions. The distinction to be made
is that unless mixing such as that caused by the liquids flowing
from different directions toward a single point is defined as
turbulence, the liquid is not turbulent during the transfer of
mass over packing. In order that the "penetration theory"
will be applicable, the liquid needs to be neither turbulent
(as commonly understood) nor even well mixed, provided that
some method exists for renewing the interface, and for dissi-
pating into the bulk of the liquid absorbed molecules which
have been concentrated in the interfacial region during the
period of absorption. Further, the degree of mixing in the
bulk of the liquid needs to be only sufficiently great so as

not to significantly limit the transfer process through the bulk
of the liquid. As a consequence, then, the major portion of the
resistance to mass transport will be retained in the vicinity
of the gas-liquid interface.

Mass Transfer Mechanism for Bubble Region

There are a number of readily observable facts in horizon-
tal gas-liquid flow in the bubble and plug regions which help
to give some insight into the fluid hydrodynamics. First of
all, the bubbles or plugs of gas moving along the top of the
tube are much less dense than the liquids. At a constant
liquid superficial velocity, very tiny bubbles (2 mm in
diameter) travel much slower than large ones (8 mm). This
is observable even if both sizes of bubbles are in the tube at
one time, and therefore, cannot be explained by supposing that
the net volumetric throughput of the gas phase is greater in
the case of the larger bubbles. The explanation would appear
to be that a velocity profile for the two phases exists in the
tube, and that a maximum velocity occurs in some position along
a vertical line through the centre of the tube. The liquid
velocity must vary from zero to the maximum from positions
at the wall to the position of the maximum. The velocity of a
bubble would appear to depend in some way on the average,

or maximum, velocity to which it was subjected. That is,
small bubbles with a small vertical dimension, and flowing
near the tube wall, would be subjected to a lower liquid
velocity and hence would travel at a slower rate than larger
bubbles having a larger vertical dimension. Because the small
bubbles move slower than large ones, the void fraction (fraction
of tube filled with gas) would be dependent on the bubble size
for equivalent gas and liquid throughput rates. The higher
velocities of the larger bubbles appear to be a result of
their deeper penetration into the tube, and hence into regions
of higher liquid velocities. Further, if it is accepted that
by the use of special entrances or nozzles, bubbles of various
sizes can be produced for any particular gas flow rate, then
it can be readily seen that for bubble flow the void fraction
is dependent on the type of entrance used.

An expression for the gas void fraction in terms of the
gas and liquid volumetric flow rates has been proposed by
Nicklin, Wilkes, and Davidson (28) for vertical gas-liquid slug
flow. This equation has been shown by Scott (29) to also apply
in a modified version for horizontal flow, by comparison with
actual void fraction data. This latter expression applies for
superficial liquid Reynolds numbers exceeding 8000, for which
the liquid velocity profile might well be expected to be

relatively flat. The expression for horizontal flow is:

$$R_G = 0.833 \frac{Q_G}{Q_G + Q_L} \tag{1}$$

where: R_G = void fraction

Q_G, Q_L = gas, liquid volumetric flow rates

Equation (1) would be expected to apply for the bubble and plug flow regions. The success of such an expression, which in no way accounts for the entrance conditions, is attributed to the fact that most investigations in the bubble flow region have been carried out using relatively large bubbles which would have penetrated well into the core of the liquid where the velocity profile was relatively flat. Bubble velocities calculated by use of equation (1) indicate that the velocities would be 1.2 times the sum of the superficial velocities of both fluids, based on the inlet volumetric flow rates, or equivalently 1.2 times the true average liquid velocity. Tiny bubbles subjected only to the liquid velocity very close to the tube wall could not be expected to flow at the same velocity as those subjected to the velocity of the liquid at a more central location in the tube. For situations when relatively large bubbles are produced, however, and for the conditions of its development, equation (1) would be expected to give good results.

Proposed Velocity Profile in Bubble Flow Region

It is possible to deduce qualitatively the shape of the velocity profile for the bubble-flow region of horizontal gas-liquid flow based on readily observable phenomena as well as on an analysis of the various forces involved. One type of behaviour in bubble flow to which no reference in the literature has been found is the particular "crawler type" of film circulation which occurs around bubbles during horizontal flow. When water, ethanol, or ethylene glycol is allowed to flow through a horizontal glass tube dusted with talc powder, and air is injected into it at a rate sufficient to produce bubble flow, the circulation of the liquid film around each bubble can be readily seen. The film circulation can best be described by considering a single bubble. As a bubble moves forward along the top of the tube, a particle of talc is picked up at the rear of the bubble and carried forward in the direction of flow along the interface and eventually deposited on the tube wall at the front of the bubble. For a short period of time, until the rear of the bubble reaches it, this particular particle deposited on the top surface of the tube is completely stationary. It is then again swept off the tube wall and circulated by the movement

of the interface from the rear of the bubble to the front. The bubbles discussed here can be generally referred to as "large", having a vertical dimension of more than one quarter that of the tube diameter, and a length of at least three or four times the depth. From observation of the movement of a particle on the bubble interface it is apparent that the interface moves at a velocity greater than the average bubble velocity. This must be true otherwise a velocity of a particle at the interface relative to the bubble itself could not be observed.

The various forces operative in the gas and liquid phase during horizontal bubble flow in a region of the tube distant from the entrance will now be considered. Three types of forces can be exerted by the gas phase on the tube wall and on the gas-liquid interface. These are a pressure force, acting at right angles to all surfaces contacted, a shear force due to a velocity profile adjacent to the tube wall or interface, and a kinetic energy force. Both the shear and kinetic energy forces would appear to be negligible in comparison to the equivalent forces in the liquid phase. Far from the tube entrance the maximum velocities possible in the gas phase would be equal to those of the liquid with which it was in contact, because there is no energy source within the gas. The shear force, and kinetic energy force in the gas, would be directly proportional to the

gas viscosity, and gas density, respectively, in the common expressions for shear and kinetic energy. A typical ratio of gas to liquid viscosity is 0.01, and of gas to liquid density is in the order of 0.001. The shear and kinetic energy forces for gases and liquids flowing at the same velocity would likewise vary roughly in the same proportions. It is assumed, therefore, that the major force exerted by the gas in bubble flow is one of pressure.

Except those of gas pressure, all the forces which determined the shape of the bubbles, and their velocity during flow are assumed to occur in the liquid phase. Obviously, if a constant pressure is assumed at all locations within a particular bubble, and all the gas pressure forces are exactly counterbalanced, then there is no net pressure force on the bubble to cause its motion. For the situation where (liquid-solid) interfacial forces confine a bubble against the tube wall, some motion of all or part of the confining interfaces is essential, therefore, to cause any motion whatsoever of the gas bubble. Motion of the gas-liquid interface around bubbles causing their flow was in fact observed as discussed earlier.

The top of the tube exposed to the gas in the bubble is presumed to be wetted by the liquid at all times. Under these conditions the bubble is confined completely by a liquid film,

albeit a thin one at the top of the tube. Interfacial (or
surface tension) forces act to reduce the total interfacial
area, and attempt to impose a spherical shape on the bubble.
The interfacial tension forces, therefore, act to cause the
bubble to penetrate deeper into the tube. The buoyancy forces
tend to maintain the bubble at the top of the tube. In addi-
tion, these forces tend to elongate the bubble opposing the
effect of interfacial tension.

Inasmuch as motion of the gas-liquid interface in the direc-
tion of flow was observed, some force must have been available
to cause this motion. The obvious force that can be considered
is one of viscous shear in the liquid phase. If a velocity
gradient adjacent to the gas-liquid interface causes its motion
in the direction of flow, it is necessary for a maximum (local)
velocity to exist at some position below the interface. If
the force required to move the gas-liquid interface is small
relative to the shearing forces at the tube wall, then the posi-
tion of the maximum velocity could be close to the interface
itself. That is, only a small velocity gradient would be
required to cause a small force at the interface.

It has already been assumed that the shear caused by
any gas velocity in the bubbles can be considered negligible.
It will also be assumed that the liquid-solid interfacial

tension at the periphery of the bubbles is small in comparison to the shear at the wall in the liquid phase. Then, if the tube is cut in half lengthwise by an imaginary plane, the area of the tube exposed to liquid is much smaller in the top half of the tube than that exposed in the bottom half. It is a necessary condition for two-phase flow that the overall pressure drop due to flow across a finite length of conduit should be the same for all positions in a given cross-section of the conduit. It is therefore assumed that the pressure drop across a finite length of tube (containing many bubbles) would be the same whether measured in the top half, or the bottom half of the tube. For this to be possible, it is apparent that the shear force (per unit area) must necessarily be greater in the top half than in the bottom half. For the shear force to be greater in the top half the mean velocity of liquid must be greater in the top half of the tube. Alternately, the top portion of the tube can be considered as offering less resis- tance to flow than the bottom half because a fraction of the wall area contacts gas. Consequently, a higher fluid velocity would result in the top portion of the tube.

Figure 2 shows a proposed velocity profile for horizontal bubble flow. The mean gas velocity as shown in Figure 2 is greater than the mean liquid velocity. A velocity gradient
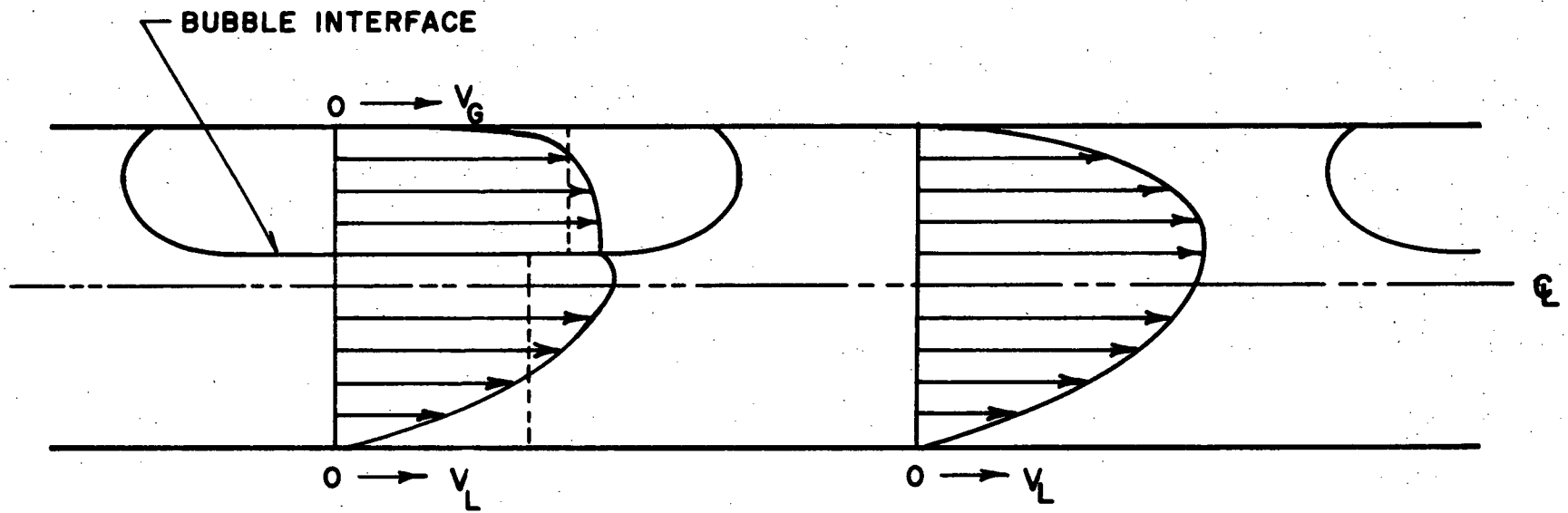
Figure 2.   Proposed Velocity Profile for Horizontal Bubble Flow

is shown adjacent to the gas-liquid interface. The maximum
liquid velocity in a portion of tube between the bubbles is
shown displaced upwards from the centre-line position. The
velocity profile has been drawn for a turbulent liquid, but
the shape of the profile would not be expected to change a
great deal for viscous flow, since the same observations and
arguments would still apply.

Proposed Mechanism for Mass Transfer in Bubble Flow

Two mechanisms will be considered, both based on the
surface-renewal or "penetration theory" model. The first one
is based on the assumption that the surface-renewal occurs by
the motion of the interface from the rear to the front of the
bubbles. The second mechanism postulates the superimposed
frequent renewal of portions of the interface during the circu-
lating motion around bubbles, as a result of eddying or mixing
within the bulk of the liquid. Although a stagnant film is
known not to exist in bubble flow, for the sake of comparison
the absorption rate assuming a film theory model will also be
estimated and compared with the observed rate.

In any consideration of the rate of mass transfer in hori-
zontal bubble flow, the relation between the gas flow rate and
bubble frequency is of considerable importance. The measurement

of bubble frequency, as well as the production of uniform bubbles by means of special nozzles, was outside the scope of this research. An attempt was made instead to simulate a practical situation by using a simple tee for introducing the gas and liquid phases into the contacting tube. For this type of entrance, the bubbles were not completely uniform in size or shape, although approximate uniformity was achieved for many of the gas and liquid flow rates. The relation between the gas flow rate and bubble frequency at a constant liquid rate was only qualitatively observed. The frequency remained roughly constant for a particular liquid flow while the gas flow rate was increased; the volume of gas contained in each bubble increased accordingly. This behaviour is consistent with that reported by Johnson (30) for bubbles formed at an orifice at relatively high gas flow rates.

A qualitative estimate of the effect on mass transfer of gas flow rate at a constant liquid rate can be made by using the following approximate model. It will be assumed that the large bubbles are geometrically similar to the small ones, and that the shape of each of them can be approximated by a right-angled parallelepiped. Then the surface area is directly proportional to the volume of a parallelepiped to the 2/3 power. If it is also assumed that the portion of each bubble in contact with

the tube wall is ineffective for mass transfer, and that a simi-
lar fraction of each bubble is made ineffective in this manner
regardless of size, then the effective interfacial area of each
bubble will still be directly proportional to the bubble volume
to the 2/3 power. Consider a length of contacting tube contain-
ing many bubbles. Even though the frequency of the bubbles
(at a constant liquid rate) is the same with an increasing gas
volumetric flow rate, the number of bubbles in a fixed length of
tube will decrease with an increased gas rate, because the total
fluid volumetric flow is increased. When the volumetric flow
of liquid greatly exceeds the gas volumetric flow (as in bubble
flow) the effect on the fluid velocity caused by variations in
gas flow only, is not large. This effect will be ignored,
therefore, in the qualitative arguments concerning the gas
flow rate and interfacial area.

Using the simplified model of parallelepiped-shaped bubbles
of constant frequency, the total interfacial area in a fixed
length of contacting tube, at a fixed liquid rate, is approxi-
mately proportional to the gas volumetric flow rate to the 2/3
power. For all models of mass transfer, the transfer rate would
be expected to be directly proportional to the effective inter-
facial area, and hence directly proportional to the gas flow
rate to the 2/3 power for the simplified model. For the mechanism

of surface renewal solely by the motion of the interface from
the rear to the front of the bubble, however, the transfer
rate is also involved with the mean contact time, or surface
age. If it is assumed that the velocity of the interface rela-
tive to that of the bubble is constant for all the sizes of
bubbles, then the net dependence of the mass transfer rate on
volumetric gas flow rate can be estimated. For this situation,
the transfer rate would be directly proportional to the effec-
tive interfacial area, and inversely proportional to the square
root of the mean contact time. If the relative velocity of the
interface is constant, then the dependence of the contact time
on any particular length dimension of a bubble would be to the
1/3 power, so that the net mass transfer rate for this mechanism
might be expected to depend on the gas volumetric flow rate to
the 1/2 power. The assumption that the bubble dimensions
increase proportionately in all directions with an increased
gas rate is somewhat in error. The dimension of length pro-
bably increases more than the width for the sizes of bubbles
actually investigated. In the extreme case of long "plug"
flow, when the bubble length greatly exceeds its depth,
bubbles tend to grow longitudinally only. In this limit of
one dimensional growth, the interfacial area is directly pro-
portional to the gas flow rate (still assuming constant bubble

frequency), and so is the contact time. Hence, the net rate of mass transfer again depends on the gas volumetric flow rate to the 1/2 power. From these two extreme cases, it may be concluded that in bubble flow the net mass transfer rate must depend on the volumetric gas flow rate to some power of 0.5 or greater, with a maximum possible value of unity for long plugs and assuming a stagnant film model.

Referring to Figure 1 (p.19), in which two typical absorption rate curves are shown (NTU vs V_G^o), it is found that in the bubble region of flow the slope on the log-log plot is nearly 2/3. Most of the absorption rate curves do in fact show a dependence on the gas volumetric flow rate, at a constant liquid rate, to an approximate power of 2/3 (but not of 1/2). Since it is known that a stagnant film does not exist at the bubble interface, the mechanism of transfer suggested, therefore, is that of the frequent renewal of portions of the interface by eddying and mixing. Subsequently much more conclusive evidence will be brought forth to indicate that in all probability this is the mechanism of mass transfer operative in bubble flow.

An actual experimental run for which a good estimate of the interfacial area can be made will be used as an illustration for comparing postulated mass transfer rates to those

experimentally measured. Run number 793 was made with the CO_2-water system at $15^{\circ}C$, using the small tube 1.228 cm in internal diameter. This particular run is used as an illustration because the bubbles produced were unusually uniform, and represented the smallest size of bubbles studied in this research. The size of bubbles was approximately 1.7 cm in overall length, and 0.6 cm in depth (almost half the tube diameter). The mean gas volumetric flow rate in the test section (between the sample points) of the absorption tube was also known. The gas input flow rate was corrected for the amount absorbed in the tube, as well as for the temperature and pressure in the tube to give a true mean value as calculated by means of an IBM-1620 computer. For this particular run the mean volumetric gas flow was 2.80 cfh which was equivalent to a superficial velocity of 0.610 fps, while the liquid flow rate was equivalent to a superficial velocity of 1.783 fps. The true bubble velocity was calculated by using the relation for void fraction given by Scott, equation (1), discussed earlier in this chapter. The conditions for the use of equation (1) included a liquid superficial Reynolds number exceeding 8000. The liquid superficial Reynolds number for run number 793 was approximately 6000, and the application of equation (1) was, therefore, not strictly justified. Since

any probable error was considered to be small in comparison to the major effect that was to be illustrated, it was used nonetheless. In essence equation (1) states that the gas (bubble) velocity is 1.2 times the true average liquid velocity. From the true bubble velocity the residence time of the bubbles in the test section could be calculated. From diagrams of the bubbles in the tube drawn to scale, it was possible to estimate the bubble cross-section area, volume, total surface area, as well as the average length of the longitudinal film surrounding each bubble. These dimensions were subsequently used to calculate the bubble frequency, number of bubbles in the test section, and the total interfacial area in the test section.

To estimate the transfer rate for the assumption of a stagnant film at the interface, a knowledge of the film thickness was required. The limit of the laminar sublayer adjacent to the wall for turbulent flow in circular channels is given by Knudsen and Katz (31). It was assumed that if the stagnant layer existed, it would have been of the same order of thickness at the bubble interface as at the tube wall. Further the liquid superficial Reynolds number was used (6000) in the evaluation of the film thickness because a true characteristic Reynolds number for two-phase flow was unknown and the film thickness was not highly dependent on Reynolds number. The thickness

obtained for the laminar sublayer was 0.0172 cm. To test the
rate of transfer for a stagnant film the most common type of
engineering rate equation was used:

$$N_A = A \mathscr{D} \frac{(C^* - C_o)}{x} \qquad (2)$$

where: $A = 162 \text{ cm}^2$

$\mathscr{D} = 1.465 \ (10^{-5}) \ \text{cm}^2 \ \text{sec}^{-1}$

$C^* = 0.0455 \ \text{millimoles cm}^{-3}$

$C_o = 0$

$x = 0.0172 \ \text{cm}$

The mass transfer rate in the test section for a stagnant
film at the interface was calculated by equation (2) to be
0.0063 millimoles per second. A maximum possible driving force
was used although the driving force for run number 793 was
actually closer to 90 per cent of the maximum. A linear concen-
tration profile was also assumed to exist in the film prior to
its arrival in the test section.

To estimate the transfer rate for the moving interface
model, it was necessary to know the rate of surface renewal,
or contact time. To determine the contact time the velocity of
the interface relative to that of the bubble was required.
Referring to Figure 2 (p.43), which shows the proposed velocity
profile for bubble flow, it appears unlikely that the interface

velocity exceeds the mean bubble velocity by more than a factor

of 1.3. The relative velocity of the interface, therefore,

would be 0.3 times the mean bubble velocity. It is noted that

the choice of the interface relative velocity was somewhat arbi-

trary, but it will be subsequently shown that this did not

significantly alter the result of this illustration. The mean

contact time was determined by dividing the interface length by

the interface relative velocity, and found to be for this

situation, 0.132 sec. The penetration depth was calculated

by the expression derived by Danckwerts (27):

$$PD = 3.6 \sqrt{\mathscr{D} \theta_c} \qquad (3)$$

where: PD = penetration depth, cm

$\mathscr{D}$ = liquid phase diffusivity, $1.465 \ (10^{-5}) \ cm^2 \ sec^{-1}$

θ_c = mean contact time, sec

The penetration depth as calculated by equation (3) was

0.0050 cm which is considerably smaller than the thickness of a

laminar sublayer calculated earlier. The penetration depth, as

defined by Danckwerts, is the depth at which the rise in concen-

tration due to unsteady-state absorption is 0.01 times that at

the interface. To calculate the rate of mass transfer in the

test section the total area exposed to the liquid was assumed

to have been renewed every 0.132 seconds. To calculate the

actual quantity of gas absorbed by the film at every exposure, it was necessary to know the concentration profile within the penetrated depth of liquid. This involved the integration of the relatively complex expression for the time dependence of the concentration and the distance from the interface. The expression for the unsteady-state absorption into a stagnant film is also given by Danckwerts (27):

$$\frac{C - C_o}{C^* - C_o} = \text{erfc} \frac{x}{2\sqrt{\mathscr{D}\theta_c}}$$ (4)

where: C = concentration at distance, x (cm), from the interface, millimoles cm^{-3}

C_o = concentration in the bulk of the liquid

C^* = saturated concentration, at the interface

θ_c = mean contact time, sec

For application to this problem if the maximum driving force is assumed, the bulk liquid concentration will be zero. The appropriate integration of equation (4) for the mass transfer rate, N_A, has been performed by Bird, Stewart, and Lightfoot (32).

$$N_A = 2 \frac{\sqrt{\mathscr{D}}}{\sqrt{\pi \theta_c}} (A) (C^* - C_o)$$ (5)

where: $A = 162 \ cm^2$

$\theta_c = 0.132 \ sec$

$$\mathscr{D} = 1.465 \ (10^{-5}) \ cm^2 \ sec^{-1}$$

$$C* = 0.0455 \ \text{millimoles} \ cm^{-3}$$

$$C_o = 0$$

N_A = average mass transfer rate for time interval θ_c, millimoles sec^{-1}

The mass transfer rate for the rolling film model as calculated from expression (5) was 0.088 millimoles per second. Again the maximum possible driving force was applied.

The actual transfer rate for run number 793 was calculated from the liquid flow rate and the CO_2 analysis at the inlet and outlet of the test section was 0.344 millimoles per second. It is of interest to note the difference in rates for the stagnant film, the rolling film, and the experimentally observed rate, 0.0063, 0.088, and 0.344 millimoles per second, respectively. It is obvious that the stagnant-film theory cannot explain the mass transfer that actually occurred. The rate calculated for the rolling film, on the other hand, was about one quarter that actually observed and was, therefore, at least of the right order of magnitude. Further, it is of interest to calculate the frequency of the surface renewal required to explain the high mass transfer rate that was experimentally observed. The frequency is the inverse of the contact time which can be solved for by using equation (5) and substituting the experi-

mentally observed mass transfer rate for N_A, the transfer rate.
It can be seen from equation (5) that the rate of transfer is
inversely proportional to the square root of the contact time,
so that to obtain a transfer rate 4 times as great would require
a contact time approximately 16 times as short. The calculated
values of contact time, and penetration depth, are, respectively,
0.0085 sec, and 0.0013 cm.

In summary, it is apparent that the rate of surface renewal
must be about 16 times as great as that accounted for by the
longitudinal motion of the interfacial film surrounding the
bubbles. Even if the estimate of the velocity of the inter-
facial film relative to the bubble was incorrect by a factor of
two or three, the rolling film model could not explain the rate
of transfer that was experimentally observed. It is, therefore,
proposed that the mechanism of transfer was the process of
surface renewal caused by turbulent eddies and mixing within
the liquid. A further argument in support of the application
of the penetration theory to bubble flow is the fact that the
dependence of the transfer rate on the liquid phase diffusivity
was found to be to the 1/2 power in accordance with the pene-
tration theory model. If the relative velocity between bubble
and fluid were very small, as might occur for very small bubbles,
it is possible to imagine a mechanism of mass transfer depending

on the complete absence of normal velocity components in the vicinity of the bubble during the residence time of bubble in the test section. This model would correspond approximately to flow past a rigid body at low Reynolds numbers and a theoretical solution for this case has been reported by Friedlander (33). This solution predicts that the transfer coefficient will be a function only of the Peclet number, with a dependence on the diffusivity to the 2/3 power. Thus, the inference of the proposed mechanism of transfer is that the transfer rate for horizontal bubble flow is largely a function of the rate of surface renewal resulting from turbulent eddies or mixing in the liquid phase. The degree of turbulence or mixing is expected to be some function of the true liquid velocity. Further, in general the transfer rate should be directly proportional to the surface area exposed to the liquid. For bubbles separated by distances equal to about one tube diameter, eddying would be promoted between the bubbles, whereas for bubbles very closely spaced (less than 3 mm) turbulent eddies for the confined spaces between them would not be expected. The dependence of the rate of transfer, therefore, must be somewhat influenced by the shape, size, and spacing of the bubbles, as well as on the actual interfacial area.

Effects of surface tension and viscosity, in addition to

that of diffusivity, can be considered in the light of the
proposed mass transfer mechanism. A variation of surface
tension should affect the size of the interfacial area, and
only indirectly, by virtue of the smaller interfacial forces,
the degree of mixing in the bulk of the liquid. One might
expect, therefore, that with liquids of lower surface tension,
longer bubbles would be produced, having comparatively larger
interfacial areas. A variation in viscosity would be expected
to greatly affect the degree of turbulence, and hence the rate
of surface renewal. It is expected that the effect of diffusi-
vity associated with changes in viscosity would be accounted
for by the usual dependence of the transfer rate for a penetra-
tion theory model, to the 1/2 power.

Proposed Mechanism for Mass Transfer in Slug Region

The pronounced difference between bubble and slug flow is
most striking. In bubble flow the interface is smooth in
appearance, wavering slowly with changing forces within the
bulk of the liquid. In slug flow the interface is very rough,
particularly in the region of the slugs themselves. Tongues of
liquid are visibly thrown out of the liquid, ripples are
extensively produced, and tiny bubbles of gas are churned
into the liquid. The speed of the motion of the interface

in the region of the slugs is far too rapid to be visually followed. For the portions of liquid between the highly agitated slugs, the rippling and agitation are greatly diminished.

The mass transfer rate in the slug flow region is generally much higher than in the bubble flow region. The transfer rate increases with gas flow rate at a constant liquid rate, typically as shown in Figure 1 (p.19). At a constant liquid rate, and for high gas rates in the slug flow region, the transfer rates are as much as 10 times as great as the maximum values obtained for bubble flow.

An accurate picture of the physical processes may be of assistance in the analysis of possible mass transfer mechanisms for slug flow. The transition between plug and slug flow is gradual. For a constant liquid flow rate, as the gas rate is increased the plug velocity also increases. The interface of each plug becomes rippled particularly near the front, the interface takes on a definite slope with the thickness or height of the plug increasing from front to rear, and the interface at the rear of the plug becomes highly agitated as if by the turbulent wake. As the gas rate is increased further, the amount of rippling increases, and the turbulence at the rear is more intense, entraining tiny bubbles which tend to circulate behind the plugs. Within the elongated plugs

small slugs or waves of liquid are propelled forward, with the
characteristic high degree of agitation at the crest. As the
gas rate is further increased, the cresting flow predominates;
however, most of the crests or slugs continue to fill the tube.
At higher gas flows still, the liquid is propelled by the gas
so rapidly that the tube contains an insufficient amount of
liquid, even at the crests, to fill its cross-section. The
turbulent crests travel along the tube at a high velocity and
at a high frequency. The quantity of liquid tends to accumu-
late at the slug crests while the amount remaining in the tube
between the slugs becomes only a small fraction of the total
amount flowing. At extremely high gas rates the liquid tends
to become more evenly distributed along the tube, annular rings,
moving in the direction of flow, begin to appear in addition to
the slugs, while the slugs increase in frequency and decrease
in size.

Some further observations about slug flow can be made.
At any instant the actual average liquid velocity is most
likely very considerably different at different positions along
the length of the tube. Similarly, at any instant at any one
cross-sectional position of the tube, the velocity of the liquid
at the interface is undoubtedly different from that of the
average at that position, especially if the position corresponds

to a crest. Because in slug flow the liquid undergoes accelera-
tion and decceleration, and because the agitation of the liquid
at the crests is so severe, it appears hopeless to attempt to
relate the condition of the liquid to a simple mean liquid
velocity component in the direction of flow. Void fraction
correlations are available, as indicated earlier, for predict-
ing average phase velocities. To successfully relate the
overall average liquid velocity to that of the interface,
or to the degree of agitation at the slug crests, would be
extremely difficult, and at the present state of knowledge,
appears impossible. However, a more qualitative approach to
mass transfer in the slug region is still available.

Mass transfer rates in the slug region compared to those
in the bubble region can easily be a factor of 10 greater. If
a surface renewal theory is assumed for the slug region similar
to the one proposed for the bubble region, some further compari-
son can be made. Although the interface is highly agitated it
is probable that the interfacial area in slug flow may be only
a factor of two or perhaps three times as great as that in the
bubble flow region. For run number 793 the estimated contact
time was 0.0085 sec and the penetration depth was 0.0013 cm.
For an increase in mass transfer rate of a factor of five, the
contact time would need to be reduced by an approximate factor

of twenty-five (assuming an interfacial area twice as great).
The order of magnitude of the contact time would then be 0.0003
sec. Such a short contact time (or even shorter) might well be
possible in the region of the slug crests. In the region
between the slugs, however, where the liquid interface is
comparable in calmness to that for bubble flow, extremely short
contact times of the order of 0.0003 seconds appear unlikely.
If transfer rates for portions of the interface between the
slugs are assumed to be comparable to those of bubble flow,
it is obvious that in the region of the slugs themselves
extremely high transfer rates would be required to account for
the high overall mass transfer rates experimentally observed.
Further, from the extremely turbulent appearance of the slug
crests, it seems entirely possible that the condition described
earlier as the "limit of turbulence" might well be reached.
For such extreme turbulence the mechanism of mass transfer by
means of a velocity component in the liquid normal to the inter-
face, as proposed by Kishinevskii (25,26), might be expected
to apply.

It is proposed that for the extreme agitation in the slug
crests themselves, the theory of transfer as proposed by
Kishinevskii applies, and that for positions in the liquid
between the slugs, the surface renewal or "penetration theory"

applies. The mass transfer rate expression according to the Kishinevskii theory is:

$$N_A = A \ (C^* - C_o) \ \bar{V}_n \tag{6}$$

where: A = interfacial area, cm^2

C^* = interfacial concentration, millimoles cm^{-3}

C_o = bulk concentration, millimoles cm^{-3}

$\bar{V}_n$ = mean velocity of liquid normal to the interface, $cm \ sec^{-1}$

For this situation, the transfer is independent of the liquid phase diffusivity. Further, it is apparent that the two transfer processes can be considered to operate in one location with the two postulated resistances occurring in parallel or in series, as discussed by Davies (34). For the model that would appear to fit the slug flow region most closely, a certain varying fraction of the interfacial area can be considered in extreme turbulence, while the remaining portion is subjected to surface renewal by eddying and mixing. The two processes would operate independently in different portions of the tube. The rate equation that would apply would be a combination of equations (5) and (6) with each equation applying to a certain fraction of the interfacial area.

It is apparent that neither the total interfacial area, nor

the portions thereof, to which the Kishinevskii theory or the penetration theory would apply, can be obtained by direct estimate or measurement. If they could be obtained, the relation between the mean surface age as well as of the mean velocity normal to the interface, and the overall mean liquid velocity in the tube would still be unknown. No direct check of the proposed mechanisms is, therefore, possible. Again, however, some significant qualitative statements concerning the effects of the various variables on the rates of absorption can be made in the light of the proposed mass transfer mechanisms.

At one liquid rate (in the slug region) with increasing gas rates, the number of slugs, and extent of agitation in them, would be expected to increase. The transfer mechanism would probably change from transfer by surface replacement only at relatively low gas rates, to that of a combination of both mechanisms at higher gas rates. The liquid phase diffusivity would have a decreasingly smaller effect on the rate of transfer, therefore, at increasing gas rates. It should be possible to compare the absorption rate curves (NTU vs V_G^o) for the CO_2-water and He-water systems, and to observe a decreasing difference between the two curves at increasing gas rates. That is, the effect of diffusivity should be diminished if the effect of the Kishinevskii theory mechanism becomes appreciable.

Further, it can be qualitatively stated that from actual observation, for identical gas rates, the degree of agitation in slug flow appeared to be noticeably increased by increases in the rate of liquid flow. Following the same line of argument as previously, the difference between the CO_2-water and He-water absorption rate curves should be smallest, therefore, for the highest liquid rate. That is, the effect of diffusivity would be least for the liquid flow rate at which the highest degree of turbulence was achieved. Again, if the mechanisms proposed do in fact apply, the experimental data should display the corresponding qualitative characteristics.

The effect of the surface tension on the absorption rates is qualitatively considered small. The kinetic energy of the liquid would most likely surpass in magnitude the interfacial forces during turbulence. The effect of interfacial tension would be expected to become less significant when the intensity of the turbulence increased. The effect of viscosity on the other hand would be expected to increase with an increase in turbulence because of the higher shear forces involved. The magnitude, and direction of such effects can be adequately determined only by experimentation.

One assumption which was made for the bubble region of flow, and thus far tacitly assumed for the slug region, may

appear to be no longer valid. It is that at the same gas

volumetric flow rates, the liquid turbulence or interfacial

area is unaffected by gas density. For much of the slug region,

the absorption tube as completely filled by consecutive slug

crests, and, as a result, portions of gas were trapped in the

tube as elongated, turbulent "plugs", by liquid completely

filling the tube at either end. For this situation, as for

the bubble region, it would appear that kinetic energy effects

in the gas phase would not be of appreciable consequence on

the interfacial conditions, compared to those in the liquid

phase. For higher gas flow rates, when annular flow was

approached, and the top portion of the tube was completely

void of liquid, the mean gas velocity would, of necessity,

be considerably greater than that of the liquid to produce

the same rate of shear at the tube wall. For this latter

condition, gas kinetic energy effects would most likely pro-

duce an increasing gas-liquid interaction (such as increases

in interfacial area, droplet entrainment, or emulsification),

for increases in gas density. For the conditions of this work,

however, the assumption that the interfacial conditions are

independent of the gas density appears to be valid for most

of the slug region of flow.

The possibility of variations in interfacial area, or other

gas-liquid interactions due to gas density for conditions of extreme turbulence, however, cannot be discounted until the Kishinevskii theory has been adequately confirmed. Conditions of such extreme turbulence as proposed by Kishinevskii may seldom be reached in any practical contacting equipment, and hence difficulty may be encountered in obtaining irrefutable experimental evidence to support or disprove his theory. Partial confirmation of the decreasing effect of diffusivity with increased turbulence is available from the reported work of Hutchinson and Sherwood (35) who found a dependence on diffusivity to the 0.25 power. Such a decreased dependence on diffusivity can be explained without the aid of the Kishinevskii theory, however, by assuming that one of the basic conditions for the use of the penetration theory becomes invalid for certain highly turbulent contacting systems. It concerns the lack of any velocity component at right-angles to the interface within the penetration depth during the period of absorption. For highly turbulent systems, if eddying or mixing occurred within the penetration depth, then the transfer rate would depend not only on the rate of unsteady-state diffusion, but also on the rate of mixing in the liquid, which would result in a decreased dependence on diffusivity, and an increased dependence on the rate of mixing for conditions of increased turbulence in the liquid.

SPECIFICATIONS AND PROPERTIES OF TEST FLUIDS

Specifications

The minimum specified purities are listed for the test fluids along with the supplier, grade, and size of purchase-lot for each.

Carbon dioxide: The CO_2 used in this research was supplied as a liquid in pressure cylinders by the Canadian Liquid Air Company and was of a commercial welding grade purity, specified at a minimum CO_2 content of 99.5 volume per cent.

Helium: The He gas was also supplied by the Canadian Liquid Air Company and was of a minimum specified purity of 99.99 volume per cent He. He was supplied as a gas in high pressure cylinders, at approximately 2200 psig, in amounts approximately 200 scf per cylinder.

Water: Vancouver city tap water was used as one of the liquids for the absorption studies.

Ethanol: The ethanol (not denatured) was purchased from the British Columbia Liquor Control Board in 10 Imperial gallon drums and specified as absolute ethanol for research use only, with a minimum purity of 99.5 volume per cent ethyl alcohol.

Ethylene glycol: The ethylene glycol was purchased as one 45 U.S. gallon lot from the Dow Chemical Company, and was of an

anti-freeze grade with a minimum purity specification of 99.5 volume per cent.

Fluid Properties, Literature Data

Except for the solubility of CO_2 in ethylene glycol, the viscosity, and the surface tension of ethylene glycol, all the fluid properties used in the calculations of the results were obtained from published sources. The density of the gases, CO_2 and He, was required for the calculation of the gas superficial velocities in the absorption tubes. The perfect gas law was used in obtaining the correct volumetric flow at the absorption conditions. Since the pressures used were close to atmospheric and the temperature close to room temperature, no significant deviation from perfect gas behaviour was expected. The presence of liquid vapour in the gas phase was accounted for by applying Dalton's law. The liquid properties and their sources are discussed further under separate headings.

Solubility

The solubility data for CO_2 in water and ethanol were obtained from the most recent review of solubilities by Linke (36). The solubilities expressed as the Bunsen coefficients are given in Table 1. The solubility data for He and water

were obtained from the Handbook of Chemistry and Physics (37).
The He solubilities expressed as the Henry's law constants are
listed in Table 2.

Viscosity and Density

The viscosity data for water and ethanol, given in Table 3,
were obtained from the Handbook of Chemistry and Physics (38).
The densities of water, ethanol, and ethylene glycol were also
obtained from the Handbook of Chemistry and Physics (39) and
these values are also listed in Table 3.

Surface Tension

Interfacial tension is the consequence of intermolecular
forces between two immiscible fluids. When one of the fluids is
a gas and the other a liquid, a change in the nature of the gas
usually does not appreciably change the interfacial tension.
Hence, for gas-liquid systems, the interfacial tension is fre-
quently referred to as surface tension and usually treated as a
property of the liquid only (40). Surface tension data avail-
able with saturated air, therefore, are considered to apply
equally well for either CO_2 or He as the gas. Surface tension
data for the air-water and air-ethanol systems were obtained
from Perry (41) and are listed in Table 4.

Liquid Phase Diffusivity

The accurate experimental determination of gas-liquid diffusion coefficients is extremely difficult and is undoubtedly subject to greater errors than the measurement of any of the other physical properties. Lack of adequate precautions to completely eliminate all sources of motion within the liquid in the diffusion path during the measurement of the diffusivities is frequently the cause of the resulting measurements being too high. The diffusivity for CO_2 in water was obtained from a reference by Davidson and Cullen in which a number of independent evaluations were compared (42). The value experimentally obtained, and used in this research, compared favourably with other values reported. The CO_2-ethanol diffusion coefficient was obtained from the International Critical Tables (43). The diffusivity of CO_2 in ethylene glycol reported by Calderbank (44) was used in this research. The diffusivity of He in water as obtained by Gertz and Loeschcke (45) was used because it was the lowest value reported. A second reason for its use was that a value calculated by means of the Wilke correlation (46) checked with the Gertz and Loeschcke value within a tolerable limit. The Wilke correlation, particularly for water, is considered by Reid and Sherwood (47) to give diffusivities

accurate to within 10 per cent. Diffusivity values were extra-
polated to temperatures other than at which they were obtained
by means of the Nernst-Einstein equation (48) when required.
The values of diffusivity as reported in the literature, extra-
polated values, and sources are given in Table 5.

Fluid Properties, Experimental Data for Ethylene Glycol

Solubility of CO_2

In his experiments with CO_2 and ethylene glycol Calderbank
(44) reported the solubility at 25^oC. Since in this research
absorption studies were performed at 15^oC and 30^oC, solubility
data at these temperatures were required. The solubility was
determined by bubbling CO_2 for a prolonged period of time
through the ethylene glycol which was maintained at a constant
temperature. Samples of the glycol were analyzed for CO_2 by
injecting known volumes into standardized excess alkali, and
back-titrating with standard hydrochloric acid.

A 2000-ml 3-necked round flask was used for the solubility
determinations. Approximately 1000 ml of glycol was poured into
the flask which was then immersed in a water bath whose tempera-
ture was controlled by a mercury thermoregulator to within
0.05^oC. A fritted-glass bubbler as well as a thermometer were

supported by a rubber stopper in the centre opening of the flask. A second opening was equipped with a glass tube and tygon connector for withdrawing samples into a pipette. The third opening was left open so that CO_2 rising through the glycol would be at essentially atmospheric pressure in the flask. Bubbling was continued for at least three hours before samples were withdrawn for analysis. Samples were taken by means of a 100-ml pipette, and were withdrawn by raising the flask out of the bath momentarily and draining the glycol into the pipette. A volume of glycol (about 50 ml) was flushed through the pipette prior to disconnecting the pipette from the flask. Exactly 100 ml of glycol was drained from the pipette into an erlenmeyer flask containing the excess caustic. The 100-ml samples were injected into 50 ml of 0.1 N caustic and back titrated with 0.1 N hydrochloric acid. This analysis was identical to that used for the regular absorption samples and is discussed in more detail in a later section.

The results of the solubility determinations are shown in Table 6.

Surface Tension

The surface tension of ethylene glycol in contact with saturated air was measured by means of a duNouy tensiometer

(model number 10402), manufactured by the Central Scientific

Company of Chicago. The procedure described for gas-liquid sur-

face tension measurements in the tensiometer technical bulletin

(49) was closely followed. The tensiometer was calibrated using

laboratory balance weights. Surface tension readings were taken

at a number of ethylene glycol temperatures and extrapolated to

15°C and 30°C. The calibration measurements and surface tension

readings are listed in Table 7. Graphs of the tensiometer

calibration, as well as the surface tension measurements taken

at various temperatures, are shown in Figure 3.

Viscosity

The viscosity of pure ethylene glycol was measured at the

two temperatures, 15°C and 30°C. In addition, the viscosities

at 15°C of glycol-water solutions containing increasing quanti-

ties of water were determined. The viscosity-water content

relationship was used as a test for the contamination of the

glycol with water and is discussed in more detail in a later

section. The viscosities were measured by Cannon-Fenske type

viscometers, following the procedure recommended in the ASTM

report D445-53T. The calibrations of the viscometers, C-8

and C-3, as obtained by De Verteuil(50), were accepted. The

viscosimeter, H-69, was calibrated by comparison with the
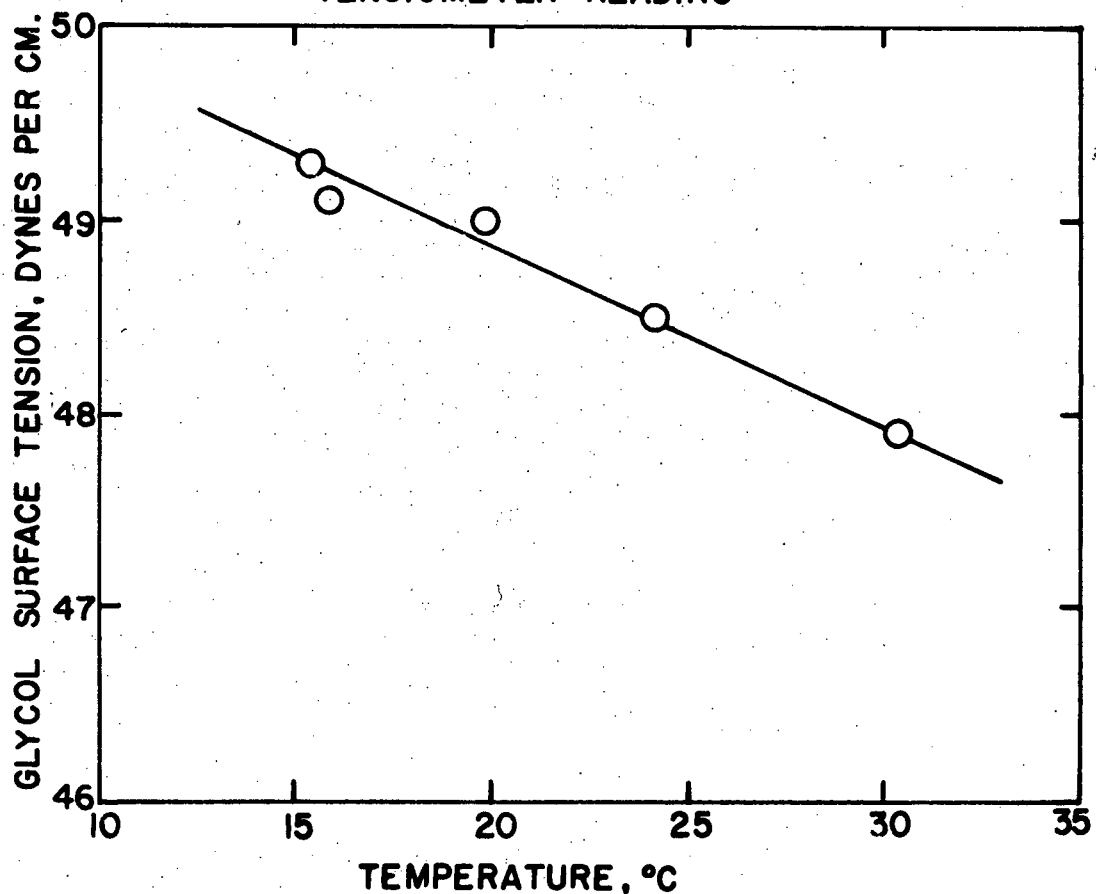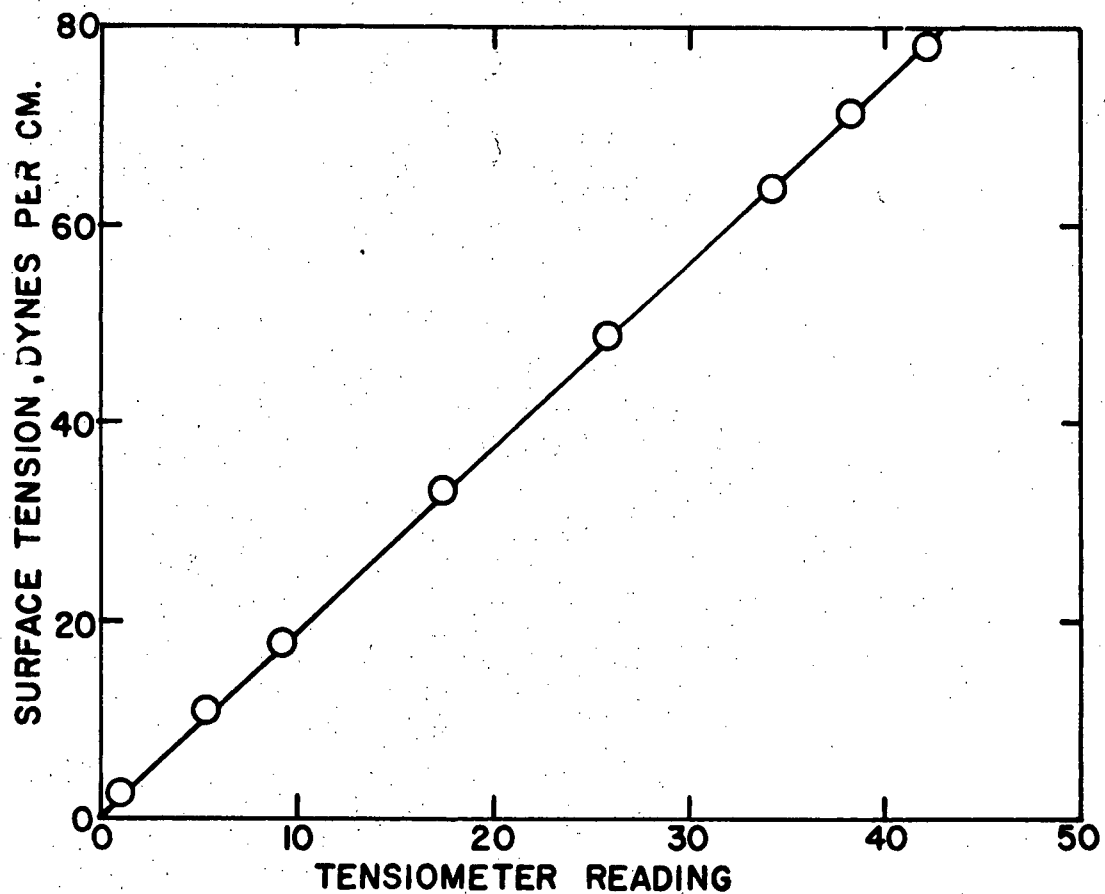
Figure 3. Graphs of Tensiometer Calibration,
Surface Tension Measurements for Ethylene Glycol

viscosity readings obtained with viscometers C-8, C-3, and H-69.

The data for all the viscosity measurements are shown in Table 8.

TABLE 1

SOLUBILITIES OF CO_2 IN WATER AND ETHANOL

Data from Linke (36)

(A) CO_2-Water

Temperature, $^\circ$C	β, Bunsen coefficient
5	1.424
5.3	1.41 (a)
10	1.194
15	1.019
20	0.878
25	0.759
30	0.664
40	0.530
45	0.480

(B) CO_2-Ethanol

5	3.899
10	3.510
13.5	3.280 (a)
15	3.194
20	2.938

(a) interpolated values

β = ml CO_2 (0°C, 760 mm) dissolved in 1 ml liquid at a
CO_2 partial pressure of 760 mm

TABLE 2

SOLUBILITY OF He IN WATER

Data from the Handbook of Chemistry and Physics (37)

Temperature, $^\circ$C	K (10^7)
0	10.0
10	10.5
15	10.71 (a)
20	10.9
30	11.1
40	10.9
50	10.5

(a) interpolated value

K = Henry's law constant

$K = \dfrac{p}{x}$

p = partial pressure in mm of mercury

x = mole fraction in liquid

TABLE 3

VISCOSITY OF WATER AND ETHANOL

Data from the Handbook of Chemistry and Physics (38)

(A) Water

Temperature, $^{\circ}$C	Viscosity, cps	Density, gm cm^{-3}
0	1.792	
5	1.519	0.9999
10	1.308	
15	1.140	0.9991
20	1.005	
25	0.894	
30	0.801	0.9957
45	0.599	0.9903
50	0.549	

(B) Ethanol

0	1.773	
10	1.466	0.7979
13.5	1.360 (a)	0.7949
20	1.200	0.7895
30	1.003	

(a) interpolated

TABLE 4

SURFACE TENSION OF WATER AND ETHANOL IN CONTACT WITH SATURATED AIR

Data from Perry (40)

(A) Water

Temperature, $^{\circ}$C	Surface tension, dynes cm^{-1}	
0	75.6	
5.3	75.1	(a)
15	73.5	(a)
20	72.8	
30	71.2	(a)
40	69.6	
45	68.8	(a)
60	66.2	

(B) Ethanol

0	24.1	
13.5	23.4	(a)
20	22.3	
40	20.6	
60	19.0	

(a) interpolated values

TABLE 5

LIQUID PHASE DIFFUSION COEFFICIENTS

(A) CO_2-Water (42)

Temperature, $^{\circ}C$	Diffusivity, times (10^5) cm^2 sec^{-1}	
5.3	1.072	(a)
15.0	1.465	(a)
25	1.92	
30	2.190	(a)
45	3.08	(a)

(B) CO_2-Ethanol (43)

13.5	2.95	(a)
17	3.20	

(C) CO_2-Ethylene glycol (44)

15	0.142	(a)
25	0.229	
30	0.285	(a)

(D) He-Water (45)

15	3.69	(a)
15	3.02	(b)
37	6.30	

(a) extrapolated using Nernst-Einstein equation (47)

(b) calculated using Wilke correlation (46)

TABLE 6

SOLUBILITY OF CO_2 IN ETHYLENE GLYCOL

(A) Temperature, $15.0^{O}C$

Barometric pressure: 758.1 mm mercury

Sample size: 100 ml

Partial pressure less than 0.1 mm mercury

Volume 0.1 N NaOH	Volume 0.1 N HCl	Solubility, millimoles per litre
50.0	2.80	47.20
50.0	2.90	47.10
50.0	2.80	47.20
50.0	2.90	47.10
	mean =	47.15

Solubility at $15.0^{O}C$, 760 mm = 47.27 millimoles per litre

(B) Temperature, $30.0^{O}C$

Barometric pressure: 758.1 mm mercury

Sample size: 100 ml

Partial pressure less than 0.1 mm mercury

38.0	1.95	36.05
38.0	2.10	35.90
38.0	2.00	36.00
38.0	2.05	35.95
	mean =	35.97

Solubility at $30.0^{O}C$, 760 mm = 36.07 millimoles per litre

(C) Solubility by Calderbank at $25.0^{O}C$, 760 mm = 39.7 millimoles per litre.

TABLE 7

SURFACE TENSION OF ETHYLENE GLYCOL

(A)   Calibration of Tensiometer

Force on ring, gm	Tensiometer Reading	Surface tension, dynes cm^{-1}
31	1.1	2.4
131	5.2	10.1
231	9.2	17.8
431	17.3	33.2
631	25.8	48.6
831	34.1	64.0
931	38.2	71.7
1031	42.5	79.4

(B)   Surface Tension Measurements

Temperature, ^{o}C	Tensiometer Reading	Surface tension, dynes cm^{-1}	
15.4	26.3	49.3	
19.7	26.1	49.0	
24.2	25.9	48.5	
24.2	25.9	48.5	
15.8	26.2	49.1	
30.4	25.6	47.9	
15.0		49.3	(a)
30.0		47.9	(a)

(a)   Read from graph of surface tension and temperature, Figure 3 (p.74).

TABLE 8

ETHYLENE GLYCOL VISCOSITY DETERMINATIONS

(A) Calibration of H-60 at 15.0°C

Liquid	Visco-meter	Time, minutes				Viscosity	
		(a)	(b)	(c)	mean	cs	cps
glycol	H-69	12.237	12.233	12.233	12.234		
glycol	C-3	3.605	3.608	3.602	3.605	23.636	26.47
1.0	H-69	11.780	11.782	11.777	11.780		
1.0	C-8	3.493	3.492	3.496	3.494	22.770	25.50

Calibration constant H-69, from C-3: 1.9320
                                      from C-8: 1.9329 mean: 1.9324

(B) Viscosity of Glycol at 15.0°C

glycol	C-3	3.605	3.608	3.602	3.605	23.636	26.47

(C) Viscosity of Glycol at 30°C

glycol	H-69	6.477	6.476	6.477	6.4767	12.516	13.90

(D) Viscosity of Water-Glycol solutions at 15.0°C

0.05	C-8	3.618	3.621	3.620	3.620	23.59	26.42
0.15	C-3	3.587	3.588	3.588	3.588	23.50	26.32
0.50	C-3	3.542	3.543	3.545	3.544	23.22	26.01
0.75	C-8	3.522	3.530	3.529	3.527	22.98	25.74
1.5	C-3	3.411	3.412	3.416	3.413	22.36	25.04
2.0	C-8	3.370	3.366	3.369	3.368	21.95	24.58

Note: numbers in liquid column represent volume per cent of

water in ethylene glycol.

Calibration constants: C-3, 6.551, cs min^{-1}

C-8, 6.516, cs min^{-1}

H-69, 1.932, cs min^{-1}

APPARATUS

An apparatus was designed and built for continuously con-
tacting various gases and liquids in a horizontal, tubular,
cocurrent absorber. A circulating system was incorporated
for the test liquids, thereby permitting the storage and reuse
of any one of the liquids. Provision was made for the contin-
uous stripping of the absorbed gas, for the cooling of the
liquid to a controlled temperature, and for measuring the flow
rate by means of one of two rotameters. The gases used in all
the experiments, He and CO_2, were supplied in the compressed,
and liquified, forms respectively, from high pressure cylinders.
Provision was also made to measure the gas flow rate, again
with one of two rotameters, to saturate the gas with the test
liquid, and to cool it to a controlled temperature prior to
contacting in the absorption tube. After contacting, the
excess gas was vented into the room or to the building exhaust
system.

A detailed flow diagram of the apparatus is shown in
Figure 4. In the description of the apparatus following,
reference is made to equipment numbers shown on this diagram,
and to drawings of individual pieces of equipment included in
Appendix I.
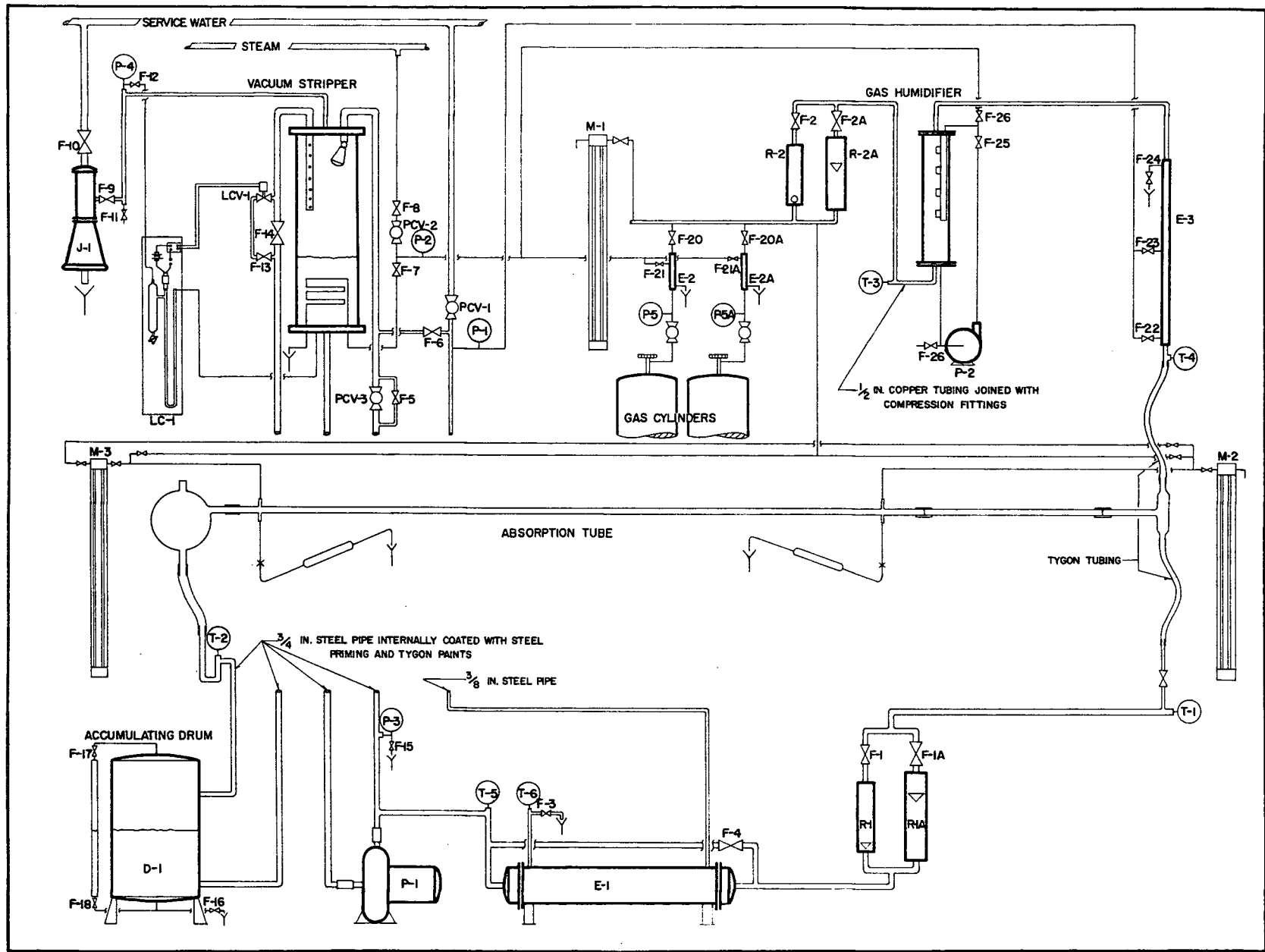
Figure 4.   Process Flow Diagram of Apparatus

A detailed list of specifications for each item of equipment is also included in Appendix I.

Liquid System

The liquid processing apparatus was used for the stripping of gas absorbed in the test section, as well as for the measurement and control of the liquid flow rate and temperature. The apparatus and its function will be briefly described by following an imaginary "packet" of liquid from the exit of the absorbed test section through the cycle that was normally followed by the liquid, back to the entrance of the test section.

After passing through the test section, the gas and liquid phases were separated in a glass cyclone. From there the liquid was allowed to drain by gravity to an accumulating drum, D-1. The liquid temperature was measured by a thermometer, T-2, mounted in the drain line. The partially saturated liquid flowed from the accumulating drum to the stripper because of the vacuum in the latter vessel. The rate of flow was automatically controlled by an on-off level-control device which maintained a constant liquid level in the stripper. The level controller, LC-1, consisted of a mercury-filled glass manometer with one leg of the manometer being completely filled with liquid

and forming a continuous column of liquid from the top of the mercury to the top of the liquid in the stripper. The other leg was open to the vapour at the top of the stripper. In this way, the mercury in the manometer always assumed a level corresponding to the liquid level in the stripper, regardless of the pressure (or vacuum) in that vessel. The side of the manometer exposed to the vapour contained two wire contacts, one immersed in the mercury, and the other placed in such a position that contact with the mercury would just be made when the desired liquid level was obtained. The two wires were connected in series with two dry cells, a switch, and the low voltage side of a relay. The relay in turn was used to operate the solenoid valve, LCV-1, which controlled the flow of partially saturated liquid into the vacuum stripper.

A drawing of the vacuum stripper showing internal details is included in Figure I-1 of Appendix I. The vacuum stripper was supported at an elevation of about 7 feet above the intake of the adjoining circulating pump, P-1, to ensure that a sufficient liquid head was provided for good operation of the pump. The stripper vacuum was maintained by means of a large-sized water ejector, J-1, while the liquid in the lower portion of the vessel was heated by a steam coil. By means of the centrifugal pump, P-1, the liquid was circulated at a rate of about

6 gpm from the bottom of the stripper to the top and through a large spray-nozzle. The circulating rate was adjusted by means of the pressure regulator, PCV-1, which also maintained constant the pressure of a side-stream of the liquid withdrawn to the test section. During the degasification of the liquid, the rate of boiling was controlled by adjusting the steam pressure regulator, PCV-2. The resulting temperature of the liquid varied from about $18^{\circ}C$ to $55^{\circ}C$ depending on the amount of saturation, the liquid throughput, and on which of the three liquids, ethanol, water, or glycol, was being processed. The pressure likewise varied widely, for the same reasons, from about 20 to 29 inches of mercury vacuum, as did the degree of saturation of the liquid leaving the vacuum stripper. The amount of gas remaining in the liquid after stripping varied anywhere from 2 to 40 per cent of the saturation value based on the absorption conditions.

A shell-and-tube heat exchanger, E-1, was provided for cooling the degassed liquid prior to its use in the test section. For a constant liquid flow rate through the test section, the temperature of the liquid was controlled within $\pm 0.3^{\circ}C$ of the absorption test temperature. This control was achieved by accurately regulating the flow of the cooling water through the exchanger, by adjusting the supply pressure

of the cooling water at the pressure regulator, PCV-1, as well as by throttling the flow of cooling water by means of the valve, F-3. In addition an exchanger by-pass valve, F-4, was provided for occasions when the heat duty was unusually low. For maximum cooling, to obtain temperatures of process liquid approaching cooling water temperatures, or while cooling the viscous ethylene glycol, it was necessary to replace the water effluent valve, F-3, with one of a larger size.

Two calibrated rotameters, R-1, and R-1A, with slightly overlapping ranges, were used to measure the flow rate of the degassed liquid to the absorption tube. When a constant temperature of the degassed liquid had been reached, no difficulty was encountered in also maintaining a constant flow through one or the other of the liquid rotameters.

Gas System

The function of the gas processing apparatus was to supply a continuous stream of gas, at a known flow rate, saturated with the vapour of the test liquid, and at the temperature at which the absorption was to take place. When CO_2 was the test gas, two CO_2 cylinders were required to supply high gas flow rates (up to 220 cfh) because of the limitation on the amount of gas that could be continuously

withdrawn from one cylinder. Without special precautions, at withdrawal rates from a single cylinder exceeding 50 cfh, icing of the pressure regulator and adjacent equipment would occur. For flow rates from both cylinders exceeding a total of 100 cfh, an infra-red heat lamp was directed towards the pressure regulators. In addition, small steam-heated double-pipe exchangers mounted adjacent to the pressure regulators were used to ensure that any CO_2 leaving the cylinders in the liquid, form, would be completely vaporized. No similar problem was encountered with the He gas which could be withdrawn at all the required flow rates from a single cylinder.

The dry gas from the cylinders was metered prior to humidification. Two calibrated rotameters, R-2, and R-2A, were used to measure the gas flow rates, one for flow rates from about 1.5 to 20 cfh of the CO_2 and the other for flow rates from about 20 to 220 cfh. The same rotameters were used for He. Pressure measurements were obtained at the gas supply header by means of a 30-inch mercury-filled Merian manometer, P-1, and the corresponding temperature measurements, downstream of the rotameter by a thermometer, T-2, mounted in the piping.

The gas was saturated with the liquid with which it was to be contacted, in a two stage process. The gas was first partially saturated in a humidifier at a temperature above that

used for the experimental runs. The partially saturated gas
was subsequently cooled in a double-pipe exchanger, E-3, to
the temperature of the experimental runs. At this latter
temperature the gas was fully saturated at all times as evi-
denced by the presence of droplets of liquid in the gas flowing
into the entrance tee. In this way, saturation was readily
attained for all gas flow rates, and the small amount of liquid
usually condensed during cooling added only negligibly to the
total liquid flow in the test section.

A detailed drawing of the gas humidifier is shown in
Figure I-2 of the Appendix I. The humidifier consisted of a
2-inch diameter pyrex glass column 24 inches long with provi-
sion for circulating liquid from the bottom through a series
of four spray nozzles into the top portion of the column.
The gas was bubbled through the liquid in the bottom and then
through the spray from the four nozzles. Sufficient heat was
normally supplied by the circulating pump, P-2, to raise the
temperature of the liquid somewhat above room temperature for
all the gas flow rates. A steam line was provided for inject-
ing live steam into the humidifier for the series of runs
using CO_2 and water at temperatures of $30^{\circ}C$ and $45^{\circ}C$. The
flow rate of steam was controlled by a small globe valve, F-24,
at a rate sufficient to saturate the gas.

The amount of cooling of the partially saturated gas to be performed in the exchanger, E-3, was determined from the gas outlet temperature as measured by the thermometer, T-4. Gross changes in the cooling duty were accomplished by closing and opening the appropriate valves, F-22 and F-23, and hence using half of the available heat exchange area or all of it as required. Finer temperature control was achieved by adjusting the cooling water valve, F-24.

Absorption Tubes

The gas-liquid contactors employed in this research consisted of glass tubes mounted horizontally with provisions for measuring the pressure and concentration at two locations along the tube near the entrance and exit. The combination of one standard type of entrance, the horizontal tee, and an absorption tube, 1.757 cm ID, was employed in the majority of the experimental runs. The dimensions of the entrance section for the 1.757 cm tube were used as a basis for constructing dimensionally similar entrance tees for the smaller (1.228 cm) and larger (2.504 cm) tubes which were used with the CO_2-water system in determining the effect of tube diameter. In a limited series of experiments three other tube entrances, having widely differing characteristics, were used with the

1.757 cm tube to determine qualitatively the effect of entrance type.

In addition to entrance type, the entrance length which is required for the development of a definite flow pattern is another important consideration of tubular flow. The entrance length in the case of single-phase flow is generally given by a number of pipe diameters, which in turn is some function of the Reynolds number. In the case of two-phase flow the dependence on some modified Reynolds number or any other parameter has not yet been established. On the basis of visual observations, the entrance length was fixed at 12.9 inches for the initial series of experimental runs, and later increased to 31.3 inches for the majority of the runs. In all the absorption measurements made, little or no quantitative difference was found between the shorter and longer entrance sections. For some test conditions, however, the shorter length seemed, on visual inspection, to be barely adequate for the clear development of the flow patterns. Hence, the longer entrance length was used for most tests.

A typical test section with its associated equipment is shown in Figure 5. Also in Figure 5 are shown the dimensions of all the tubes and entrance types investigated in this research.

GLASS ABSORPTION TUBE AND ASSOCIATED EQUIPMENT

GAS INLET

ENTRANCE SECTION   TEST SECTION   OUTLET CYCLONE

A
D
B
C
INLET PRESSURE POINT   OUTLET PRESSURE POINT
F
E
G
TYGON SLEEVES
4 NIPPLES 6 MM. NOMINAL O.D. TUBING, 1¼ INCHES LONG
INLET SAMPLE LOCATION   OUTLET SAMPLE LOCATION
H

LIQUID INLET   TYGON TUBING
RUBBER HOSE
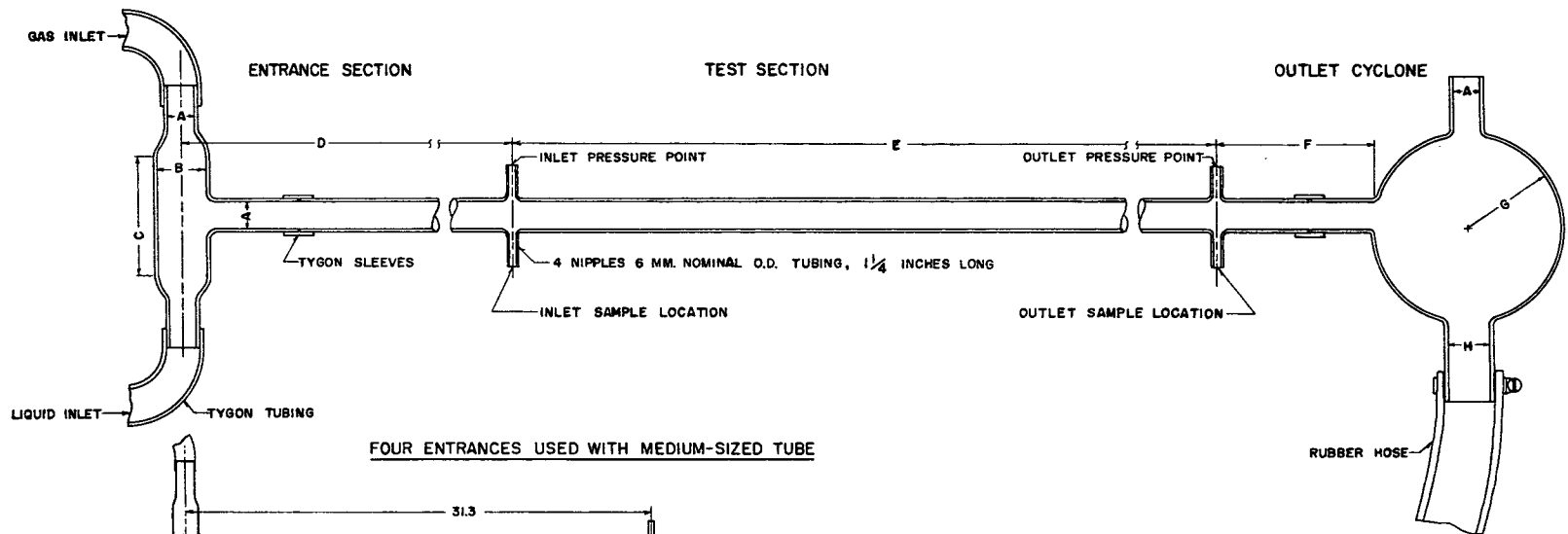
FOUR ENTRANCES USED WITH MEDIUM-SIZED TUBE

31.3

REGULAR ENTRANCE AS SHOWN ABOVE

31.3

ENTRANCE TEE AND TUBE SAME INTERNAL DIAMETER

12 MM. NOMINAL O.D.
6   31.3

LIQUID THROUGH RUN OF TEE

2.3

6   31.3

RUBBER SLEEVE
12 MM. NOMINAL O.D.   6 MM. NOMINAL O.D.   CONCENTRIC GAS ENTRANCE
2.3
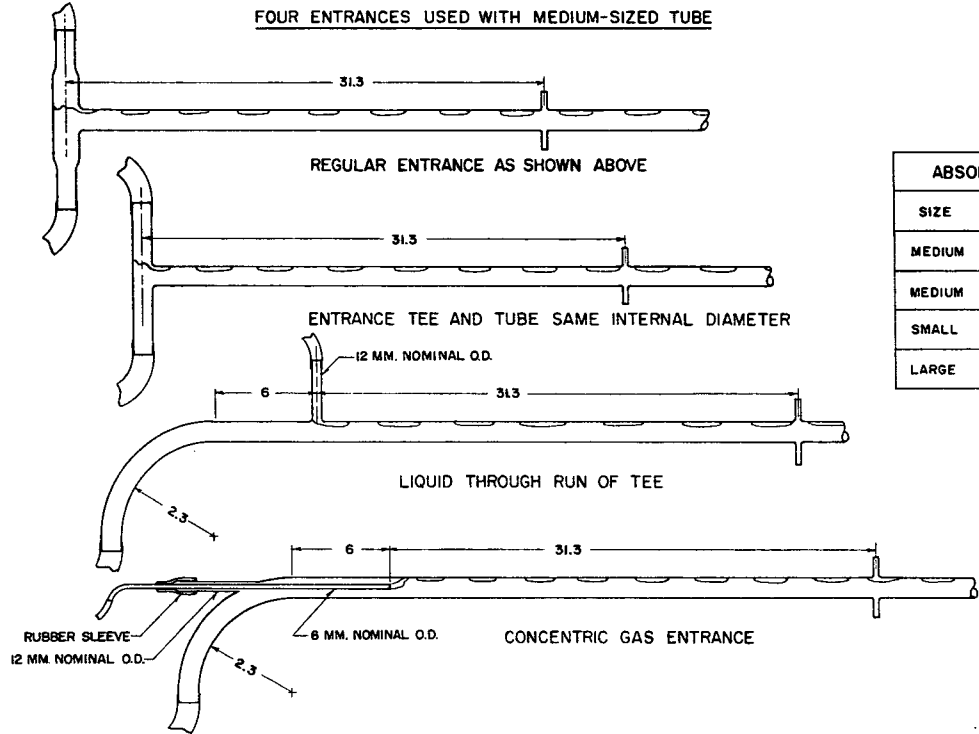
ABSORPTION TUBE DIMENSIONS, INCHES								
SIZE	A	B	C	D	E	F	G	H
MEDIUM	0.692 1.757 CM.	1.20	3.8	12.9	92.3	4.1	2.44	1.07
MEDIUM	0.692 1.757 CM.	1.20	3.8	31.3	92.3	4.1	2.44	1.07
SMALL	0.483 1.226 CM.	0.81	3.2	31.3	92.3	4.6	1.82	0.63
LARGE	0.986 2.504 CM.	1.61	5.4	31.3	92.3	5.8	3.10	1.31

NOTE: (1) ALL DIMENSIONS NOT TO SCALE
(2) DIMENSIONS IN INCHES UNLESS OTHERWISE STATED

Figure 5.   Dimensions of Absorption Tubes and Entrances Used

Since the absorption tubes played a key role in this work the construction, mounting, and related procedures will be described in some detail. Each absorption tube was constructed from two sections of pyrex glass tube both having the same internal diameter when measured by callipers, and a length of approximately 4 feet. After the two sections had been joined by glass blowing, glass nipples were installed diametrically opposite to one another at two positions 92.25 inches apart along the tube, corresponding to inlet and outlet sampling locations. The average internal diameter for each absorption tube was subsequently obtained to a high degree of accuracy by measuring the internal volume of a portion of the tube. One end of the tube was sealed with a cork, the sampling and pressure nipples were carefully sealed with plasticine, and water from a volumetric flask was poured into the tube. The height of the column of water with the tube in the vertical position, along with the known volume, was used to calculate the average internal diameter.

The entrance tees were blown from standard sizes of pyrex glass tubing, while the outlet cyclone separators were blown from round-bottomed pyrex flasks of a suitable size. The portions of entrance tee and outlet cyclone directly adjoining the absorption tubes were carefully matched in size, in each

case, to that of the absorption tube itself.

In preparation for a series of experimental runs one of the absorption tubes, as well as the associated entrance tee and outlet cyclone, was supported on a metal framework by means of laboratory clamps. The sections of the entrance tee, absorption tube, and outlet cyclone were butted together and held by means of tightly-fitting tygon sleeves. The gas and liquid supply lines were connected to the entrance tee by tygon tubing. The outlet tube of the cyclone was connected to the liquid drain line by means of a rubber hose held in place by hose-clamps. Precautions were taken to ensure that the absorption tube was mounted horizontally and that the entrance and exit sections were properly aligned. It was estimated that the maximum deviation from a horizontal position was less than 0.1 inch in the full length of the tube of over 100 inches.

When the absorption tube was in operation, the liquid phase was sampled at the entrance and outlet sample locations by means of the sampling nipples provided. A detailed description of the sampling procedure is given in the section on Sampling and Analysis. The pressure corresponding to the sampling locations was obtained in the gas phase at the top of the absorption tube by means of two 30-inch Merian manometers, M-2 and M-3. The manometers were filled with water,

carbon tetrachloride, or mercury, depending on the range of pressures to be measured. The glass pressure nipples were connected to the manometers with transparent tygon tubing, so that any liquid carried into the tubing could be readily observed. A gas supply line and valve connected to each manometer line permitted a small amount of gas to be passed through the line and into the absorption tube prior to taking a pressure reading. The gas used for this purpose was the same as that used in the absorption experiment, hence it did not constitute an impurity. The flow was always small and infrequent, hence it added to the measured gas flow rate in the absorption only negligible. The manometers were also provided with small globe valves for damping extreme pressure fluctuations. Especially during slug flow, pressure fluctuations were of such a magnitude that, without damping, suitable pressure measurements could not be taken. The test section inlet pressure was measured relative to the atmospheric pressure in all the experiments. For some experiments the test section outlet pressure was similarly measured. In most runs, however, the second manometer was used to measure the pressure drop in the test section.

Materials of Construction

As indicated in Figure 4 (p.85), all of the interconnecting

liquid flow lines were constructed of standard steel pipe,

coated on the inside for added protection against corrosion.

A coating was also applied to all the other steel surfaces ex-

posed to the circulating liquid including the casing of the

pump, P-1, the heads of the exchanger, E-1, and the liquid rota-

meter entrance and exit blocks. For an initial series of experi-

mental runs with CO_2 and water, however, the steel surfaces were

exposed to the dilute carbonic acid solutions without the

internal protective coating. It was found that when a single

charge of water was circulated continuously in the equipment

for a period of about 7 hours, ferric ion was detectable in the

circulating liquid. Small amounts of hydroxide precipitate

were observed when samples of the liquid were injected into

dilute caustic solutions. Since the equipment was to be used

with ethanol and ethylene glycol, liquids which could not be

replaced daily for economic reasons, it was necessary to prevent

the contamination of these liquids. All the appropriate piping

and liquid processing equipment was disassembled and subjected

to a coating procedure. The surfaces were washed with soap and

water to remove any oily film, and scraped free of rust where

necessary. The cleaned surfaces were then dried and coated with a lead-based metal primer. After the primer-coat had been thoroughly dried, tygon paint, diluted with acetone to a suitable consistency, was applied, providing a second protective coating. In this way, the steel surfaces were protected by a smooth semi-flexible resistant coating. No significant deterioration of the protective coating was observed after repeated service of the equipment for a period of time in excess of one year.

Several of the initial runs with CO_2 and water were duplicated after the liquid processing equipment had been coated, and the results indicated that the presence of a small amount of ferric ion in the water did not significantly affect its absorption characteristics.

The remaining portions of the liquid processing equipment were all constructed from brass, copper, and glass, all three of which were resistant to the liquid solutions used. The gas handling equipment was also constructed from these same three materials, and no corrosion problem was encountered.

PROCEDURE

The procedure for operating the experimental equipment will be described in two sections, one pertaining to the liquid system, the other to the gas system. The preparation of the gases, CO_2 and He, was essentially identical; however, the preparation of the equipment and the test procedures differed somewhat for the three liquids. The operating procedures for water, ethanol, and ethylene glycol, therefore, will be described separately.

Liquid System

For all three liquids the general procedure was to establish a constant liquid flow rate through the test section, and to maintain it for a series of experimental measurements at the varying gas flow rates. The liquid flow and temperature could be kept constant, with a minimum of adjustments to the equipment, for long periods of time and even for widely varying gas flow rates.

Water as the test liquid

With water as the test liquid, the equipment was recharged daily during a given series of runs. A flow of service water was started into the vacuum stripper, and also to the water-

cooled exchangers, E-1 and E-3. When a sufficient quantity of water appeared in the stripper, the circulating pump, P-1, was started. A water flow was then directed through the test section at approximately the rate desired for the experimental runs, anywhere from 0.6 to 4.2 gpm. The water leaving the test section was allowed to accumulate in the drum, D-1, until the drum was about one half full, equivalent to about 7 gallons in quantity. The water ejector was then put into operation, evacu-ating the stripper, and causing the water to flow from the accumulating drum back into the vacuum stripper completing the cycle. Next the fresh water supply line was shut off. Subse-quent adjustments were concerned with achieving a suitable stripping rate, and obtaining the desired liquid flow and temperature in the test section.

A flow of steam was started into the heating coil of the vacuum stripper, which was then adjusted to provide vigorous boiling, but without bumping, of the water in the stripper. The steam flow rate was adjusted by resetting the steam supply pressure as controlled by the regulator, PCV-2, to some value between 2 and 20 psig, depending on the throughput of the process water. The cooling rate of the water leaving the strip-per was regulated to obtain the desired temperature at the absorption tube entrance, usually $15.0^{\circ}C$. It was adjusted

primarily by throttling the cooling water flow out of the exchanger, E-1. When the outlet valve, F-3, was nearly open or closed, however, the pressure regulator, PCV-1, was adjusted to some value between 4 and 30 psig, as required, to maintain control of the temperature at the cooling-water flow valve, F-3. Final small adjustments were made to obtain the exact flow rate of water to the test section, prescribed for that particular series of runs, and to obtain the temperature to within $0.3^{\circ}C$. A small gas flow of approximately 2 cfh was started through the test section about 20 minutes before any measurements were to be taken. This gas flow displaced any air present in the equipment and also aided in deaerating the circulating process water itself.

At the completion of a series of experimental runs, the equipment was shut down by first breaking the vacuum in the stripper (opening valve F-11) and then stopping the circulating pump, P-1. The steam and cooling water flows were next stopped, and the equipment was completely drained by means of valves, F-15 and F-16.

Ethanol as the test liquid

Absolute ethanol was employed as the test liquid for the investigation of the effect of surface tension on the absorption

rate. Because water had been previously used in the equipment, a thorough drying of the equipment was necessary to avoid contamination of the ethanol with water. First the equipment was dismantled where necessary to ensure that all the water completely drained. The partly dismantled lines and equipment were allowed to dry overnight. Air from the building air supply was temporarily connected with rubber tubing to the long sections of piping, and these sections were dried by means of a small flow of air again left overnight. After the dried equipment was assembled, a small amount of ethanol was flushed through the equipment, then approximately 12 U.S. gallons of ethanol was charged into the accumulating drum through the cyclone at the outlet of the test section. The ethanol was allowed to drain into the accumulating drum and stored there between each successive series of experiments.

Because of its hygroscopic nature, special precautions were taken to avoid contamination of the ethanol with water from the air. When the equipment was idle, all the outlets opening directly into the room were closed. In this way contact with the room air was minimized. Also, in case of leakage in the exchanger, E-1, the supply pressure of the cooling water was always maintained at a pressure below that of the ethanol.

Frequent additions of fresh ethanol to that initially

charged were required because of the relatively high evaporation and sampling losses.

Apart from those differences already mentioned, the operation of the equipment with ethanol was very similar to that with water. The initial filling of the vacuum stripper before starting the circulating pump, was accomplished by first starting the water ejector and causing ethanol to flow from the accumulating drum to the stripper. In all other respects the method of operation was the same as for water.

Ethylene glycol as the test liquid

Ethylene glycol was used as the test liquid for determining the effect of viscosity on the absorption rate. The experimental runs using He and water were performed after CO_2 and ethanol had been processed in the equipment; therefore, as for ethanol, a thorough drying procedure was required before the glycol could be charged into the equipment without contamination.

Because ethylene glycol is highly hygroscopic, more rigid precautions were taken against its contamination with water vapour from the air, than were taken with ethanol. In addition a viscosity test was devised and used at frequent intervals during the experimentation for determining the water

content of the glycol. As measured by the test, at no time during the experimentation did the water content increase more than 0.4 volume per cent above that already present in the newly purchased material.

A 15 U.S. gallon plastic carboy was used to charge the ethylene glycol into the equipment. The carboy was equipped with a silica gel dryer for the top opening into which the dryer was installed immediately after filling. An outlet valve at the bottom of the carboy was used to drain the glycol into the equipment. A temporary platform was erected above the absorption tube outlet cyclone to support the carboy while the glycol was being charged into the cyclone. Every outlet of the equipment which could expose the glycol to the room air was subsequently protected by a silica gel air dryer. Silica gel dryers were installed at the outlet cyclone, in the accumulating drum vent line, and in the vacuum-breaking line at the valve, F-11. The dryers did not keep air out of the equipment but were effective in removing the water from the air which entered. When the equipment was being used, however, the silica gel dryer at the outlet cyclone was removed, and later reinstalled at the completion of each series of experiments. The procedure for operating the equipment using ethylene glycol as the test liquid was the same as for ethanol in all

other respects.

A series of ethylene glycol-water solutions containing from 0 to 2 per cent water by volume, was accurately prepared. The viscosities of these solutions were obtained at 15°C using Cannon-Fenske type viscosimeters, and the procedure described in a previous section. A graph showing the effect of the low concentrations of water on the viscosity of ethylene glycol solutions is shown in Figure 6, and the measured values are given in Table 8 (p.83). Because of the sensitivity of the viscosity measurements, a water content in the glycol as low as 0.1 volume per cent was detectable.

Calibration of the liquid rotameters

The liquid rotameters were calibrated by diverting the liquid flow normally passing through the absorber test section, to a 15 U.S. gallon capacity carboy mounted on a platform scale, and recording the time taken to accumulate a measured weight of liquid. A glass tee was installed by means of tygon tubing into the liquid line adjacent to the entrance of the absorption tube. A drain line for diverting the liquid into the carboy, was joined to the temporarily installed tee and provided with a screw clamp. It was therefore possible to circulate liquid through the normal flow channels, to attain
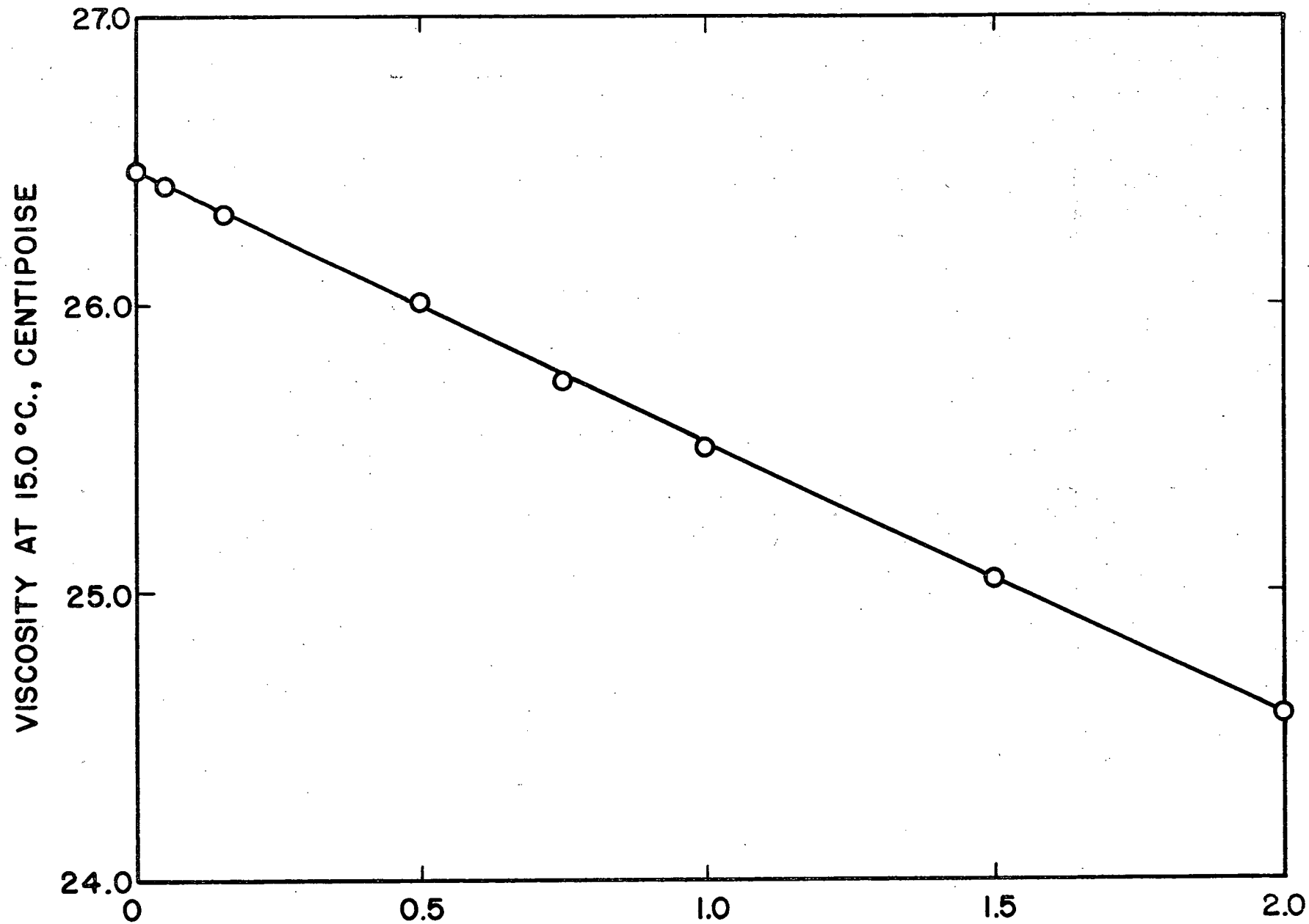
Figure 6. Viscosities of Ethylene Glycol-Water Solutions

a desired temperature and flow through the rotameters and absorp-
tion tube, and then to divert the flow from the absorption tube
to the weigh-tank for calibration. When calibrating the rota-
meters for ethanol or ethylene glycol, the contents of the car-
boy were returned into the equipment, by way of the outlet
cyclone, when the carboy became about one half full.

During calibration, the liquid temperature was maintained
to within $0.3^{\circ}C$. The scales could be read within one ounce,
and had been recently tested and approved by the Weights and
Measures Section of the Department of Trade and Commerce.
The accuracy of the calibration, therefore, appeared to be
limited primarily by the ability to read the position of the
float.

The rotameter calibrations are shown in graphical form
in Figures II-1, -2, -3 and the tabulated data appears in
Tables II-1, -2, -3 of Appendix II.

Gas System

An accuracy of within 3.0 per cent of the true gas flow
for all flow ranges from 1.5 to 220 cfh was desirable, but
difficult to achieve, because of the compressibility of the
gas. Such an acceptable accuracy with the gas rotameters was
obtained by calibrating the rotameters at specific pressure

settings, and thereafter using the rotameters at these pressures only. The control of the gas flow, as well as the humidification of the gas, were relatively simple. The measurement of the pressure at the entrance and exit of the test section, however, was complicated by the extreme pressure fluctuations which occurred during plug and slug flows.

Calibrations of the gas rotameters

The gas rotameter, R-2, for use with CO_2, and covering a flow range from approximately 1.5 to 20 cfh at room conditions, was calibrated using a wet test meter. The wet test meter, manufactured by the Precision Scientific Company of Chicago, had a maximum capacity of 50 cfh and a rated accuracy in the range used, of 0.5 per cent. The rotameter was calibrated at three pressures, 4, 8, and 12 inches of mercury above atmospheric pressure. This rotameter, when calibrated in the same way for He, gave a range from 1.5 to 50 cfh at room conditions, at pressures of 4, 12, and 24 inches of mercury.

The calibration procedure consisted of temporarily diverting the flow of gas from the absorption tube entrance through the wet test meter. The time taken for a suitable volume of gas to flow through the meter as well as the rotameter pressure, temperature, and float position were recorded. A particular gas

flow rate was obtained by alternately adjusting the gas flow

valve, F-2, and the gas supply pressure to give the desired

rotameter pressure as read by the manometer, M-1, and the

desired rotameter float position. The gas temperature at the

rotameter was measured by the thermometer, T-3, and remained

in the range from $18^{\circ}C$ to $25^{\circ}C$ for the calibration measurements.

The gas rotameter, R-2A, was calibrated for both CO_2 and

He by means of a large dry gas displacement meter. The

displacement meter, meter number A65630, was manufactured by

the Canadian Meter Company of Hamilton, Canada, and had a

maximum rated capacity of 900 cfh. The rotameter, R-2A, was

calibrated using CO_2 for pressures of 4, 8, 12, 16, and 24

inches of mercury above atmospheric pressure, and in the approxi-

mate range from 20 to 220 cfh. The corresponding calibration

pressures for He were 4, 12, and 24 inches of mercury, and the

approximate range from 30 to 250 cfh. The procedure for cali-

bration using the dry gas meter was identical to that using

the wet test meter. The calculations associated with the cali-

bration measurements, and the resulting calibration graphs for

CO_2 and He are given in Appendix II.

The calibrations for the gas rotameters, and all subse-

quent gas flow measurements, were made in volumetric units,

cubic feet per hour, of dry gas at $15^{\circ}C$ and 756 mm of mercury

absolute pressure. Appropriate corrections for temperature,

pressure, liquid vapour pressure, as well as for the quantity

of gas absorbed by the liquid, were made when the true volume-

tric flow rates at the entrance and exit of the test section

were required. The calculations involved are discussed in

more detail in the chapter on the Treatment of Data.

Gas flow measurement and control

The procedure for obtaining a particular gas flow rate,

as for example 18 cfh of CO_2 (at $15^{\circ}C$ and 756 mm of mercury

pressure), consisted of referring to the gas rotameter calibra-

tion graphs and choosing the appropriate rotameter, and rota-

meter settings at a fixed pressure for the desired flow.

The actual mechanical procedure of obtaining a particular

gas flow consisted of successively adjusting the gas supply

pressure, and the position of the flow valve, F-2 (or F-2A).

Adjustments to the flow valve changed the gas supply pressure

as well as the flow. A number of alternate adjustments to the

flow valve and one or both of the cylinder pressure regulators

was usually required to obtain a particular float position and,

at the same time, a particular rotameter pressure. The method

for obtaining any desired flow rate for He was exactly com-

parable.

An approximation was made in measuring the gas flow rates. For the purpose of the calibration, the rotameter temperature was adjusted to 21°C and the barometric pressure to 756 mm of mercury. Gas density corrections were applied to the calibration measurements when the actual temperature and barometric pressure differed from 21°C and 756 mm of mercury, as indicated in the Appendix II. For all subsequent flow measurements, however, the rotameter temperature and the barometric pressure were assumed to be 21°C and 756 mm of mercury, respectively, and no correction for the gas density was made. This approximation greatly simplified the use of the calibration graphs and introduced only small absolute errors to the flow measurements. The magnitude of the errors thus introduced can be readily estimated. It is known (51) that for a gas the volumetric flow rate through a rotameter, for a particular float position, usually varies inversely as the square root of the gas density. The rotameter temperature and barometric pressure for the majority of the experiments varied in the range $21\pm4^\circ$C and 756 ± 8 mm of mercury, respectively. Since the density varies inversely as the absolute temperature and directly as the absolute pressure, the assumed value of the gas density could be in error by a maximum of 1.4 per cent because of temperature variations, and 0.93 per cent at the

lowest rotameter pressure used, because of barometric pressure
variations. The rotameter flow, however, varying inversely as
the square root of the gas density, would have a maximum possible
error of 0.7, and 0.47 per cent, introduced by ignoring the
actual rotameter temperature, and barometric pressure, respec-
tively. These errors could be tolerated, since they were
usually much less than the maximum values, and since the ability
to read the float position was liable to errors of a somewhat
greater magnitude.

Gas humidification and saturation

As briefly described in the section on Apparatus, after
being partially saturated with the vapour of the test liquid
in the gas humidifier, the test gas was cooled to the absorp-
tion temperature and at this temperature was completely satur-
ated. If Raoult's law was assumed to hold for the three
liquids concerned, the molar concentrations of vapour in the
gas at saturation would be proportional to the liquid vapour
pressures. It is evident that the concentration of the
ethylene glycol vapour in the gas would be small indeed, while
the presence of ethanol vapour in the gas would significantly
increase the gas volume.

Prior to start up, the humidifier was charged with approxi-

mately 500 ml of the test liquid. The operation of the humidi-
fier consisted only of starting the circulating pump, P-2, and
recharging the humidifier when most of the liquid had vaporized.

For the majority of the absorption runs the gas temperature
was allowed to vary in the range from 1 degree less to 4 degrees
more than the prescribed test temperature. Better temperature
control was considered unnecessary for two reasons. First, the
total heat content of the gas stream, for all the gas and
liquid flow rates encountered, was small when compared to that
of the liquid stream. Temperature differences of the gas of
several degrees, therefore, had a negligible effect on the
liquid temperature. Next, a considerably amount of contact
between the gas and liquid occurred in the entrance tee and
entrance section, prior to any concentration measurements.
Hence the gas was cooled to the liquid temperature, and the
excess vapour simultaneously condensed, because of the direct
contact between the two phases. As indicated earlier the
temperature rise of the liquid was negligible. For these
reasons the gas was usually maintained in a temperature
range slightly above the absorption temperature.

The temperature of the gas flowing into the absorption
tube was measured by the thermometer, T-4, mounted in the
piping. The cooling rate in the water-cooled exchanger, E-3,

was regulated by adjusting the rate of flow of cooling water
and, when necessary, closing and opening the appropriate
valves, F-22 and F-23, to double or halve the effective heat
exchange area.

Measurement of pressure in the absorption tube

A number of difficulties are involved in measuring
pressures in two-phase flow. The pressure gradient along the
tube is not constant, particularly for the bubble, plug, and
slug flow regions. The interruption of phases as observed
at any one position of the tube, as well as the associated
pressure surges, are characteristic of two-phase flow. For
this situation some "average" pressure must be measured.
Two-phase flow pressure measurements can be made in either
the gas phase (at the top of the tube) or the liquid phase
(at the bottom of the tube). There is a disadvantage in
measuring the liquid phase pressure; a second non-miscible
heavier liquid (such as mercury) is usually required as the
manometer fluid. With mercury the manometer would become
insensitive to the rapid pressure fluctuations due to the
inertia of the fluid in the pressure line and manometer.
The measurement of pressure in the gas phase was adopted
for this work because any desired manometer fluid could be

used, and because of the relatively rapid response of this type of system.

The two manometers, M-2 and M-3, were mounted adjacent to their respective inlet and outlet sampling locations. The inlet manometer, always measuring the higher pressure, was filled with water, carbon tetrachloride, or mercury, depending on the range of pressures to be measured. The fluids used in the outlet manometer were either water or carbon tetrachloride. The procedure for taking a pressure reading consisted of first clearing the manometer line of any liquid by passing a small amount of test gas through it. If the manometer fluctuated widely the fluctuations were dampened by partly closing the needle valve in the manometer line. The reading finally taken was a "time-averaged" one, a pressure reading that persisted for the longest period of time. Because of the nature of the fluctuations, the time-averaged reading did not usually corres- pond to the average of the maximum and minimum readings. The method of taking a time-averaged pressure reading was employed whether the particular manometer was used to measure pressure relative to the atmosphere, or to measure the pressure drop between the inlet and outlet sample locations.

It should be mentioned that the measurement of two-phase pressures by the method just described was not considered

highly accurate. The accuracy of the pressure measurements did not limit the accuracy of the absorption rate determinations, however. In all cases, the pressures measured were small relative to the atmospheric pressure, or to the absolute pressure. The gas solubility and hence driving force for mass transfer depended on the absolute pressure. Any errors in the measurement of pressure above atmospheric, therefore, had little effect on the accuracy of the absolute pressure or on the absorption rate determinations.

SAMPLING AND ANALYSIS

Sampling

In general, it was desirable to obtain liquid samples which yielded the average or "mixing cup" concentrations. Such samples would be obtained if all the liquid flowing through a given cross-section of tube in a fixed time interval was trapped, removed into a sealed container, and then thoroughly mixed. Although this was not possible in practice, suitable samples which were equivalent to the mixing cup variety could be readily obtained, nonetheless. For all the experimental runs, the liquid phase was in either a well mixed, or in a turbulent, region of flow. The concentration gradient through the bulk of the liquid phase, therefore, could be expected to be insignificant compared to that in a very small region near the gas-liquid interface. Figure 7 shows vertical concentration profiles for the CO_2-water system in the bubble, and slug flow regions, as well as for the CO_2-ethylene glycol system in the bubble region. The method for obtaining samples at the different vertical positions in the absorption tube is discussed in a following section. It is apparent from Figure 7 that the concentration gradient through the bulk of the liquid was very
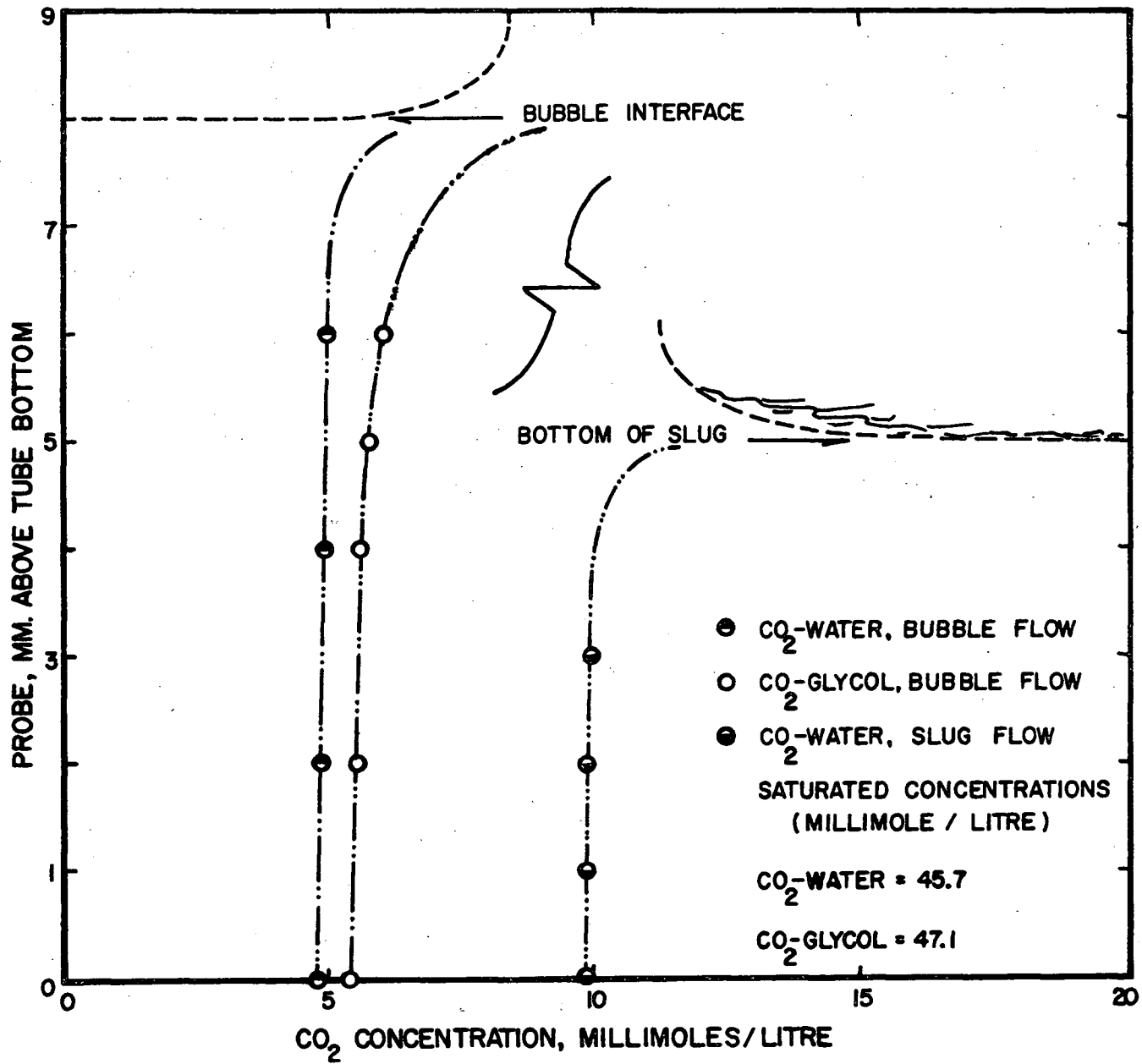
Figure 7. Concentration Profiles for CO_2-Water and CO_2-Glycol

small relative to the overall gradient, from saturation at the interface to the lowest value at the bottom of the tube. It is also evident that any concentration chosen in a fairly wide region between the bottom of the tube and the gas-liquid interface would yield a good approximation to the average or mixing cup concentration. A sample drawn from a position approximately midway between the bottom of the tube and the minimum gas-liquid interface, therefore, on analysis would be expected to give a good approximation of the mixing cup concentration.

Liquid samples were taken at the inlet and outlet sample locations to determine the concentration change in the test section. The method of sampling and analysis for each of the gas-liquid combinations studied was usually somewhat different. When CO_2 was absorbed in any of the three liquids, water, ethanol, or ethylene glycol, the samples were withdrawn into pipettes, charged into caustic solutions and subsequently analyzed by titration. For the He-water experimental runs, small water streams were continuously withdrawn at both the inlet and outlet locations and passed through stripping columns provided at these two locations. The He was stripped out of the water by a CO_2 gas stream which was then passed through a thermal conductivity-cell (TC-cell) for analysis. Details of the sampling apparatus for the four gas-liquid combinations
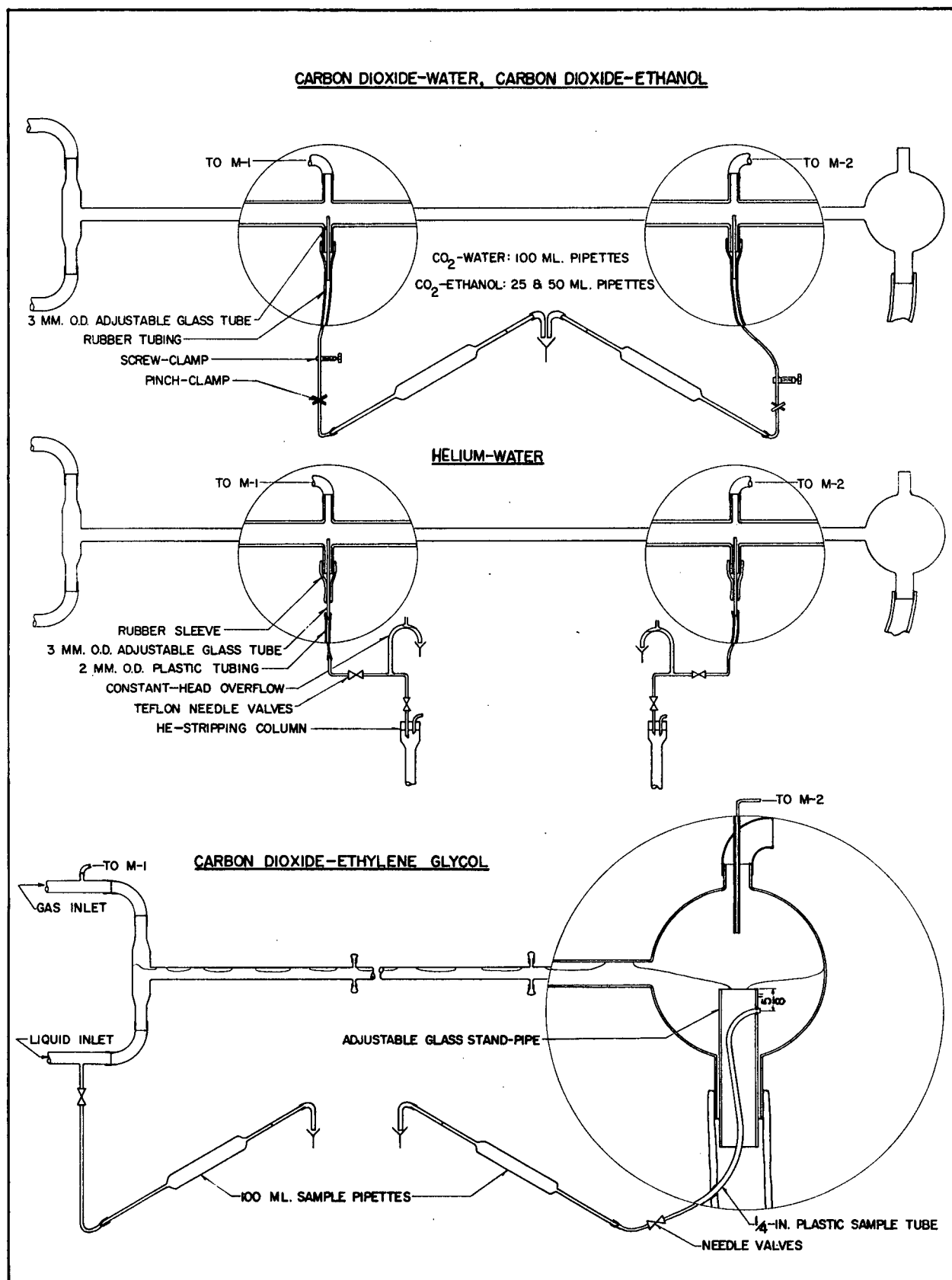
Figure 8. Methods of Sampling for Absorption Rate Determinations

are shown in Figure 8.

CO_2-Water and CO_2-Ethanol

The sampling methods for the CO_2-water and CO_2-ethanol systems were almost identical. As indicated in Figure 8, liquid samples were obtained by means of 3 mm OD glass tubes inserted inside the glass sample nipples of the absorption tube. The small diameter sample tubes were held in place by pieces of rubber tubing connected to the glass nipples. Liquid samples could be taken from any vertical position in the absorption tube, at both the inlet and outlet sample locations. During the progress of the experimental runs, the inlet and outlet samples were always taken at the same sample position in the absorption tube, approximately midway between the bottom of the absorption tube and the minimum elevation of the gas-liquid interface. For very turbulent slug or annular flow regions however, when bubbles of gas became entrained in the liquid, precautions were required to prevent withdrawal of the gas bubbles with the liquid samples. For these turbulent flows, the sample tubes were lowered into the sample nipples, with the top of each tube placed 10 to 15 mm below the bottom of the large absorption tube. In this way, the sample nipples effectively served as gas-liquid separators, removing entrained bubbles from the

liquid samples. The concentration profiles shown in Figure 7 (p.119) were obtained at constant liquid and gas flow rates through the absorption tube, by varying the inlet and outlet sample tube positions simultaneously in measured increments.

Because of the low solubilities of CO_2 in water and ethanol, relatively large samples of these liquids were required for analysis by titration. Samples were accumulated in pipettes mounted below the absorption tube and joined to the sampling tubes with rubber tubing, as shown in Figure 8 (p.121). While the samples were being taken it was important to avoid exposure to the air to prevent loss of the absorbed gas. Each sample pipette was arranged so that, during sampling, the liquid entered at the point of the pipette, and slowly filled it to overflowing. The liquid overflow was diverted to a drain. A volume of liquid approximately equal to the sample volume was normally purged through the pipette to ensure that the sample finally contained in the pipette was a representative one.

The pipette size for all the CO_2-water samples was 100 ml. For the CO_2-ethanol runs smaller pipettes of 25 and 50 ml were used. The pipettes were clamped in location with the supply and overflow tubes connected at all times except when the samples were actually being transferred to the sample flasks.

The sampling rate was normally kept in the range from 10 to 40 ml per minute. Samples were taken simultaneously at the inlet and outlet sample locations for each different combination of gas and liquid flow rates.

CO_2-Ethylene glycol

In addition to the concentration profile measurements, a second qualitative test was performed to determine the extent of mixing in the ethylene glycol phase. Ink was injected with a syringe into the liquid near the entrance of the absorption tube. Sketches of the different visual patterns observed with different CO_2 and ethylene glycol flows are shown in Figure 9. The mixing in the liquid phase appeared to be good, as already suggested by the flatness of the concentration profile. The superficial Reynolds numbers for the liquids were of the order of 8000 (turbulent) for water and 200 (laminar) for ethylene glycol. Because of the low Reynolds number great care was initially taken in sampling the glycol, and was subsequently found unnecessary. In fact the similarity of the concentration profiles for the two liquids seems anomalous, and this simi- larity is discussed further in a later section.

The sampling method used for ethylene glycol was a some- what elaborate one, chosen to obtain representative samples
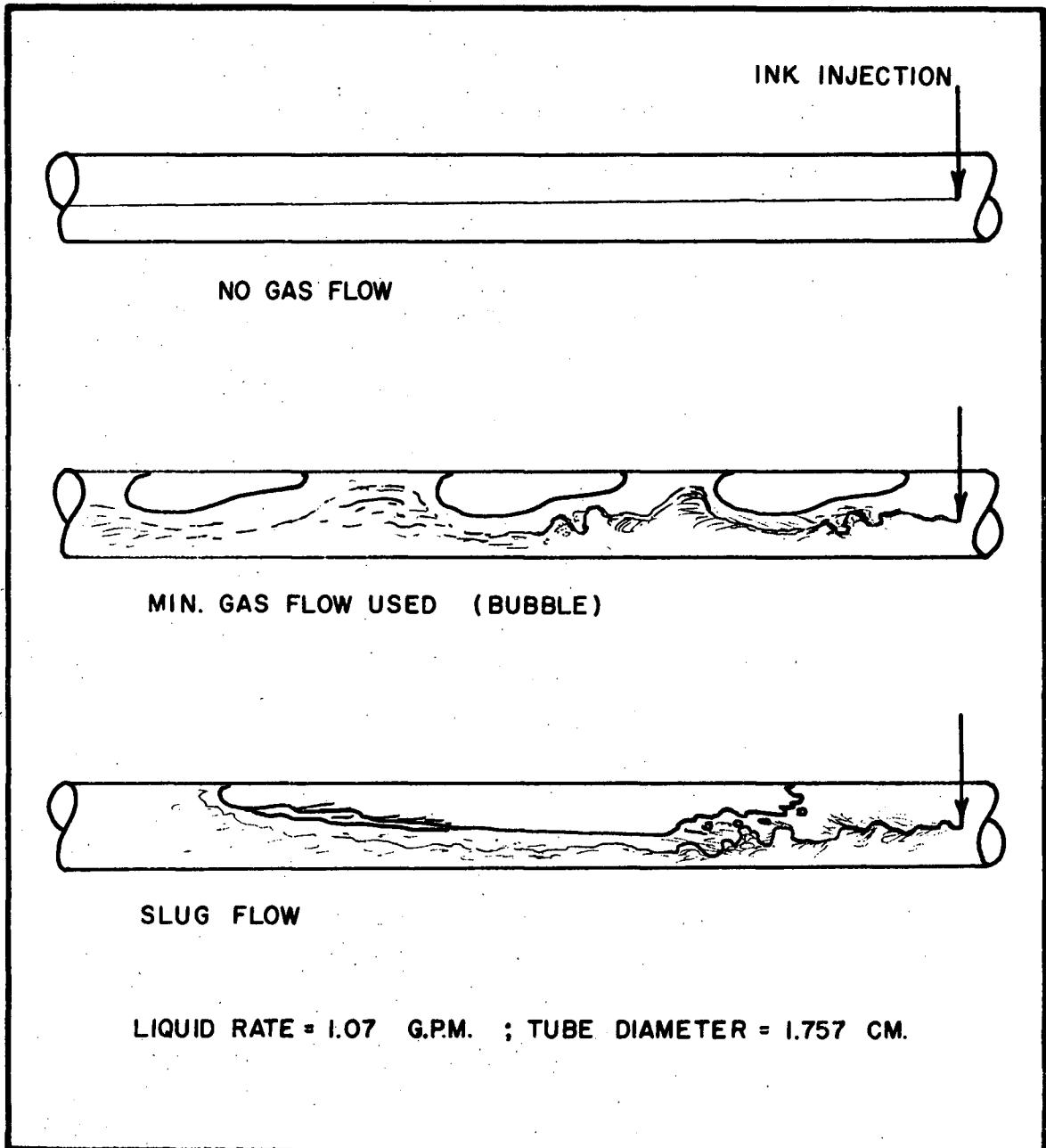
Figure 9. Induced Turbulence in Ethylene Glycol
by Ink Injection Tests

even for large concentration profiles in the liquid phase.

Details of the sampling equipment are shown in Figure 8 (p.121).

The test section for the CO_2-ethylene glycol series of experi-

ments included the entrance tee, the total length of the absorp-

tion tube, and the outlet cyclone separator as well. Inlet and

outlet samples were taken from the liquid supply line upstream

of the entrance tee, and from the outlet cyclone, respectively,

to measure the concentration increase in the test section.

Even if a large concentration gradient existed in the liquid

phase of the absorption tube, an average outlet concentration

could still be obtained by utilizing the cyclone action for

mixing the liquid in the cyclone separator, and withdrawing

a sample from there. The inlet sample was necessarily of a

uniform concentration. This method of sampling had the inherent

complication of including in the contacting system the entrance

tee, an initial tube section where uniform flow may not have

been established, and the outlet cyclone. The assumption was

made that the flow pattern in the initial section of the absorp-

tion tube was rapidly established and its contacting effective-

ness was equivalent to that of any other portion of tube. This

appeared to be a good assumption because the visual flow pattern

was fully established in most cases within 12 to 18 inches from

the entrance tee, and because the entrance length (12 to 18

inches) was a small proportion of the total effective tube

length of 127.1 inches. Further, it was possible to make

measurements of the amount of absorption which occurred in

the entrance tee and outlet cyclone for all the ethylene

glycol flow rates used, and to correct the overall absorption

rates accordingly.

Mixing of the ethylene glycol was promoted in the outlet

cyclone to achieve a uniform concentration. As indicated in

Figure 8 (p.121) a moveable glass stand-pipe was installed

inside the cyclone drain line, with very little clearance

between the two. Any ethylene glycol flowing into the cyclone

filled it to the level of the stand-pipe, and overflowed into

the stand-pipe and then through the regular drain line. A

small hole was blown in the glass stand-pipe approximately

5/8-inch below the top edge to serve as a sample point.

A sample line consisting of stiff 1/4-inch diameter polyeth-

ylene tubing was forced through the small hole in the stand-

pipe and was held there by a ridge cut around the tubing.

The other end of the polyethylene tubing was inserted through

a small hole drilled for it in the rubber hose connecting

the drain line to the cyclone. In this way, the sample tubing

supported the stand-pipe and permitted external adjustment of

its position. By adjusting the position of the stand-pipe the

outlet cyclone was maintained about one half full for all the CO_2- ethylene glycol experimental runs. The liquid in the cyclone appeared to be well mixed by the action of the liquid flowing into the cyclone. In the cyclone most of the surface liquid layer which had been in contact with the CO_2 tended to flow radially toward the stand-pipe and then out the drain line. This was a desirable effect since a sample taken from below the liquid surface then showed a CO_2 content which largely excluded that resulting from absorption in the cyclone itself.

Inlet and outlet samples were taken by means of two 100 ml pipettes. Needle valves were installed in both the inlet sample line, as well as in the polyethylene outlet sample line to regulate the sampling rates. In all other respects the method of sampling was the same as for water and ethanol.

An estimate of the amount of absorption occurring in the entrance tee and outlet cyclone was made separately for each different combination of flow rates and temperature that were used during the absorption experiments. The method consisted of passing the ethylene glycol through the absorption tube as a single phase and permitting contact with the CO_2 gas only in the entrance tee and outlet cyclone. Prior to each test, CO_2 was passed through the entrance tee and absorption tube to ensure that the entrance tee was adequately purged. By means

of a temporary line, CO_2 was allowed to flow continuously into the outlet cyclone during the test to ensure that the cyclone contained only CO_2 gas. Inlet and outlet samples were taken by the same procedure used for the regular ethylene glycol absorption runs. The only absorption which occurred during these tests, therefore, was that in the entrance tee and outlet cyclone. It was assumed that the amount of absorption in the entrance tee and outlet cyclone remained the same for one ethylene glycol flow and temperature regardless of the gas flow rate. In all probability this was not a highly accurate assumption, particularly for high gas flow rates, when an increase in liquid turbulence at both the entrance and outlet was evident. The amount of absorption due to these sections was a very small fraction of the total amount of absorption in the tube, especially at high gas flow rates. The error in measurement of the overall absorption rates would be in little error even if the amount absorbed in the entrance tee and outlet cyclone was in error by a factor of two or more.

He-water

During the He-water experimental runs the liquid samples were withdrawn from the same two locations in the absorption tube (92.2 inches apart) that were used for the CO_2-water,

and CO_2-ethanol experiments. The sampling for He-water differed from that of the latter two systems in that the samples were continuously withdrawn and continuously analyzed at both the inlet and outlet sampling locations. The accuracy of the analysis depended on maintaining constant sample flows through small stripping columns. Because of the pressure surges characteristic of some regions of two-phase flow, maintaining constant sample flows was no simple task. Since the details of the control of the sample flow rates were so closely associated with the He analysis itself, a more detailed description will be deferred to the next section.

Analysis

The analysis for dissolved CO_2 in the three liquids, water, ethanol, and ethylene glycol, was almost identical. The analysis entailed the reaction of the sample with an excess of a known volume of standard sodium hydroxide solution and back-titration with standard acid. The system CO_2-water has frequently been used for mass transfer studies because of the relative simplicity of the analysis. An identical method of analysis was shown to be suitable for solutions of CO_2 in ethanol and ethylene glycol, as well as in water. Solutions of He in water, on the other hand, presented a

much greater problem since He is chemically inert in solution, and only sparingly soluble. Because of its relatively high gaseous thermal conductivity, however, gas-phase He mixtures could be analyzed by means of a calibrated TC-cell. A method of stripping He from the water solutions by a carrier gas was developed for obtaining gas-phase mixtures suitable for analysis by thermal conductivity.

CO_2-Water

The titration of carbonates and bicarbonates with acid is usually considered to be a double-indicator titration, with the first end point occurring when all the carbonate has been converted to the bicarbonate, and the second, when all the bicarbonate has been converted to dissolved CO_2. The first, and second-end points occur at approximate pH values of 9, and 4, respectively. The analysis of dissolved CO_2 was similar to, but not identical with, that for carbonate solutions. In the initial step, the volatile CO_2 in the sample was converted to a stable carbonate-bicarbonate mixed solution by injecting the sample into a volume of standard sodium hydroxide sufficiently large to convert at least some of the CO_2 to carbonate. An indicator in the solution for a pH of 9, corresponding to the first end point, confirmed the presence of the carbonate.

When titrated with acid to the carbonate-bicarbonate end point (pH 9) the sample solution then contained an amount of bicarbonate equivalent in number of moles to that amount of CO_2 originally present in the sample. Back-titration with acid to the first end point, therefore, yielded by difference the molar quantity of bicarbonate, or of original CO_2, in the sample. Titration to the second end point could have been performed as a check on the amount of standard caustic used, but was not required for the determination of the CO_2 originally present in the sample.

The normality of both the sodium hydroxide and the hydrochloric acid solutions used in the volumetric analysis was 0.100. This normality was chosen to provide sufficiently large volumes of titration to ensure a reasonably accurate analysis even for low concentrations of CO_2 in the water samples. For the 100 ml sample size used, the maximum volume of sodium hydroxide required was 45.47 ml, for a water sample completely saturated with CO_2 at $15°C$ and 1 atm pressure.

The end-point for the carbonate-bicarbonate titration was not expected to be as sharp as for most alkalimetric titrations (52), but by means of a special mixed indicator an adequate accuracy was obtained for most of the analyses. The mixed indicator chosen was cresol red-thymol blue which,

according to Simpson (53), was expected to give a relatively

sharp colour change at the carbonate-bicarbonate end point.

The maximum probable error due to analysis was estimated to be

equivalent to 0.1 ml of solution for a titration volume of

5.0 ml, or about 2 per cent.

Prior to a series of experimental runs, a 250 ml erlen-

meyer flask was prepared for each sample that was to be taken.

A volume of 0.1 N sodium hydroxide corresponding to the

expected CO_2 content was drained from a burette into each

flask, a few drops of indicator were added, and the flask was

then sealed with a stopper. During the sampling, the tip of

the pipette was kept below the caustic surface to avoid loss

of CO_2. The sample flasks were sealed and set aside for titra-

tion when the experimental runs had been completed.

CO_2-Ethanol and CO_2-Ethylene glycol

For the absorption runs with the CO_2-ethanol and CO_2-

ethylene glycol systems, the method of analysis for the

dissolved CO_2 was identical with that outlined above for CO_2

dissolved in water. Before the method was adopted for ethanol

and ethylene glycol, however, it was necessary to show that

the reaction of CO_2 with sodium hydroxide produced the same

reaction in these two liquids, and that the mixed indicator

changed colour at the carbonate-bicarbonate end point for both liquids. The suitability of the procedure was tested by using solutions of water containing increasing proportions of ethanol (or ethylene glycol). Equal quantities of sodium carbonate were dissolved in pure water, and in a number of ethanol-water solutions with increasing ethanol content, and pH curves for titration with acid were obtained. The same procedure was followed in the preparation of solutions of water and ethylene glycol. Figure 6 (p.107) shows the resulting titration curves for the ethanol solutions, and the titration volumes for the ethylene glycol solutions. In both cases the analysis of the carbonate was independent of the liquid concentration. In fact, the carbonate-bicarbonate end point was somewhat sharper in solutions containing ethanol than in water itself.

For the CO_2-ethanol experimental runs sample volumes of 25 and 50 ml were taken, because the solubility of CO_2 was considerably higher in ethanol than in water. The solubility of CO_2 in the ethylene glycol was much closer to that in water so that 100 ml samples were taken for runs with this system.

He-Water

For the absorption runs with the He-water system the water was continuously sampled and analyzed at both the inlet and
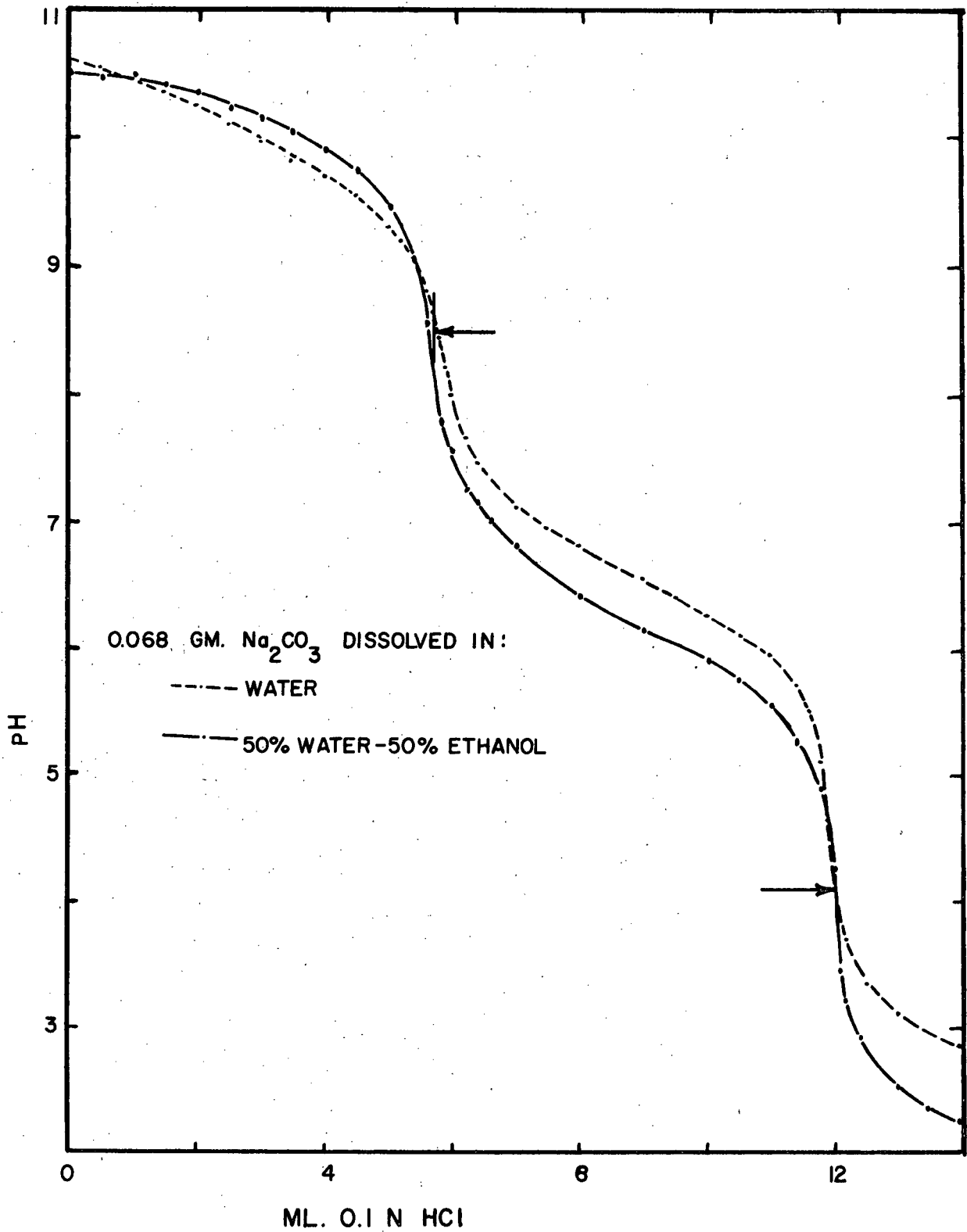
Figure 10. pH Curves for Carbonate Titration
in Solutions of Water and Ethanol
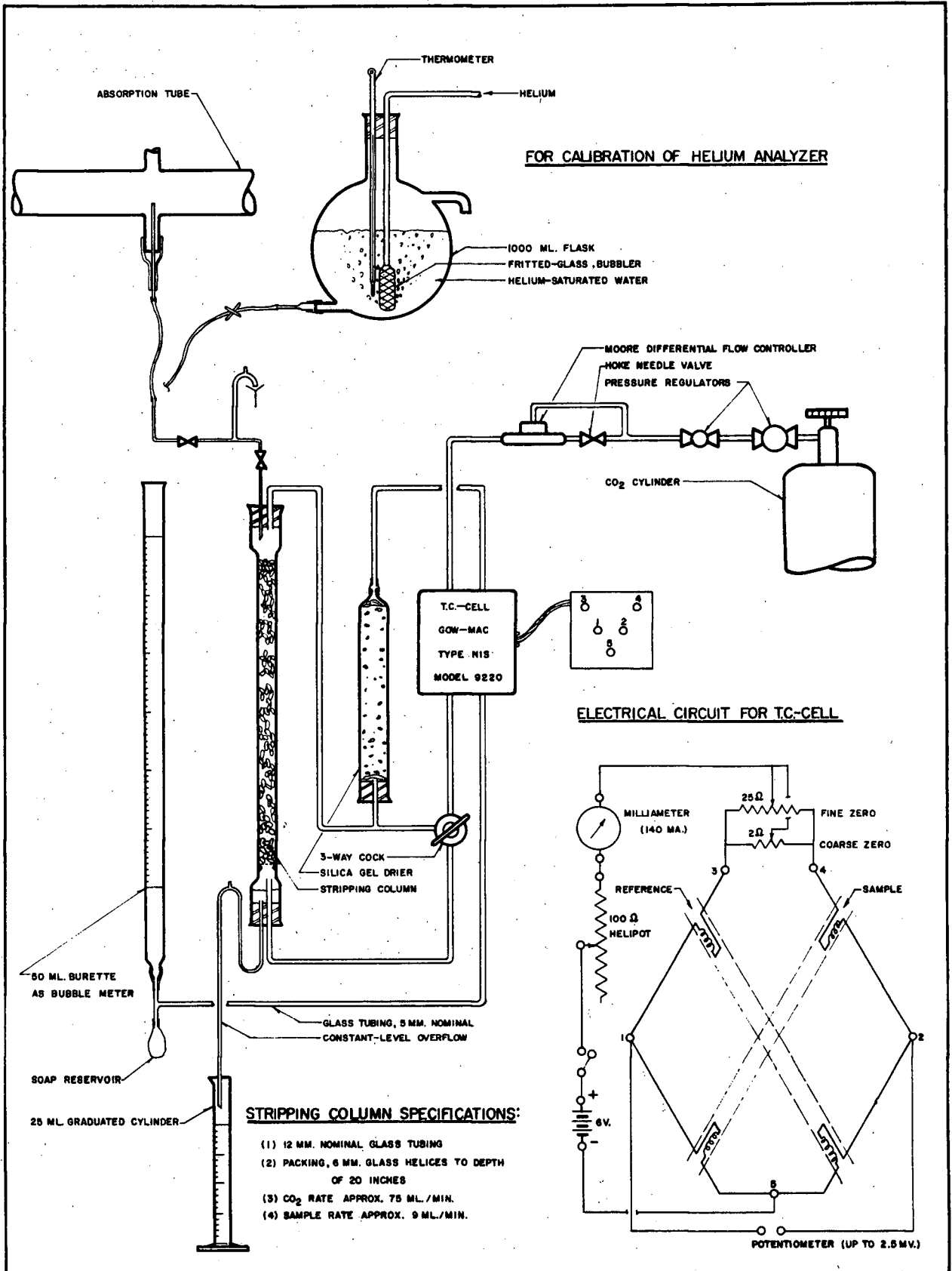
Figure 11. Flow Diagram for Helium Analyzers

outlet sample locations by means of two identical specially

designed He analyzers. The operation of the analyzers entailed

the counter-current stripping of the He from the water in minia-

ture packed columns using CO_2 as a carrier gas. The column

effluent water, stripped of its He, was discarded, while the

effluent CO_2, containing the He, was passed through a calibrated

TC-cell for analysis. A flow diagram for one of the units is

shown in Figure 11.

Accurate analysis for He depended on maintaining the flow

rates of both the water sample and CO_2 stripping gas constant,

and then measuring them accurately. To keep the liquid sample

flow constant a constant-head overflow tube was installed

above the stripping column. A sample flow was continuously

withdrawn through a 2 mm diameter plastic sample line. A

portion of the stream was passed into the stripping column

while the remainder was allowed to overflow by way of the

constant-head tube. The rates of both streams were controlled

by small Teflon needle valves. The constant-head tube, pro-

viding a low and constant liquid head, enabled accurate flow

control into the stripping column. The column itself was

constructed from a 24-inch long 12 mm nominal OD section of

glass tubing with enlarged inlet and outlet sections. The

column was packed to a depth of 20 inches with 6 mm glass

helices. The water level was kept constant in the bottom of the column by an inverted U-tube with a small hole blown at the top of it to eliminate a siphoning effect. The liquid sample flow was measured at the column effluent line by means of a 25 ml graduated cylinder and a stop watch, and maintained between 7 and 11 ml per minute.

A constant flow rate of CO_2 to each stripping column was accurately maintained by a Moore constant-differential flow controller, in conjunction with a high quality 40-turn Hoke needle valve. The flow of CO_2 to each column was passed through the reference side of the TC-cell then up through the column, through a silica gel dryer, and then through the measuring side of the TC-cell. The CO_2 flow rates were measured by soap-bubble meters installed downstream of the TC-cells. The flows were maintained in the range from 60 to 75 ml per minute.

Good stripping was expected in each of the columns because of the low water flow rates and relatively high gas flow rates. The stripping action was enhanced by keeping the concentration of the He in the CO_2 very low, less than 0.01 mole fraction for all analyses, so that the driving force for stripping was always nearly the maximum. Both of the TC-cells were calibrated by using water saturated with He,
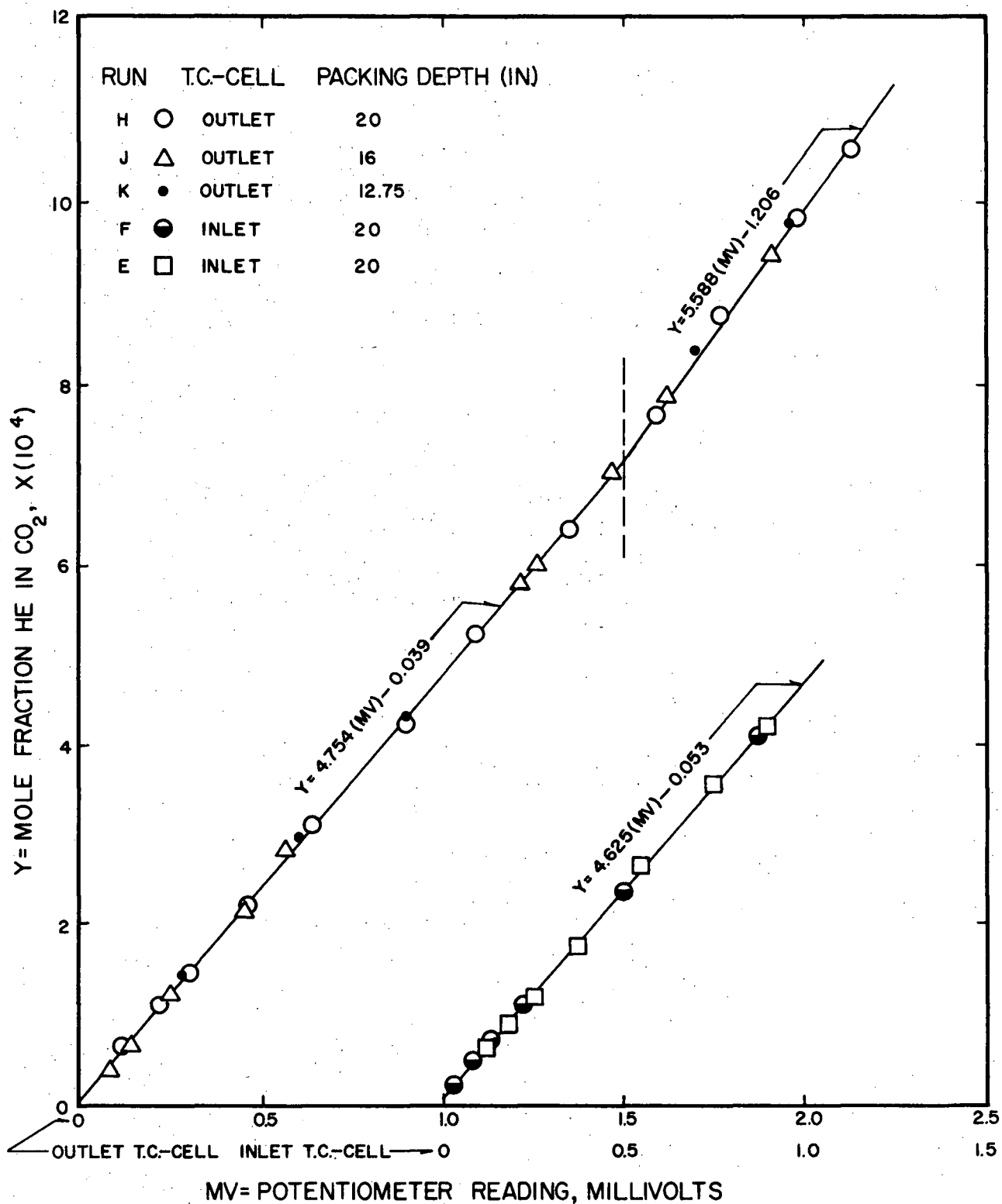
Figure 12. He Analyzer Calibration Curve

and passing various measured flow rates of the He-saturated water through each of the stripping columns. For one column, the calibration was repeated using packing depths in the column of 12.75, 16, and 20 inches. The three resulting calibrations gave a single line. All these calibrations are shown in Figure 12, and supporting data are listed in Table III-3 of Appendix III. The fact that the various depths of packing gave identical calibrations for the one column, indicated that the stripping of the He from the water was essentially complete even for the 12.75-inch packing depth. The calibration of the TC-cells with He-saturated water was simplified because of the nearly constant (although small) solubility of He in water with changing temperatures.

The electrical circuit for each of the TC-cells shown in Figure 11 (p.136) was a standard one for such detectors. A current of 140 ma was supplied to the heating circuits of both TC-cells. In each case the same milliammeters were used during calibration and subsequent analyses so that any absolute errors in the milliammeter readings were not reflected in the analyses. The TC-cell signals were measured by two Student potentiometers graduated in divisions of 0.1 mv. The zero reading of the TC-cells was taken when the water in the equipment had been deaerated for a period of at least 1/2-hour.

The flow of He was then started through the equipment and the experimental runs were allowed to proceed. Because of the very rapid sampling and the analysis possible with the TC-cells, only 15 to 20 minutes elapsed between successive pairs of concentration measurements. At the completion of a series of measurements the flow was stopped, and the water in the equipment was again circulated for about 1/2-hour for a check on the zero positions of the TC-cells. Any shift of the TC-cell potential readings, usually small, was corrected for by assuming a drift linear with time. The TC-cell method for the analysis of the He in water as employed in this research was considered highly successful in view of the problems normally encountered during analyses of this type. The maximum probable error of analyses was estimated to be about $\pm$ 4 per cent of the measured values.

Preparation and Maintenance of Standard Solutions

The 0.1 N sodium hydroxide and hydrochloric acid solutions used for the volumetric analysis of CO_2 were prepared by diluting commercially prepared sealed ampoules of the concentrated liquids. The solutions were prepared in large quantities of about 8 to 10 liters of the sodium hydroxide and 3 to 4 liters of the acid. To check the normality of the sodium hydroxide solution a standard solution of potassium acid

phthalate was prepared. The concentrated liquids, as supplied

by The British Drug Houses (Laboratory Chemicals) Company, were

specified to have a maximum concentration tolerance on dilution

of 0.1 per cent. The concentration of the initial batch of

the standard caustic was determined using the potassium acid

phthalate standard and was found to be within the 0.1 per cent

tolerance specified by the supplier (British Drug Houses Ltd.).

The concentration of the diluted acid prepared in the same way

as the caustic was within the same limit of accuracy when

titrated with the standard sodium hydroxide. Thereafter, when

new batches of the 0.1 N acid and base were prepared from

ampoules of the concentrated materials, by suitable dilution,

they were titrated one against the other. If the titration

volumes were within 0.4 per cent of one another (or within

0.1 ml in 25-ml volumes), the concentration of both solutions

was assumed to be, therefore, 0.1000 ± 0.0004 N.

The normal procedures for ensuring that the standard

solutions were carbonate-free were followed. The ampoules of

concentrated caustic were guaranteed by the suppliers to be

carbonate-free, and on testing after dilution with specially

prepared CO_2-free water, a negligible amount of carbonate was

found. Special precautions were taken to keep the stock

solutions of standard acid and base in a carbonate-free

condition. Concentration changes of the standard solutions over a period of three months were negligible.

TREATMENT OF DATA

The absorption data were obtained as mean or "mixing cup"
concentrations at the extremities of the test section. Pressure
measurements were also obtained to permit the calculation of
absolute pressures at the inlet and outlet. In the following
section, the methods of calculating the NTU (number of transfer
units), and the mean volumetric gas flow rate for the absorption
tube test interval, are presented and discussed.

At a constant temperature, pressure, and constant condi-
tions of contacting, the driving force for absorption would be
expected to decrease along the absorption tube due to an increas-
ed concentration of absorbed gas in the liquid. For all experi-
mental runs the absorption temperature was measured and found
to be essentially constant, the pressure change in the test
section, also measured, was found to be small with respect to
the absolute pressure, and the volume of gas absorbed when
compared with the total gas flow through the tube was also
usually small. Except for the concentration in the liquid,
therefore, it appeared that with reasonable accuracy the
conditions along the tube could be taken as constant at their
average values. For such a system, where the potential
(driving force) is linear in the variable defining the amount

transferred, the logarithmic mean potential applies over the
entire tube length (54). If the properties of the liquid were
changed appreciably by the presence of the absorbed gas, then
the logarithmic mean driving force would be inaccurate. To
conclusively determine whether the amount absorbed was, in
fact, linearly dependent on the logarithmic mean driving force
over the entire concentration range, an experimental test
was carried out using the CO_2-water system at constant gas
and liquid flow rates but with increasing inlet concentrations
of absorbed gas. The variation in inlet concentrations was
achieved by changing the boiling rate in the vacuum stripper.
Table 9 shows the experimentally obtained values of logarithmic
mean concentration driving force and amounts absorbed (as well
as the conditions of the experiments). Figure 13 graphically
shows the results, which clearly show the linear relationship.
The range of concentrations for this test far exceeded those
covered in most of the experimental runs, and hence the use
of the logarithmic mean driving force for absorption in this
work appears to be well justified. It follows from the
definition of NTU that the values of NTU must be independent
of the concentration of the entering liquid, when calculated
from the quantity of gas absorbed and the logarithmic mean
driving force. The calculated values of NTU for the tests

TABLE 9

AMOUNT OF CO_2 ABSORBED AND LOGARITHMIC MEAN DRIVING FORCE

Absorption tube: 1.757 cm ID; test section 7.983 ft

Sample size: 100 ml; 1.0 ml 0.1 N NaOH equivalent to 1.0 milli-

moles per litre

Flow rates: water, 1.50 gpm; CO_2, 86.5 cfh (slug flow)

Barometric pressure: 764.5 mm mercury

Run	Amount absorbed millimoles per litre	Concentration driving force millimoles per litre		LMDF millimoles per litre	NTU
		In	Out		
901	8.80	42.0	32.4	37.2	0.237
902	8.80	42.1	32.5	37.25	0.236
903	7.15	34.45	26.5	30.47	0.235
904	7.10	34.55	26.65	30.6	0.232
905	4.4	22.1	17.9	20.0	0.220
906	4.75	22.95	17.4	20.2	0.235
907	2.9	13.5	9.8	11.65	0.249
908	2.8	13.4	9.7	11.60	0.241
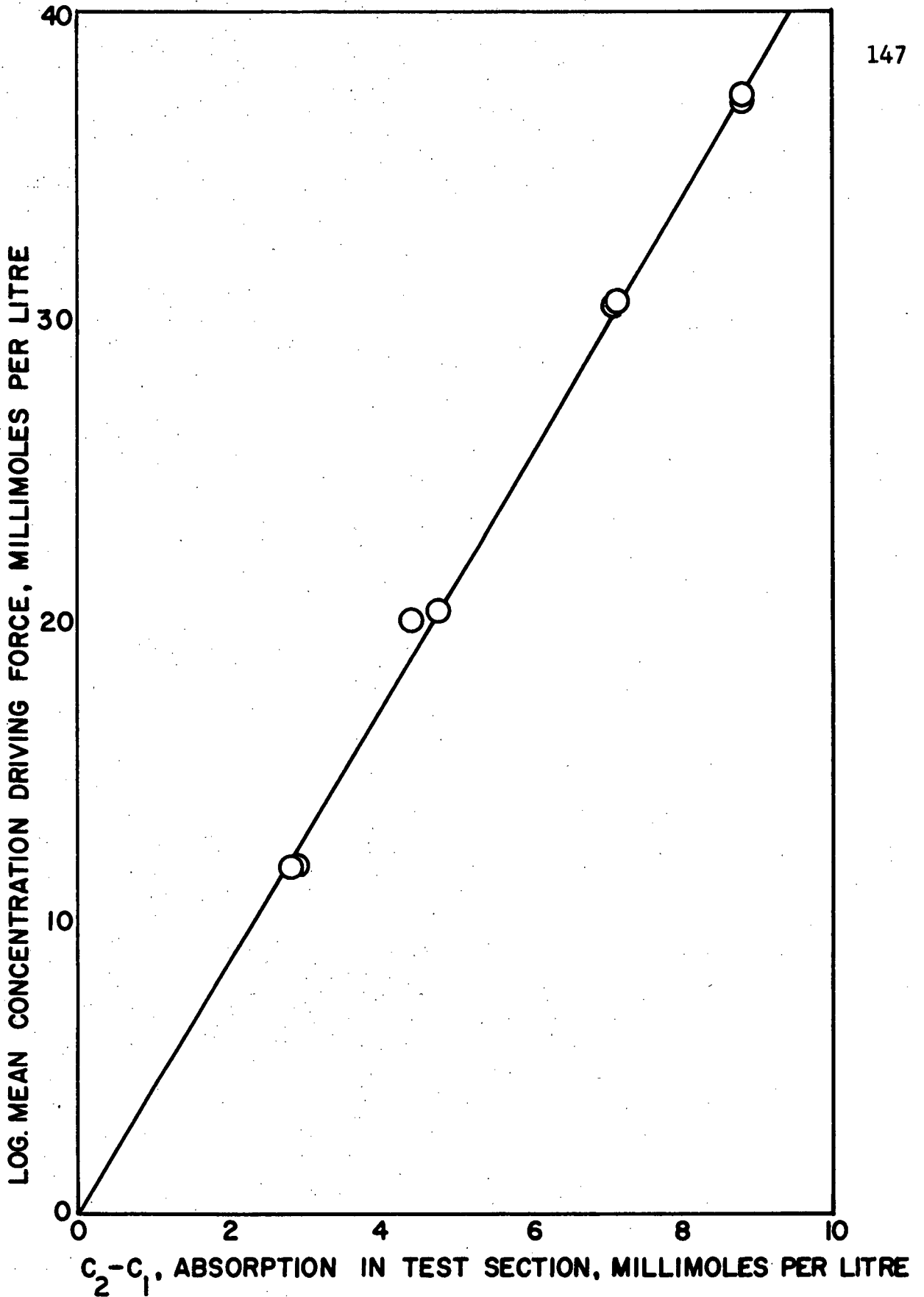
Figure 13. Quantity of Absorption for Varying Inlet
Concentrations and Logarithmic Mean Driving Force

described above are also listed in Table 9, and can be seen to be essentially independent of inlet concentration. The definition of NTU applicable to this work is then,

$$
NTU = \frac{(C_2 - C_1)}{\dfrac{(C_1^* - C_1) - (C_2^* - C_2)}{\ln \dfrac{C_1^* - C_1}{C_2^* - C_2}}} = \frac{k_L (A)}{Q_L^o} \tag{7}
$$

where C_1, C_2 = inlet, and outlet concentrations, millimoles per litre

C_1^*, C_2^* = inlet, and outlet saturated concentrations, millimoles per litre

k_L = mass transfer coefficient, cm sec^{-1}

A = interfacial area, cm^2

Q_L^o = liquid volumetric flow rate, cm^3 sec^{-1}

As stated above, the assumption was made that the conditions for mass transfer along the test section were essentially constant. Some gas was in fact absorbed in the test section, however, as well as in that portion of tube upstream of the test section, thus, decreasing the total quantity of gas flowing, and, in addition, the pressure along the tube did change, even if only by a small amount relative to the absolute pressure. These factors were taken into account in calculating the mean gas volumetric flow through the test section. The

amount absorbed in the entrance section was calculated by assuming that the same flow pattern and transfer conditions existed there as in the remaining portion of the tube, and that, therefore, the NTU per unit length of entrance likewise was the same. From the NTU in the test section, the amount of absorption therein, and the length, the appropriate con-centration driving force, and the amount of absorption were calculated for the entrance section. It can be shown that the amount of absorption in the entrance section is closely given by the following expression,

$$C_1 - C_0 = \frac{\frac{E}{L} (NTU) (C_1^* - C_1)}{1 - \frac{E}{2L} (NTU)} \tag{8}$$

where C_0 = tube inlet concentration (millimoles per litre)

C_1 = test section inlet concentration

C_1^* = test section inlet saturated concentration

E = length of entrance, ft

L = length of test section, ft

NTU = number of transfer units in test section

The arithmetic mean quantity of gas flowing through the test section is then given by,

$$(Q_G)m = Q_G^o - f \left[(C_1 - C_0) - \tfrac{1}{2}(C_2 - C_1) \right] \tag{9}$$

where $(Q_G)_m$ = mean dry gas flow in test section, cfh at $15^{\circ}C$,

756 mm

Q_G^o = gas flow at tube inlet, cfh at $15^{\circ}C$, 756 mm

f = conversion factor, from millimoles CO_2 per litre

liquid, to gas volumetric units, cfh at $15^{\circ}C$,

756 mm (depends on liquid rate and gas solubility).

The final correction for the mean gas volumetric flow was that

for temperature and pressure, which was simply a conversion from

cfh at $15^{\circ}C$ and 756 mm to the actual absorption temperature

and actual mean test section pressure. The above calculations

were incorporated in the main IBM 1620 computer programs which

were used in processing all the absorption data, and which

are listed separately in Appendix IV for the different gas-

liquid systems. The experimental data and calculated values

for all the runs as listed in Appendix V include the actual

quantitative corrections to the gas volumetric flow resulting

from transfer into the absorbing liquids, and the test section

pressures being different from those at which the flows were

originally measured. The magnitude of these corrections was

usually small in comparison to the total gas flow rates in the

absorption tubes, the maximum occurring for the CO_2-ethanol

system, for which the gas solubility was greatest.

EXPERIMENTAL RESULTS

In this section the experimental results are shown graphi-
cally on logarithmic plots of NTU and mean gas superficial
velocity (V_G^O), at constant liquid rates. The range of gas
velocities at each liquid rate includes the regions of bubble,
plug, slug, and (sometimes) annular flow. A graph showing the
effect of entrance type is also included. Lines drawn through
the data points on all of these graphs are visually estimated
mean representations.

The computations of NTU, mean gas superficial velocity,
and other information from the raw experimental data were
accomplished by means of an IBM 1620 computer. The FORTRAN
programs for these computations are given in Appendix IV.
In Appendix V are to be found the raw experimental measurements
and calculated data for various systems, from which all the
values were taken for the plotted graphs. The experimental
data for each series of runs (performed in a single day)
include the gas and liquid flow rates, flow region, the titra-
tion volumes, pressures (or pressure drops) for the inlet
and outlet locations of the test section, tube diameter,
absorption temperature, and barometric pressure. The calcu-
lated values include the amount of absorption, logarithmic

mean concentration driving force, NTU, mean gas volumetric

flow, gas volumetric correction, and mean gas superficial

velocity.

Effect of Gas Density

A graph of the absorption curve for the CO_2-water system,

obtained from measurements taken at a single liquid rate but at

two absorption pressures (10 and 20 psia) is shown in Figure 1

in the section on Theoretical Aspects. The absorption condi-

tions were as follows: temperature, $15^{\circ}C$, tube diameter 1.757

cm, and liquid flow rate 1.07 gpm. When the gas superficial

velocity is used as the ordinate, the data for both pressures

fall closely on a single curve.

Absorption Curves at Three Liquid Superficial Velocities

Absorption data were obtained at three superficial liquid

velocities for each of the four gas-liquid systems, CO_2-water,

He-water, CO_2-ethanol, and CO_2-glycol using the 1.757 cm

absorption tube. Absorption data were also obtained using

the CO_2-water system for two additional tube sizes, 1.228

and 2.504 cm in diameter, and at the same three velocities.

To permit comparisons of the absorption behaviour for the

different systems at the same liquid superficial velocities

three separate graphs are given. In Figures 14, 15, and 16, absorption curves at superficial liquid velocities of approximately 0.5, 0.9, and 1.8 fps, respectively, are shown. The effects of the primary variables cannot be observed directly by an inspection of these graphs since the primary variables could not be independently varied, as discussed in some detail in the section on the Design of Experiments, so that in most cases combinations of effects only can be observed. The values of liquid phase diffusivity, surface tension, and liquid phase viscosity, for each of the gas-liquid systems corresponding to the absorption curves shown in Figures 14, 15, and 16, can be obtained from Tables 3, 4, and 5.

Effect of Increased Liquid Flow Rate

Absorption data for the CO_2-water system using the 1.757 cm tube were obtained at three liquid superficial velocities in addition to the three already mentioned, namely at 1.2, 2.6 and 3.6 fps. The resulting absorption curves, including a repetition of the one for a liquid superficial velocity of 0.5 fps, are shown in Figure 17.
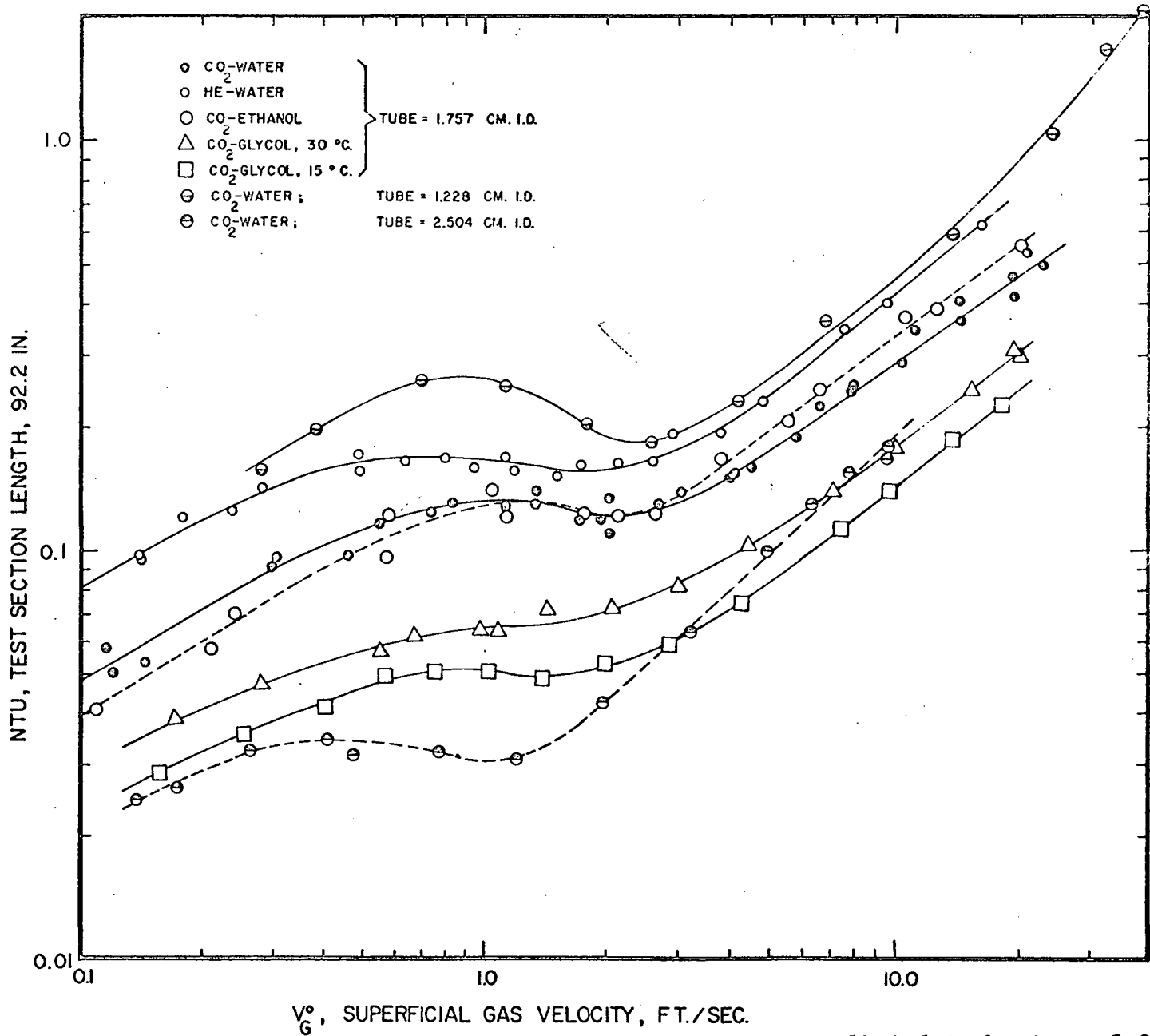
Figure 14. NTU vs Gas Superficial Velocity, for Liquid Superficial Velocity of 0.5 fps
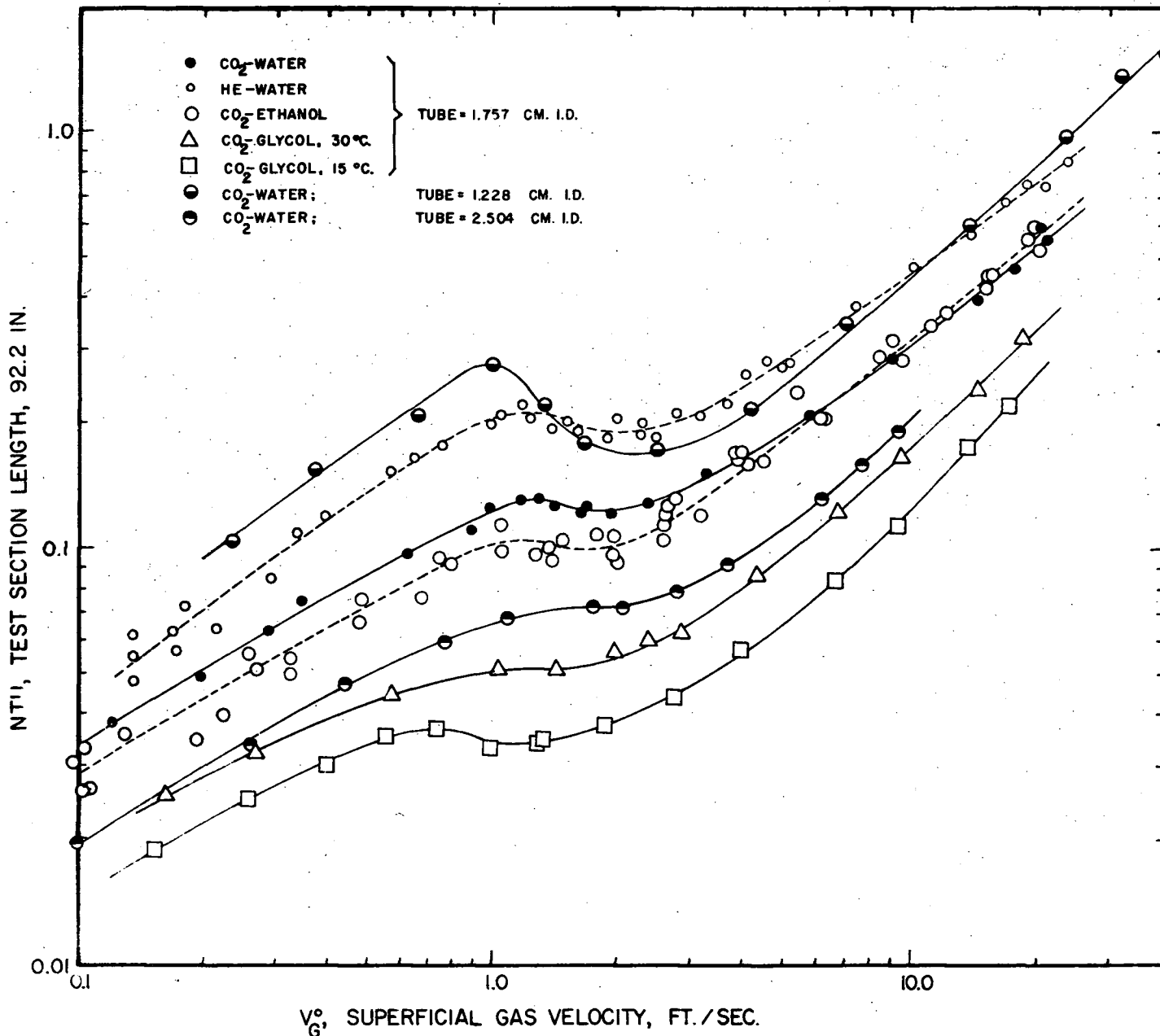
Figure 15. NTU vs Gas Superficial Velocity, for Liquid Superficial Velocity 0.9 fps
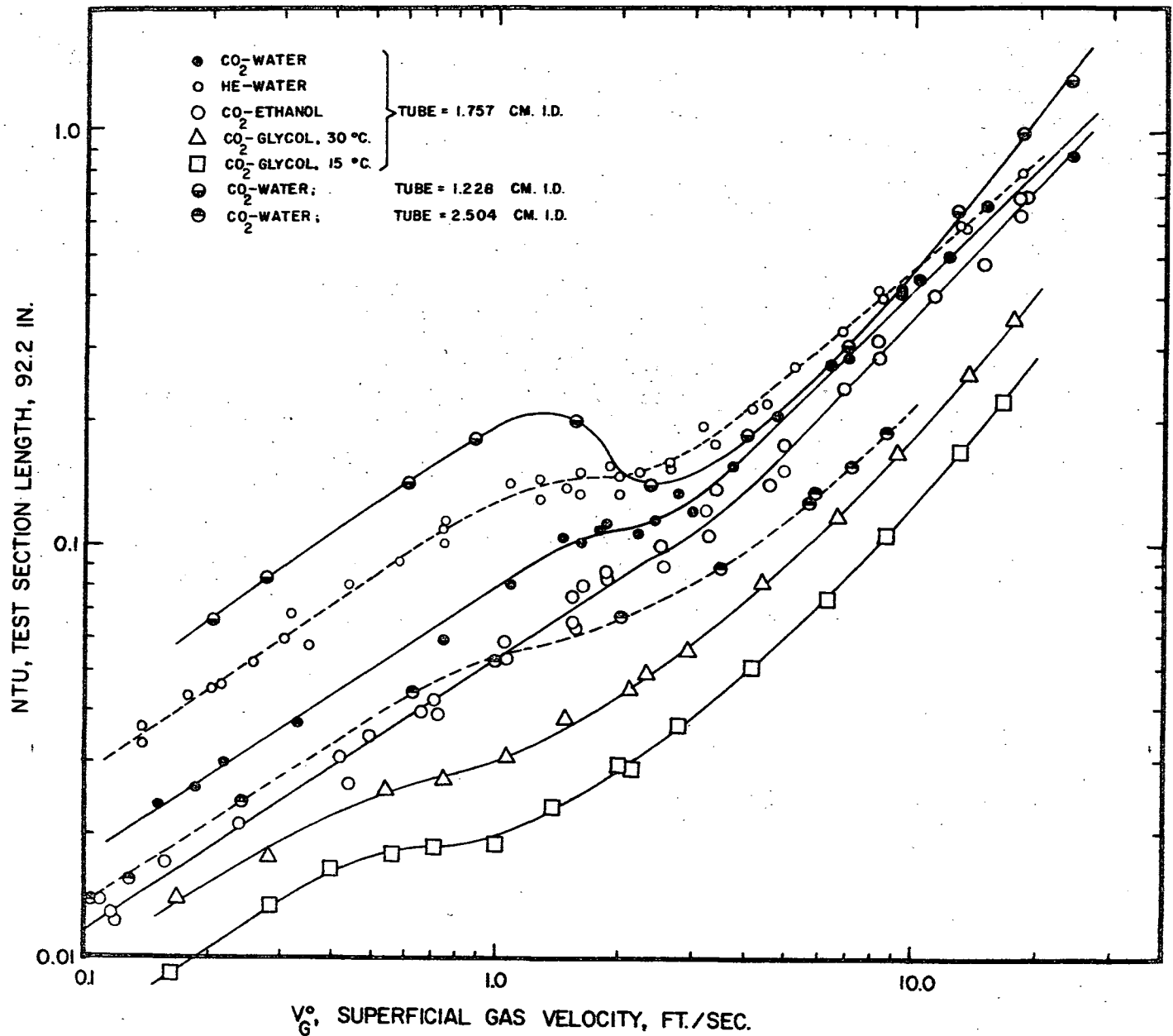
Figure 16. NTU vs Gas Superficial Velocity, for Liquid Superficial Velocity of 1.8 fps
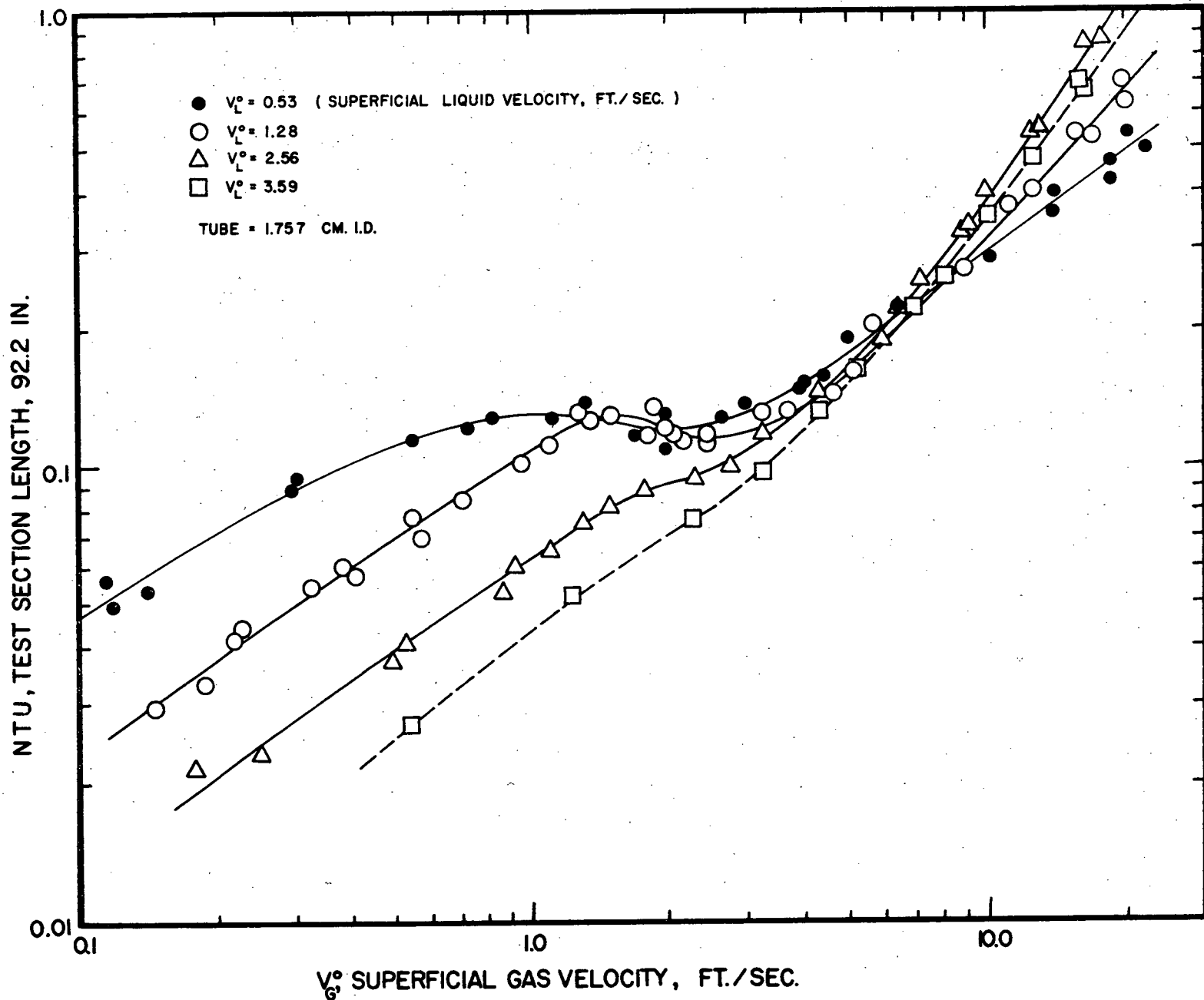
Figure 17.   Effect of Gas and Liquid Flow Rates for the CO_2-Water System

Effect of Entrance Type

The effect of the type of entrance was measured using the CO_2-water system and the 1.757-cm tube. In addition to the standard horizontal tee entrance, three other types of entrances were used (please refer to Figure 5). The amount of absorption was determined in the test section for each of the entrances using three particular gas flow rates, a constant liquid rate, and (except for the type of entrance) identical absorption conditions. The entrance types provided widely different mixing characteristics. It was therefore expected that if the type of entrance in any way affected the absorption rate downstream of the entrance, this would have been readily observable. The resulting amounts of absorption in the test section, correspond-ing to the different entrances, are shown in Figure 18 as values superimposed on the absorption curve for the equivalent conditions of flow and the regular type of entrance.

Effect of Temperature on Absorption Rate

A number of additional absorption runs were performed using the CO_2-water system, and the 1.757-cm absorption tube, but at three other temperatures, 5.3, 30.0 and $45.0^{\circ}C$. For these experimental runs the liquid rate was held constant at 1.07
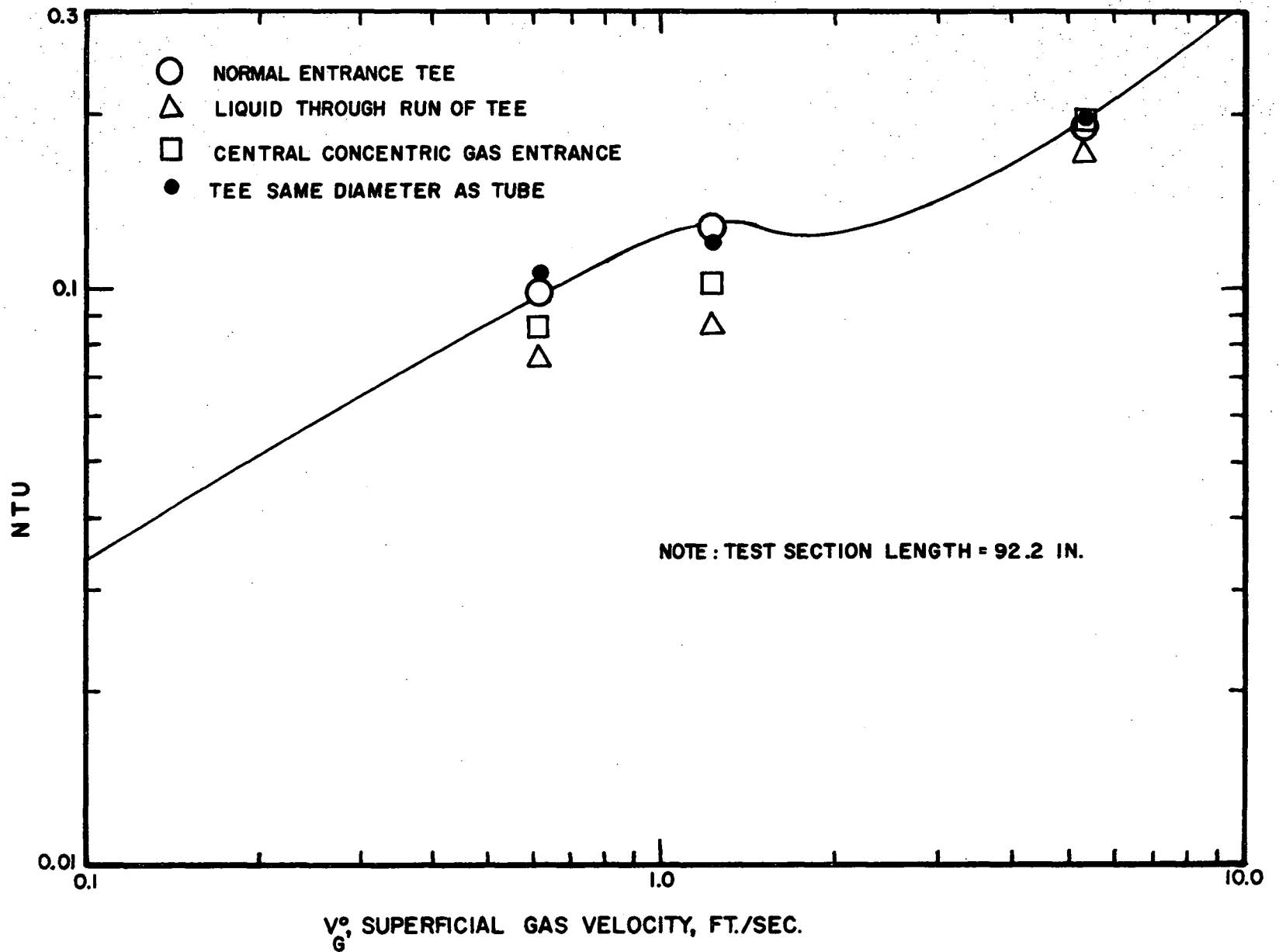
Figure 18.   Effect of Entrance Type on the Absorption Rate for the CO_2-Water System

gpm (equivalent to a superficial liquid velocity of 0.9 fps).

The effect of temperature in these experiments should be largely

that of the resulting changes in the liquid phase diffusivity,

and liquid viscosity, since the corresponding change in surface

tension is small. These data were not included when correlations

were developed, but were used as a check on the reliability of

the correlating expressions for predicting the behaviour of

the CO_2-water system.

DEVELOPMENT OF CORRELATIONS

The extreme differences between the bubble and slug flow regions, in hydrodynamics, shape of the interface, and mechanisms for mass transfer, suggests the treatment of these two regions as distinctively separate contacting processes. In the following sections two different correlations will be presented, one pertaining to the bubble region and extending at least in part into the plug region of flow, and the other representing slug flow behaviour but including part of the plug region, and extending at least to the slug-annular transition. Both correlations are particularly designed to illustrate, as far as possible, the major flow characteristics and probable transport mechanisms of their respective regions, rather than to merely give an empirical description of experimental data. The correlation pertaining to the bubble-plug region was obtained by direct deduction from observed qualitative and quantitative experimental facts. This correlation is more general than that for the slug region and, in all probability, therefore, can be extrapolated without much loss in accuracy. The correlation for the slug region, on the other hand, was purposely restricted to a narrow region of liquid rates for which the relation between NTU and gas superficial velocity, at constant liquid rates, was

linear on an arithmetic plot. Because of this restriction, it was possible to obtain an unusual insight into the mechanisms of mass transfer and support for the theory proposed by Kishinevskii (discussed previously) for highly turbulent transfer processes. The general criteria for extrapolating the slug correlation can be qualitatively deduced, however, as considered in the section on Discussion and Conclusions. These developments will now be discussed in detail.

Bubble Region

In the development of a mass transfer correlation for the bubble region, a typical test section containing many bubbles will be considered. For this transfer process, where the logarithmic mean concentration driving force applies, the material balance for CO_2 has the form,

$$N_A = Q_L^o (C_2 - C_1) = k_L(A) \frac{(C_1^* - C_1) - (C_2^* - C_2)}{\ln \dfrac{C_1^* - C_1}{C_2^* - C_2}} \qquad (10)$$

where: N_A = transfer rate, millimoles sec^{-1}

Q_L^o = liquid superficial flow, ml sec^{-1}

C = concentrations millimoles cm^{-3}

A = interfacial area in test section, cm^2

$$k_L = \text{transfer coefficient, cm sec}^{-1}$$

To avoid consideration of the actual concentrations and mean concentration driving forces in the test section, expression (10) can be rewritten to a good approximation as,

$$Q_L^O \text{ NTU} = k_L (A) \tag{11}$$

It is recognized that the transfer coefficient in the above expressions is in all probability dependent on the square root of the product of the liquid diffusivity and surface renewal rate, according to the penetration theory model.

The development will first be undertaken for the case for which the volumetric liquid feed rate is constant, and also considerably greater than that of the gas rate, $(Q_L^O \gg Q_G^O)$. The absorption curves for such a situation can be observed in Figure 16. Two assumptions will be made concerning the frequency and shape of the bubbles produced with varying gas rates, in accordance with the discussion in the section on Theoretical Aspects. First, the frequency of the bubbles remains constant with an increasing gas rate at constant liquid rate and therefore, the increase in bubble volume is directly proportional to the volumetric rate of flow. This assumption is based on qualitative observations that not only for one liquid, but for all liquids tested, at the same superficial liquid velocities,

the frequency of the bubbles appeared to be approximately constant. The second assumption is that the bubbles maintain geometric similarity while increasing in size with increasing gas rates. As pointed out earlier, the amount of transfer area would be expected to be proportional to the 2/3 power of the gas volumetric flow rate for bubbles which expand uniformly in all dimensions, or nearly directly proportional to the gas rate for plugs expanding unidimensionally with increased gas flow. The first situation corresponds approximately to low ratios of gas to liquid volumetric flow rates, while the plug case corresponds to higher ratios.

The values for the NTU for all the liquids used, at a constant liquid velocity, show the same approximate dependence on the superficial gas velocity. For example, this similarity for two liquids of widely differing viscosity is well shown in Figure 16 for water and ethylene glycol. Such a similarity of behaviour with gas velocity, together with the observed constant bubble frequency at a constant liquid rate, implies that k_L, the transfer coefficient, must be reasonably constant in a given gas-liquid system as the gas velocity increases, and the observed variation in NTU with gas flow is a consequence largely of changes in interfacial transfer area, at least at low gas rates. Additional support for this conclusion may be drawn from

experimental observations made concerning the mixing effects in bubble flow. These effects are illustrated in Figure 9 for horizontally flowing bubbles in ethylene glycol. Even in this case, where the superficial liquid Reynolds number was about 200, the mixing and eddying due to "induced turbulence" was rather astoundingly vigorous. Any local concentration differences would be quickly and efficiently dispersed by this action, and the concentration profiles actually measured in the glycol solutions, shown in Figure 8, confirm this conclusion. For any liquid, therefore, flowing at a constant rate, changes in bubble size would be expected to have much less effect on the transfer rate than changes in bubble frequency.

Although it is difficult to describe quantitatively the shapes and surface areas of the bubbles as gas flow varies, some useful relationships can be derived. The surface area of each bubble has already been shown to vary as $(Q_G^0)^n$, where n has values between 2/3 and 1. The surface area in a test section of length, L, and containing a certain number of bubbles, will be proportional to the number of bubbles times the area of each bubble, that is,

$$A \propto \frac{fL}{V_B} (Q_G^0)^n \tag{12}$$

where f is the bubble frequency, sec^{-1}, and V_B is the bubble

velocity. The bubble frequency appears to depend primarily on the liquid flow rate, Q_L^O, and so it can be assumed that $f \propto (Q_L^O)^m$. The bubble velocity, V_B, is proportional to the true average liquid velocity, $(V_G^O + V_L^O)$, so one can also express this proportionality as $V_B \propto (Q_G^O + Q_L^O)^P$. Making these substitutions in (12),

$$A \propto \frac{(Q_L^O)^m L}{(Q_L^O + Q_G^O)^P}(Q_G^O)^n \tag{13}$$

The transfer coefficient, k_L, for a submerged object is known to be generally a function of the degree of turbulence in the ambient fluid, and hence for this case of horizontally moving bubbles, it must depend strongly on the number of bubbles per unit length of tube because of the induced turbulence, due to presence of these bubbles, and probably to a rather lesser degree, on the true average liquid velocity itself. On these assumptions, one can write,

$$k_L \propto k_L' \frac{(Q_L^O)^q}{(Q_L^O + Q_G^O)^n} \tag{14}$$

The k_L' is the part of the transfer coefficient dependent on parameters other than the flow quantities.

The above relationships are now substituted into equation (11) giving,

$$Q_L^O \ NTU = k_L A \propto k_L' \left[\frac{(Q_L^O)^b}{(Q_L^O + Q_G^O)} \right]^a (Q_G^O)^n \qquad (15)$$

For the case of $Q_L^O \gg Q_G^O$, that is, for bubbles approaching spherical or elliptical shapes, "n" in the above equation should have a value of approximately 2/3. If the exponent "b" is assumed to be equal to unity, than equation (15) assumes a particularly simple form,

$$Q_L^O \ NTU \propto k_L' (Q_G^O)^{2/3} \qquad (16)$$

and this expression should apply for all liquid rates at low gas rates in a given system. A logarithmic plot of $Q_L^O(NTU)$ vs Q_G^O for the CO_2-water system is shown in Figure 19. Values of $Q_L^O(NTU)$ (which are equal to $k_L A$) can be seen to fall on a single line in the region of low gas rates for a range of liquid volumetric flow rates from 5 to 34 cfh. This provides a good deal of support for the foregoing assumptions in general, and particularly for the assumption that the exponent, b, can be taken as equal to unity. Equivalent tests for the effect of liquid and gas flow on the mass transfer rate for all other gas-liquid systems investigated yielded essentially identical results. In all cases the exponent "n" for low gas flow rates had a value approximately equal to 2/3.
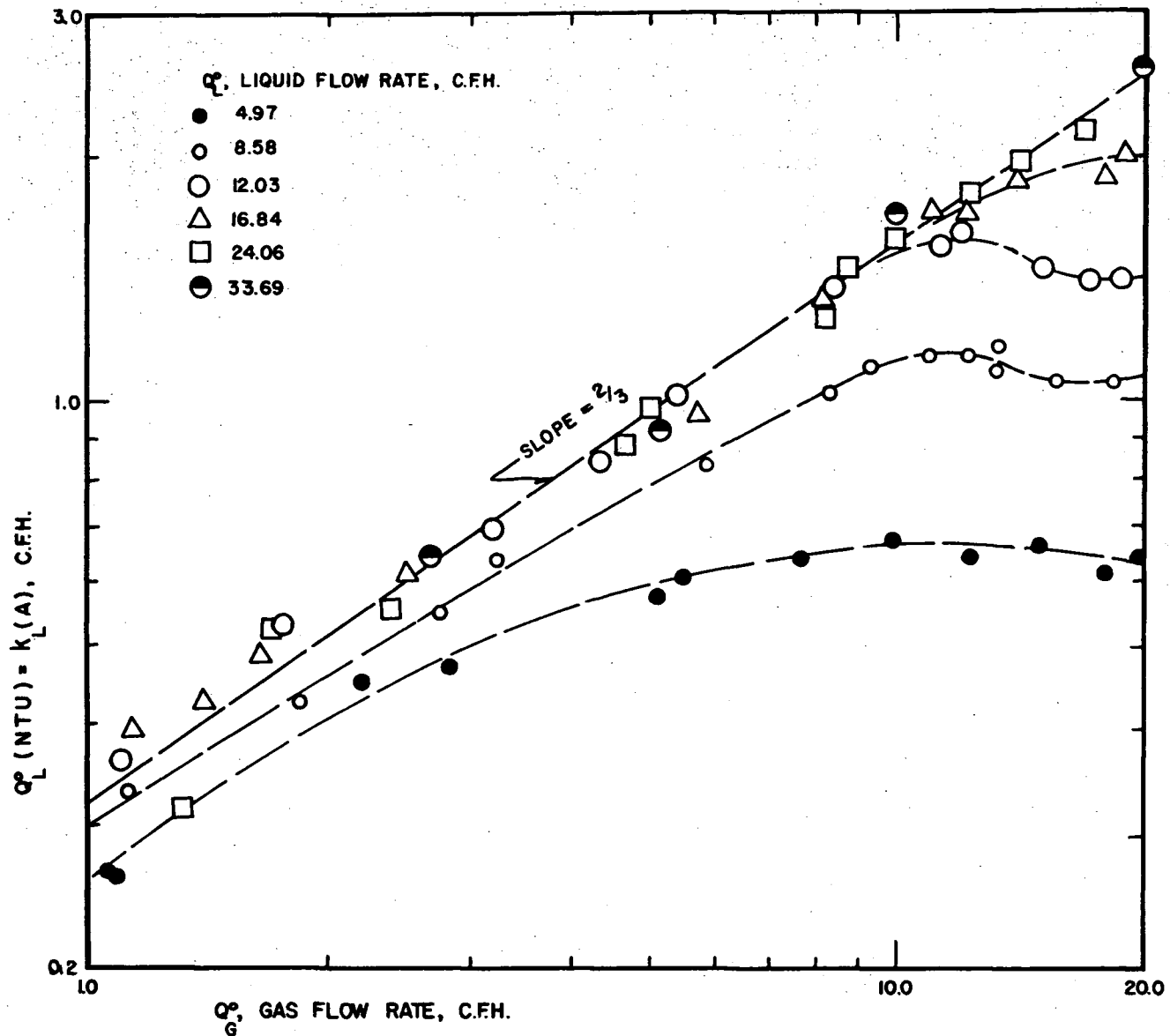
Figure 19. Effect of Liquid Flow Rate at Low Gas Rates, on the Rate of Absorption Using the CO_2-Water System

As the gas flow rate increases relative to the liquid flow, the slope of the $k_L(A)$ vs Q_G^O curve should become a decreasing function of Q_G^O as the gas volumetric flow becomes of the same order of magnitude as the liquid flow. If the exponent, a, is sufficiently large, that is, greater than 2/3, then when $Q_G^O \gg Q_L^O$, maximum values of the quantity $k_L(A)$ might be observed. This maximum would show most clearly at low liquid rates. If long plug flow occurred at flows of gas high relative to those of the liquid, (n=1), then it might be possible for $k_L(A)$ to become essentially independent of the gas rate. These characteristics are exactly observed in Figure 19 for the lowest liquid rate. The inference is that the index, a, is greater than 2/3, and has a value between 2/3 and unity.

The original equation (15) can be considerably simplified if the exponent, a, is taken as equal to unity, and the final correlating equation then becomes,

$$(V_L^O + V_G^O)\text{NTU} \propto k_L'(V_G^O)^S \tag{17}$$

This expression brings all the data for each of the gas-liquid systems into good agreement over wide ranges of the bubble and plug flow regions. The ability of equation (17) to bring together all the data for each of the gas-liquid systems studied, particularly those for CO_2-water and CO_2-glycol, and for the

index, S, to be very nearly the same for all systems and between 2/3 and unity, provides considerable evidence that the model for mass transfer chosen for this region of flow is correct.

The effects of the variables, diffusivity, viscosity, surface tension, and tube diameter, were introduced into expression (17) as simple dimensionless ratios with the basis of comparison being the CO_2-water system at $15^{o}C$ and the tube dimension of 1.757 cm in diameter. Thus in the bubble region the correlating expression for all the variables becomes:

$$Z = (V_L^O + V_G^O)NTU\left[\frac{\mathscr{D}_w}{\mathscr{D}_x}\right]^d\left[\frac{\sigma_w}{\sigma_x}\right]^e\left[\frac{\mu_w}{\mu_x}\right]^g\left[\frac{D_x}{D_w}\right]^h \propto (V_G^O)^S \qquad (18)$$

where: $\mathscr{D}$ = diffusivity

σ = surface tension

μ = viscosity

D = tube diameter

V_G^O, V_L^O = gas and liquid superficial velocities, fps

indices:

d = 0.50

e = 0.50

g = 0.14

h = 2.0

subscripts:

w = values for CO_2-water system at $15^{\circ}C$, tube diameter

1.757 cm

x = equivalent property for each of the other gas-liquid

systems and conditions.

The powers chosen for the dimensionless ratios were those which tended to bring the data into closest agreement with the reference system. The experimental data as correlated using equation (18) were calculated by means of an IBM 1620 computer, and are graphically represented in Figure 20. A linear relationship on the logarithmic plot was fitted to these data, and the equation of the best straight line was fitted by the method of least squares. The resulting equation is as follows:

$$Z = (0.2024)(V_G^o)^{(0.8075)} \qquad (19)$$

Equation (19) was derived for a range of gas superficial velocities from approximately 0.1 to 3.0 fps. This range included bubble flow and was extended well into the plug flow region. The number of transfer units for a length of tube 92.2 in, can be predicted from equation (19) with a probable error not exceeding 15 per cent.
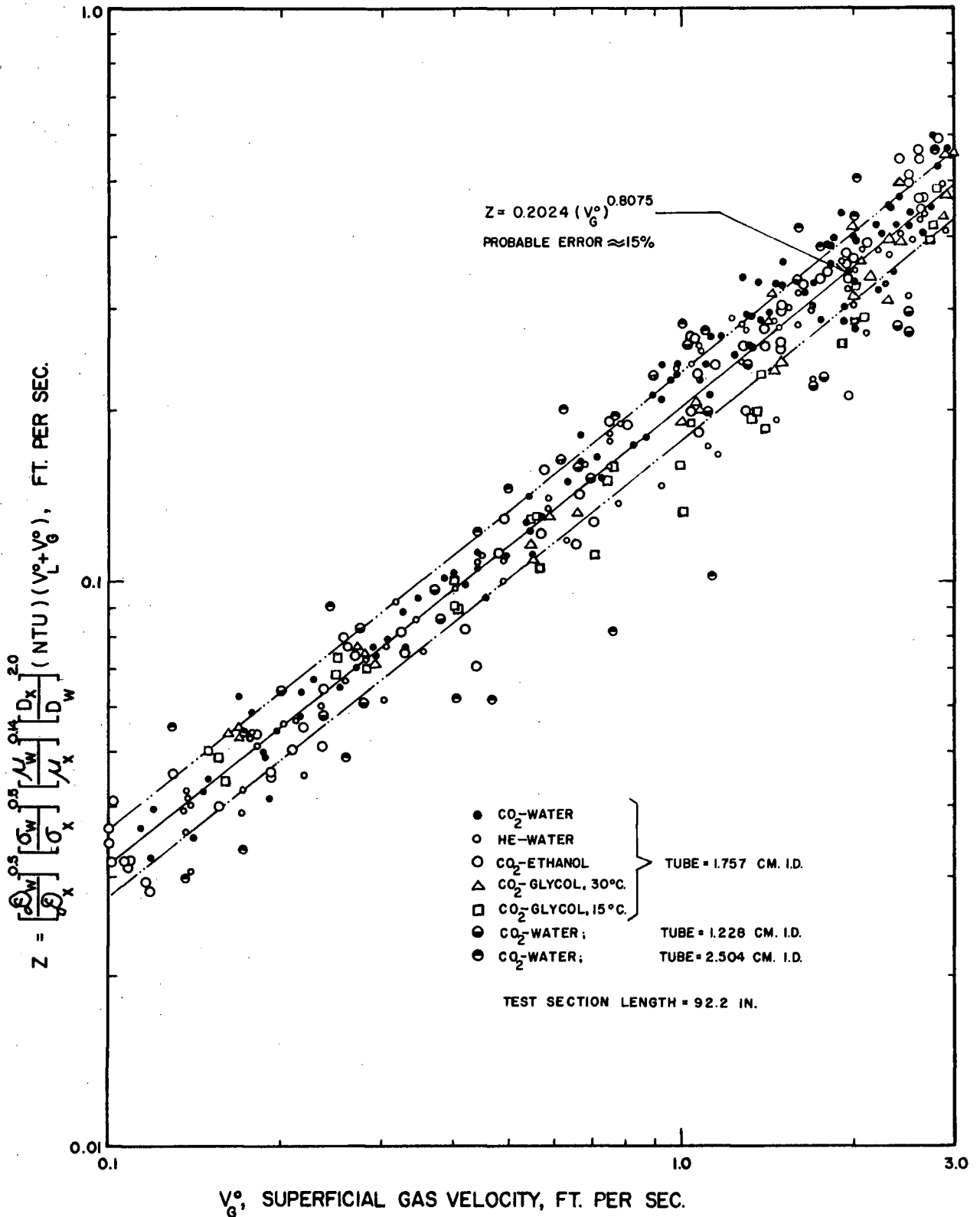
Figure 20. Correlation for Two-Phase Flow Absorption Rates
for the Bubble and Plug Regions

Slug Region

For the turbulent slug region an attempt was made to show
quantitatively that the degree of turbulence _itself_ affected
the extent to which the various system variables, diffusivity,
viscosity, surface tension, and tube diameter, influenced the
rate of mass transfer. That is to say, for example, that the
effect on the transfer rate of the liquid phase molecular diffu-
sivity was in turn affected by the degree of turbulence. Such
an interaction between the molecular properties, diffusivity,
and viscosity, at least would be expected if either the Kishi-
nevskii theory, as discussed earlier, or some other transfer
process in addition to that of simple surface renewal, were
operative in the slug region of flow.

The linear relationship on an arithmetic plot of the NTU
and gas superficial velocities for essentially all the gas-liquid
systems and conditions, made it possible to readily separate the
effects of the various variables. Except for the experimental
runs with the CO_2-water system at two liquid superficial velo-
cities exceeding approximately 2 fps., a good linear NTU-V_G^o
relationship was obtained.

The methods and reasoning which were used in producing
the particular type of empirical correlation developed here

are outlined in the following section. Figures 21, 22, and
23 show NTU and V_G^o data for all the gas-liquid systems, plotted
on linear coordinates, each graph corresponding to a single
superficial liquid velocity, respectively, 0.53, 0.91 and 1.79
fps. The values for these plots were taken directly from the
best visually estimated lines through the actual experimental
data of Figures 14, 15, and 16. Actual experimental data and
appropriate computer programs could have been used for establish-
ing best straight lines fitted by the method of least mean
squares; however, as subsequent analysis will show, the omission
of such procedures does not significantly limit the accuracy of
the overall results.

The major underlying assumption for the slug region (which
was also assumed in the bubble region) will be restated here.
It is, at equal gas and liquid superficial velocities, the mass
transfer rates are directly comparable and any difference in
transfer rates that is observed for different systems, therefore,
is the consequence of system variables other than flow. It is
recognized that such an assumption becomes more dubious as the
velocities of both phases increase, generally increasing the
probability of kinetic energy effects and flow interactions.
In addition, it is known that the fraction of the tube volume
occupied by liquid is governed not only by the flow variables,
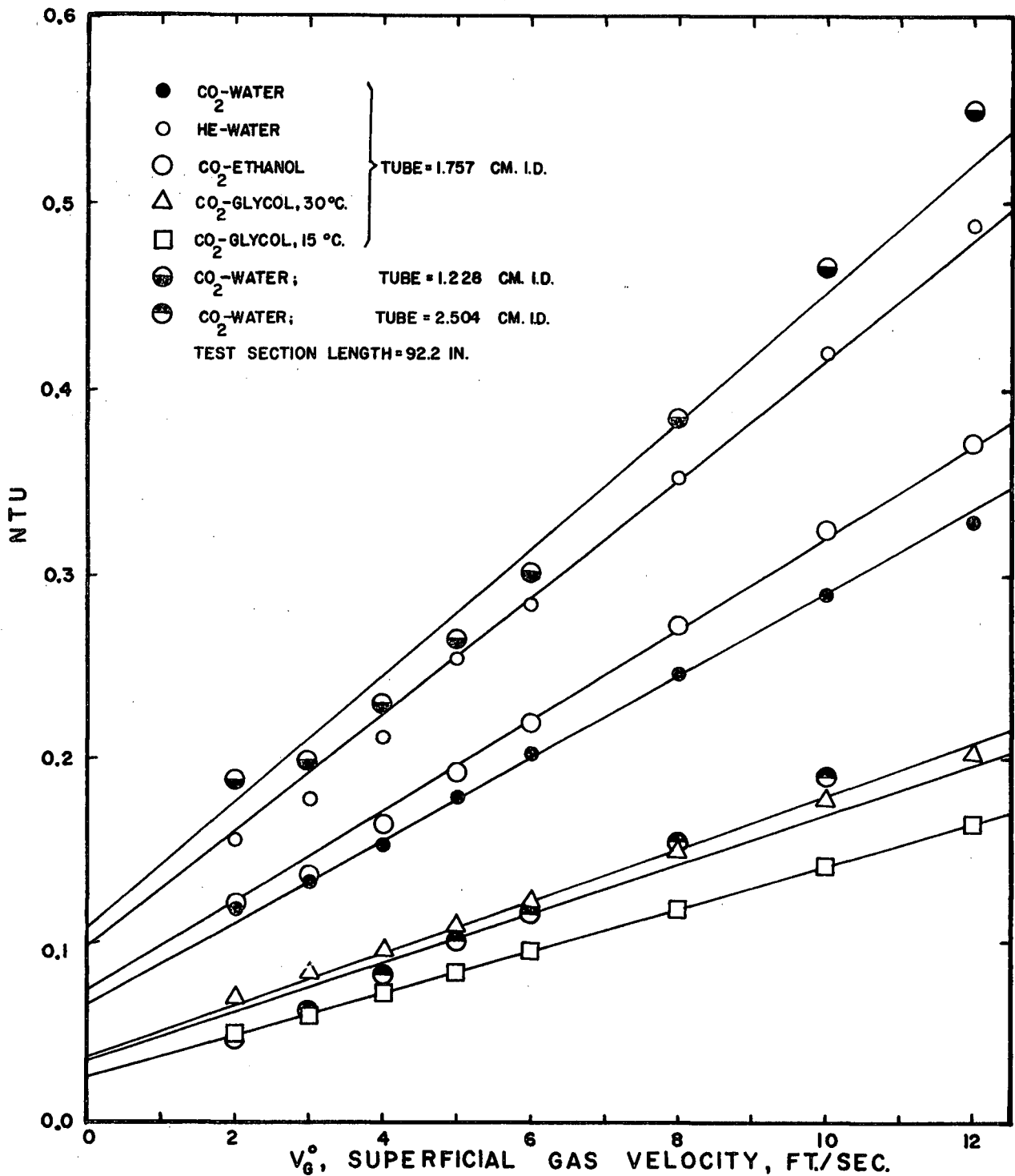
Figure 21. Absorption Rate vs Gas Superficial Velocity for
Slug Region at a Liquid Superficial Velocity of 0.53 fps
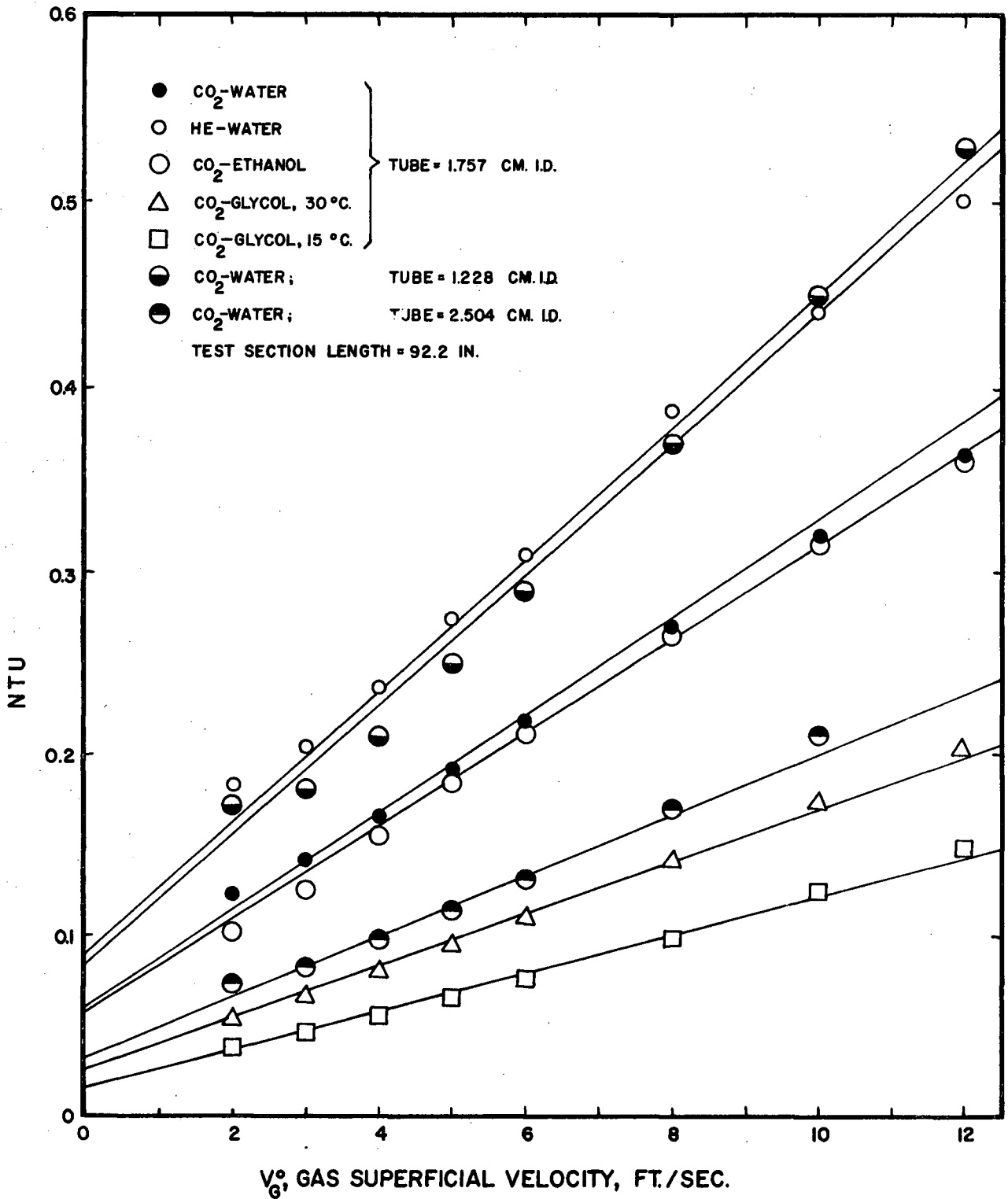
Figure 22.   Absorption Rate vs Gas Superficial Velocity for
Slug Region at a Liquid Superficial Velocity of 0.91 fps
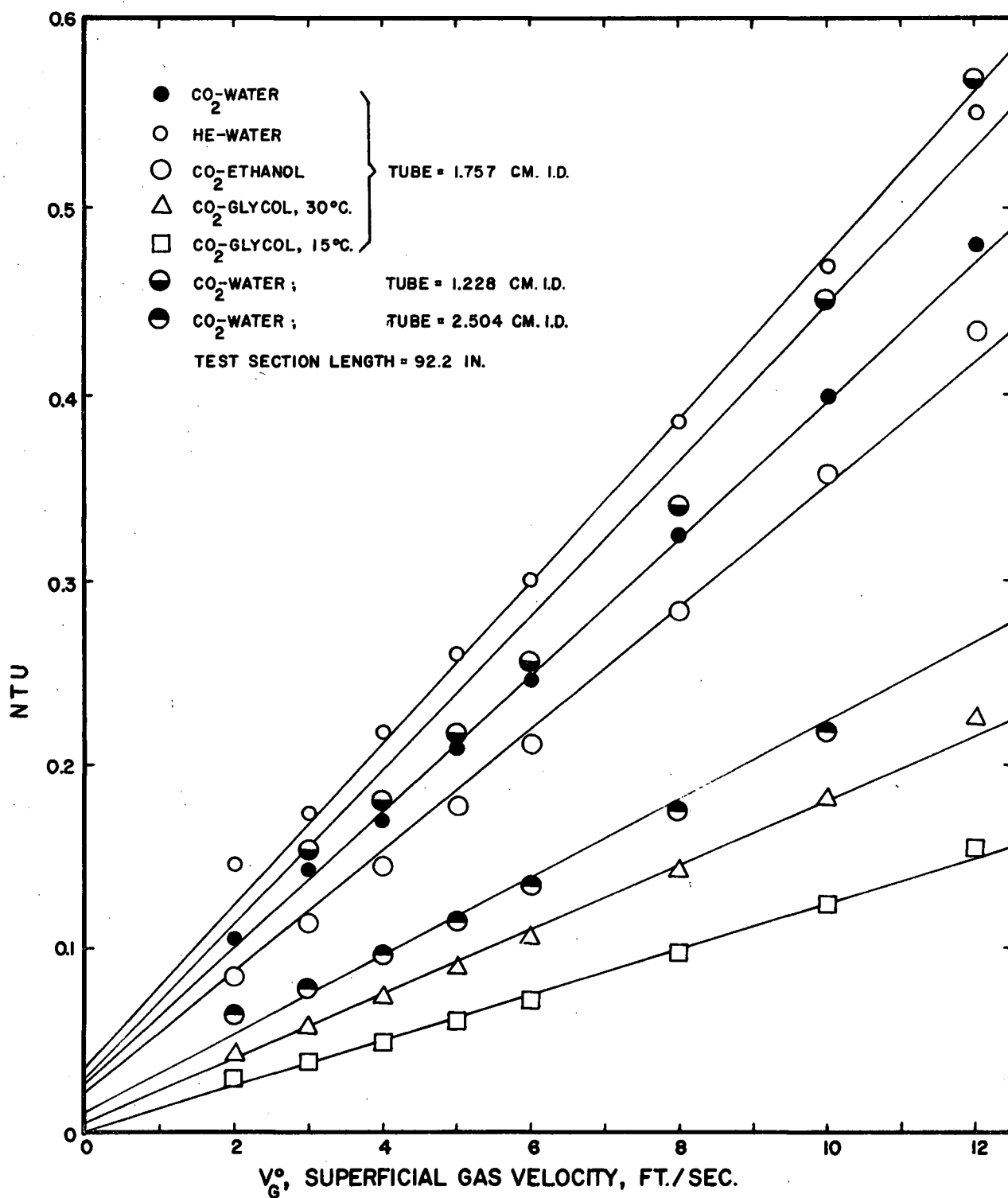
Figure 23. Absorption Rate vs Gas Superficial Velocity for Slug Region at a Liquid Superficial Velocity of 1.79 fps

but to a lesser extent by viscosity and surface tension. An estimate of the effect of these liquid properties on the liquid volume fraction can be obtained from void fraction correlations such as those of Lockhart and Martinelli (55), or Hughmark and Pressburg (56). The evidence that specific limits for the slug and slug-annular regions at fixed gas rates correspond approximately to constant values of the liquid superficial velocity, is also not completely convincing. Results obtained in these studies, however, indicate that the magnitude of the liquid flow effects themselves, without changes in any other of the liquid properties or conditions, is small (but not negligible) in comparison to that caused by these other properties and conditions. Referring to Figures 21, 22, and 23, for any one gas-liquid system (and temperature), a variation in liquid superficial velocity by a factor of more than three changes the slope of the NTU-V_G^o line somewhat, but changes the magnitude of the actual value of NTU at a specific gas velocity by only a small amount compared to the changes in NTU between different gas-liquid systems. This is particularly evident when comparing the relationships for He-water and CO_2-glycol.

A further observation can be made from Figures 21, 22, and 23. Increasing slopes invariably correspond to increasing intercepts. An empirical equation suggested for each of the

systems, therefore, is as follows:

$$NTU + k = b\,c + b\,V_G^O = b\,(c + V_G^O) \qquad (21)$$

where: $b\,c - k$ = intercept at $V_G^O = 0$

NTU = number of transfer units for 7.683 ft of tube

V_G^O = gas superficial velocity, fps

b = slope of NTU-V_G^O relationship and factor which

determines the position of the intercept;

depends on physical properties for each of

the gas-liquid systems, and also on V_L^O

c = proportionality constant which depends only

on V_L^O, for all gas-liquid systems

k = single constant for all systems and conditions

In equation (21) only the variable "b" is a function of the liquid flow rate as well as of the properties of the gas-liquid systems. The variable "c" is a function of the liquid superficial velocity only, and is therefore constant for any one liquid rate, while the constant "k" is completely invariant with flow rates and system properties.

The particular form of equation (21) was chosen because only the single variable "b" was dependent on the physical properties of the contacting fluids. It was therefore possible to relate the slopes of any two NTU-V_G^O straight lines, corres-

ponding to different properties but at the same liquid super-

ficial velocity, directly to the effect of the difference in

the properties concerned. The determination of the constant

"k", and variables, "b" and "c", involved an extensive trial-

and-error procedure. It was somewhat simplified because the

value of the constant, "k", necessary to fit the experimental

data was obviously small. Because of the trial-and-error

procedure used, it was easiest to evaluate the variable "c"

for the three values of V_L^o. These values of "c", along with

the effect of V_L^o on the variable "b", are graphically shown in

Figure 24. For the limited range of liquid flows, the effect

of V_L^o on both of the quantities "b" and "c" is linear.

In the same way as was done for the bubble region, the

effects of the different system variables were expressed as

simple dimensionless ratios, which appeared to best describe

the experimental data. Separate exponents for these dimension-

less ratios were determined, however, for each of the three

liquid rates, these rates corresponding to changes in degree

of turbulence. The correlating equation for the slug region,

obtained by comparing the NTU-V_G^o slopes for the different

systems, and based on liquid superficial velocities not

exceeding 2 fps, is then as follows:
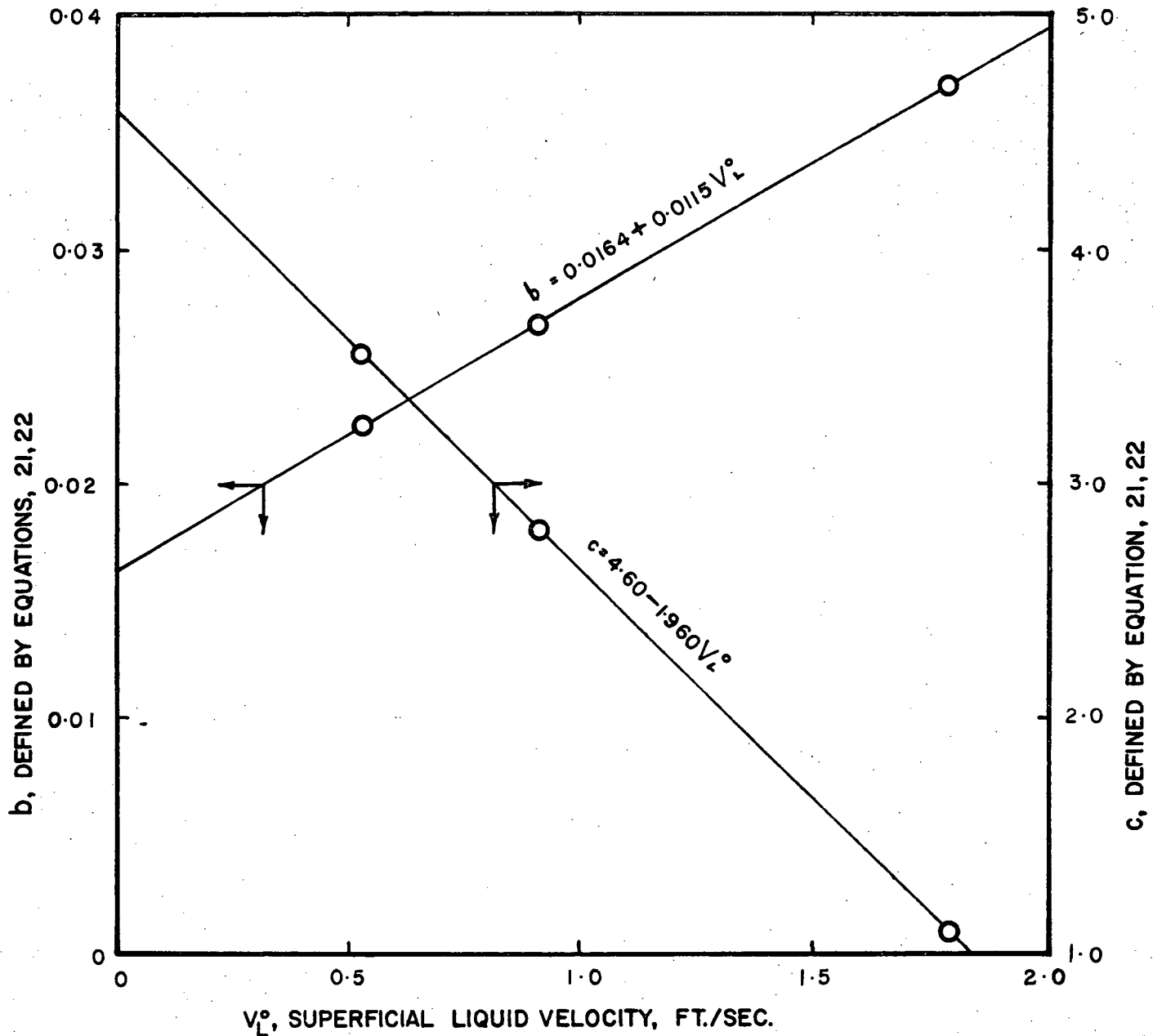
Figure 24. Values of "b" and "c" vs Liquid Superficial Velocity to be Used in Equation (21)

$$X = NTU + k = F b (c + V_G^O) \qquad (23)$$

where: $k = 0.014$

$b = 0.0164 + 0.115(V_L^O)$

$c = 4.60 - 1.960(V_L^O)$

V_L^O, V_G^O = liquid and gas superficial velocities, fps

$F = 1.0$ for the CO_2-water system at $15^O C$, tube diameter 1.757 cm

$$F = \left[\frac{\mathscr{D}_x}{\mathscr{D}_w}\right]^d \left[\frac{\sigma_x}{\sigma_w}\right]^e \left[\frac{\mu_x}{\mu_w}\right]^f \left[\frac{D_w}{D_x}\right]^g \qquad (24)$$

where: $\mathscr{D}$ = diffusivity

σ = surface tension

μ = viscosity

D = tube diameter, cm

w = values for the CO_2-water system at $15^O C$, tube diameter 1.757 cm

x = equivalent property for each of the other gas-liquid systems and conditions

For each liquid flow rate the exponents for the four dimensionless ratios were obtained by the general method outlined in the section on the Design of Experiments. The variability in the effects of the molecular properties, viscosity

and diffusivity, due to the changes in liquid flow rate, is most pronounced. Figure 25 graphically shows the changes of the exponents with the liquid flow rates, for the effects of the three physical properties and the tube diameter. The data for the values of the exponents which apply to equation (24) are also listed in Table 10.

Figure 26 shows a plot of NTU and V_G^o for the CO_2-water system for the two additional liquid superficial velocities exceeding 2 fps. The relationships are no longer linear. If values of the NTU at superficial liquid velocities exceeding 2 fps and for other gas-liquid systems are required, it seems likely that the CO_2-water curves shown in Figure 26 could be applied, and suitable extrapolated indices for use in equation (24) could be obtained from Figure 25, to give acceptable values for the mass transfer rates in this portion of the slug region.

The gas superficial velocities for the proposed correlation ranged from 2 to 40 fps, while the liquid superficial velocities ranged from 0.53 to 1.79 fps. A test for the proposed correlation is graphically shown in Figure 27, where the experimental NTU values are plotted against those predicted by equations (23) and (24). The relatively small scatter from the 45° line, with a probable error of approximately 10%, indicates the satisfactory degree of correlation achieved.
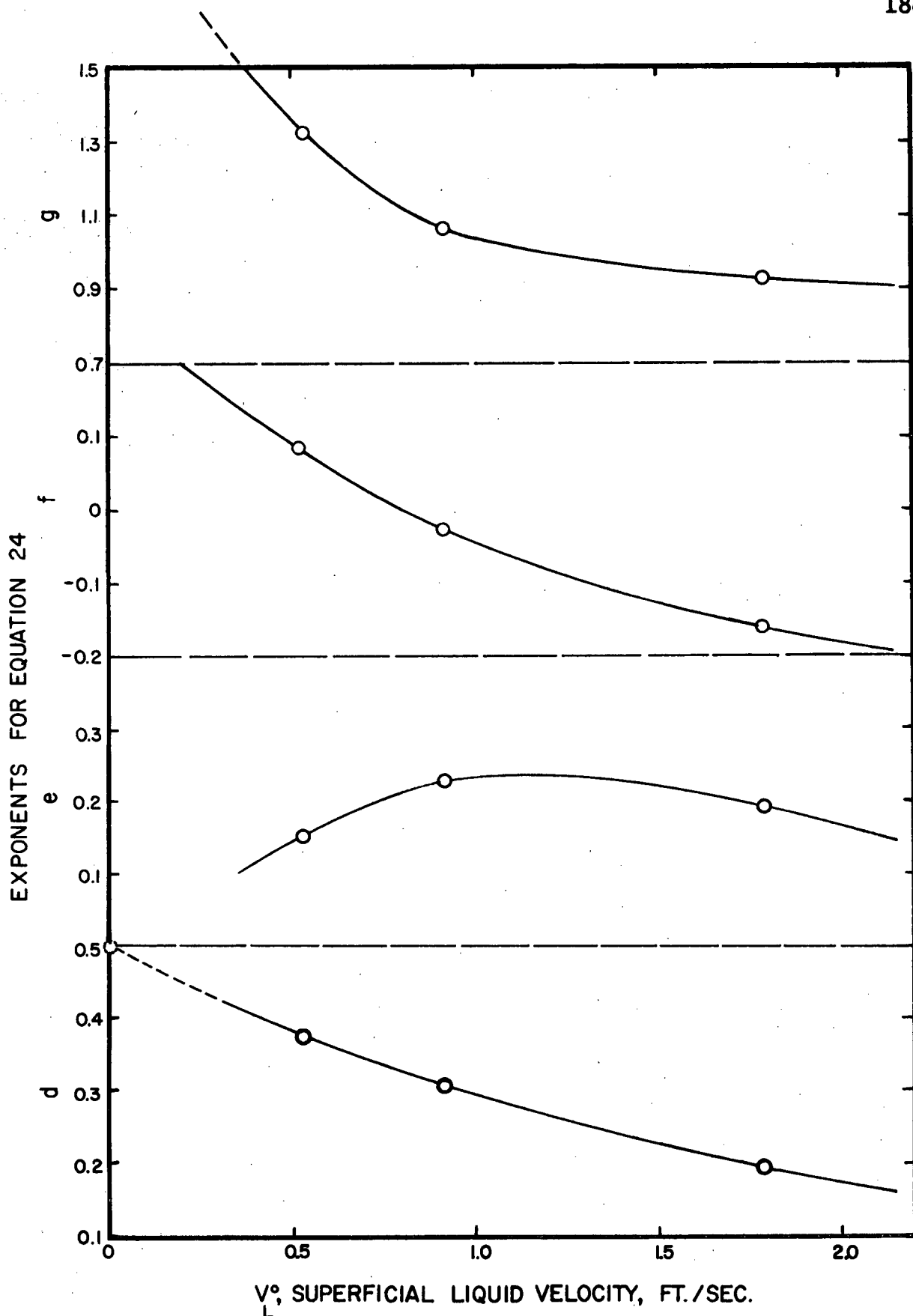
Figure 25. Exponents for Dimensionless Ratios in Equation (24)
as Functions of Liquid Superficial Velocity

TABLE 10

EXPONENTS FOR DIMENSIONLESS RATIOS IN EQUATION (24),

VARIABLE WITH LIQUID SUPERFICIAL VELOCITY

V_L^O = liquid superficial velocity, fps

Ratio	Exponent	$V_L^O = 0.53$	$V_L^O = 0.91$	$V_L^O = 1.79$
Diffusivity	d	0.374	0.307	0.193
Surface tension	e	0.151	0.228	0.193
Viscosity	f	0.086	-0.028	-0.161
Tube diameter	g	1.32	1.063	0.913
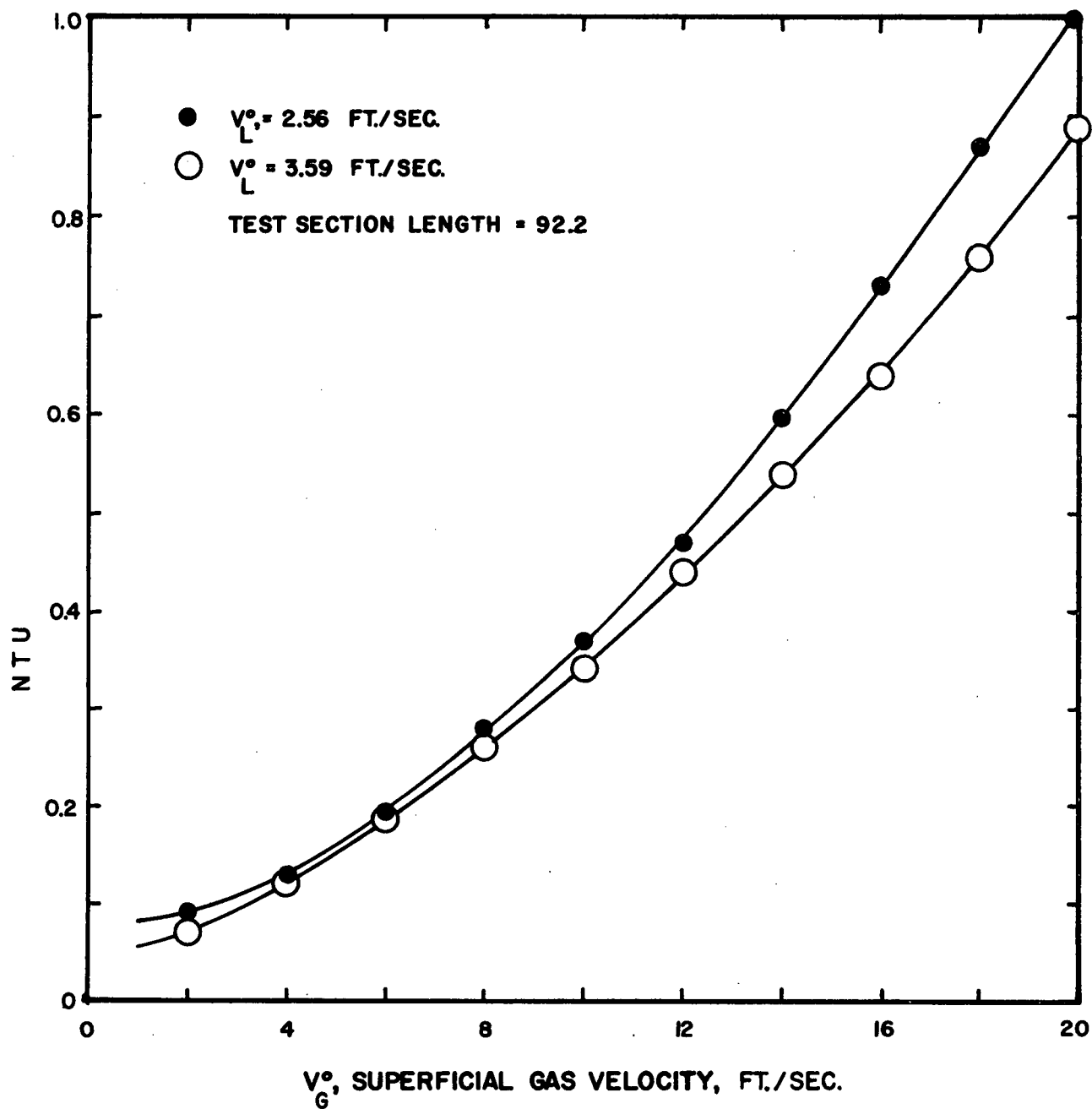
Figure 26. Graph of NTU vs Gas Superficial Velocity for the
CO_2-Water System at Liquid Superficial Velocities
Exceeding 2 fps
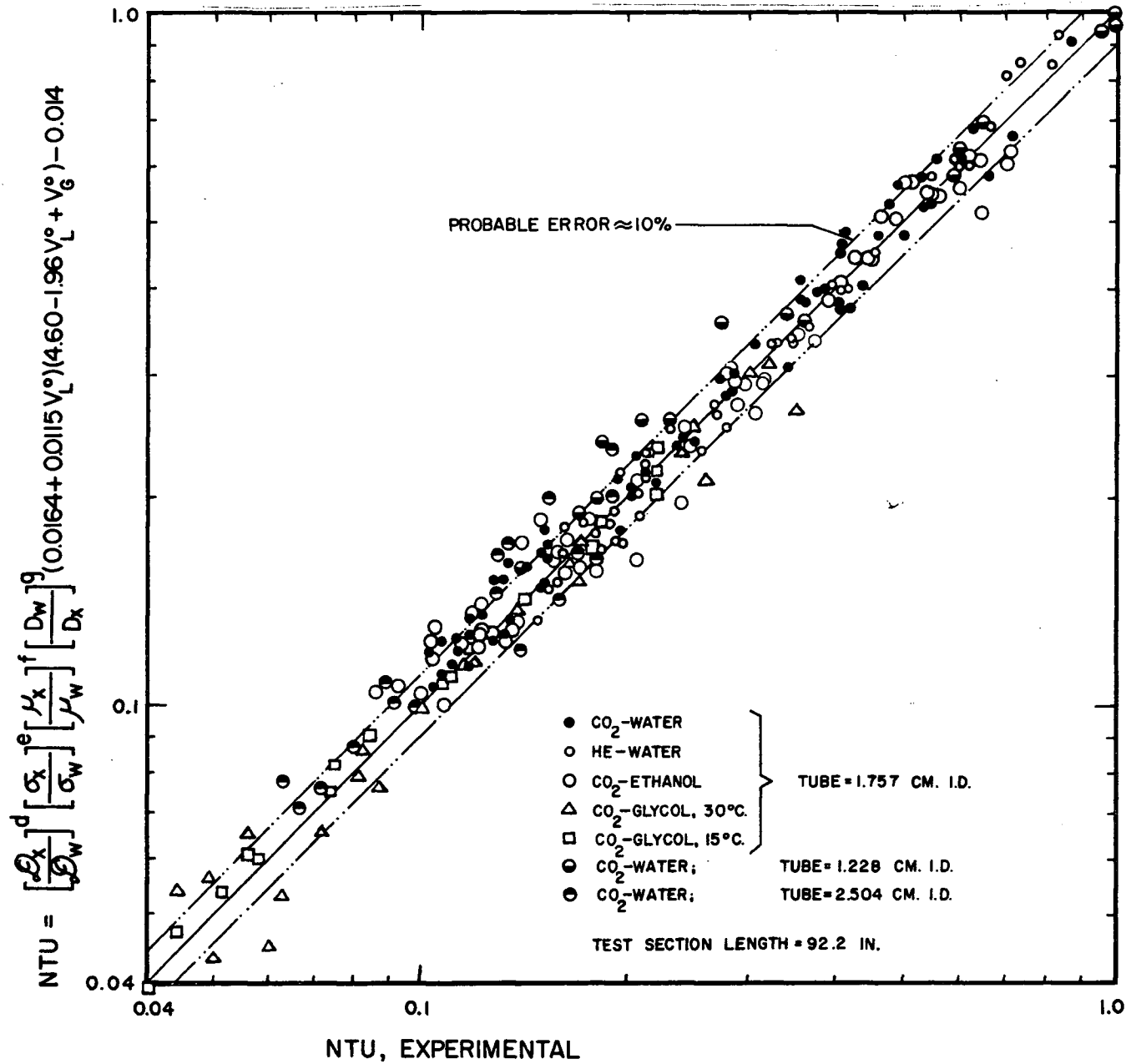
Figure 27. Correlation for Slug Region, Calculated vs Observed Values of NTU

DISCUSSION AND CONCLUSIONS

One of the major observations from the results of this investigation concerns the role of turbulence with respect to the rates of mass transfer. The mixing and eddying effects which have been observed in ethylene glycol at superficial Reynolds numbers well in the laminar region indicate that "induced turbulence" caused by changing directions of flow within the bulk of the liquid can be a much more significant source of mixing than that due to an average velocity vector in the direction of flow. For both the bubble and slug regions, it would appear that there are two major causes of the accentuated turbulence which seems to be a characteristic feature of two-phase flow. They are first, the effectively changing cross-sectional area of the flow channel for each phase, and next the existence of a movable interface which permits an interaction of forces between the phases.

The success of the model for liquids of widely differing properties, which relates the source of turbulence in bubble flow to the presence of the bubbles themselves, suggests that a simple Reynolds number based on tube dimensions and the flows of one or both phases is not a satisfactorily descriptive quantity for the flow characteristics for the bubble region.

Similarly in slug or annular flow, a Reynolds number based on

tube dimensions and true linear velocities of one or both phases

might be very useful, but is again difficult to relate to true

two-phase flow characteristics. For these reasons, the condi-

tions of flow have been described simply by phase superficial

velocities. It is probable that a "bubble" Reynolds number

might be a significant parameter in bubble flow, but such a

Reynolds number is difficult to define explicitly because of

the unsymmetrical nature of bubble flow.

Because of its complexity, and lack of similarity to

that for single-phase flow, the mass transfer process in two-

phase flow would seldom appear to warrant treatment in a manner

similar to that for single-phase flow. Mass transfer in single-

phase flow is involved with transfer from a solid boundary which

is (normally) immobile. The shear force at the wall is mani-

fested as pressure drop and (for single-phase flow) is well

defined by the flow rate, physical properties, and channel

dimensions. The transfer of both shear and mass occurs at the

same location, at the channel wall, and is governed by related

flow characteristics, and for this reason relationships between

mass and momentum transfer have been successful. In two-phase

flow, on the other hand, although the shear at the wall is also

manifested as pressure drop as for single-phase flow (but not

so well defined), the mass transfer occurs at another location in the flow channel altogether, at the interface, and is therefore dependent on the host of variables influencing the conditions of the interface. Further, as a result of this work, it appears likely that the mechanism of transfer changes in different regions of two-phase flow. Hence, for two-phase flow the relationships between shear at the wall and mass transfer at the interface, if they can be determined, will, in all probability, be highly complex. The methods of study most likely to be successful in two-phase flow are those which are fundamental in nature, and which avoid direct comparison with the usually completely dissimilar phenomena for single-phase flow unless such a comparison is logically justified.

Bubble Flow

The physical model as developed for bubble flow in the section on Development of Correlations, and the resulting correlation as described by equation (18) will be discussed in this section. One of the most significant factors in these results is the dependence of the transfer rate on the liquid phase diffusivity to the 0.5 power. This gives strong support to the usefulness of the surface renewal or penetration theory models for mass transfer in this region. The 0.5 exponent for

the diffusivity ratio is further substantiated by applying the

bubble flow correlating equation to the CO_2-water results

obtained at various temperatures. As indicated earlier, absorp-

tion data were obtained at one liquid rate, 1.07 gpm, one tube

size, 1.757 cm, and at three temperatures (in addition to $15^{\circ}C$),

$5.3^{\circ}C$, $30^{\circ}C$, and $45^{\circ}C$. For this range of temperatures, the vis-

cosity ranged from 0.60 cp to 1.50 cp, while the liquid diffus-

ivity ranged from 3.08 (10^{-5}) to 1.07 (10^{-5}) cm^2 sec^{-1}. As

would be expected, the temperature variation had only a small

effect on the surface tension. The exponent on the viscosity

ratio in the correlating equation (0.14) was small, so that

the viscosity effect on the absorption rate would be expected

to be likewise, small. The approximately three-fold variation

in diffusivity was used as a further check on the effect of

diffusivity on the absorption rate. Figure 28 shows a plot of

the least mean squares line and the 15% probable error limits

for the bubble flow correlation, and the CO_2-water data obtain-

ed at the various temperatures. The fact that these latter

data fall exactly on the same correlating line constitutes an

independent check of the applicability of the correlating equa-

tion particularly with respect to the effect of liquid phase

diffusivity on the mass transfer rate in bubble flow.

There is what appears to be an anomalous effect of viscosity
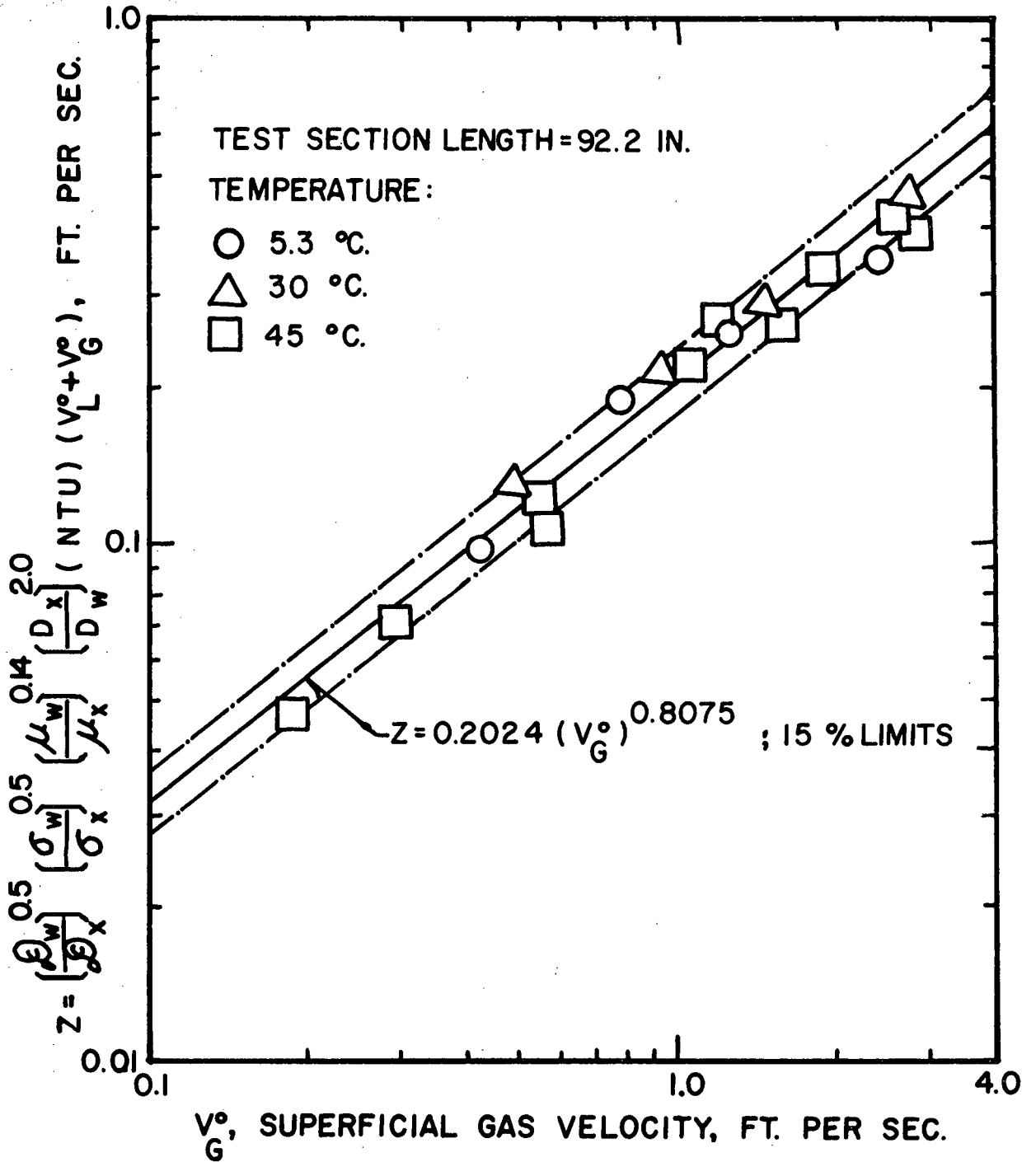
Figure 28. Application of the Bubble Flow Correlation to CO_2-Water System Data at Various Temperatures

on the transfer rate in the bubble region. One might expect
that the assumption that the degree of turbulence is a result
of the number of bubbles or "mixing stages", if not completely
accurate, would err in the direction of reduced turbulence with
increased viscosity. From expression (18) it is noted that the
index of the viscosity ratio although small (0.14) as might be
expected, is in the direction which indicates an increased
transfer rate with higher viscosity liquids. The likely explan-
ation might be that for more viscous liquids a greater fraction
of the area of each bubble is exposed to the liquid. For
ethylene glycol the assumption that a constant fraction of each
bubble supposedly ineffective for mass transfer because of
direct contact with the tube wall, may not be accurate.
Because of the liquid viscosity, as each bubble moves, more
time may elapse for the drainage of liquid down the sides of
the tube, in this way effectively increasing the fraction of
interfacial area per bubble available for mass transfer. This
appeared to be at least qualitatively true from visual observa-
tion of bubble flow with ethylene glycol. The increase in
transfer rate for the more viscous liquids would then be a
direct consequence of an increased interfacial area.

For large "chain bubbles" rising up through a liquid, two
observations which appear pertinent to this work have been

reported by Calderbank (57). The first is that liquid phase mass transfer coefficients for a continuous sequence of bubbles rising through a depth of liquid are found to be appreciably greater than those for individual bubbles, which are equal in size and under otherwise identical conditions. The difference is ascribed to the effect of the bubbles wakes which leave the liquid in a more turbulent state in the case of the "chain bubbles". This effect gives more credence to the phenomenon referred to as "induced turbulence" in horizontal bubble flow.

The second observation made by Calderbank is that the liquid phase coefficients of mass transfer for large bubbles rising in a liquid can be expressed by the common type of relationship:

$$Sh \propto (Sc)^{0.5} (Re)^n \tag{25}$$

where: Sh = Sherwood number

Sc = Schmidt number

Re = Reynolds number

n = 0.77

Another explanation for the observed dependence on viscosity of the mass transfer rate in a two-phase bubble flow is that the interfacial area remains constant, and that equation (25) is applicable. For such a situation, whatever the true definition

of the Reynolds number, the exponent "n" would of necessity

have to be less than 0.5 (actually 0.36) in order for the

observed net dependence of the transfer rate to be directly

proportional to the liquid viscosity to the 0.14 power. Mass

transfer coefficients increasing with viscosity have not been

reported in any of the reviewed literature. It appears most

likely, therefore, that the first explanation for the effect of

viscosity is the more probable.

As indicated in the section on Theoretical Aspects, one

would probably expect that bubbles in liquids having lower

surface tensions, but otherwise having comparable physical

conditions and properties, would be longer and thinner and hence

provide a larger interfacial area per bubble. In comparing the

results for the CO_2-ethanol and CO_2-water systems a slightly

higher transfer rate for the CO_2-ethanol systems might be

expected, therefore, after accounting for the difference in

liquid diffusivities for these two systems. This behaviour was

not observed, however. On the contrary, as indicated by the

correlating equation (18), the lower surface tension greatly

reduced the rate of transfer for comparable conditions. This

effect is similar in this respect to the damping effect of

monolayers which reduce surface rippling, and thereby reduce

surface areas and transfer rates. The damping effect of

monolayers has normally been considered a consequence of the
"resistance to local compression". Since the reduction in
transfer rate was observed for pure (absolute) ethanol as the
test liquid, the interface was expected to have been free of any
monolayer. For a turbulent "clean" interface according to
Levich (58), a reduction in surface tension should enhance the
transfer rate. For a number of reasons this writer is not will-
ing to accept that for the experiments with the CO_2-ethanol
system, the observed reduction in the transfer rate could have
been caused by the presence of a monolayer, even although this
would seem to explain the experimentally measured effect.
The reasons are that absolute ethanol was used in the experi-
mental equipment, which was initially flushed with this liquid,
and then charged for a series of experiments. After a period
of experimentation of several weeks, a noticeable drop in trans-
fer rate at equivalent flow conditions occurred, then indicating
the presence of contaminants. After a second flushing and
complete recharging with fresh absolute ethanol, original
results were reproduced, and again after a period of operation
a reduction in transfer rate was observed. The results for
the reduced rates of transfer were discarded because of presumed
contamination. The results, duplicated for the fresh ethanol,
therefore, are considered to reflect the true effect of the

surface tension of a pure liquid. No completely logical explan-
ation for this observed effect of surface tension has been found
in recent publications, nor have any experiments designed to
separate the effects in such dynamic systems as two-phase flow
been found in the current literature. Although it is outside
the scope of this research, a purely hypothetical reason
for the observed effect of surface tension can be suggested if
one makes the following assumptions:

(a) The interface can be treated as a membrane which vibrates
     because of localized eddying.

(b) The amplitude of vibration is mainly determined by buoy-
     ancy and other hydrodynamic conditions.

(c) A vibrating string represents a one-dimensional view of
     the two-dimensional situation of a vibrating membrane.

(d) The transfer coefficient is directly proportional to
     the frequency of vibration, at constant amplitude, for
     the two-dimensional membrane.

If the foregoing rather gross assumptions were true, the fre-
quency of vibration would be directly proportional to the
square root of a tension force of a string (59), and equi-
valently the mass transfer coefficient would be directly pro-
portional to the square root of a surface tension force for the
interfacial membrane, as obtained in equation (18). The above

hypothesis illustrates that there may be a completely logical

reason for the dependence of mass transfer on surface tension.

A second explanation for the decreasing effect on the mass

transfer rate with liquids of lower surface tension can be

obtained from the work of Baird and Davidson (60). They observed

that for large single bubbles immersed in a "pure" liquid, the

mass transfer rates were approximately 50% higher than the rates

calculated from surface renewal theory. They attributed these

high transfer rates to the presence of interfacial capillary

ripples, which had a marked effect on the transfer rate exceed-

ing the contribution of the ripples to the interfacial area,

by providing a source of mixing in the interfacial region.

The interfacial ripples were eliminated by the addition of a low

concentration of n-hexanol. While this additive was expected

to lower the surface tension, and hence reduce rippling, it was

not considered to otherwise affect the surface renewal rate.

Baird and Davidson continued their experiments with "Lissapol",

which was more strongly adsorbed, forming a continuous monolayer

at the interface, and reduced the transfer rate even further.

The relation between the work of Baird and Davidson and this

research is that if one assumes that capillary rippling was

present at the interface with water in bubble flow, then the

absence of such rippling could be expected with ethanol, having

a much lower surface tension. Any slight increase in surface area with ethanol, due to bubble elongation, would appear to be more than offset by the absence of rippling, which might well be the cause of the observed reduction in the mass transfer rate in this work, as in that of Baird and Davidson.

The role of the horizontal tee entrance as a bubble form-ing device is of considerable interest in estimating the effect of tube diameter on the rates of mass transfer in bubble flow. If this type of entrance is likened to an orifice in a horizon-tal plate, use can be made of the work on bubble formation of Van Krevelin and Hoftijzer (61). For the occurrence of "chain-bubbling", equivalent to high gas rates, the bubble volume was found to be independent of viscosity effects, surface tension, and even of orifice diameter. The proposed equation relating bubble diameter and the other variables was as follows:

$$D_B = 0.279(Q_G)^{0.4} \left[\frac{\rho_L}{\rho_L + \rho_G}\right]^{0.2} \tag{26}$$

where: D_B = diameter of equivalent spherical bubble, ft

Q_G = volumetric gas flow rate per orifice, cfh

ρ_L, ρ_G = liquid and gas densities

This equation supports the previously mentioned observation that in this work the bubble frequency appeared to be independent of

viscosity and surface tension. Measurements were not made to test the effect of the density ratio, which must approach unity closely for the gas-liquid systems used in this work. A significent conclusion of equation (26), if the analogy to the horizontal orifice is still maintained, is that the bubble frequency would also be expected to be independent of the tube entrance size for the two-phase absorber. If this were true, then equation (17) would still be expected to express the relationship between the transfer rate and the variables V_L^o and V_G^o, the liquid and gas superficial velocities. The parallel between the vertical rising chain-bubbles and bubbles formed in a horizontal tee must break down, however, since the bubble frequency was visually observed to be much higher in the small diameter (1.228 cm) absorption tube than in the larger ones. The large exponent of 2.0 for the diameter ratio in equation (18) is indicative of the high dependence of the absorption rate on tube diameter. Particularly for the large (2.504 cm) tube, and at the lowest liquid rate, a considerable deviation from the proposed correlation is noted, probably due to the bubbles in the larger tube flowing proportionately nearer to the top of the tube, and hence affecting the degree of agitation in the bulk of the liquid to a lesser extent. This behaviour suggests that the ratio of bubble diameter to tube

diameter would be a necessary parameter of a correlation, for smaller values of this ratio.

Slug Region

As discussed in the section on Theoretical Aspects, two effects were to be expected with regard to the mass transfer rates in the turbulent slug region of flow if the Kishinevskii theory was applicable to portions on the gas-liquid interface. The first was that at a constant liquid rate, increasing gas rates might be expected to increase the fraction of the extremely turbulent "slug crest" area in the test section and, therefore, cause a decreased dependence on diffusivity at the higher gas rates. As can be observed from the NTU-V_G^o lines in Figures 21, 22, and 23 for the CO_2-water and He-water systems at any one liquid rate, if such a decreased dependence on diffusivity was obtained at all, it was small indeed. Further consideration of the mass transfer process at any one liquid rate, suggests that the accelerating effect of the increased gas flow on the liquid phase may be significant. The consequence of this acceleration is that less liquid is present in the tube at higher gas velocities, and the liquid, slug crests included, travels at a much higher velocity through the tube. The total amount of liquid in the tube at any one time is obviously less

at higher gas rates (that is, the void fraction increases), and, therefore, the number of slug crests present in the test section is probably smaller. The velocity of the liquid as well as the number of slug crests present in the test section are assumed to be comparable for equivalent gas (CO_2 and He) superficial velocities. In consequence, a comparison of the absorption rate curves at any one liquid rate is not useful in either supporting or disproving the theory of Kishinevskii.

The second effect expected in the slug region was that at constant gas rates, increased liquid rates would decrease the effect of molecular diffusivity. It was qualitatively observed during experimentation that the quantity of liquid in the tube increased with increasing liquid rates, and in addition the degree of agitation increased also to a pronounced degree. By a comparison of the slopes of the NTU-V_G^o lines in Figures 21, 22 and 23, it is evident that the slope for the He-water system approaches that for the CO_2-water system at the highest liquid rate (1.792 fps). This indicates that the effect of the molecular liquid phase diffusivity appears to be decreasing in its influence on the rates of mass transfer at higher degrees of turbulence. The magnitude of this effect is quantitatively shown by the indices to be used in conjunction with equation (24), in Figure 25 and Table 10. The exponents of

the viscosity ratios appear to give further qualitative confir-

mation of the Kishinevskii theory, showing that viscosity plays

an increasingly important role in the rates of mass transfer as

the turbulence increases.

Recent work by Davies, Kilner, and Ratcliff (62) discredits

the work of Kishinevskii on the grounds that in their experiments

in a stirred vessel, the transfer rates, in the absence of

splashing and emulsification, were dependent on the square root

of the liquid phase diffusivity for comparable conditions,

regardless of the stirring rate. Although it is unfortunate

that the experiments of Kishinevskii were not described in

enough detail to indicate the extent of the agitation, and

condition of the interface, it appears likely that the condition

of the interface for his work was not comparable to that of

Davies et al. The application of the Kishinevskii theory to

this present research was made because of the obvious extremely

turbulent behaviour of the liquid which included splashing and

emulsification at the interface. Because of the successful

application of the principles of the Kishinevskii theory to

this work, it appears that the Kishinevskii theory is an entirely

possible explanation for the observed absorption phenomena in

two-phase flow.

The dependence of the mass transfer coefficients on

diffusivity to an exponent of less than 0.5 can be independently

observed by the use of the experimental CO_2-water data obtained

in the slug region of flow, at various temperatures. As indi-

cated earlier, absorption data were obtained at one liquid

rate, 1.07 gpm, with one tube size, 1.757 cm, and at the

three temperatures, $5.3^{\circ}C$, $30^{\circ}C$, and $45^{\circ}C$. Also as indicated

earlier, the diffusivity range for these temperatures was a

factor of three. For this particular liquid volumetric flow

rate, the effect of both the surface tension, and viscosity,

were very small because the former was only slightly tempera-

ture dependent, and the latter had an exponent for the viscosity

ratio of 0.028. Figure 29 shows a graph of the experimental NTU

values plotted against those predicted using the slug flow

correlation. It is noted that although the exponent for the

diffusivity ratio is 0.307, the data for the three temperatures

lie along a single straight line parallel and close to the 45°

line. The conditions for this series of experiments make it a

relatively stringent test of the effect of diffusivity. The

comparison of the absorption rates does not depend on the

accuracy of independent diffusivity determinations for two

systems, one including the gas H_2 or He, for which such deter-

minations are invariably difficult to make with accuracy, but

instead on the values of diffusivity frequently measured over

$$NTU = \left[\frac{\rho_x}{\rho_w}\right]^a \left[\frac{\sigma_x}{\sigma_w}\right]^b \left[\frac{\mu_x}{\mu_w}\right]^c \left[\frac{D_w}{D_x}\right]^d (0.0164 + 0.0115 V_L^\circ)(4.60 - 1.96 V_L^\circ + V_G^\circ) - 0.04$$

TEMPERATURE
○ 5.3 °C.
△ 30 °C.
□ 45 °C.
TEST SECTION LENGTH = 92.2 IN.

45° LINE, 10% LIMITS

N T U, EXPERIMENTAL
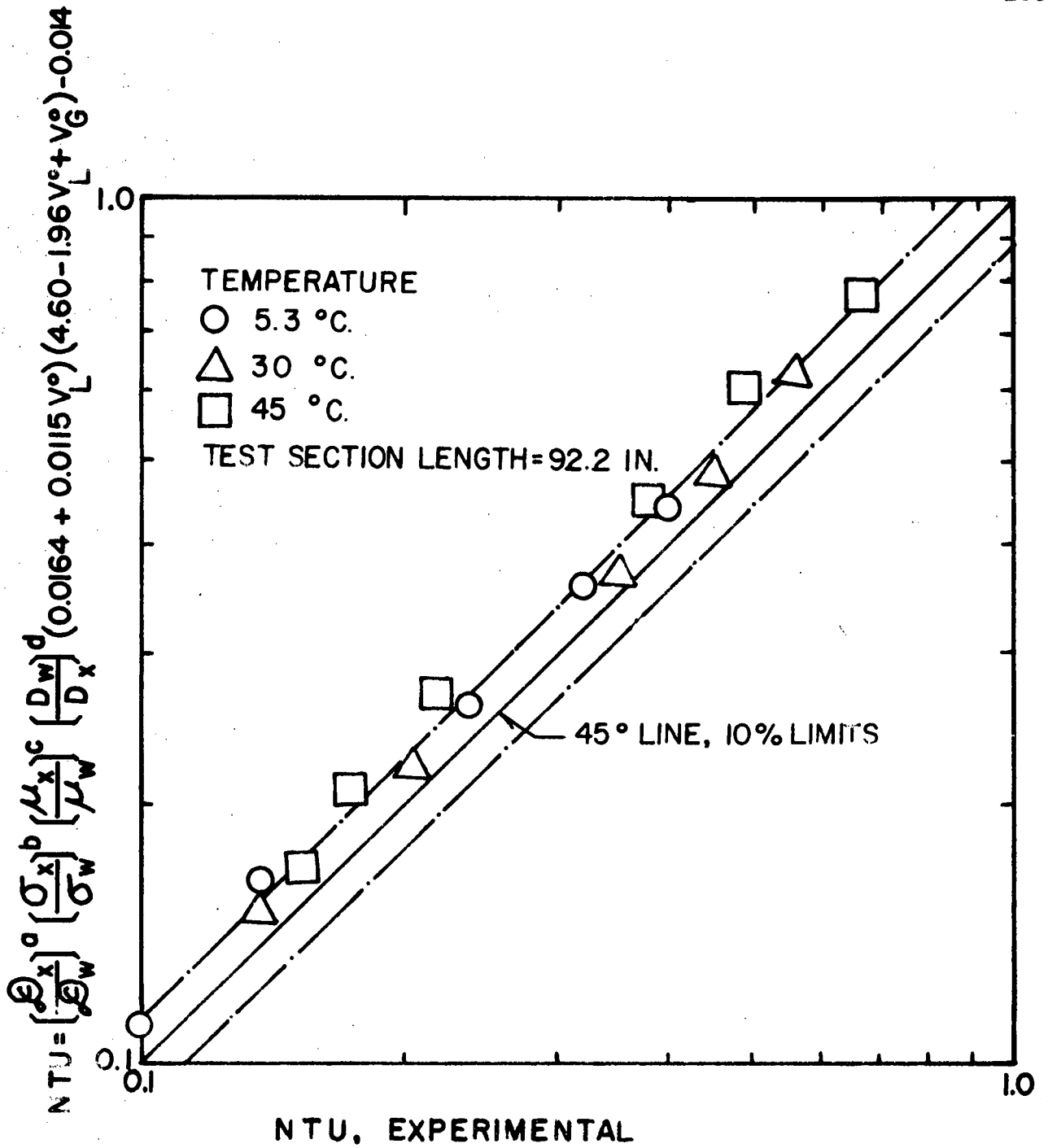
Figure 29. Application of Slug Flow Correlation to
CO_2-Water Absorption Data at Various Temperatures

a wide temperature range for the one gas-liquid system, CO_2-water. In addition, the gas density for these experiments can be considered constant in comparison to the variations between that of He or H_2 and such gases as CO_2 and O_2. This provides a second independent check that the exponent for the effect of diffusivity for this particular condition of turbulence is, in fact, less than 0.5, or 0.307.

The fact that the data all lie slightly above the 45° line suggests that a gas density ratio parameter, raised to a small exponent should possibly be introduced into the correlation for higher accuracy. It is recalled that the effect of the difference in gas densities between He and CO_2 was ignored in the determination of the effect of diffusivity. It is obvious from Figure 29 that the effect of gas density is small, and may result in predicted values of NTU being approximately 5 to 10% too high, depending on the particular gas density.

The effect of surface tension is noted to be smaller in the slug region than in the bubble region. The reason for the direction of the effect of surface tension is not immediately obvious, decreasing values decreasing the rates of transfer. It might also be expected, in the light of the reduction in the effect of surface tension in slug flow when compared to

bubble flow, that a continuing reduction would be obtained at higher degrees of turbulence in the slug region itself. The effect of surface tension would be expected to be reflected in changes in interfacial area, or in the degree of microscopic turbulence of the interface. In slug flow, the former seems to be the more likely explanation for the decrease in transfer rates with decreasing surface tension, and would possibly be due to the variation in void fraction with a change in this property of the liquid. According to Hughmark and Pressburg (63), the liquid fraction will vary approximately as σ^n, where σ is the surface tension, and the exponent, n, is estimated to be of the order of 0.2. Thus, if one assumes the surface area at equal gas and liquid rates to be directly proportional to the amount of liquid in the tube, the effect of a decrease in surface tension of the pure liquid will be to decrease the transfer rate. Because both of these effects of interfacial tension on the transfer rate act in the same direction, the rather appreciable dependence of the absorption rate on this property in the slug region of flow becomes understandable.

The dependence of transfer rates on tube diameter was found to be less in the slug region than in the bubble region, and was consistently reduced with increased liquid turbulence.

It would appear logical that tube geometry would be of lesser importance at higher liquid rates. The interaction of the phase velocities in increasing the turbulence, would be decreasingly affected by the tube walls. It is interesting to note that in Figure 25 at the intercept of the $d-V_L^o$ curve the value of "d" (2.0) obtained for the bubble region falls directly on the extrapolated line determined by the other values of "d" for the slug region.

In conclusion, there is a need to conclusively determine for increasingly turbulent two-phase flows whether a different mechanism of mass transfer is beginning to operate, for example, Kishinevskii's theory, or whether the observed results are the consequence of the same process occurring at very different rates at the same time and in different locations, because of a great variation in the amount of transfer area existing per unit volume of fluid. Although the present work does not settle this point, nor was it intended to do so, present evidence seems to favour the former viewpoint. Now that the pattern of absorption behaviour is known, and the relative importance of the system variables, it should be possible to design unique experiments to investigate the rate process under more carefully controlled conditions.

REFERENCES

1. Nicklin, D. J., Wilkes, J. O. and Davidson, J. F., *Trans. Inst. Chem. Engrs.* 40, 61 (1962).

2. Anderson, G. H. and Mantzouranis, B. G., *Chem. Eng. Sci.* 16, 222 (1961).

3. Collier, J. G. and Hewitt, G. F., *Trans. Inst. Chem. Engrs.* 39, 127 (1961).

4. Varlamov, M. L., Manakin, G. A. and Staroselskii, Ya. I., *Zh. Prikl. Khim.* (USSR) 32, 2504 (1959).

5. Varlamov, M. L., Manakin, G. A. and Staroselskii, Ya. I., *Zh. Prikl. Khim.* (USSR) 32, 2511 (1959).

6. Anderson, J. D., Bollinger, R. E. and Lamb, D. E., "Mass Transfer in Two-Phase Annular Horizontal Flow". Presented at A.I. Che. Eng. Natl. Meeting, Los Angeles, February, 1962.

7. Martinelli, R. C. and Nelson, D. B., *Trans. Am. Soc. Mech. Eng.* 70, 695 (1948).

8. Isbin, H. S., Fauske, H., Grace, T. and Gracia, J., "Symposium on Two-Phase Fluid Flow". Paper No. 10, Inst. Mech. Engrs., London, February, 1962.

9. Hughmark, G. A. and Pressburg, B. S., *A. I. Ch. E. Journal* 7, 677 (1961).

10. Schiel, K., German Patent No. 1,074,391, issued January 28, 1960.

11. Alves, G. E., *Chem. Eng. Progr.* 50, 449 (1954).

12. Govier, G. W. and Omer, M. M., *Can. Chem. Eng.* 40, 93 (1962).

13. Harriot, R. J., *Can. J. Chem. Eng.* 40, 60 (1962).

14. Scriven, L. E. and R. L. Pigford, *A.I. Ch. E. Journal* 5, 397 (1959).

15. Vivien, J. E. and D. W. Peaceman, <u>A. I. Ch. E. Journal</u> <u>2</u>, 437 (1956).

16. Davies, J. T. and Rideal, E. K., "Interfacial Phenomena" 2nd Ed. pp.311-313, Academic Press, New York, 1963.

17. Drew, T. B., Hoopes Jr., J. W. and T. Vermeulen, Editors, "Advances in Chemical Engineering", Vol. 4, p.1, Academic Press, New York, 1963.

18. Blank, M., <u>J. Phys. Chem.</u> <u>65</u>, 1698 (1961).

19. Harvey, G. A. and Smith, W., <u>Chem. Eng. Sci.</u> <u>10</u>, 274 (1959).

20. Drew, T. B., Hoopes Jr., J. W. and T. Vermeulen, Editors, "Advances in Chemical Engineering", Vol. 4, pp.3, 7, Academic Press, New York, 1963.

21. Ibid., p.5.

22. Lewis, W. K., and Whitman, W. G., <u>Ind. Eng. Chem.</u> <u>16</u>, 1215 (1925).

23. Higbie, R., <u>Trans. Am. Inst. Chem. Engrs.</u> <u>31</u>, 365 (1935).

24. Sherwood, T. K. and Pigford, R. L., "Absorption and Extraction", pp.20, 22, 265-267, McGraw-Hill, New York, 1952.

25. Kishinevskii, M. K. and Pamfilov, A. V., <u>Zh. Prikl. Khim.</u> <u>22</u>, 1173 (1949).

26. Kishinevskii, M. K. and Serebryansky, V. T., <u>Zh. Prikl. Khim.</u> <u>29</u>, 27 (1956).

27. Danckwerts, P. V., <u>Ind. Eng. Chem.</u> <u>43</u>, 1450 (1951).

28. Nicklin, D. J., Wilkes, J. O. and Davidson, J. F., <u>Trans. Inst. Chem. Engrs.</u> <u>40</u>, 61 (1962).

29. Scott, D. S., <u>Can. J. Chem. Eng.</u> <u>40</u>, 224 (1962).

30. Bowman, R. L. and Johnson, A. I., <u>Can. J. Chem. Eng.</u> <u>40</u>, 139 (1962).

31. Knudsen, J. G. and Katz, D. L., "Fluid Dynamics and Heat Transfer", p.214, McGraw-Hill, New York, 1958.

32. Bird, R. B., Stewart, W. E. and Lightfoot, E. N., "Transport Phenomena", p.541, Wiley, New York, 1960.

33. Friedlander, S. K., A. I. Ch. E. Journal 7, 347 (1961).

34. Ref. 20, p.10.

35. Hutchinson, M. H. and Sherwood, T. K., Ind. Eng. Chem. 29, 836 (1937).

36. Linke, W. F., "Solubilities Inorganic and Metal Organic Compounds", Vol. 1, 4th Ed., Van Nostrand, New York, 1958.

37. Hodgman, C. D., "Handbook of Chemistry and Physics", 44th Ed., p.1708, Chemical Rubber Publishing Company, Cleveland, 1962.

38. Ibid., pp.2257, 2260.

39. Ibid., p.2197.

40. Perry, J. H., Editor, "Chemical Engineers Handbook, 3rd Ed., p.363, McGraw-Hill, New York, 1950.

41. Ibid., p.363.

42. Davidson, J. F. and Cullen, E. J., Trans. Faraday Soc. 53, 51 (1957).

43. "International Critical Tables", Vol. 5, McGraw-Hill, New York, 1929.

44. Calderbank, P. H., Trans. Inst. Chem. Engrs. 37, 176 (1959).

45. Gertz, K. H. and Loeschcke, H. H., Z. Naturf. 9b, 1 (1954).

46. Wilke, C. R., Chem. Eng. Progr. 218 (1949).

47. Reid, R. C. and Sherwood, I. K., "The Properties of Gases and Liquids", p.286, McGraw-Hill, New York, 1958.

48. Ibid., p.284.

49. Bulletin No. 101, "The Ring Method for Surface and Interfacial Tensions", Central Scientific Company, Chicago.

50. De Verteuil, G. H., "The Viscosity of Liquids", M.A.Sc. Thesis, University of British Columbia, 1958.

51. Rhodes, T. J., "Industrial Instruments for Measurement and Control", p.303, McGraw-Hill, New York, 1941.

52. Simpson, S. G., Ind. Eng. Chem. 16, 709 (1924).

53. Hamilton, L. F. and Simpson, S. G., "Quantitative Chemical Analysis", p.170, 10th Ed., Macmillan, New York, 1952.

54. Ref. 24, p.130.

55. Lockhart, R. W. and Martinelli, R. C., Chem. Eng. Progr. 45, 39 (1949).

56. Hughmark, G. A. and Pressburg, B. S., A. I. Ch. E. Journal 7, 677 (1961).

57. Ref. 44.

58. Levich, V. G., "Physicochemical Hydrodynamics", pp.135, 136, Prentice-Hall, Englewood Cliffs, 1962.

59. Mendenhall, C. E., Eve, A. S., Keys, D. A. and Sutton, R. M., "College Physics", 4th Ed., p.197, Heath, Boston, 1956.

60. Baird, M. H. I. and Davidson, J. H., Chem. Eng. Sci. 17, 87 (1962).

61. Van Krevelin, D. W. and Hoftijzer, P. J., Chem. Eng. Prog. 46, 29 (1950).

62. Davies, J. T., Kilner, A. A. and Ratcliff, G. A., Chem. Eng. Sci. (in press)(1964).

63. Ref. 56.

APPENDIX I

PROCESS EQUIPMENT SPECIFICATIONS

1. Rotameters

   R-1, R-1A (liquid)

   Manufacturer: Brooks Rotameter Company

   Model: R-1, R-8M-25-2; float, 8-RV-14-2

   　　　　R-1A, R-9M-25-2; float, 9-RV-14

   Capacities: see calibration curves Appendix II

   R-2, R-2A (gas)

   Manufacturer: Brooks Rotameter Company

   Model: R-2, R-6M-25-1; float, pyrex (spherical)

   　　　　R-2A, R-9M-25-2; float, 8-RV-3

   Capacities: see calibration curves Appendix II

2. Pumps

   P-1

   Supplier: Pumps and Power, Vancouver

   Model: MPJS-33-H, deep-well jet self-priming, centrifugal

   Capacity: 6.1 gpm at NPSH of 6 ft, inlet and discharge

   　　　　　pressures, full vacuum and 30 psig (water)

   Motor: 1/3 hp, 3450 rpm, directly connected

   Special features: mechanical shaft seal suitable for vacuum

P-2

Manufacturer: Eastern Industries Company

Model: E-1, type 100, laboratory, centrifugal

Capacity: approximately 0.25 gpm at head of 30 ft (water)

Motor: 1/15 hp, 5000 rpm, directly connected

3. Heat Exchangers

E-1

Type: shell-and-tube, single-pass both shell and tube

Tubes: approximately 320, 5/16-in OD copper tubes, 42 in long,
arranged in a triangular pitch, ½-in on centres

Shell: 6-in OD

Baffles: approximately 25% cut, every 6 in

Heads: flanged to match shell flanges, steel, coated with
primer and tygon paints

Area: approximately 50 sq ft, based on tube outside area

E-2, E-2A

Type: double-tube, internal tube 3/8-in copper, external
5/8-in copper, 4 in long.

Construction: brass end-pieces silver soldered, inlet and
outlet nipples, ¼-in also silver soldered

E-3

Type: double-tube, internal tube ½-in copper, external
3/4-in copper, overall length 30 in

Construction: brass end-pieces and three ½-in copper

nipples silver soldered

4. **Drum**

D-1

Size: 11-in diameter, 26-in length, approximate volume

11 U.S. gallons

Material of construction: stainless steel

5. **Water Ejector**

J-1

Manufacturer: Schutte and Koerting

Model: O

Capacity: approximately 1.5 scfh gas at 26 in mercury vacuum

6. **Thermometers**

T-1, T-2, T-4

Manufacturer: W. H. Kessler

Type: ASTM, solid point, range 0°C to 30°C, 0.1^{o}C divisions

T-3, T-5, T-6

Manufacturer: Kimble Glass

Range: -10°C to 100°C, 1°C divisions

7. **Pressure Gauges**

P-1, P-2

Range: 0 to 30 psig

P-3

Range: 0 to 50 psig

From D-1

To J-1

From P-1

1/4-in. brass end-plates

Shower head

3/4-in. iron pipe, tygon-
coated, 12 in. long, with
40 1/8-in. holes drilled

Q.V.F. section, 6-in.,
36 in. long

Liquid depth, 12 in.

3/8-in. coiled copper
tube, approx. 15 ft.

Note: not to scale

To drain

Steam inlet

To P-1
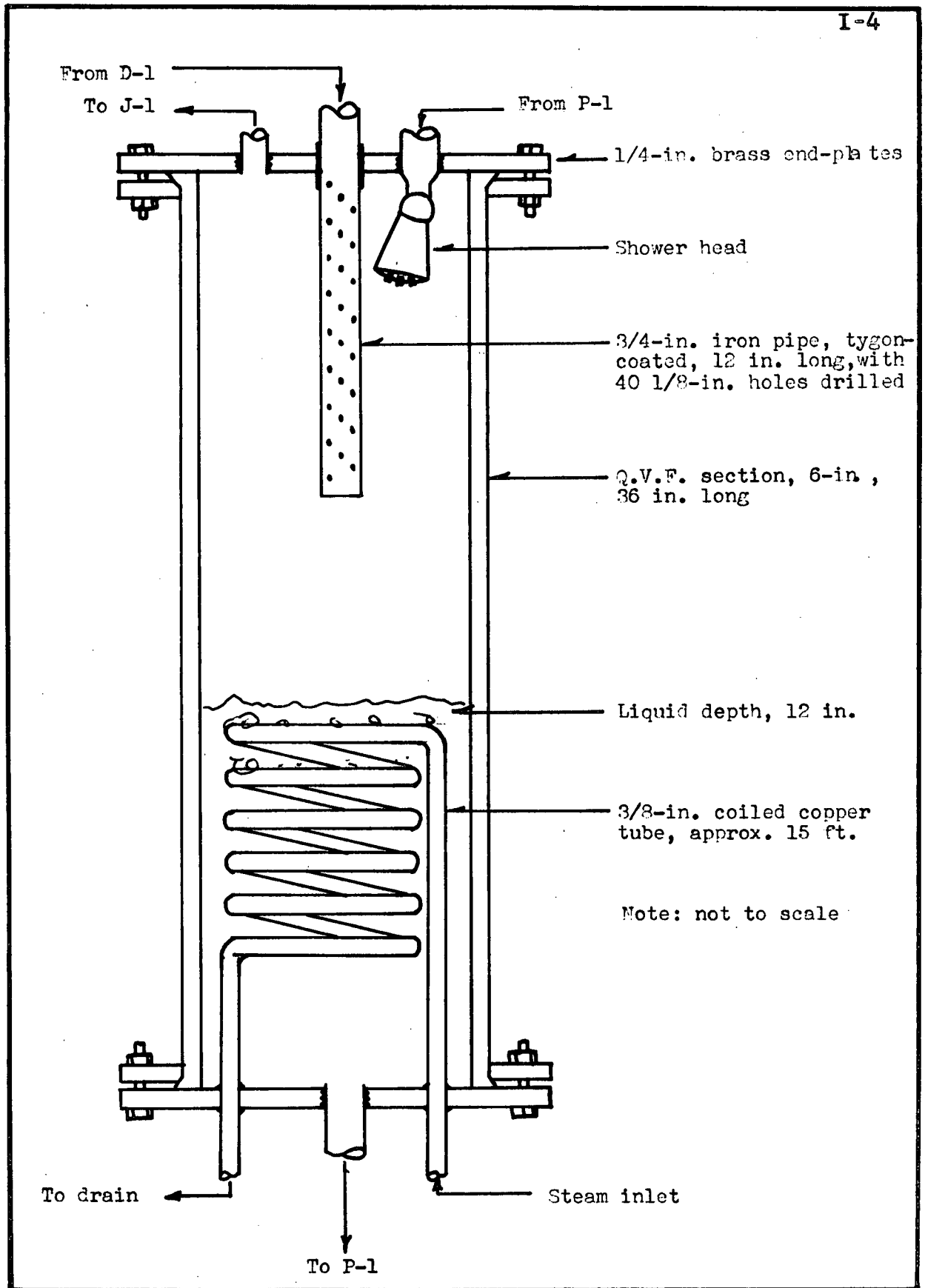
Figure I-1. Details of Vacuum Stripper

From P-2

Humidified gas

1/4-in. brass
end-plates

4, 1/8-in. diameter
nozzles

1/2-in. brass pipe

Q.V.F. section, 2-in.,
24 in. long

Note: not to scale

To P-2

Dry gas inlet
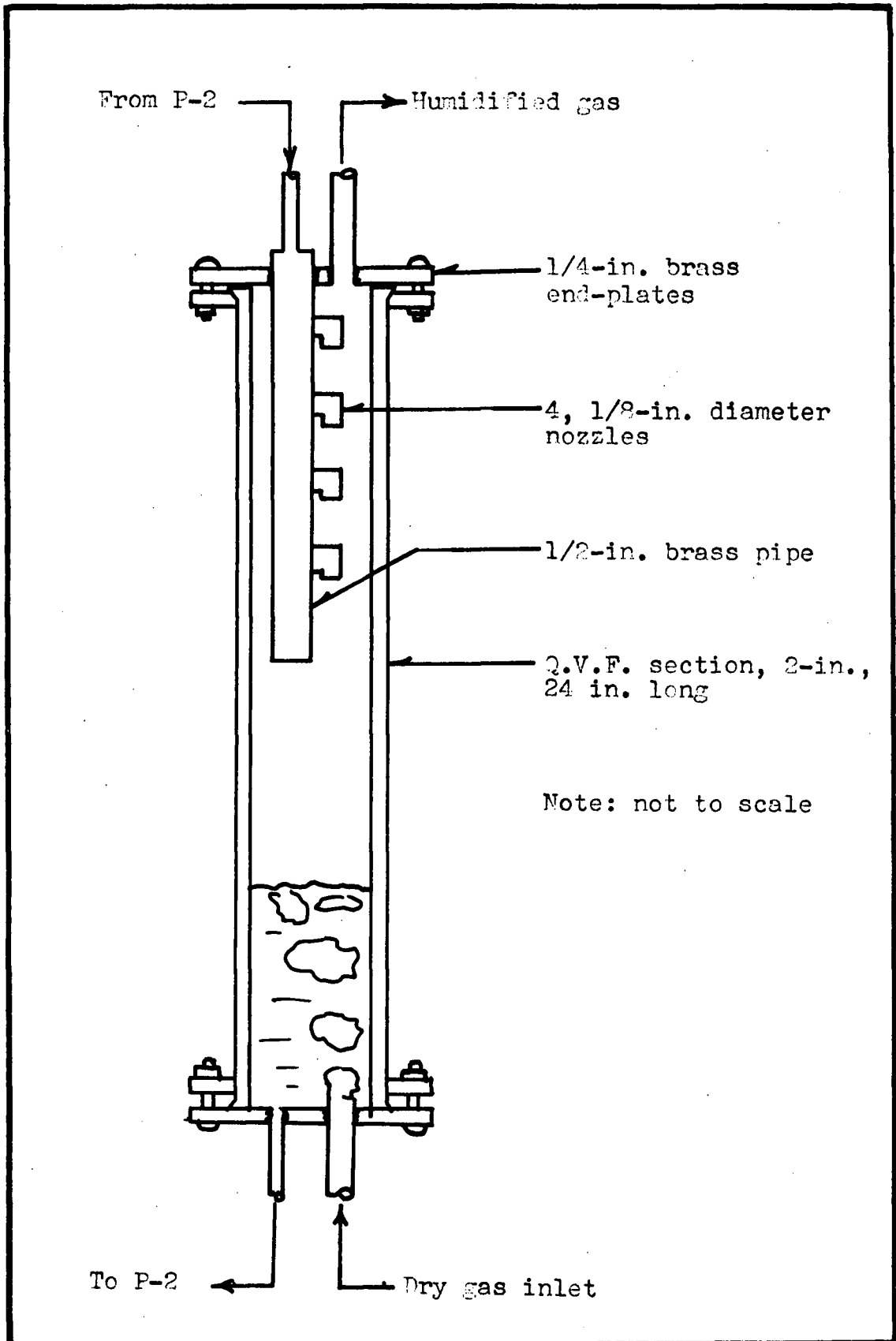
Figure I-2.   Details of Gas Humidifier

APPENDIX II

CALIBRATION OF GAS AND LIQUID ROTAMETERS

TABLE II-1

CALIBRATION OF LIQUID ROTAMETER, R-1, FOR WATER AND ETHANOL

Liquid	Temperature °C	Weight lb	Time min	Flow rate gpm	Rotameter Reading
	(15.0)				
Water	15.2	25	2.92	1.027(a)	1.00
	14.7	25	2.91	1.031	1.00
	15.0	20	2.92	0.822	0.80
	15.1	15	2.91	0.619	0.60
	15.1	10	2.90	0.414	0.40
	15.3	5	2.90	0.207	0.20

(a) calculation of flow rate based on water density of 8.334 lb/gal

Liquid	Temperature °C	Weight lb	Time min	Flow rate gpm	Rotameter Reading
	(13.5)				
Ethanol	13.4	6.0	0.813	0.608(b)	0.540
	13.5	6.0	0.860	0.899	0.797
	13.8	6.0	1.01	1.056	0.923
	13.6	6.0	1.49	1.117	0.979

(b) calculation of flow rate based on ethanol density of 6.605 lb/gal

Liquid	Temperature °C	Weight lb	Time min	Flow rate gpm	Rotameter Reading
Water	30.0	15	1.675	1.078(c)	1.04

(c) calculation of flow rate based on water density of 8.307 lb/gal

Liquid	Temperature °C	Weight lb	Time min	Flow rate gpm	Rotameter Reading
Water	45.2	15	1.69	1.074(d)	1.04

(d) calculation of flow rate based on water density of 8.263 lb/gal

TABLE II-2

CALIBRATION OF LIQUID ROTAMETER, R-1A, FOR WATER AND ETHANOL

Liquid	Temperature °C	Weight lb	Time min	Flow rate gpm	Rotameter Reading
	(15.0)				
Water	15.3	10	2.76	0.435(a)	0.40
	15.3	15	1.78	1.011	1.00
	14.7	25	1.99	1.508	1.50
	14.8	25	1.47	2.042	2.00
	15.3	25	1.19	2.52	2.50
	15.1	35	1.41	2.98	3.00

(a) calculation of flow rate based on water density of 8.334 lb/gal

	(13.5)				
Ethanol	13.7	6.0	0.730	1.24(b)	1.12
	13.5	6.0	0.579	1.57	1.43
	13.4	6.0	0.419	2.17	1.96

(b) calculation of flow rate based on ethanol density of 6.605 lb/gal

TABLE II-3

CALIBRATION OF LIQUID ROTAMETER, R-1A, FOR ETHYLENE GLYCOL

Temperature $^{\circ}$C	Weight lb	Time min	Flow rate gpm	Rotameter Reading
(15.0)				
15.0	5	2.290	0.234(a)	0.97
14.9	8	1.492	0.574	1.66
15.1	11	1.070	1.101	2.72
15.0	15	0.915	1.75	3.82
15.1	20	0.914	2.34	4.90

(a) calculation based on glycol density of 9.337 lb/gal

(30.0)				
29.9	6	2.004	0.324(b)	0.79
30.0	8	1.249	0.692	1.40
29.9	11	1.037	1.146	2.10
30.0	15	0.981	1.65	2.90
30.1	20	0.997	2.17	3.70
29.9	30	1.359	2.39	4.04

(b) calculation based on glycol density of 9.253 lb/gal
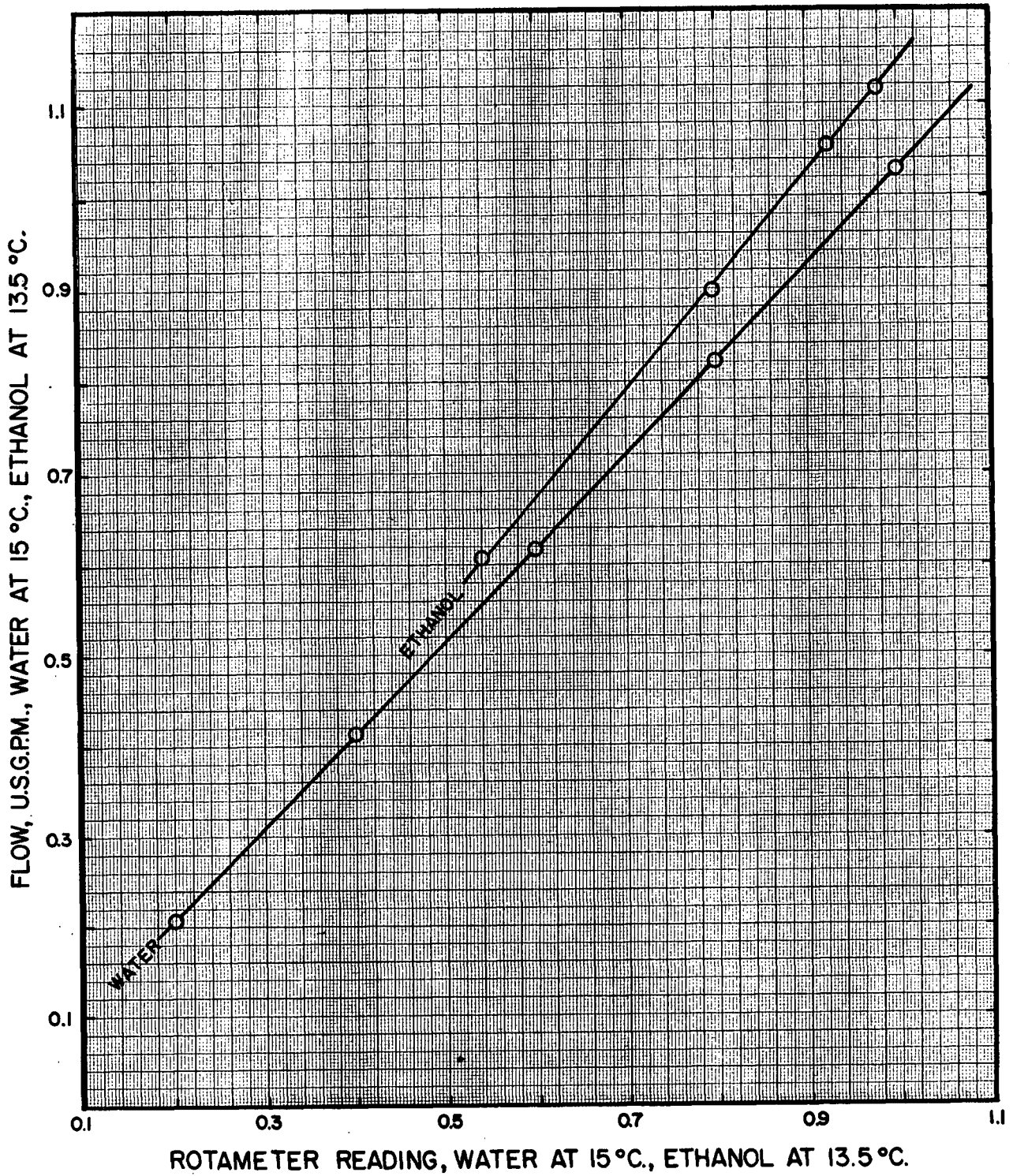
Figure II-1. Calibration of Liquid Rotameter,
R-1, for Water and Ethanol
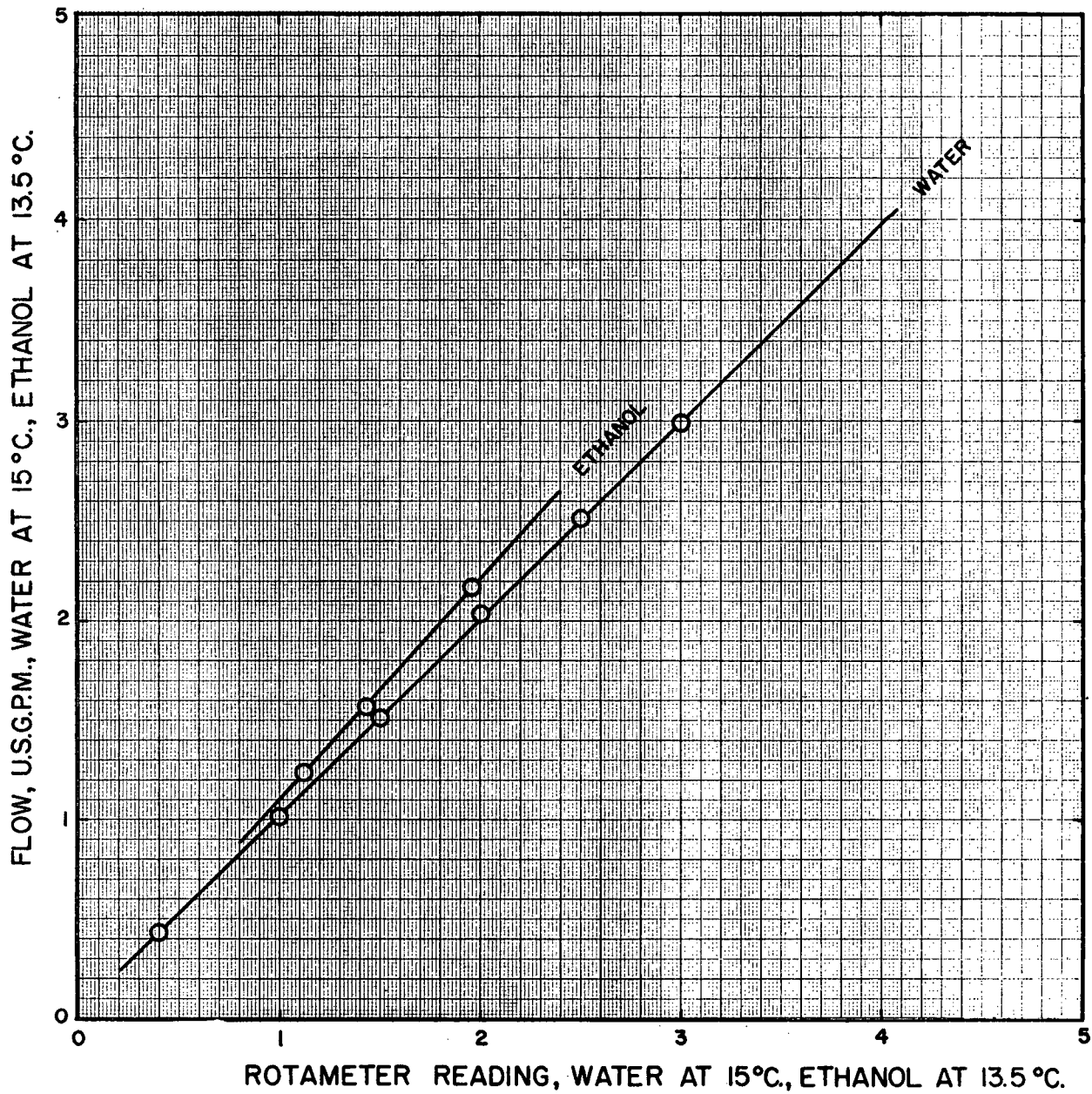
Figure II-2. Calibration of Liquid Rotameter,
R-1A, for Water and Ethanol
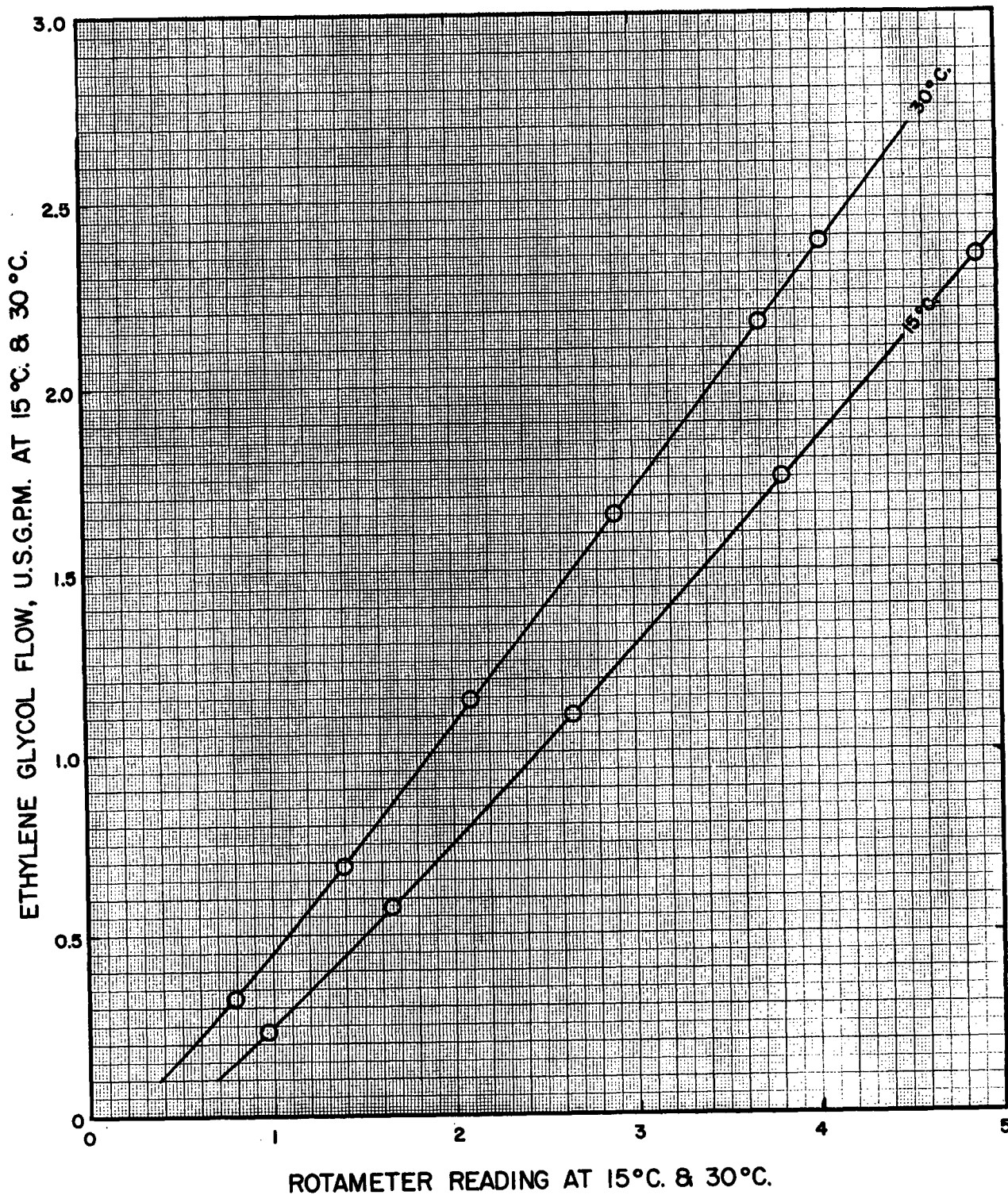
Figure II-3. Calibration of Liquid Rotameter,
R-1A, for Ethylene Glycol

TABLE II-4

CALIBRATION OF GAS ROTAMETER, R-2, FOR CO_2 FLOW

Rotameter			Wet Test Meter		Flow Rate	
Reading	Temp. °C	Pressure in Hg	Volume cf (a)	Time min	cfh 15°C,756mm (b)	cfh 15°C,756mm (c)
4.0	23.1	4.0	0.05	2.33	1.218	1.229
4.0	23.6	12.0	0.05	1.97	1.440	1.456
10.0	23.8	12.0	0.10	1.28	4.44	4.49
10.0	24.0	4.0	0.10	1.45	3.92	3.97
20.0	24.0	4.0	0.20	1.26	9.01	9.11
20.0	20.0	12.0	0.20	1.12	10.10	10.10
30.0	18.4	4.0	0.30	1.23	13.76	13.66
30.0	19.0	8.0	0.40	1.56	14.50	14.44
30.0	17.8	12.0	0.40	1.47	15.38	15.27
40.0	21.0	4.0	0.50	1.57	18.00	18.04
40.0	21.0	8.0	0.50	1.49	18.96	19.00
40.0	21.2	12.0	0.50	1.40	20.16	20.10
48.0	21.5	4.0	0.50	1.34	21.06	21.20
48.0	22.2	8.0	0.50	1.27	22.26	22.40
48.0	23.2	12.0	0.50	1.20	23.52	23.72

(a) volume of CO_2 at barometric pressure 757 mm, saturated with water at 74°F, using wet test meter Ch.E. 1668.

(b) volumetric flow rate of CO_2, dry basis.

(c) volumetric flow rate of CO_2, dry basis, for rotameter conditions of 21.0°C and 756 mm (nominal) pressure.

TABLE II-5

CALIBRATION OF GAS ROTAMETER, R-2A, FOR CO_2 FLOW

Rotameter			Displacement Meter			Flow Rate
Reading	Temp. °C	Pressure in Hg	Volume cf (a)	Time min	Volume cf (b)	cfh 15°C,756mm (c)
20.0	21.5	24.0	0.50	1.00	0.488	29.5
52.0	21.0	"	2.0	2.19	1.976	54.25
98.0	20.0	"	2.0	1.30	1.976	91.1
150	16.0	"	4.0	1.73	3.905	134.2
200	12.5	"	5.0	1.64	4.88	174.
231	7.6	"	5.0	1.41	4.89	203.
20.0	19.5	16.0	1.0	2.16	0.976	27.0
98.0	15.0	"	2.0	1.39	1.976	84.1
150	14.0	"	3.0	1.42	2.976	123.7
200	14.5	"	5.0	1.79	4.88	160.8
50.0	22.0	"	1.5	1.82	1.454	48.2
20.0	22.0	12.0	1.0	2.29	0.976	25.7
52.0	21.5	"	2.0	2.48	1.976	48.1
98.0	21.5	"	3.0	2.20	2.908	79.6
150	18.8	"	4.0	2.01	3.91	116.3
178	16.0	"	5.0	2.12	4.89	136.4
20.0	22.0	8.0	1.0	2.46	0.976	24.0
50.0	22.3	"	1.5	1.99	1.454	44.1
100	22.7	"	3.0	2.26	2.91	78.0
150	22.0	"	4.0	2.09	3.88	112.2
2.0	22.5	4.0	0.25	1.91	0.244	7.75
7.0	22.7	"	0.50	2.14	0.489	13.83
12.0	22.8	"	0.50	1.71	0.489	17.92
20.0	23.0	"	1.0	2.64	0.977	22.44
35.0	20.2	"	2.0	3.63	1.944	32.18
50.0	20.6	"	2.0	2.79	1.940	41.75
75.0	20.8	"	2.0	2.03	1.940	57.4
98.0	23.0	"	2.0	1.65	1.954	71.8
106	20.0	"	3.0	2.24	2.908	78.0

(a) volume of CO_2 at barometric pressure of 756 mm and temperature of 23°C, passing through dry gas displacement meter.

(b) volume of CO_2 at barometric pressure of 756 mm and temperature of 15°C (dry basis).

(c) volumetric flow rate of CO_2, dry basis, for rotameter conditions of 21°C and 756 mm (nominal) pressure.

TABLE II-6

CALIBRATION OF GAS ROTAMETER, R-2, FOR He FLOW

Rotameter			Wet Test Meter		Flow Rate	
Reading	Temp. °C	Pressure in Hg	Volume cf (a)	Time min	cfm (b)	cfh 15°C,756mm (c)
5.3	23.3	4	0.050	1.602	0.03121	1.786
8.9	23.3	"	0.050	1.629	0.07673	4.391
12.5	22.0	"	0.125	1.510	0.1656	9.480
16.6	22.0	"	0.250	0.910	0.2747	15.72
20.0	22.0	"	0.250	0.684	0.3655	20.92
23.2	22.3	"	0.500	1.120	0.4464	25.55
7.0	23.0	"	0.050	0.999	0.05005	2.864
4.0	22.9	"	0.050	2.130	0.0235	1.343
4.0	21.0	12	0.025	0.890	0.02809	1.608
5.9	21.0	"	0.050	1.183	0.04227	2.419
10.7	21.5	"	0.125	0.865	0.1445	8.269
17.7	21.0	"	0.250	0.707	0.3536	20.23
24.8	21.0	"	0.500	0.906	0.5519	31.58
32.1	21.0	"	0.750	1.006	0.7455	42.66
8.1	23.0	"	0.125	1.507	0.08295	4.747
14.0	23.0	"	0.250	1.020	0.2451	14.03
40.7	22.5	"	1.00	1.050	0.9524	54.50
47.9	22.5	"	1.00	0.906	1.104	63.18
9.3	22.5	24	0.150	1.073	0.1398	8.00
12.9	"	"	0.250	0.970	0.2577	14.75
17.2	"	"	0.375	0.910	0.4121	23.58
22.9	"	"	0.750	1.263	0.5938	33.98
30.1	"	"	1.00	1.228	0.8143	46.60
39.2	"	"	1.00	0.938	1.066	61.00
48.1	"	"	1.00	0.783	1.277	73.08

(a) volume of He at 753 mm, saturated at 75.0°F, using wet test meter 1668.

(b) volumetric flow rate of He, dry basis, at 753 mm pressure and 75.0°F.

(c) volumetric flow rate of He, dry basis, at 756 mm pressure and 15.0°C, for rotameter conditions of 21.0°C, and 756 mm (nominal) pressure.

TABLE II-7

CALIBRATION OF GAS ROTAMETER, R-2A, FOR He FLOW

Rotameter			Displace. Meter		Flow Rate	
Reading	Temp. °C	Pressure in Hg	Volume cf (a)	Time min	cfm (b)	cfh 15°C,756mm (c)
8.20	23.5	24	1.00	1.117	10.8784	52.7
36.5	"	"	2.50	1.023	2.398	143.9
43.6	"	"	3.00	1.090	2.700	162.0
54.4	"	"	3.5	1.087	3.160	189.6
62.0	"	"	4.0	1.133	3.446	207.8
72.3	"	"	4.0	1.007	3.898	233.9
85.8	"	"	5.0	1.107	4.432	265.9
3.8	23.3	24	0.50	0.912	0.5380	32.27
6.9	"	"	1.00	1.288	0.7619	45.71
11.0	"	"	1.00	0.952	1.030	61.80
14.6	"	"	1.50	1.210	1.217	73.02
21.2	"	"	1.50	0.925	1.592	95.52
10.7	"	"	1.00	0.978	1.003	60.18
16.6	"	"	1.50	1.080	1.363	81.78
20.5	"	"	1.50	0.917	1.605	96.30
30.0	"	"	2.0	0.943	2.081	124.9
3.6	23.2	12	0.50	1.097	0.4473	26.84
6.2	"	"	0.75	1.180	0.6237	37.42
9.0	"	"	1.00	1.249	0.7856	47.14
15.6	"	"	1.25	1.063	1.154	69.24
22.6	"	"	1.50	1.007	1.462	87.72
28.8	"	"	1.50	0.849	1.734	104.0

(a) volume of He at 753 mm and 75.0°F, dry basis.

(b) volumetric flow rate of He, dry basis, at 756 mm and 15°C.

(c) volumetric flow rate of He, dry basis, at 756 mm and 15°C, at rotameter conditions of 21.0°C and 756 mm (nominal) pressure.
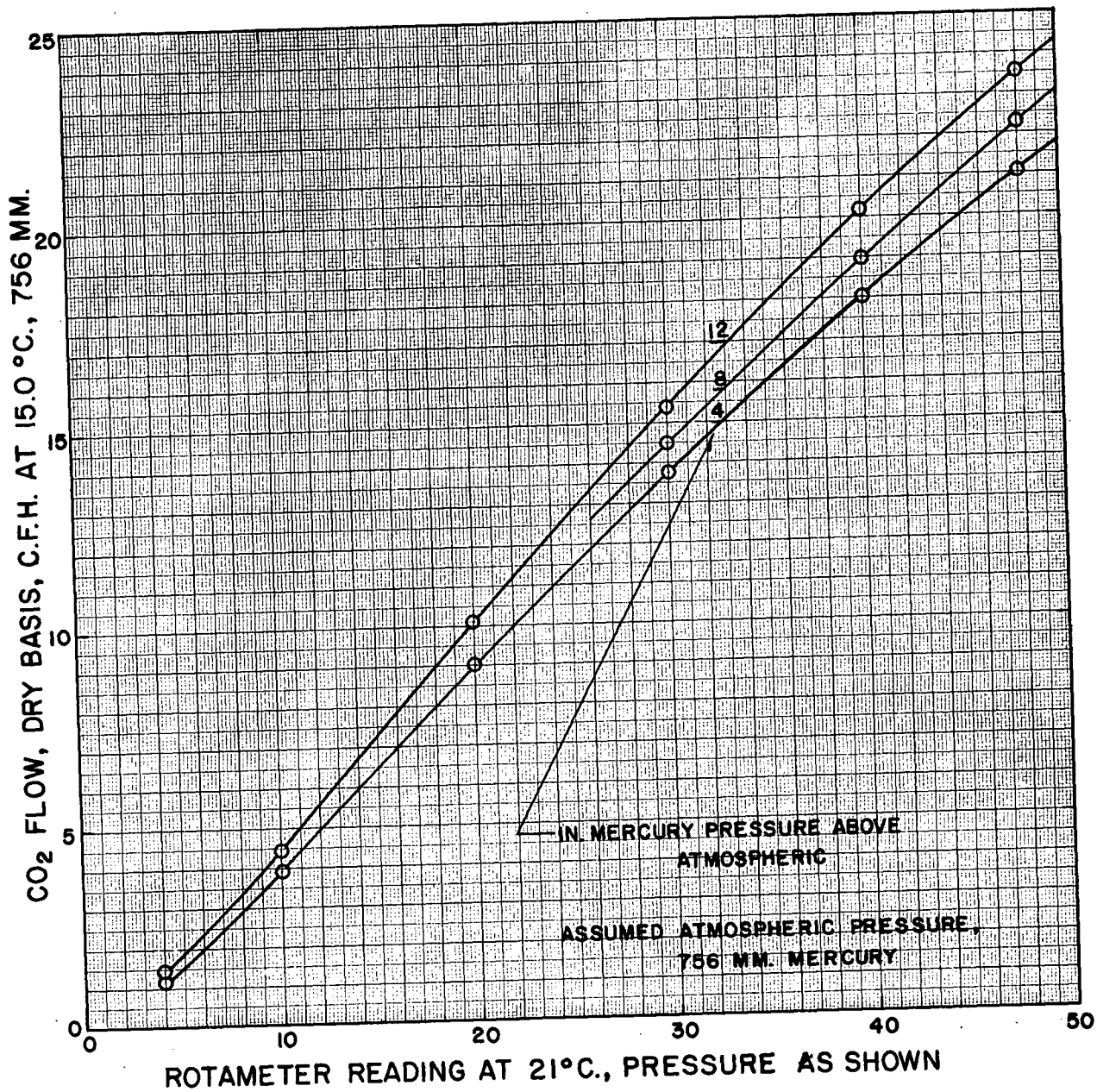
Figure II-4. Calibration of Rotameter,
R-2, for CO_2
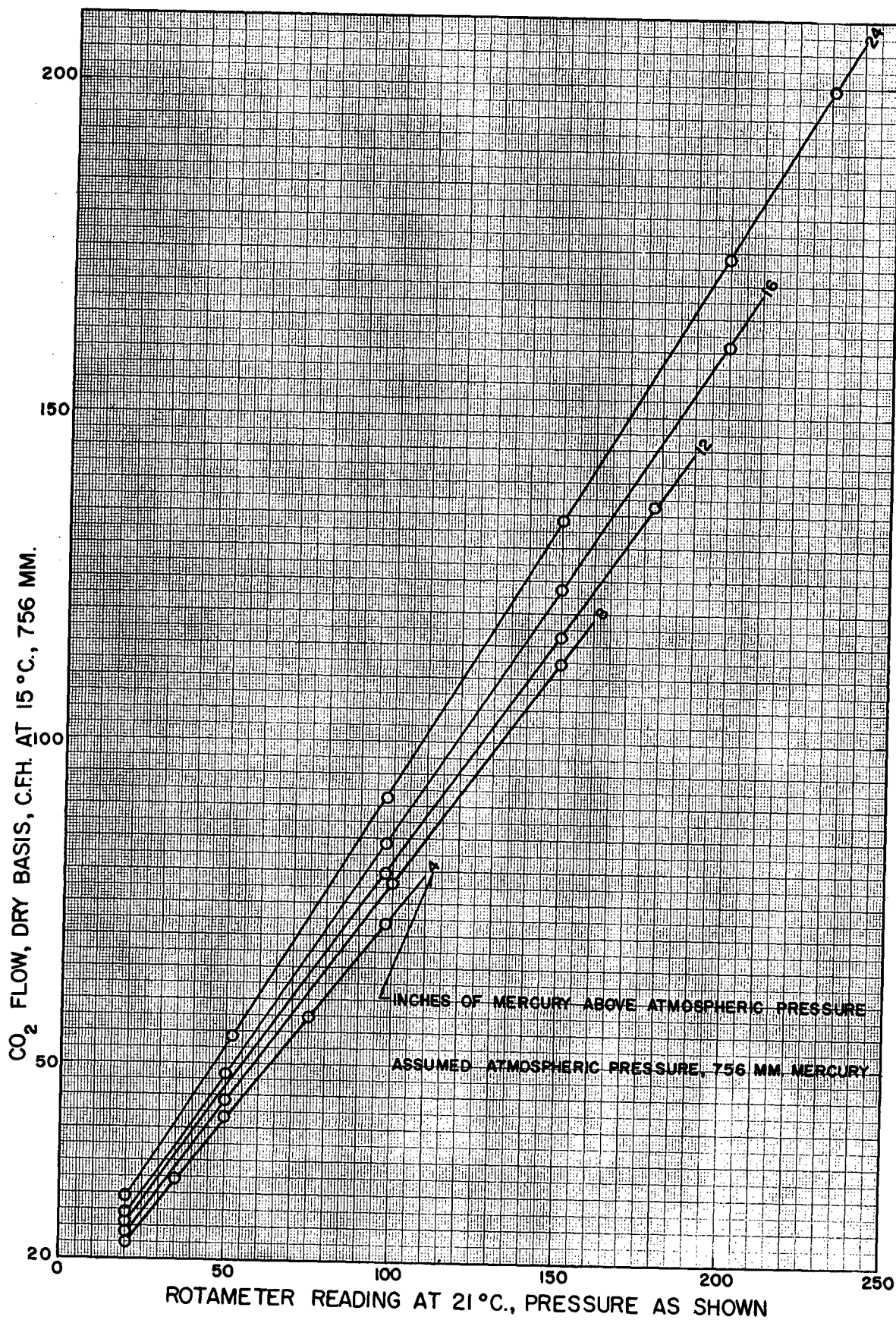
Figure II-5.   Calibration of Rotameter,
R-2A, for CO_2
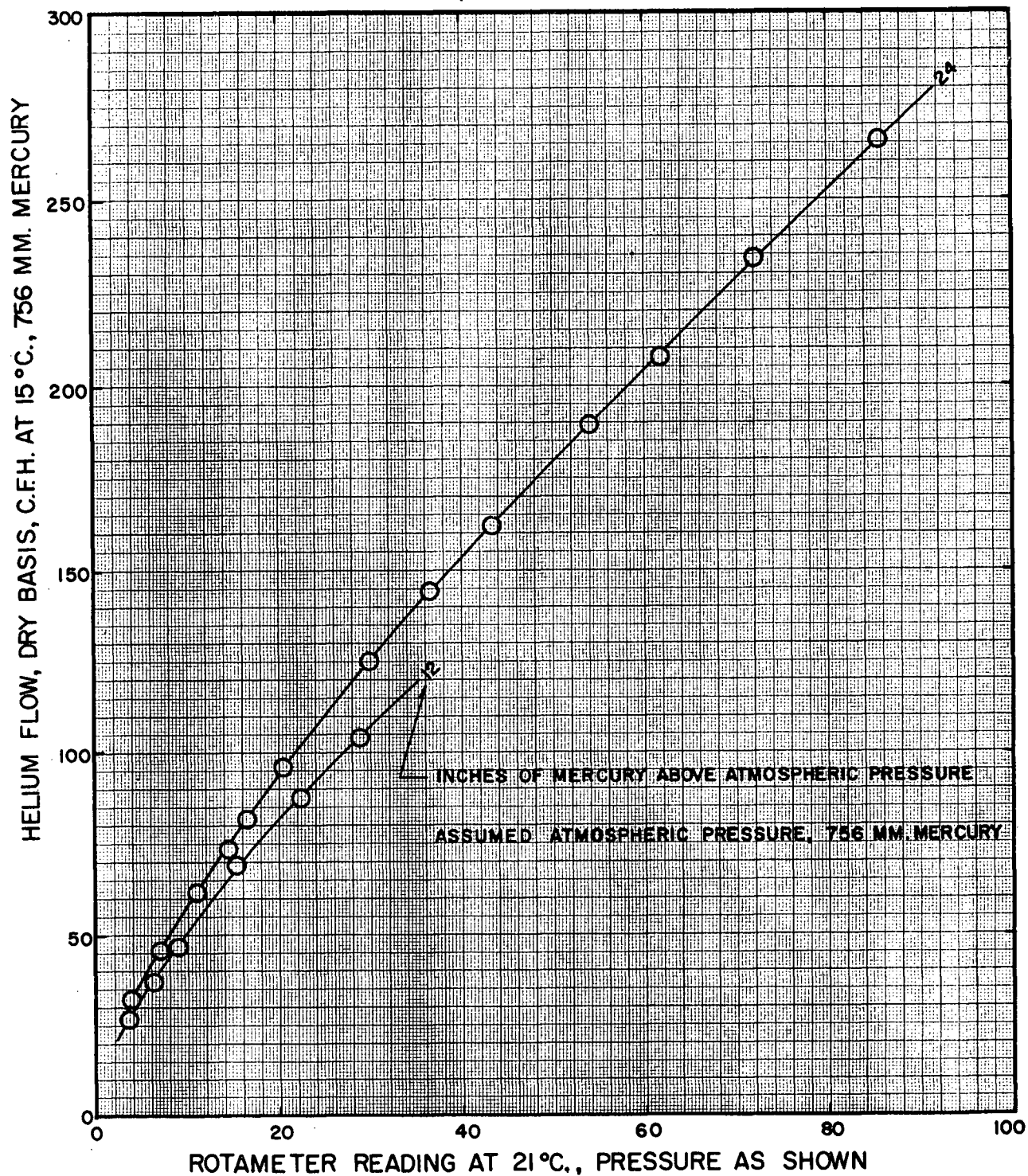
Figure II-6. Calibration of Rotameter,
R-2, for He
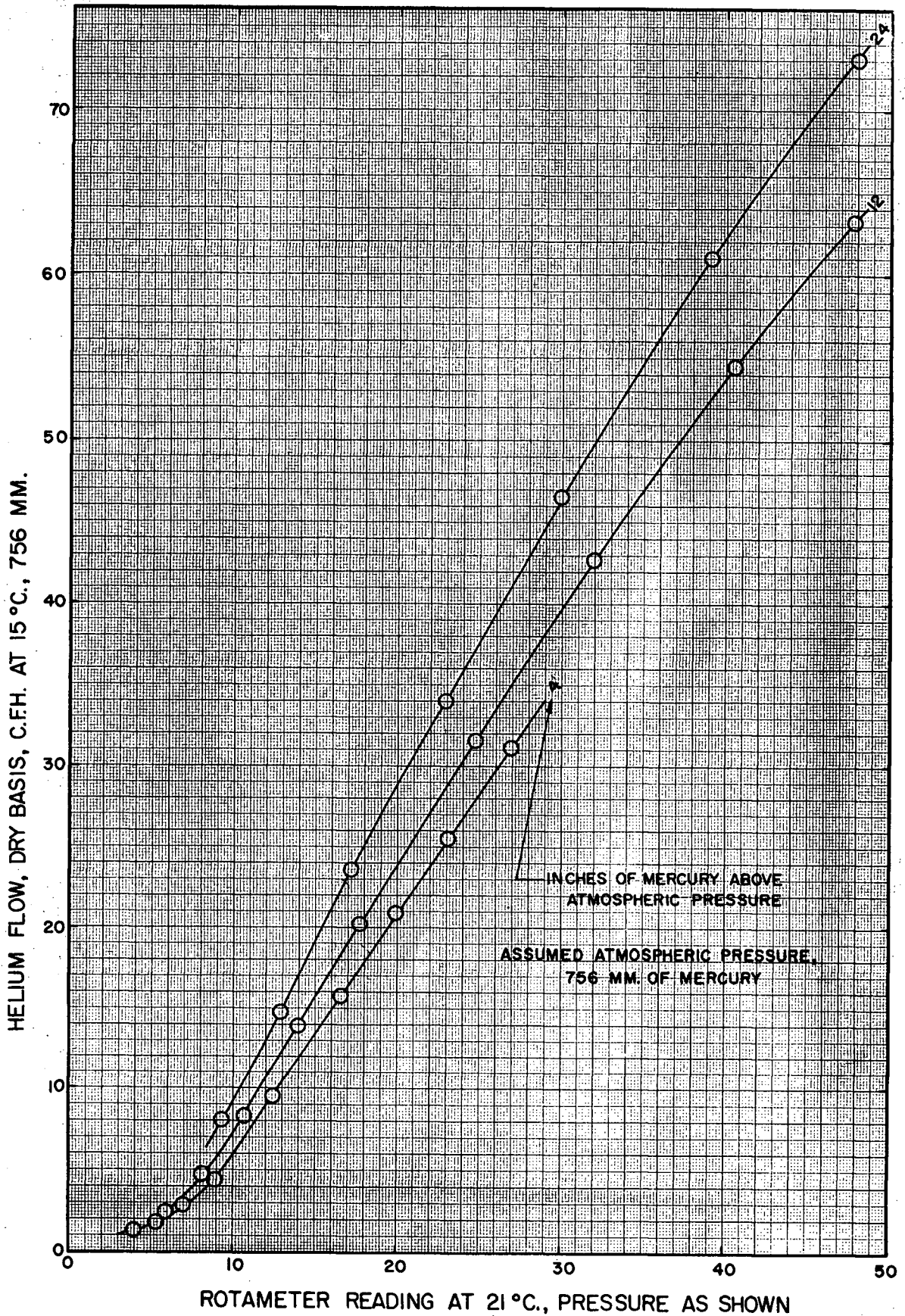
Figure II-7. Calibration of Rotameter,
R-2A, for He

APPENDIX III

SAMPLING AND ANALYSIS

TABLE III-1

CONCENTRATION PROFILE IN LIQUID, IN BUBBLE AND SLUG FLOWS

WITH CO_2-WATER SYSTEM

1. Bubble Flow:

Probe Position mm (a)	Concentration (inlet sample point) millimoles/l
-2	4.70
0	4.85
2	4.90
4	4.95
6	5.00

Note: bottom of bubbles approximately 8 mm from tube bottom.

2. Slug Flow:

-1	9.85
0	9.90
1	9.90
2	9.90
3	10.00

Note: bottom of slugs approximately 5 mm from tube bottom.

(a) probe position measured from inside bottom level of absorption tube 17.57 mm in diameter.

Note: saturated concentration approximately 45.7 millimoles per litre.

TABLE III-2

ABSORPTION RATES IN ENTRANCE TEE AND OUTLET CYCLONE

FOR ETHYLENE GLYCOL

Glycol Flow Rate gpm	NTU at 15°C	NTU at 30°C
0.62	0.00386	0.00421
1.07	0.00333	0.00281
2.10	0.00114	0.00112

Note: NTU values calculated with no gas flowing through the tube, but with the liquid in the tee and cyclone exposed to the gas.

TABLE III-3

DATA FOR CALIBRATION OF He ANALYZER FOR INLET SAMPLE POINT

Run	Water rate ml/min	CO_2 rate ml/min	Ratio of rates(10^2) ml water/ ml CO_2	Mole fraction He in CO_2(10^4)	Potential millivolts
E	0.495	76.5	0.647	0.601	0.120
	0.696	76.3	0.912	0.847	0.180
	0.960	75.9	1.265	1.175	0.255
	1.420	75.6	1.878	1.745	0.375
	2.14	75.2	2.846	2.644	0.545
	2.85	74.7	3.815	3.546	0.750
	3.36	74.4	4.516	4.196	0.895
F	0.178	76.6	0.232	0.215	0.031
	0.387	76.4	0.506	0.470	0.077
	0.576	76.2	0.756	0.702	0.128
	0.885	76.0	1.164	1.081	0.214
	1.92	75.3	2.550	2.368	0.500
	2.80	74.7	3.748	3.481	0.736
	4.46	73.5	6.068	5.636	1.182
L	0.564	75.5	0.747	0.681	0.118
	1.04	74.4	1.398	1.274	0.280
	1.90	73.6	2.580	2.351	0.503
	3.28	72.7	4.510	4.110	0.875

Note: column length in each case 20 in of packing.

TABLE III-4

DATA FOR CALIBRATION OF He ANALYZER FOR OUTLET SAMPLE POINT

Run	Water rate ml/min	CO_2 rate ml/min	Ratio rates(10^2) ml water/ ml CO_2	Mole fraction He in $CO_2(10^4)$	Potential millivolts
H	0.526	77.40	0.680	0.6195	0.110
	0.909	77.16	1.178	1.074	0.214
	1.23	76.92	1.599	1.458	0.304
	1.85	76.69	2.412	2.199	0.458
	2.58	75.64	3.411	3.109	0.643
	3.49	74.74	4.669	4.256	0.897
	4.25	73.96	5.746	5.238	1.092
	5.15	73.21	7.035	6.413	1.346
	6.12	72.78	8.409	7.665	1.586
	6.88	71.84	9.577	8.730	1.775
	7.69	71.43	10.77	9.817	1.980
	8.26	71.12	11.61	10.58	2.129
J	0.292	77.90	0.375	0.342	0.078
	0.521	76.95	0.677	0.617	0.136
	0.990	76.16	1.300	1.185	0.248
	1.77	75.50	2.344	2.137	0.456
	2.32	74.95	3.095	2.822	0.564
	4.65	73.40	6.335	5.776	1.216
	4.80	72.84	6.590	6.008	1.259
	5.55	72.15	7.692	7.013	1.472
	6.20	71.80	8.635	7.473	1.614
	7.34	71.16	10.31	9.400	1.907
K	1.19	76.00	1.566	1.427	0.278
	2.45	74.75	3.278	2.987	0.603
	3.53	73.90	4.777	4.354	0.895
	6.64	72.15	9.203	8.387	1.703
	7.63	71.20	10.716	9.766	1.954

Note: depth of column packing: H, 20 in

J, 16 in

K, 12-3/4 in

APPENDIX IV

IBM-1620 FORTRAN PROGRAMS USED IN

CALCULATIONS OF EXPERIMENTAL RESULTS

Programs for Computing NTU Values for the Various Gas-Liquid
Systems

The general method consisted of calculating the absolute
pressures, and subsequently the concentration driving forces
(correcting for the vapour pressure of the liquid), at the inlet
and outlet of the test section. The NTU values were calculated
according to equation (7) in the section on Treatment of Data.
The correction for the amount of gas absorbed in the entrance
section was made by applying equation (8), and the arithmetic
mean gas flow rate in the test section was calculated from
equation (9). The arithmetic mean gas volumetric flow rate
was calculated at the mean test section temperature and pres-
sure, and from it, the mean superficial gas velocity. The
length of a transfer unit (LTU) was also calculated. A coded
number system to describe the type of flow (bubble, plug, etc.)
was also included for reproduction in the computer print-out
of the data and calculated values. The small variations in
the programs will be separately described:

1. $\underline{CO_2\text{-Water}}$: The two values of E/L in equation (8) were introduced directly into the program. These values corresponded to 0.13964 for the 12.75-in entrance length (E), and to 0.33947 for the 30-in entrance length. Constants A and B were introduced to convert the pressure measurements in inches of manometer fluid to mm of mercury.

2. $\underline{CO_2\text{-Ethanol}}$: The calculations followed an identical pattern to those for the CO_2-water system.

3. $\underline{CO_2\text{-Ethylene Glycol}}$: The entrance length was zero for the CO_2-glycol system. The NTU values were calculated for the entire tube length therefore, and were corrected for the amount of absorption in the entrance tee and outlet cyclone. The amount of the corrections is listed in Appendix III. The NTU values were multiplied by a factor (0.72541) so that the values were then based on a length of tube 92.2 in, comparable to that used as the test section for all the other systems.

4. $\underline{He\text{-Water}}$: The calculation for the concentration driving force for the He-water system differed from that for the CO_2-water system, because of the difference in method of analysis. The ratios of water to CO_2 flow rates were required, along with the potentiometer reading to give the liquid-phase He concentrations. The equations for the He concentrations vs millivolt readings, as shown in Figure 12, were used directly in the

program for the concentration determinations.

Program for Computing the Correlation Variables for the Bubble and Plug Regions

The program was mainly involved with the calculation of the correlating variable according to equations (17, 18). Absorption data for gas superficial velocities exceeding 3.0 fps (slug region) were excluded. A regression line of the correlating variable on V_G^o, the gas superficial velocity, was obtained by the method of least squares.

Program for Computing the Correlation Variables for the Slug Flow Region

The program was involved with the calculation of the correlating variable for the slug region. Absorption data for gas superficial velocities of less than 2.0 fps were excluded. The various coefficients for the dimensionless ratios, as shown in Figure 25, were used for the corresponding values of liquid superficial velocity.

PROGRAMS FOR COMPUTATION OF NTU AND CORRELATING VARIABLES

```
FORTRAN 2 COMPILE.
C         COMPUTATION OF NTU FOR CARBON DIOXIDE WATER
60        PRINT 1
1         FORMAT (/53HSYSTEM   TUBE CM BP MM    OL GPM  TEMP CA SATC ML VP MM)
          READ2,LIQ,D,BP,OL,TEMP,CSAT,VP,A,B,C
2         FORMAT (I4,1F7.3,2F8.3,2F6.2,3F8.3,1F8.5)
          IF (LIQ) 70,80,70
70        PRINT 3,LIQ,D,BP,OL,TEMP,CSAT,VP
3         FORMAT (I6,6F8.3)
          AREA = 0.0008454*D*D
          PRINT 14
14        FORMAT(/67H RUN OG CFH P IN    PD   C IN  C OUT TYPE OGM  VCOR   TUN
         1     TUL   VG )
50        READ 4,NO,OG,P1,PD,C1,C2,J
4         FORMAT (I8,5F10.4,I4)
          IF(NO)51,60,51
51        PIN  = BP+A*P1
          POUT = PIN-B*PD
          PMEAN= 0.5*(PIN+POUT)
          FD = (PIN-POUT)/2.99
          PPIN = PIN-VP
          PPOUT= POUT-VP
          DFIN = PPIN*CSAT/760.0-C1
          DFOUT= PPOUT*CSAT/760.-C2
          DFLM = (DFIN-DFOUT)/LOG(DFIN/DFOUT)
          TUN  = (C2-C1)/DFLM
          TUL  = 7.683/TUN
          CONCE= 0.33947*TUN*DFIN/(1.0-.16974*TUN)
          TITR = 8.0203*OL*C
          VOLE = TITR*(CONCE+0.5*(C2-C1))*(273.2+TEMP)/273.2*760.0/(PMEAN-VP
         1)
          OGCOR= OG*756.0/(PMEAN-VP)*(273.2+TEMP)/288.2
          OGM  = OGCOR-VOLE
          VELG = OGM/AREA/3600.0
          PRINT 7,NO,OG,P1,FD,C1,C2,J,OGM,VOLE,TUN,TUL,VELG
7         FORMAT (I4,1F7.2,4F6.2,I3,1F7.2,1F6.2,1F7.4,1F6.1,1F7.3 )
          PUNCH 8,NO,J,OGM,TUN,TUL,VELG
8         FORMAT (I4,I3,1F7.2,1F7.4,1F6.1,1F7.3)

          GO TO 50
80        STOP
          END
```

```
FORTRAN 2 COMPILE.
C         COMPUTATION OF NTU FOR CARBON DIOXIDE ETHANOL
60        PRINT 1
1         FORMAT (/53HSYSTEM   TUBE CM BP MM    OL GPM  TEMP C  SATC ML VP MM)
          READ2,LIQ,D,BP,OL,TEMP,CSAT,VP,A,B,C
2         FORMAT (I4,1F7.3,2F8.3,2F6.2,3F8.3,1F8.5)
          IF (LIQ) 70,80,70
70        PRINT 3,LIQ,D,BP,OL,TEMP,CSAT,VP
3         FORMAT (I6,6F8.3)
          PRINT 14
14        FORMAT(/67H RUN OG CFH P IN    PD   C IN  C OUT TYPE OGM   VCOR   TUN
         1     TUL   VG )
50        READ 4,NO,OG,P1,PD,C1,C2,J
4         FORMAT (I8,5F10.4,I4)
          IF(NO)51,60,51
51        PIN  = BP+A*P1
          POUT = PIN-B*PD
          PMEAN= 0.5*(PIN+POUT)
          PPIN = PIN-VP
          PPOUT= POUT-VP
          DFIN = PPIN*CSAT/760.0-C1
          DFOUT= PPOUT*CSAT/760.-C2
          DFLM = (DFIN-DFOUT)/LOG(DFIN/DFOUT)
          TUN  = (C2-C1)/DFLM
          TUL  = 7.683/TUN
          CONCE= 0.33947*TUN*DFIN/(1.0-.16974*TUN)
          TITR = 8.0203*OL*C
          VOLE = TITR*(CONCE+0.5*(C2-C1))*(273.2+TEMP)/273.2*760.0/(PMEAN-VP
         1)
          OGCOR= OG*756.0/(PMEAN-VP)*(273.2+TEMP)/288.2
          OGM  = OGCOR-VOLE
          VELG = OGM/3600.0/0.002610
          PRINT 7,NO,OG,P1,PD,C1,C2,J,OGM,VOLE,TUN,TUL,VELG
7         FORMAT (I4,1F7.2,4F6.2,I3,1F7.2,1F6.2,1F7.4,1F6.1,1F7.3 )
          PUNCH 8,NO,J,OGM,TUN,TUL,VELG
8         FORMAT (I4,I3,1F7.2,1F7.4,1F6.1,1F7.3)
          GO TO 50
80        STOP
```

PROGRAMS FOR COMPUTATION OF NTU AND CORRELATING VARIABLES

```
FORTRAN 2 COMPILE.
      C      COMPUTATION OF NTU FOR HELIUM WATER
      60     PRINT 1
      1      FORMAT (/53HSYSTEM  TUBE CM  BP MM   OL GPM  TEMP C  SATC MF VP MM)
             READ2,LIO,D,BP,OL,TEMP,CSAT,VP,A,B,C
      2      FORMAT (I4,1F7.3,2E8.3,1E5.1,1F7.3,3E8.3,1E8.5)
             IF (LIO) 70,80,70
      70     PRINT 3,LIO,D,BP,OL,TEMP,CSAT,VP
      3      FORMAT (I6,6F8.3)
             AREA = 0.0008454*D*D
             PRINT 14
      14     FORMAT (/71H  NO  OG CFH  P1    PO   H IN H OUT TYPE OGM   VOLE
             1NTU  LTU  VELG   )
      50     READ 4,NO,OG,P1,PO,VIN,VOUT,TGIN,TGOUT,WIN,WOUT,J
      4      FORMAT (I4,1F7.2,2F6.2,6E7.3,I4)
             IF(NO)51,60,51
      51     PIN  = BP+A*P1
             POUT = PIN-B*PO
             PO   = PO/1.598
             PMEAN= 0.5*(PIN+POUT)
             PPIN = PIN-VP
             PPOUT= POUT-VP
             RIN  =50.0/TGIN/WIN
             ROUT =50.0/TGOUT/WOUT
             XIN  =RIN*(4.6250*VIN+0.053)
             YFIN =XIN*0.91925*BP/760.0*18.064/22.411
             IF   (VOUT-1.50) 10,10,11
      10     XOUT =ROUT*(4.7541*VOUT+0.039)
             GO TO 12
      11     XOUT =ROUT*(5.5830*VOUT-1.2262)
      12     YFOUT=XOUT*0.91925*BP/760.0*18.064/22.411
             DFIN =PPIN*CSAT/760.0-YFIN
             DFOUT=PPOUT*CSAT/760.0-YFOUT
             DFLM = (DFIN-DFOUT)/LOG(DFIN/DFOUT)
             TUN  =(YFOUT-YFIN)/DFLM
             TUL  = 7.683/TUN
             TITR = 8.0203*OL*C
             CONCE=0.33947*TUN*DFIN/(1.0-0.16974*TUN)

             VOLE =TITR*(CONCE+0.5*(YFOUT-YFIN))*996.36/(PMEAN-VP)
             OGCOR= OG*756.0/(PMEAN)
             OGM  = OGCOR-VOLE
             VELG =OGM/AREA/3600.0
             PRINT 7,NO,OG,P1,PO,YFIN,YFOUT,J,OGM,VOLE,TUN,TUL,VELG
      7      FORMAT (I4,1F7.2,4F6.2,I3,1F7.2,1F6.2,1F7.4,1F6.1,1F7.3 )
             PUNCH 8,NO,J,OGM,TUN,TUL,VELG
      8      FORMAT (I4,I3,1F7.2,1F7.4,1F6.1,1F7.3)
             GO TO 50
      80     STOP
             END
```

```
FORTRAN 2 COMPILE.
      C      COMPUTATION OF NTU FOR CARBON DIOXIDE ETHYLENE GLYCOL
      60     PRINT 1
      1      FORMAT (/53HSYSTEM  TUBE CM  BP MM   OL GPM   TEMP C   SATC ML CYCLO)
             READ2,LIO,D,BP,OL,TEMP,CSAT,CY,A,B,C
      2      FORMAT (I4,1F7.3,2F8.3,2F6.2,1F8.5,2F8.3,1F8.5)
             IF (LIO) 70,80,70
      70     PRINT 3,LIO,D,BP,OL,TEMP,CSAT,CY
      3      FORMAT (I6,6F8.3)
             PRINT 14
      14     FORMAT(/67H RUN OG CFH P IN    PO   C IN  C OUT TYPE OGM   VCOR   TUN
             1    TUL   VG )
      50     READ 4,NO,OG,P1,PO,C1,C2,J
      4      FORMAT (I8,5F10.4,I4)
             IF(NO)51,60,51
      51     PIN  = BP+A*P1
             POUT = PIN-B*PO
             PMEAN= 0.5*(PIN+POUT)
             PPIN = PIN-0.1
             PPOUT= POUT-0.1
             DFIN = PPIN*CSAT/760.0-C1
             DFOUT= PPOUT*CSAT/760.-C2
             DFLM = (DFIN-DFOUT)/LOG(DFIN/DFOUT)
             TUN  = 0.72541*((C2-C1)/DFLM-CY)
             TUL  = 7.683/TUN
             TITR = 8.0203*OL*C
             VOLE = TITR*0.5*(C2-C1)*(273.2+TEMP)/273.2*760.0/(PMEAN-0.1)
             OGCOR= OG*756.0/(PMEAN-.1)*(273.2+TEMP)/288.2
             OGM  = OGCOR-VOLE
             VELG = OGM/3600.0/0.002610
             PRINT 7,NO,OG,P1,PO,C1,C2,J,OGM,VOLE,TUN,TUL,VELG
      7      FORMAT (I4,1F7.2,4F6.2,I3,1F7.2,1F6.2,1F7.4,1F6.1,1F7.3 )
             PUNCH 8,NO,J,OGM,TUN,TUL,VELG
      8      FORMAT (I4,I3,1F7.2,1F7.4,1F6.1,1F7.3)
             GO TO 50
      80     STOP
```

```
FORTRAN 2 COMPILE.
C        CORRELATION OF VARIABLES FOR BUBBLE AND PLUG REGIONS
         READ 1,N,SUMX,SUMY,SUMXX,SUMXY
1        FORMAT (I4,4F10.4)
4        READ 2,LIQ,DT,QL,DIFF,ST,VISC
2        FORMAT (I4,3F6.3,2F7.3)
         IF (LIQ) 80,80,5
5        VELL = QL/7.481/60.0/(0.0008454*DT*DT)*
         PRINT 9
9        FORMAT (/42H LIQ TUBE QL GPM DIFF  S TENS VISC    VELL   )
         PRINT 8,LIQ,DT,QL,DIFF,ST,VISC,VELL
8        FORMAT (I4,3F6.3,3F7.3)
         PRINT 11
11       FORMAT (/50H NO J    QGM    NTU    LTU   VELG  FACTOR CORR Y   )
         F =SQRTF(1.465/DIFF*73.53/ST)*(1.14/VISC)**0.14*DT/3.0876*DT
60       READ 3,NO,J,QGM,TUN,TUL,VELG
3        FORMAT (I4,I3,1F7.2,1F7.4,1F6.1,1F7.3)
         IF (NO) 4,4,70
70       IF (VELG - 3.0) 95,95,60
95       Z = TUN*F*(VELL + VELG)
         Y = 0.43429*LOGF(Z)
         X = 0.43429*LOGF(VELG)
         PRINT 6,NO,J,QGM,TUN,TUL,VELG,F,Z
6        FORMAT (I4,I3,1F7.2,1F7.4,1F7.2,1F7.3,2F7.4)*
         PUNCH 14,NO,J,QGM,TUN,TUL,VELG,F,Z
14       FORMAT (I4,I3,1F7.2,1F7.4,1F7.2,1F7.3,2F7.4)
         N = N+1
         SUMX = SUMX + X
         SUMY = SUMY + Y
         SUMXY = SUMXY + X*Y
         SUMXX = SUMXX + X*X
         GO TO 60
80       DN =N
         XB = SUMX/DN
         YB = SUMY/DN
         B = (SUMXY - DN*XB*YB)/(SUMXX - DN*XB*XB)
         A = YB - B*XB
         PRINT 12,N,SUMX,SUMY,SUMXX,SUMXY,A,B
12       FORMAT(7I4,4F12.5,2F7.5)
         STOP
         END
```

PROGRAMS FOR COMPUTATION OF NTU AND CORRELATING VARIABLES

```
      FORTRAN 2 COMPILE.
C         CORRELATION FOR SLUG REGION
          READ 1,N,SUMX,SUMY,SUMXX,SUMXY
1         FORMAT (I4,4F10.4)
4         READ 2,LIQ,DT,QL,DIFF,ST,VISC
2         FORMAT (I4,3F6.3,2F7.3)
          IF (LIQ) 80,80,5
5         VELL = QL/7.481/60.0/(0.0008454*DT*DT)*
          PRINT 9
9         FORMAT (/42H LIQ TUBE QL GPM DIFF  S TENS VISC   VELL   )
          PRINT 8,LIQ,DT,QL,DIFF,ST,VISC,VELL
8         FORMAT (I4,3F6.3,3F7.3)
          PRINT 11
11        FORMAT (/50H NO J    QGM   NTU    LTU   VELG  FACTOR CORR Y   )
          IF (VELL-0.75) 20,30,30
20        F=(1.465/DIFF)**.374*(73.53/ST)**.151*(1.14/VISC)**.086*(DT/1.757)
          1**1.32
          GO TO 60
30        IF (VELL-1.3) 40,50,50
40        F=(1.465/DIFF)**.307*(73.53/ST)**.228*(VISC/1.14)**00.028*(DT/1.75
          17)**1.063
          GO TO 60
50        F=(1.465/DIFF)**.193*(73.53/ST)**.193*(VISC/1.14)**00.161*(DT/1.75
          17)**0.913
60        READ 3,NO,J,QGM,TUN,TUL,VELG
3         FORMAT (I4,I3,1F7.2,1F7.4,1F6.1,1F7.3)*
          IF (NO) 4,4,70
70        IF (VELG - 2.0) 60,60,95
95        Y=1.0/F*(.0164 + .0115*VELL)*(4.608- 1.96*VELLA+ VELG) - 0.014
          X  = TUN
          PRINT 6,NO,J,QGM,TUN,TUL,VELG,F,Y
6         FORMAT (I4,I3,1F7.2,1F7.4,1F7.2,1F7.3,2F7.4)
          PUNCH 14,NO,J,QGM,TUN,TUL,VELG,F,Y
14        FORMAT (I4,I3,1F7.2,1F7.4,1F7.2,1F7.3,2F7.4)
          N = N+1
          SUMX =SUMX + X
          SUMY = SUMY + Y

          SUMXY = SUMXY + X*Y
          SUMXX = SUMXX + X*X
          GO TO 60
80        DN =N
          XB = SUMX/DN
          YB = SUMY/DN
          B = (SUMXY - DN*XB*YB)/(SUMXX - DN*XB*XB)
          A = YB - B*XB
          PRINT 12,N,SUMX,SUMY,SUMXX,SUMXY,A,B
12        FORMAT (/I4,1F10.4,1F10.6,1F10.3,1F10.4,2F9.6)
          STOP
          END
```

APPENDIX V

LISTS OF EXPERIMENTAL DATA, CALCULATED VALUES OF

CORRELATION VARIABLES, AND RELATED CALCULATED RESULTS

Lists of Experimental Data and Calculated Values of NTU for

the Various Systems

The experimental runs were all numbered so that values

from the three separate lists of calculated results could be

related, if desired. Two number-codes were used, the first

referring to "system":

Number	System	
1	CO_2-Water.............	
2	He-Water..............	
3	CO_2-Ethanol..........	Tube size, 1.757 cm
4	CO_2-Glycol at 30°C...	
5	CO_2-Glycol at 15°C...	
6	CO_2-Water.............	Tube size, 1.228 cm
7	CO_2-Water.............	Tube size, 2.504 cm

The second number-code referring to "type" or flow region is as

follows:

Number	Type (flow region)
1	bubble
2	bubble-plug transition
3	plug
4	plug-slug transition
5	slug
6	slug-annular transition
7	annular

The values for "SATC ML" are saturated concentrations at the

absorption temperature and 760 mm pressure, and are given in
the same units as "C IN" and " OUT" for the particular series
of experiments, usually ml of 0.1 N equivalent base for a
100-ml sample, or millimoles per litre.

The units of the various other listed variables are as
follows:

Variable	Definition and Units
QG CFH	gas flow, cfh at 15°C, 756 mm (dry gas)
P IN, PD	pressure, pressure drop; inches of carbon tetra-chloride (at 21°C), unless otherwise noted
QGM	mean gas flow rate, cfh at absorption temperature and mean test section pressure, saturated
VCOR	the sum of the volume of gas absorbed in the entrance section and one half that absorbed in the test section; units same as for QGM
TUN	NTU, dimensionless
TUL	LTU, ft
VG	gas superficial velocity, fps

Lists of Calculated Correlation Variables for the Bubble
and Slug Regions

The listed variables not previously defined, and their
units, are as follows:

Variable	Definition and Units
DIFF	diffusion coefficient, cm^2/sec (10^5)
S TENS	surface tension, dynes/cm
VISC	viscosity, cp
VELL	liquid superficial velocity, fps
J	same as "TYPE", defined by second code-number
FACTOR	products of all dimensionless groups raised to appropriate exponents, dimensionless
CORR Y	(a) ordinate for bubble correlation; fps (b) predicted NTU value for slug correlation; dimensionless

COMPUTATION OF NTU

EXECUTE FORTRAN PROGRAM.

SYSTEM	TUBE CM	BP MM	OL GPM	TEMP C	SATC ML	VP MM
1	1.757	754.000	.620	15.000	45.475	12.800

RUN	OG CFH	P IN	PD	C IN	C OUT	TYPE	UGM	VCOR	TUN	TUL	VG
41	135.40	4.90	1.58	3.40	17.20	5	132.74	1.10	.4023	19.0	14.128
42	105.10	3.20	1.82	5.60	15.50	5	103.24	.95	.3414	22.4	10.089
43	72.70	2.00	1.37	4.00	13.00	5	73.04	.71	.2508	30.6	7.774
44	36.90	1.50	1.18	1.20	7.20	5	37.02	.47	.1491	51.5	3.041
45	1.24	.50	.31	1.20	3.60	1	1.07	.18	.0571	134.4	.114
46	4.52	.55	.29	1.40	5.30	1	4.29	.30	.0950	80.8	.457
47	8.82	.70	.41	1.60	5.30	2	8.69	.28	.0903	85.0	.024
48	12.88	.80	.48	1.70	5.70	3	12.79	.31	.0982	78.1	1.361
49	18.08	1.00	.68	1.90	6.60	5	18.02	.36	.1170	65.6	1.018
50	28.20	1.30	.92	2.00	7.50	4	28.23	.43	.1386	55.4	3.005
51	47.00	1.70	1.32	1.70	9.30	5	47.13	.59	.1953	39.3	5.017
52	60.40	1.90	1.33	1.70	10.30	5	60.62	.67	.2239	34.3	6.452

SYSTEM	TUBE CM	BP MM	OL GPM	TEMP C	SATC ML	VP MM
1	1.757	758.200	2.100	15.000	45.470	12.800

RUN	OG CFH	P IN	PD	C IN	C OUT	TYPE	UGM	VCOR	TUN	TUL	VG
53	4.84	2.50	2.50	8.60	10.50	1	4.38	.49	.0538	142.5	.467
54	7.86	3.05	2.95	9.30	12.20	1	7.16	.75	.0850	95.5	.762
55	11.18	3.60	3.28	9.90	13.70	1	10.25	.99	.1148	66.9	1.091
56	13.28	3.70	3.38	9.70	15.10	1	11.95	1.42	.1663	46.1	1.270
57	16.71	4.00	3.62	12.20	16.30	3	15.72	1.37	.1556	57.4	1.673
58	20.22	5.00	4.06	7.60	12.00	3	19.11	1.14	.1247	61.5	2.054
59	27.00	5.00	3.37	8.40	13.00	5	25.82	1.20	.1336	57.4	2.748
60	36.60	6.10	4.28	9.60	14.70	5	35.20	1.33	.1542	49.8	3.747
61	46.00	8.10	5.97	10.60	17.00	5	44.93	1.67	.2021	37.8	4.782
62	68.60	10.80	7.86	12.10	20.30	5	65.54	2.16	.2792	27.3	6.976
63	93.40	12.80	8.98	13.90	24.90	5	88.72	2.04	.4201	18.2	9.444
64	150.00	17.00	10.09	13.80	29.60	6	141.08	4.33	.6621	11.6	15.016
65	122.00	14.90	10.02	13.60	26.40	6	115.56	3.44	.4984	15.4	12.390
66	102.50	12.90	8.45	13.40	25.30	5	97.35	3.10	.4392	17.4	10.362
67	93.40	12.50	8.24	13.30	24.20	5	88.74	2.90	.4056	18.9	9.445

SYSTEM	TUBE CM	BP MM	OL GPM	TEMP C	SATC ML	VP MM
1	1.575	757.200	1.500	15.000	45.470	12.800

RUN	OG CFH	P IN	PD	C IN	C OUT	TYPE	UGM	VCOR	TUN	TUL	VG
74	1.32	1.10	1.10	2.20	3.45	1	1.13	.23	.0299	256.9	.146
75	2.03	1.15	1.15	3.60	5.40	1	1.72	.35	.0448	171.2	.227
76	3.58	1.30	1.30	5.50	7.40	1	3.27	.35	.0497	154.4	.433
77	5.85	1.45	1.41	5.30	8.50	1	5.32	.59	.0847	90.6	.795
78	9.11	1.95	1.88	4.70	9.00	1	8.43	.49	.1136	67.5	1.113

SYSTEM	TUBE CM	BP MM	OL GPM	TEMP C	SATC ML	VP MM
1	1.575	759.600	1.500	15.000	45.470	12.800

RUN	OG CFH	P IN	PD	C IN	C OUT	TYPE	UGM	VCOR	TUN	TUL	VG
79	12.29	2.35	2.16	4.10	9.10	1	11.44	.93	.1307	58.7	1.515
80	15.84	2.45	2.23	4.00	8.70	1	15.06	.88	.1220	62.9	1.996
81	19.30	2.70	2.44	5.30	9.50	3	18.63	.78	.1120	66.5	2.468
82	28.90	3.30	2.98	6.90	11.60	5	28.14	.89	.1343	57.2	3.728
83	36.90	3.90	3.39	6.70	11.80	5	36.07	.95	.1426	53.8	4.778
84	48.30	4.80	4.04	6.90	12.80	5	47.25	1.10	.1675	45.8	6.258

SYSTEM	TUBE CM	BP MM	OL GPM	TEMP C	SATC ML	VP MM
1	1.575	758.200	1.500	15.000	45.470	12.800

RUN	OG CFH	P IN	PD	C IN	C OUT	TYPE	UGM	VCOR	TUN	TUL	VG
90	3.57	1.25	1.25	4.00	6.30	1	3.18	.42	.0581	132.0	.421
91	4.79	1.40	1.40	4.90	7.60	1	4.34	.50	.0702	109.4	.574
92	19.30	2.60	2.50	8.10	12.20	3	18.70	.76	.1183	64.9	2.476
93	57.30	5.10	4.59	8.20	16.80	5	55.83	1.63	.2656	28.0	7.395
94	115.30	7.30	6.61	11.40	26.10	5	112.18	2.91	.5738	13.4	14.859
95	190.70	11.00	9.68	12.50	34.40	6	184.05	4.69	1.0966	7.0	24.379

SYSTEM	TUBE CM	BP MM	OL GPM	TEMP C	SATC ML	VP MM
1	1.575	759.200	.620	15.000	45.470	12.800

RUN	OG CFH	P IN	PD	C IN	C OUT	TYPE	OGM	VCOR	TUN	TUL	VG
112	1.24	.27	.28	1.70	3.90	1	1.08	.16	.0525	146.2	.143
113	2.48	.34	.35	1.70	5.40	1	2.22	.28	.0900	85.3	.294
114	5.80	.45	.46	1.90	6.80	2	5.48	.38	.1216	63.1	.727
115	10.39	.63	.63	2.00	7.50	3	10.08	.42	.1378	55.7	1.335
116	15.30	.73	.70	2.10	7.40	3	15.06	.41	.1327	57.8	1.994
117	20.22	.88	.84	2.40	7.50	3	20.04	.39	.1283	59.8	2.655
118	30.80	1.20	1.13	2.30	8.30	5	30.64	.46	.1523	50.4	4.059

SYSTEM	TUBE CM	BP MM		QL GPM	TEMP C	SATC ML	VP MM
1	1.575	757.620		.620	15.000	45.470	12.800

RUN	QG CFH	P IN	PD	C IN	C OUT	TYPE	QGM	VCOR	TUN	TUL	VG
119	41.10	1.35	1.22	2.20	11.50	5	40.85	.73	.2470	31.0	5.412
120	60.70	1.60	1.41	2.70	13.50	5	60.53	.85	.2971	25.8	8.018
121	85.00	1.80	1.58	3.30	13.50	5	85.12	.82	.2826	27.1	11.274
122	113.50	2.40	2.05	3.50	15.10	5	113.65	.92	.3298	25.2	15.053
123	144.00	2.95	2.38	3.60	17.50	5	144.02	1.11	.4109	18.6	19.076
124	169.00	3.60	2.84	4.00	19.90	5	168.76	1.29	.4921	15.4	22.353

SYSTEM	TUBE CM	BP MM		QL GPM	TEMP C	SATC ML	VP MM
1	1.575	753.300		2.100	15.000	45.470	12.800

RUN	QG CFH	P IN	PD	C IN	C OUT	TYPE	QGM	VCOR	TUN	TUL	VG
125	1.36	1.92	2.01	3.10	4.05	1	1.13	.24	.0252	350.6	.150
126	2.82	2.12	2.18	4.10	5.55	1	2.48	.37	.0365	210.1	.329
127	14.80	3.70	3.57	9.40	13.10	1	14.01	.07	.1139	69.2	1.856
128	130.60	14.60	10.47	16.00	28.50	6	125.05	3.42	.5458	14.1	16.564
129	191.70	18.60	14.09	18.20	34.40	6	182.33	4.65	.8747	8.7	24.151

SYSTEM	TUBE CM	BP MM		QL GPM	TEMP C	SATC ML	VP MM
1	1.575	752.500		2.100	15.000	45.470	12.800

RUN	QG CFH	P IN	PD	C IN	C OUT	TYPE	QGM	VCOR	TUN	TUL	VG
130	1.91	2.05	2.11	4.40	5.55	1	1.64	.30	.0291	263.5	.217
131	6.17	2.52	2.52	6.70	8.80	1	5.72	.55	.0571	134.3	.757
132	12.79	3.42	3.29	10.20	13.50	1	12.10	.87	.1009	76.8	1.603
133	14.53	3.60	3.41	11.20	14.60	1	13.84	.89	.1074	71.5	1.833
134	19.14	4.20	3.88	12.50	15.90	3	18.48	.89	.1117	68.7	2.448
135	11.67	3.30	3.20	12.70	15.80	1	11.02	.81	.1024	75.0	1.460
136	1.64	1.98	2.01	4.30	5.30	1	1.40	.26	.0252	304.4	.186
137	8.73	2.90	2.90	8.25	11.00	1	8.14	.72	.0788	97.4	1.079
138	17.44	3.96	3.64	10.70	14.10	3	16.77	.89	.1056	72.7	2.222
139	23.30	4.90	3.96	11.90	15.60	3	22.54	.07	.1194	64.3	2.988
140	30.10	5.80	4.48	12.10	16.00	3	29.30	1.02	.1266	60.6	3.881

SYSTEM	TUBE CM	BP MM		QL GPM	TEMP C	SATC ML	VP MM
1	1.575	755.000		1.500	15.000	45.470	12.800

RUN	QG CFH	P IN	PD	C IN	C OUT	TYPE	QGM	VCOR	TUN	TUL	VG
141	1.64	1.11	1.20	5.20	6.50	1	1.42	.24	.0356	228.3	.188
142	2.83	1.20	1.26	5.30	7.40	1	2.48	.39	.0550	139.5	.328
143	7.81	1.74	1.75	7.60	11.20	1	7.25	.67	.1024	74.9	.063
144	10.96	2.12	2.08	7.90	12.30	1	10.28	.83	.1277	60.1	1.362
145	15.03	2.40	2.33	8.50	13.20	1	14.34	.88	.1394	55.1	1.000
146	25.10	2.94	2.81	9.00	13.40	4	24.58	.82	.1316	58.3	3.255
147	40.00	4.14	3.70	9.70	15.00	5	39.37	1.30	.1637	46.9	5.214
148	69.00	5.60	4.53	10.90	19.00	5	67.80	1.54	.2715	28.2	8.961

SYSTEM	TUBE CM	BP MM		QL GPM	TEMP C	SATC ML	VP MM
1	1.757	757.300		1.500	15.000	45.470	12.800

RUN	QG CFH	P IN	PD	C IN	C OUT	TYPE	QGM	VCOR	TUN	TUL	VG
149	2.34	1.15	1.21	3.80	5.50	1	2.05	.31	.0425	180.6	.218
150	3.99	1.27	1.29	4.30	6.70	1	3.59	.44	.0613	125.2	.382
151	20.14	2.67	2.55	7.10	11.30	3	19.54	.78	.1181	65.0	2.383
152	55.20	5.26	4.69	8.40	15.20	5	54.11	1.28	.2253	37.4	5.767
153	107.50	7.90	5.62	10.90	21.60	5	105.29	2.06	.3735	20.5	11.207
154	151.50	9.39	7.76	12.40	26.30	5	147.77	2.73	.5468	14.0	15.728
155	190.60	11.43	9.55	13.80	30.00	6	185.24	3.26	.7147	10.7	19.716

SYSTEM	TUBE CM	BP MM		QL GPM	TEMP C	SATC ML	VP MM
1	1.757	750.300		1.500	15.000	45.470	12.800

RUN	QG CFH	P IN	PD	C IN	C OUT	TYPE	QGM	VCOR	TUN	TUL	VG
156	5.59	1.43	1.46	5.20	8.15	1	5.15	.55	.0785	97.7	.548
157	12.74	2.25	2.25	5.40	10.30	1	12.06	.93	.1345	57.0	1.284
158	17.58	2.46	2.40	5.55	9.80	3	17.12	.80	.1163	66.2	1.822
159	121.20	7.82	6.69	9.00	26.90	5	119.70	2.32	.4035	19.0	12.741
160	163.80	9.86	8.48	10.20	24.50	5	161.33	2.83	.5294	14.5	17.172
161	194.70	11.70	9.82	11.30	27.00	6	191.09	3.14	.6253	12.3	20.439
162	21.65	2.79	2.63	6.05	10.20	4	21.27	.78	.1145	67.0	2.264

SYSTEM	TUBE CM	BP MM		QL GPM	TEMP C	SATC ML	VP MM
1	1.757	759.200		1.070	15.000	45.470	12.800

RUN	QG CFH	P IN	PD	C IN	C OUT	TYPE	QGM	VCOR	TUN	TUL	VG
163	18.76	1.55	1.51	5.00	8.60	4	18.31	.62	.1220	62.9	1.949
164	22.60	1.70	1.64	4.10	9.00	4	22.15	.65	.1282	59.9	2.350
165	31.50	2.12	1.93	4.30	10.00	5	30.09	.76	.1514	50.7	3.298
166	86.40	3.52	3.08	5.10	15.00	5	85.47	1.34	.2853	26.9	9.097
167	137.60	4.97	4.24	5.90	18.00	5	136.05	1.70	.4029	19.0	14.481
168	198.30	7.05	5.86	7.10	24.30	5	195.15	2.43	.5985	12.8	20.771

COMPUTATION OF NTU

SYSTEM	TUBE CM	BP MM	OL GPM	TEMP C	SATC ML	VP MM
1	1.757	751.500	1.070	15.000	45.470	12.800

RUN	OG CFH	P IN	PD	C IN	C OUT	TYPE	QGM	VCOR	TUN	TUL	VG
169	1.52	.46	.49	1.90	3.50	1	1.13	.21	.0385	199.4	.129
170	3.02	.65	.66	2.40	5.00	1	2.73	.34	.0641	119.7	.291
171	8.77	1.12	1.13	3.30	7.90	1	8.33	.62	.1190	64.5	.886
172	11.40	1.26	1.26	3.70	8.70	2	10.95	.67	.1314	58.4	1.166
173	13.66	1.36	1.36	3.40	8.30	5	13.27	.66	.1275	60.2	1.413
174	16.27	1.45	1.39	3.30	8.20	5	15.63	.66	.1271	60.4	1.696
175	54.90	3.03	2.46	4.20	11.90	5	54.72	1.05	.2120	36.2	5.825
176	167.10	6.02	5.26	5.80	20.50	5	166.63	2.07	.4742	16.2	17.735
177	198.30	7.21	6.14	6.40	22.70	5	197.28	2.31	.5518	13.0	20.898

SYSTEM	TUBE CM	BP MM	OL GPM	TEMP C	SATC ML	VP MM
1	1.757	749.400	1.070	15.000	45.470	12.800

RUN	OG CFH	P IN	PD	C IN	C OUT	TYPE	QGM	VCOR	TUN	TUL	VG
178	2.07	.59	.62	2.30	4.30	1	1.85	.26	.0490	156.7	.197
179	3.57	.72	.73	2.40	5.40	1	3.25	.40	.0746	102.0	.346
180	6.26	.91	.92	3.30	7.10	1	5.89	.51	.0976	78.6	.627
181	9.70	1.19	1.19	3.30	8.20	1	9.26	.66	.1277	60.1	.986
182	12.69	1.32	1.30	3.30	8.40	3	12.29	.69	.1352	57.6	1.330
183	15.84	1.41	1.37	3.50	8.20	5	15.57	.63	.1227	62.6	1.657

SYSTEM	TUBE CM	BP MM	OL GPM	TEMP C	SATC ML	VP MM
1	1.757	760.400	.620	15.000	45.470	12.800

RUN	OG CFH	P IN	PD	C IN	C OUT	TYPE	QGM	VCOR	TUN	TUL	VG
193	1.32	.27	.38	2.60	4.65	1	1.12	.20	.0498	154.0	.119
194	3.22	.37	.47	2.85	6.65	1	2.86	.39	.0950	83.8	.304
195	5.53	.40	.50	2.90	7.45	1	5.11	.47	.1150	66.7	.544
196	8.20	.55	.65	3.40	8.40	1	7.76	.51	.1288	59.6	.826
197	10.96	.60	.70	3.40	8.40	20	10.55	.51	.1288	59.6	1.123
198	12.74	.62	.72	3.30	8.30	3	12.35	.51	.1284	59.8	1.314
199	16.31	.73	.81	3.45	8.00	3	16.00	.47	.1166	65.8	1.703
200	19.26	.86	.94	3.75	8.00	4	19.00	.43	.1093	70.2	2.025
201	31.20	1.19	1.26	4.85	9.15	5	31.03	.44	.1138	67.5	3.303 ×

SYSTEM	TUBE CM	BP MM	OL GPM	TEMP C	SATC ML	VP MM
1	1.757	759.900	.620	15.000	45.470	12.800

RUN	OG CFH	P IN	PD	C IN	C OUT	TYPE	QGM	VCOR	TUN	TUL	VG
202	42.50	1.51	1.19	3.60	9.55	5	42.22	.62	.1557	49.3	4.494
203	54.30	1.68	1.27	4.15	11.15	5	53.96	.73	.1871	41.0	5.746
204	72.60	1.84	1.37	4.55	13.15	5	72.20	.92	.2397	32.0	7.685
205	96.60	2.48	1.66	5.00	14.95	5	96.03	1.07	.2861	26.8	10.221
206	134.10	3.62	2.21	5.90	17.75	5	133.03	1.30	.3596	21.3	14.160
207	177.00	5.14	2.54	7.53	21.60	5	174.78	1.59	.4651	16.5	18.603
208	197.20	6.04	3.38	8.30	23.80	5	194.33	1.80	.5425	14.2	20.604

SYSTEM	TUBE CM	BP MM	OL GPM	TEMP C	SATC ML	VP MM
1	1.757	760.200	3.000	15.000	45.470	12.800

RUN	OG CFH	P IN	PD	C IN	C OUT	TYPE	QGM	VCOR	TUN	TUL	VG
209	1.59	6.88	3.45	3.45	4.00	1	1.31	.26	.0131	585.4	.139 ×
210	2.87	6.90	3.48	4.20	5.15	1	2.38	.45	.0231	351.2	.254
211	5.81	7.47	3.91	6.00	7.60	1	4.97	.77	.0411	186.7	.520
212	9.80	8.57	4.77	10.00	12.10	1	8.65	1.01	.0604	127.1	.021
213	15.58	10.03	5.57	13.40	16.00	1	14.07	1.23	.0815	94.1	1.498
214	23.70	11.73	6.52	13.90	16.80	3	21.77	1.40	.0940	81.6	2.318
215	35.10	13.05	7.13	14.50	18.15	5	30.37	1.77	.1209	63.5	3.252
216	44.70	16.30	8.41	15.55	19.80	5	41.05	2.07	.1463	52.6	4.569
217	75.40	22.70	11.69	17.75	24.50	5	68.09	3.35	.2560	30.0	7.247
218	97.00	25.50	12.74	19.60	27.70	5	87.03	4.10	.3358	22.8	9.263

SYSTEM	TUBE CM	BP MM	OL GPM	TEMP C	SATC ML	VP MM
1	1.757	758.900	3.000	15.000	45.470	12.800

RUN	OG CFH	P IN	PD	C IN	C OUT	TYPE	QGM	VCOR	TUN	TUL	VG
219	2.07	3.46	3.57	5.50	6.35	1	1.66	.41	.0217	352.5	.177
220	7.57	4.55	4.23	7.50	8.80	1	6.96	.63	.0352	218.1	.740 ×
221	11.49	5.46	4.74	10.40	12.00	1	10.41	1.08	.0659	116.5	1.108
222	18.45	6.79	5.47	11.40	14.30	3	16.96	1.43	.0893	86.0	1.805
223	65.80	13.76	10.75	16.00	22.00	5	61.45	3.05	.2226	34.5	6.541
224	102.30	18.30	13.92	19.15	28.10	5	94.36	4.78	.3967	19.3	10.044
225	134.30	21.80	16.48	22.00	32.55	6	123.13	5.03	.5553	13.8	13.106
226	172.00	26.70	20.13	24.70	37.60	7	155.29	8.10	.8612	8.0	16.528
227	187.40	27.80	20.98	25.00	37.80	7	169.52	8.04	.8633	8.8	18.043

SYSTEM	TUBE CM	BP MM	OL GPM	TEMP C	SATC ML	VP MM
1	1.757	747.600	3.000	15.000	45.470	12.800

RUN	OG CFH	P IN	PD	C IN	C OUT	TYPE	OGM	VCOR	TUN	TUL	VG
228	5.08	4.09	3.93	7.35	8.70	10	4.67	.50	.0371	236.6	.497
229	8.72	5.09	4.63	8.45	10.30	1	8.17	.60	.0527	145.6	.870
230	13.10	6.13	5.21	9.95	12.45	1	12.34	.03	.0749	102.5	1.314
231	27.20	8.21	6.64	11.15	14.35	5	26.23	1.20	.0998	76.9	2.792
232	59.30	13.12	10.05	13.80	19.15	5	57.05	2.01	.1858	41.3	6.072
233	89.30	16.04	12.89	15.65	23.95	5	84.05	3.15	.3232	25.7	9.242
234	125.20	20.70	15.75	17.80	29.60	6	117.80	4.61	.5426	14.1	12.539
235	164.60	24.80	18.90	19.30	32.50	6	154.15	5.25	.6715	11.6	16.637

SYSTEM	TUBE CM	BP MM	OL GPM	TEMP C	SATC ML	VP MM
1	1.757	752.400	1.070	5.300	62.910	6.600

RUN	OG CFH	P IN	PD	C IN	C OUT	TYPE	OGM	VCOR	TUN	TUL	VG
236	4.63	.96	.97	6.15	9.70	1	3.92	.60	.0658	116.6	.417
237	8.48	1.16	1.15	6.85	12.20	1	7.36	.02	.1022	75.1	.783
238	12.79	1.37	1.36	7.45	12.90	3	11.55	.03	.1054	72.8	1.229
239	24.30	1.91	1.85	8.25	12.95	5	22.90	.80	.0915	83.0	2.437
240	45.70	3.13	2.98	9.00	15.85	5	43.28	1.18	.1380	55.6	4.607
241	87.20	3.88	3.53	10.00	21.00	5	82.73	1.06	.2565	32.6	8.806
242	122.00	4.90	4.45	10.90	25.05	5	116.52	2.58	.3217	25.8	12.402
243	164.70	5.65	5.05	13.15	29.30	5	156.31	3.01	.3971	19.3	16.637

SYSTEM	TUBE CM	BP MM	OL GPM	TEMP C	SATC ML	VP MM
1	1.757	753.300	1.070	30.000	29.630	31.900

RUN	OG CFH	P IN	PD	C IN	C OUT	TYPE	OGM	VCOR	TUN	TUL	VG
244	4.68	.74	.73	1.65	4.25	1	4.64	.50	.1031	74.4	.494
245	8.44	.96	.94	1.95	5.30	1	8.62	.65	.1366	56.2	.918
246	12.83	1.18	1.16	2.10	5.50	3	13.44	.66	.1395	55.0	1.430
247	23.80	1.71	1.68	2.45	5.85	5	25.46	.65	.1392	55.1	2.712
248	45.70	3.27	3.18	3.15	7.80	5	49.10	.02	.2043	37.6	5.226
249	88.10	4.53	4.34	4.05	11.25	5	94.68	1.49	.3509	21.9	10.077
250	125.30	5.26	4.81	4.75	13.20	5	132.52	1.82	.4414	17.3	14.125
251	165.80	6.49	5.96	6.10	15.75	5	178.01	2.13	.5645	13.6	18.046

SYSTEM	TUBE CM	BP MM	OL GPM	TEMP C	SATC ML	VP MM
1	1.757	757.000	1.070	45.000	21.420	71.000

RUN	OG CFH	P IN	PD	C IN	C OUT	TYPE	OGM	VCOR	TUN	TUL	VG
252	4.73	.68	.66	1.15	2.70	1	5.42	.33	.0892	86.2	.577
253	8.48	.91	.89	1.55	3.95	1	9.79	.52	.1448	53.0	1.042
254	12.65	1.07	1.03	1.55	3.75	5	14.89	.47	.1318	58.2	1.585
255	23.10	1.60	1.53	1.75	3.85	5	27.58	.45	.1268	60.5	2.936 X
256	45.30	2.53	2.28	2.10	5.50	5	54.10	.75	.2185	35.1	5.759
257	86.00	3.34	3.04	2.50	7.90	5	102.70	1.25	.3837	20.0	10.931
258	122.00	4.09	3.67	3.15	9.50	5	146.75	1.52	.4926	15.5	15.620
259	165.00	5.63	5.17	3.05	11.05	5	196.36	2.02	.6651	11.5	20.900

For runs number 260 to 306 inclusive only, the inlet pressure, P IN, given in inches of mercury; (PD) given in inches of CCl_4 as previously.

SYSTEM	TUBE CM	BP MM	OL GPM	TEMP C	SATC ML	VP MM
1	1.757	753.100	1.070	15.000	45.470	12.800

RUN	OG CFH	P IN	PD	C IN	C OUT	TYPE	OGM	VCOR	TUN	TUL	VG
260	6.27	9.95	.81	5.10	9.45	1	4.19	.58	.0836	91.8	.446
261	9.20	9.90	.96	5.20	11.10	1	6.22	.70	.1155	66.4	.662
262	13.31	9.95	1.41	6.15	12.55	2	9.28	.86	.1283	59.8	.988
263	28.30	10.05	1.58	7.00	12.10	4	20.85	.68	.1023	75.0	2.219
264	55.70	9.90	2.63	9.80	16.75	5	41.67	.95	.1519	50.5	4.435
265	86.00	9.95	3.12	11.15	21.45	5	64.33	1.44	.2417	31.7	6.847
266	127.80	10.00	3.50	11.70	24.20	5	95.89	1.79	.3558	25.1	10.276
267	165.00	10.05	4.00	13.75	27.40	5	122.53	1.98	.3575	21.4	13.042

SYSTEM	TUBE CM	BP MM	OL GPM	TEMP C	SATC ML	VP MM
1	1.757	762.400	4.200	15.000	45.470	12.800

RUN	OG CFH	P IN	PD	C IN	C OUT	TYPE	OGM	VCOR	TUN	TUL	VG
268	3.42	1.05	5.93	4.00	5.00	1	2.69	.66	.0241	318.1	.287 X
269	5.97	1.13	6.56	4.95	6.05	1	5.13	.73	.0271	282.6	.546
270	13.23	1.35	8.11	6.80	8.80	1	11.61	1.34	.0521	147.3	1.236
271	24.10	1.61	9.54	8.35	11.15	5	21.58	1.88	.0704	109.5	2.297
272	34.50	1.91	11.12	10.05	13.45	5	31.07	2.29	.0973	78.9	3.307
273	54.30	2.43	13.74	12.55	18.30	5	47.96	3.04	.1813	42.3	5.104
274	74.20	2.99	16.90	15.65	22.05	5	65.67	4.42	.2224	34.5	6.989

COMPUTATION OF NTU

SYSTEM	TUBE CM	BP MM	OL GPM	TEMP C	SATC ML	VP MM
1	1.757	755.700	4.200	15.000	45.470	12.800

RUN	OG CFH	P IN	PD	C IN	C OUT	TYPE	OGM	VCOR	TUN	TUL	VG	
275	2.12	1.02	5.79	3.25	4.00	1	1.60	.50	.0179	428.6	.170	x
276	19.87	1.55	9.16	10.15	12.10	1	18.22	1.32	.0559	137.2	1.039	
277	28.50	1.78	10.62	12.70	15.50	5	25.99	1.91	.0873	87.0	2.766	x
278	45.20	2.20	12.63	14.65	18.65	5	41.06	2.74	.1337	57.4	4.371	
279	87.70	3.38	18.81	18.60	25.15	5	78.21	4.59	.2547	30.1	8.325	
280	109.00	3.79	20.79	21.05	29.05	5	96.21	5.76	.3509	21.8	10.240	
281	137.60	4.33	23.58	25.65	33.10	6	120.15	7.07	.4782	16.0	12.788	
282	176.10	5.10	28.52	26.20	37.70	6	151.09	9.34	.7050	10.8	16.081	
283	180.20	5.32	30.09	27.20	37.80	7	155.03	8.50	.6611	11.6	16.501	

SYSTEM	TUBE CM	BP MM	OL GPM	TEMP C	SATC ML	VP MM
1	1.757	757.700	1.070	15.000	45.470	12.800

RUN	OG CFH	P IN	PD	C IN	C OUT	TYPE	OGM	VCOR	TUN	TUL	VG
284	2.70	11.18	1.55	6.05	9.20	1	1.58	.40	.0585	131.1	.168
285	5.86	11.18	1.63	7.50	11.634	1	3.78	.52	.0791	97.1	.405
286	12.02	11.18	1.82	7.70	14.05	1	8.63	.88	.1343	57.1	.918
287	25.90	11.19	1.88	8.80	14.40	3	16.87	.72	.1125	68.2	1.796
288	31.00	11.19	1.93	9.05	14.35	4	22.14	.68	.1067	71.9	2.357
289	47.90	11.19	2.02	10.85	17.60	5	34.33	.88	.1433	53.5	3.654
290	85.50	11.19	2.83	10.50	21.20	5	61.62	1.44	.2365	32.4	6.558
291	155.60	11.20	4.03	14.65	26.75	5	112.06	1.08	.3609	21.2	12.023
292	163.00	11.22	4.12	14.95	29.65	5	110.27	2.09	.3846	19.0	12.588

SYSTEM	TUBE CM	BP MM	OL GPM	TEMP C	SATC ML	VP MM
1	1.757	757.700	1.070	15.000	45.470	12.800

RUN	OG CFH	P IN	PD	C IN	C OUT	TYPE	OGM	VCOR	TUN	TUL	VG	
293	2.98	-8.30	.68	2.50	4.20	1	2.52	.41	.0595	126.0	.269	
294	4.95	-8.29	.91	3.40	6.20	1	6.32	.70	.1034	74.2	.472	
295	12.29	-8.14	1.23	4.20	7.05	3	16.61	.70	.1078	71.2	1.768	
296	18.98	-8.15	1.45	4.95	8.10	5	25.09	.78	.1235	62.1	2.766	
297	26.50	-7.91	2.40	7.80	11.30	5	38.99	.87	.1540	49.8	4.150	
298	37.20	-8.15	2.65	12.60	16.15	5	51.75	.91	.2029	37.8	5.508	
299	41.40	-7.51	3.58	16.65	20.80	5	55.95	1.07	.2970	25.8	5.955	x

SYSTEM	TUBE CM	BP MM	OL GPM	TEMP C	SATC ML	VP MM
1	1.757	762.700	1.070	15.000	45.470	12.800

RUN	OG CFH	P IN	PD	C IN	C OUT	TYPE	OGM	VCOR	TUN	TUL	VG
300	1.51	-8.03	.60	2.45	3.55	1	1.83	.24	.0571	206.7	.194
301	3.42	-8.06	.72	3.15	5.35	1	4.21	.53	.0777	98.7	.448
302	7.19	-8.16	1.09	4.25	7.50	2	9.24	.80	.1228	62.5	.983
303	9.90	-8.07	1.20	5.15	8.40	3	12.83	.80	.1265	65.7	1.366
304	15.84	-8.15	1.60	5.70	9.35	4	21.50	.65	.1048	73.3	2.288
305	25.40	-8.12	2.20	6.10	9.25	5	31.95	.78	.1279	60.0	3.401
306	38.70	-7.80	9.09	15.35	18.30	5	53.59	.76	.1933	39.7	5.754

COMPUTATION OF NTU

SYSTEM	TUBE CM	BP MM	QL GPM	TEMPΔC	SATC ML	VP MM
3	1.757	747.500	1.040	13.500	36.600	28.700

RUN	QG CFH	P IN	PD	C IN	C OUT	TYPE	QGM	VCOR	TUN	TUL	VG
351	1.98	.47	.77	1.45	2.65	1	1.22	.84	.0368	208.6	.130
352	4.04	.55	.88	1.90	3.50	1	3.09	1.12	.0500	153.4	.329
353	5.99	.67	.99	2.70	5.05	1	4.58	1.66	.0763	100.6	.488
354	8.68	.81	1.22	3.90	6.70	1	7.06	1.99	.0953	80.5	.751
355	15.48	1.09	1.59	4.90	7.85	3	14.04	2.11	.1042	73.6	1.494
356	25.80	1.39	2.08	5.50	8.35	5	24.87	2.03	.1026	74.8	2.647
357	34.50	1.85	2.68	6.20	8.75	5	34.12	1.81	.0935	82.1	3.632 X
358	59.60	2.47	3.46	7.35	12.50	5	58.21	3.78	.2077	36.9	6.195
359	107.40	3.72	5.07	9.80	17.10	5	105.79	5.58	.3437	22.3	11.259

SYSTEM	TUBE CM	BP MM	QL GPM	TEMP C	SATC ML	VP MM
3	1.757	750.700	1.040	13.500	36.600	28.700

RUN	QG CFH	P IN	PD	C IN	C OUT	TYPE	QGM	VCOR	TUN	TUL	VG
375	1.66	.42	.71	1.25	2.35	1	.95	.76	.0333	230.4	.102
376	2.92	.51	.79	1.65	2.95	1	2.12	.91	.0399	192.0	.226
377	5.73	.60	.99	2.95	5.00	1	4.51	1.44	.0665	115.5	.480
378	9.06	.86	1.31	4.15	6.85	1	7.50	1.91	.0921	83.4	.798
379	16.67	1.17	1.70	5.45	7.95	3	15.54	1.77	.0888	86.4	1.654 X
380	20.53	1.30	1.97	5.55	8.05	4	19.55	1.77	.0891	86.1	2.080
381	27.40	1.52	2.25	6.15	9.75	5	25.85	2.58	.1338	57.3	2.752
382	43.80	2.06	2.98	7.20	11.35	5	42.40	3.20	.1621	47.3	4.513
383	84.40	2.89	4.07	7.70	13.25	5	83.24	4.08	.2273	33.7	8.859
384	115.30	3.73	5.25	9.40	15.65	5	114.40	4.67	.2792	27.5	12.175
385	166.70	5.83	7.87	12.40	18.10	6	166.99	4.26	.2874	26.7	17.772
386	190.80	6.89	9.28	12.95	18.65	6	191.25	4.26	.2944	26.0	20.354

SYSTEM	TUBE CM	BP MM	QL GPM	TEMP C	SATC ML	VP MM
3	1.757	750.700	1.040	13.500	36.600	28.700

RUN	QG CFH	P IN	PD	C IN	C OUT	TYPE	QGM	VCOR	TUN	TUL	VG
387	1.54	.43	.72	1.50	2.50	1	.90	.69	.0304	251.9	.096
387	1.54	.43	.72	1.75	2.60	1	1.00	.59	.0260	294.8	.107
389	3.52	.53	.84	2.80	4.55	1	2.43	1.23	.0562	136.6	.258
389	3.52	.53	.84	2.95	4.55	1	2.53	1.12	.0515	149.1	.270
390	26.30	1.45	2.20	5.80	9.30	5	24.79	2.51	.1282	59.9	2.639
390	26.30	1.45	2.20	6.00	9.60	5	24.72	2.58	.1331	57.6	2.631
391	38.10	1.88	2.72	6.80	11.05	5	36.44	3.07	.1639	46.8	3.878
391	38.10	1.88	2.72	6.85	11.25	5	36.32	3.19	.1705	45.0	3.866
392	53.60	2.24	3.24	6.95	13.30	5	50.82	4.72	.2573	29.8	5.409 X
392	53.60	2.24	3.24	7.20	13.15	5	51.14	4.40	.2414	31.8	5.443
393	88.10	2.97	4.21	8.90	15.55	5	86.14	4.99	.2942	26.1	9.168
393	88.10	2.97	4.21	8.70	15.80	5	85.77	5.36	.3148	24.4	9.129
394	145.10	4.83	6.61	10.80	19.65	5	142.46	6.96	.4523	16.9	15.162
394	145.10	4.83	6.61	11.15	19.45	5	142.95	6.47	.4249	18.0	15.214
395	193.00	6.87	9.19	12.65	21.55	6	190.66	7.09	.4998	15.3	20.292
395	193.00	6.87	9.19	12.75	21.85	6	190.46	7.29	.5176	14.8	20.270

SYSTEM	TUBE CM	BP MM	QL GPM	TEMP C	SATC ML	VP MM
3	1.757	747.000	1.040	13.500	36.600	28.700

RUN	QG CFH	P IN	PD	C IN	C OUT	TYPE	QGM	VCOR	TUN	TUL	VG
396	11.45	.88	1.47	4.60	7.40	2	9.96	2.00	.0978	78.5	1.060
396	11.45	.88	1.47	5.15	7.95	2	9.96	2.00	.0997	77.0	1.060
397	14.52	.95	1.61	4.95	7.60	3	13.28	1.89	.0934	82.2	1.413
397	14.52	.95	1.61	4.90	7.75	3	13.13	2.04	.1006	76.3	1.397
398	19.97	1.18	1.88	5.15	7.75	4	19.00	1.85	.0921	83.3	2.022
398	19.97	1.18	1.88	5.15	8.15	4	18.70	2.15	.1071	71.7	1.990
399	25.60	1.37	2.17	5.40	8.30	5	24.64	2.07	.1042	73.6	2.623
399	25.60	1.37	2.17	5.50	8.65	5	24.46	2.26	.1142	67.2	2.603
400	40.20	1.81	2.81	6.40	10.40	5	39.02	2.90	.1522	50.4	4.153
400	40.20	1.81	2.81	6.15	10.35	5	38.87	3.05	.1590 A	48.3	4.137
401	91.00	2.91	4.28	9.10	15.40	5	89.91	4.74	.2812	27.3	9.569
401	91.00	2.91	4.28	8.90	15.20	5	89.92	4.73	.2787	27.5	9.570
402	186.00	6.57	8.92	13.00	22.25	6	184.20	7.52	.5435	14.1	19.604
402	186.00	6.57	8.92	12.95	22.90	6	183.48	8.23	.5981	12.8	19.528

COMPUTATION OF NTU

SYSTEM	TUBE	CM	BP MM	QL GPM	TEMP C	SATC ML	VP MM
3	1.757	749.700		2.100	13.500	36.600	28.700

RUN	QG CFH	P IN	PD	C IN	C OUT	TYPE	QGM	VCOR	TUN	TUL	VG
403	1.62	1.45	2.49	2.05	2.45	1	1.12	.56	.0122	625.5	.119
403	1.62	1.45	2.49	1.90	2.40	1	.98	.70	.0153	501.9	.104
404	3.01	1.51	2.62	2.70	3.55	1	1.93	1.19	.0268	266.4	.205
404	3.01	1.51	2.62	2.65	3.50	1	1.93	1.19	.0267	266.0	.205
405	8.12	1.82	3.05	4.45	5.70	1	6.66	1.76	.0419	182.0	.709
405	8.12	1.82	3.05	4.40	5.55	1	6.81	1.62	.0385	199.5	.725
406	14.04	2.32	3.76	6.60	8.05	1	12.51	2.05	.0526	145.0	1.352
406	14.04	2.32	3.76	6.60	8.05	1	12.51	2.05	.0526	145.9	1.332
407	20.02	2.83	4.39	7.70	9.95	3	17.53	3.22	.0862	89.0	1.866
407	20.02	2.83	4.39	7.80	9.95	3	17.68	3.07	.0825	93.0	1.881
408	33.20	3.78	5.53	10.45	12.00	5	30.81	3.52	.1051	73.1	3.279
408	33.20	3.78	5.53	10.30	13.15	5	30.22	4.11	.1225	62.6	3.216
409	84.70	7.93	7.90	13.70	19.10	5	78.30	8.08	.2850	26.9	8.333
409	84.70	7.93	7.90	13.85	19.70	5	77.54	8.84	.3155	24.3	8.253
410	182.80	14.20	17.30	17.35	25.80	6	169.91	14.05	.6117	12.5	18.083
410	182.80	14.20	17.30	16.90	25.80	6	169.05	14.91	.6360	12.0	17.991

SYSTEM	TUBE	CM	BP MM	QL GPM	TEMP C	SATC ML	VP MM
3	1.757	756.300		2.100	13.500	36.600	28.700

RUN	QG CFH	P IN	PD	C IN	C OUT	TYPE	QGM	VCOR	TUN	TUL	VG
411	2.17	1.48	2.58	2.35	2.75	1	1.67	.55	.0122	625.8	.178
411	2.17	1.48	2.58	2.30	2.85	1	1.47	.76	.0168	454.8	.156
412	5.13	1.62	2.73	3.80	4.60	1	4.16	1.11	.0258	247.2	.443
412	5.13	1.62	2.73	3.75	4.70	1	3.95	1.32	.0307	250.0	.421
413	11.82	2.15	3.52	6.00	7.65	1	9.84	2.32	.0581	132.0	1.047
413	11.82	2.15	3.52	5.95	7.45	1	10.05	2.10	.0526	145.8	1.070
414	16.71	2.53	4.02	7.65	9.65	1	14.35	2.82	.0753	102.0	1.527
414	16.71	2.53	4.02	7.50	9.20	1	14.78	2.39	.0632	121.3	1.573
415	26.50	3.18	4.89	9.40	11.85	3	23.71	3.48	.0994	77.2	2.524
415	26.50	3.18	4.89	9.75	11.80	3	24.30	2.90	.0837	91.7	2.586
416	51.20	5.33	6.96	11.90	15.70	5	46.73	5.50	.1757	43.7	4.974
416	51.20	5.33	6.96	12.05	15.30	5	47.57	4.67	.1493	51.4	5.062
417	150.20	12.70	15.00	17.35	24.60	6	138.82	11.47	.4897	15.6	14.774
417	150.20	12.70	15.00	17.50	24.40	6	139.46	10.83	.4642	16.5	14.843

SYSTEM	TUBE	CM	BP MM	QL GPM	TEMP C	SATC ML	VP MM
3	1.757	751.000		2.100	13.500	73.200	28.700

RUN	QG CFH	P IN	PD	C IN	C OUT	TYPE	QGM	VCOR	TUN	TUL	VG
418	1.60	1.45	2.51	3.75	4.65	1	1.03	.63	.0137	559.6	.109
419	3.09	1.55	2.69	6.80	8.75	1	2.76	1.37	.0314	244.2	.294
420	10.07	1.95	3.29	10.65	14.55	1	7.66	2.77	.0681	112.6	.816
421	17.66	2.62	4.14	16.65	20.75	1	15.36	2.92	.0800	95.0	1.634
422	25.30	3.10	4.80	19.00	24.25	3	22.39	3.77	.1086	70.7	2.383
423	35.20	3.85	5.70	21.05	27.40	5	31.74	4.59	.1385	55.4	3.378
424	75.80	7.47	8.95	28.50	39.70	5	68.95	8.46	.3075	24.0	7.358
425	152.30	13.30	15.50	38.20	54.20	5	139.74	13.47	.6498	11.8	14.872
426	187.40	16.00	18.60	43.30	57.90	6	174.64	12.58	.7082	10.8	18.586

SYSTEM	TUBE	CM	BP MM	QL GPM	TEMP C	SATC ML	VP MM
3	1.757	750.100		1.070	13.500	73.200	28.700

RUN	QG CFH	P IN	PD	C IN	C OUT	TYPE	QGM	VCOR	TUN	TUL	VG
427	1.40	.40	.79	4.45	6.30	1	.79	.66	.0288	266.3	.084
428	4.10	.50	.91	6.35	9.70	1	3.05	1.21	.0544	141.0	.325
429	11.76	.88	1.53	10.60	16.95	2	9.90	2.33	.1138	67.4	1.053
430	18.28	1.12	1.84	11.80	17.70	3	16.94	2.16	.1076	71.3	1.792
431	24.70	1.32	2.19	12.75	19.25	5	23.28	2.39	.1212	63.3	2.478
432	39.20	1.79	2.83	14.80	23.40	5	37.49	3.21	.1702	45.1	3.991
433	81.40	2.77	4.28	18.95	31.75	5	79.41	4.94	.2896	26.5	8.451
434	149.80	5.03	7.22	25.65	41.85	5	147.82	6.57	.4522	16.0	15.732
435	182.50	6.61	9.05	28.85	46.65	5	179.86	7.46	.5590	13.7	19.142

SYSTEM	TUBE	CM	BP MM	QL GPM	TEMP C	SATC ML	VP MM
3	1.757	751.700		.610	13.500	73.200	28.700

RUN	QG CFH	P IN	PD	C IN	C OUT	TYPE	QGM	VCOR	TUN	TUL	VG
436	1.51	.12	.32	3.25	5.00	1	1.02	.54	.0407	188.6	.109
437	3.02	.16	.41	5.45	9.80	1	2.24	.90	.0701	109.4	.238
438	6.70	.26	.53	5.65	12.95	1	5.43	1.53	.1210	63.4	.578
439	11.08	.39	.77	6.70	15.05	2	9.75	1.76	.1422	54.0	1.038
440	17.27	.42	.93	7.50	14.75	3	16.43	1.52	.1239	61.9	1.748
441	25.30	.71	1.15	8.70	15.80	5	24.78	1.49	.1236	62.1	2.638
442	52.20	1.10	1.65	11.45	22.30	5	51.83	2.33	.2057	37.3	5.516
443	98.70	1.79	2.45	14.25	31.55	5	98.33	3.00	.3722	20.6	10.465
444	179.30	3.00	4.05	23.45	43.15	6	180.03	4.67	.5466	14.0	19.160

SYSTEM	TUBE CM	BP MM	QL GPM	TEMP C	SATC ML	VP MM
3	1.757	747.400	.610	13.500	36.600	28.700

RUN	QG CFH	P IN	PD	C IN	C OUT	TYPE	QGM	VCOR	TUN	TUL	VG
445	1.99	.20	.48	2.05	4.05	1	1.25	.83	.0633	121.2	.133
446	4.04	.25	.55	2.65	5.80	1	2.90	1.32	.1037	74.0	.308
447	7.67	.45	.69	3.05	6.60	2	6.52	1.49	.1191	64.4	.693
448	12.74	.56	.97	4.10	7.70	2	11.79	1.52	.1253	61.2	1.255
449	20.85	.75	1.24	4.55	8.40	3	20.15	1.63	.1368	56.1	2.144
450	43.30	1.03	1.70	5.50	11.15	5	42.76	2.44	.2152	35.6	4.551
451	79.40	1.69	2.21	6.30	17.05	5	77.71	5.03	.4748	16.1	8.270
452	146.60	3.36	4.35	9.85	25.35	5	143.60	8.53	.9684	7.9	15.283

SYSTEM	TUBE CM	BP MM	QL GPM	TEMP C	SATC ML	VP MM
3	1.757	749.900	1.070	13.500	73.200	28.700

RUN	QG CFH	P IN	PD	C IN	C OUT	TYPE	QGM	VCOR	TUN	TUL	VG
480	1.51	.37	.81	3.80	5.50	1	.96	.61	.0262	293.0	.102
481	2.49	.46	.91	4.95	7.10	1	1.82	.77	.0338	226.8	.193
482	7.71	.77	1.40	6.40	10.95	1	6.37	1.65	.0747	102.7	.678
483	13.68	1.04	1.78	7.50	13.25	3	12.13	2.10	.0971	79.0	1.290
484	19.83	1.30	2.13	8.15	13.80	4	18.55	2.06	.0965	79.7	1.974
485	31.20	1.82	2.67	8.90	15.75	5	29.88	2.52	.1194	64.3	3.180
486	61.70	2.44	3.39	10.85	21.85	5	59.82	4.14	.2063	37.2	6.367
487	118.00	4.17	5.90	15.60	32.40	5	115.23	6.63	.3688	20.8	12.264
488	186.60	7.28	10.10	21.80	42.05	6	182.90	8.41	.5378	14.2	19.465

SYSTEM	TUBE CM	BP MM	QL GPM	TEMP C	SATC ML	VP MM
3	1.757	757.200	2.100	13.500	73.200	28.700

RUN	QG CFH	P IN	PD	C IN	C OUT	TYPE	QGM	VCOR	TUN	TUL	VG
489	1.64	1.61	2.74	3.40	4.25	1	1.09	.59	.0127	601.5	.116
490	3.07	1.69	2.84	4.80	6.15	1	2.21	.94	.0207	369.4	.236
491	7.76	2.16	3.65	5.50	8.00	1	6.22	1.74	.0392	195.7	.662
492	16.80	2.88	4.67	8.00	11.90	1	14.49	2.74	.0643	119.3	1.542
493	27.20	3.65	5.62	9.20	14.30	3	24.25	3.60	.0865	88.7	2.581
494	47.90	5.03	7.55	10.95	18.80	5	43.28	5.62	.1403	54.7	4.606
495	73.40	7.45	9.80	15.35	27.45	5	65.53	8.89	.2434	31.5	6.974

SYSTEM	TUBE CM	BP MM	QL GPM	TEMP C	SATC ML	VP MM
3	1.757	751.900	.610	13.500	73.200	28.700

RUN	QG CFH	P IN	PD	C IN	C OUT	TYPE	QGM	VCOR	TUN	TUL	VG
471	1.63	.10	.28	3.50	6.15	1	1.15	.54	.0408	187.0	.122
472	2.62	.11	.32	3.95	7.55	1	1.98	.74	.0563	136.3	.210
473	6.32	.21	.48	5.15	10.80	1	5.39	1.17	.0916	83.8	.574
474	11.76	.40	.79	6.15	13.40	2	10.70	1.52	.1211	63.4	1.138
475	20.67	.52	1.01	7.25	14.40	3	19.97	1.50	.1215	63.1	2.126
476	35.60	.82	1.40	9.65	19.00	5	34.97	1.98	.1690	45.4	3.722
477	61.90	1.20	1.73	11.90	24.60	5	61.43	2.76	.2474	31.0	6.538
478	117.10	2.18	3.00	16.45	33.70	6	117.24	3.90	.3889	19.7	12.478

SYSTEM	TUBE CM	BP MM	QL GPM	TEMP C	SATC ML	VP MM
2	1.757	751.000	1.070	15.000	70.962	12.800

NO	QG CFH	PI	PD	H IN	H OUT	TYPE	QGM	VOLE	NTU	LTU	VELG
505	1.54	.49	.48	2.03	7.55	1	1.54	0.00	.3861	89.1	.164 X
506	2.20	.53	.58	1.85	8.43	1	2.20	0.00	.1330	74.5	.234 X
507	6.24	.78	.78	2.95	12.85	1	6.26	.01	.1620	47.4	.666
508	14.43	1.20	1.15	5.20	16.58	3	14.47	.01	.1962	39.1	1.541
509	21.90	1.52	1.48	5.27	15.89	4	21.96	.01	.1849	41.5	2.338
510	39.20	2.42	2.42	7.48	21.56	5	39.25	.01	.2588	29.6	4.178
511	66.30	3.48	3.47	9.15	29.50	5	66.25	.02	.4148	18.5	7.052 X
512	114.00	4.60	4.25	11.59	37.95	5	114.50	.03	.5072	12.6	12.187 X
513	174.00	5.78	6.07	13.41	45.48	5	174.11	.04	.8919	8.6	18.552 X

SYSTEM	TUBE CM	BP MM	QL GPM	TEMP C	SATC ML	VP MM
2	1.757	754.100	1.070	15.000	70.962	12.800

NO	QG CFH	PI	PD	H IN	H OUT	TYPE	QGM	VOLE	NTU	LTU	VELG
514	1.32	.53	.56	3.32	6.31	1	1.31	0.00	.2463	155.7	.140
515	2.08	.55	.58	3.85	7.86	1	2.07	0.00	.3632	121.3	.221
516	5.50	.78	.78	5.75	14.58	1	5.49	0.00	.1494	51.3	.585
517	10.13	1.10	1.08	6.93	18.63	2	10.12	.01	.2276	36.9	1.377
518	11.45	1.14	1.12	7.01	19.17	2	11.44	.01	.2169	35.4	1.217
519	19.40	1.39	1.32	6.81	18.30	4	19.38	.01	.2028	37.9	2.062
520	26.85	1.84	1.65	7.76	19.44	5	26.79	.01	.2396	36.4	2.852
521	44.15	2.70	2.47	9.81	24.38	5	43.99	.01	.2793	27.5	4.662

COMPUTATION OF NTU

SYSTEM	TUBE CM	BP MM	QL GPM	TEMP C	SATC MF	VP MM
2	1.757	754.600	1.070	15.000	70.962	12.800

NO	QG CFH	P1	PD	H IN	H OUT	TYPE	QGM	VOLE	NTU	LTU	VELG
522	1.30	.51	.55	3.24	5.45	1	1.29	0.00	.0343	225.5	.138 ×
523	1.67	.53	.58	3.97	7.56	1	1.66	0.00	.0563	136.2	.177
524	3.79	.70	.70	5.22	12.36	1	3.78	0.00	.1180	65.1	.432
525	9.83	.98	1.08	7.28	18.43	1	9.81	.01	.1977	38.8	1.045
526	13.58	1.07	1.20	7.58	18.33	3	13.66	.01	.1910	40.2	1.454
527	15.72	1.19	1.25	7.39	17.95	3	15.70	.01	.1860	41.1	1.671
528	23.90	1.60	1.53	7.88	18.04	5	23.85	.01	.1802	42.6	2.539
529	49.20	3.00	2.79	10.34	24.26	5	48.96	.01	.2675	28.7	5.211
530	70.50	3.82	3.34	12.50	30.11	5	70.01	.01	.3673A	20.9	7.452
531	159.50	5.15	4.56	13.99	41.03	5	157.96	.03	.6605	11.6	16.813
532	227.00	5.83	5.60	15.04	45.78	5	224.68	.03	.8221	9.3	23.914

SYSTEM	TUBE CM	BP MM	QL GPM	TEMP C	SATC MF	VP MM
2	1.757	756.300	1.070	15.000	70.962	12.800

NO	QG CFH	P1	PD	H IN	H OUT	TYPE	QGM	VOLE	NTU	LTU	VELG
533	1.30	.51	.53	2.73	6.29	1	1.29	0.00	.0547	140.2	.157
534	1.62	.53	.56	3.88	7.85	1	1.61	0.00	.0624	123.1	.171
535	2.84	.59	.61	5.26	10.21	1	2.83	0.00	.0801	95.8	.301
536	7.39	.95	.93	7.09	17.21	1	7.36	.01	.1768	43.4	.785
537	11.97	1.16	1.20	6.33	17.89	2	11.92	.01	.2019	38.0	1.269
538	18.50	1.34	1.45	6.36	16.75	3	18.43	.01	.1796	42.7	1.962
539	22.50	1.54	1.57	6.73	17.09	5	22.41	.01	.1972	38.9	2.385
540	30.80	2.07	2.12	7.50	19.03	5	30.65	.01	.2051	37.4	3.262
541	66.80	3.61	3.22	11.36	28.42	5	66.23	.01	.3444	22.3	7.049
542	97.00	3.98	3.50	13.04	35.75	5	96.09	.02	.4521	16.9	10.227
543	133.40	4.85	4.25	14.14	37.66	5	131.00	.02	.5455	14.0	14.039
544	200.10	5.35	4.69	14.66	42.67	5	197.63	.03	.7037	10.9	21.056

SYSTEM	TUBE CM	BP MM	QL GPM	TEMP C	SATC MF	VP MM
2	1.757	752.000	2.100	15.000	70.962	12.800

NO	QG CFH	P1	PD	H IN	H OUT	TYPE	QGM	VOLE	NTU	LTU	VELG
555	1.30	1.66	1.80	1.52	4.55	1	1.29	0.00	.0457	168.1	.138 ×
556	1.67	1.74	1.88	2.21	5.64	1	1.66	0.00	.0525	146.2	.177 ×
557	2.44	1.82	1.92	2.27	6.47	1	2.43	0.00	.0648	118.4	.259 ×
558	4.13	2.09	2.16	4.06	8.92	1	4.12	0.00	.0774	99.2	.439
559	7.05	2.55	2.54	5.37	12.03	1	7.03	.01	.1098	69.9	.749
560	12.00	3.22	3.08	7.05	14.48	1	11.96	.01	.1267	60.6	1.273
561	15.06	3.39	3.25	7.53	15.18	3	15.01	.01	.1317	58.3	1.598
562	18.80	3.87	3.56	7.87	15.29	3	18.72	.01	.1282	59.9	1.993
563	25.00	4.99	3.94	7.54	16.67	5	24.81	.01	.1585	48.4	2.641
564	32.30	5.85	4.56	7.83	18.57	5	31.99	.02	.1898	40.4	3.405
565	42.90	7.12	5.35	8.94	20.68	5	42.35	.02	.2127	36.1	4.508
566	65.20	9.75	7.00	11.50	27.92	5	63.92	.03	.3250	23.6	6.803

SYSTEM	TUBE CM	BP MM	QL GPM	TEMP C	SATC MF	VP MM
2	1.757	752.000	2.100	15.000	70.962	12.800+

NO	QG CFH	P1	PD	H IN	H OUT	TYPE	QGM	VOLE	NTU	LTU	VELG
567	1.30	1.66	1.80	1.88	4.03	1	1.29	0.00	.0325	236.3	.138
568	1.90	1.74	1.88	3.20	6.35	1	1.89	0.00	.0446	172.0	.202
569	2.44	1.82	1.92	3.72	7.03	1	2.43	0.00	.0516	148.6	.259
570	4.13	2.09	2.16	4.38	9.39	1	4.12	0.00	.0802	95.7	.439
571	7.05	2.55	2.54	5.31	12.22	1	7.03	.01	.1142A	67.2	.749
572	12.00	3.22	3.08	6.23	14.80	1	11.96	.01	.1456	52.7	1.273
573	15.06	3.39	3.25	6.49	15.28	3	15.01	.01	.1502	51.1	1.598
574	18.80	3.87	3.56	7.28	15.77	3	18.72	.01	.1464	52.4	1.993
575	25.00	4.99	3.94	8.07	16.81	5	24.81	.01	.1524	50.3	2.641
576	32.30	5.85	4.56	9.52	19.06	5	31.99	.01	.1716	44.7	3.405
577	42.90	7.12	5.35	10.58	21.95	5	42.35	.02	.2115	36.3	4.508
578	65.20	9.75	7.00	12.42	28.70	5	63.92	.03	.3277	23.4	6.803

SYSTEM	TUBE CM	BP MM	QL GPM	TEMP C	SATC MF	VP MM
2	1.757	751.600	2.100	15.000	70.962	12.800

NO	QG CFH	P1	PD	H IN	H OUT	TYPE	QGM	VOLE	NTU	LTU	VELG
579	1.67	1.84	1.90	2.83	5.61	1	1.66	0.00	.0427	179.6	.177
580	3.31	2.01	2.03	3.97	7.50	1	3.30	0.00	.0556	138.0	.352
581	7.07	2.53	2.50	5.37	11.46	1	7.06	.01	.1001	75.7	.751
582	13.96	3.35	3.24	6.78	14.73	3	13.92	.01	.1356	56.6	1.482
583	21.00	4.25	3.81	7.52	16.11	3	20.91	.01	.1489	51.5	2.225
584	30.00	5.87	4.47	8.52	17.63	5	29.72	.02	.1924	39.9	3.163
585	49.90	8.68	6.19	9.03	23.57	5	49.07	.02	.2701	28.4	5.223
586	80.00	12.25	8.01	12.49	32.51	5	77.86	.04	.4178	18.3	8.208
587	121.20	16.30	10.58	16.11	41.28	5	122.47	.05	.6017	12.7	13.035
588	185.00	19.50	12.14	19.51	46.82	6	176.58	.06	.7284	13.5	19.794

COMPUTATION OF NTU

SYSTEM	TUBE CM	BP MM	OL GPM	TEMP C	SATC MF	VP MM
2	1.757	754.600	2.100	15.000	70.962	12.800

NO	OG CFH	P1	PD	H IN	H OUT	TYPE	UGM	VOLE	NTU	LTU	VELG
589	2.01	1.89	1.85	2.87	5.83	1	2.00	0.00	.0453	169.2	.212
590	3.01	2.03	2.04	3.35	7.82	1	2.09	0.00	.0699	109.8	.318
591	10.13	3.06	2.88	5.25	13.75	1	10.06	.01	.1415	54.2	1.071
592	18.00	4.03	3.54	6.74	15.82	3	17.85	.01	.1554	49.4	1.933
593	39.90	7.18	5.19	9.28	21.01	5	39.25	.02	.2127	36.1	4.176
594	82.20	12.26	8.38	11.62	31.05	5	79.76	.04	.3936	19.5	8.089
595	130.00	15.67	10.32	15.35	40.51	5	124.97	.05	.5889	13.0	13.332
596	182.20	19.30	11.82	17.54	48.10	5	173.26	.07	.8110	9.4	18.442

SYSTEM	TUBE CM	BP MM	OL GPM	TEMP C	SATC MF	VP MM
2	1.757	750.400	.620	15.000	70.962	12.800

NO	OG CFH	P1	PD	H IN	H OUT	TYPE	UGM	VOLE	NTU	LTU	VELG
597	1.30	.31	1.30	2.81	8.95	1	1.30	0.00	.0975	78.7	.138
598	1.67	.36	.35	2.96	10.45	1	1.67	0.00	.12054	63.7	.178
599	2.56	.40	.41	2.98	11.76	1	2.67	0.00	.1428	53.7	.284
600	4.56	.45	.46	3.32	13.69	2	4.59	0.00	.1719	44.6	.487
601	7.39	.51	.50	3.35	13.35	2	7.43	0.00	.1655	46.4	.799
602	10.90	.58	.56	3.14	12.64	3	10.96	0.00	.1558	49.2	1.166
603	15.98	.72	.71	3.73	13.38	3	16.07	0.00	.1600	48.0	1.710

SYSTEM	TUBE CM	BP MM	OL GPM	TEMP C	SATC MF	VP MM
2	1.757	746.900	.620	15.000	70.962	12.800

NO	OG CFH	P1	PD	H IN	H OUT	TYPE	UGM	VOLE	NTU	LTU	VELG
604	1.30	.30	.31	2.76	8.77	1	1.31	0.00	.0956	80.3	.139
605	2.20	.34	.36	3.57	11.18	1	2.22	0.00	.1244	61.7	.236
606	5.90	.46	.48	4.27	13.95	2	5.96	0.00	.1650	47.1	.634
607	10.30	.60	.55	4.13	14.06	3	10.40	0.00	.1672	45.9	1.107
608	19.70	.79	.77	4.59	14.17	3	19.90	0.00	.1621	47.3	2.118
609	27.00	.91	.98	4.42	15.59	4	27.27	0.00	.1910	40.2	2.003
610	44.60	1.47	1.32	6.13	19.00	5	44.98	0.00	.2300	33.3	4.788
611	69.60	1.95	1.65	8.48	26.26	5	70.11	.01	.3490	22.0	7.463

SYSTEM	TUBE CM	BP MM	OL GPM	TEMP C	SATC MF	VP MM
2	1.757	749.400	.620	15.000	70.962	12.800

NO	OG CFH	P1	PD	H IN	H OUT	TYPE	UGM	VOLE	NTU	LTU	VELG
612	4.56	.44	.47	4.61	13.91	2	4.59	0.00	.1564	49.1	.688
613	8.77	.56	.52	4.74	14.17	2	8.83	0.00	.1591	48.2	.939
614	13.88	.68	.63	5.42	14.26	3	13.97	0.00	.1500	51.1	1.487
615	24.10	.94	.88	5.04	15.34	4	24.25	0.00	.1615	47.5	2.581
616	35.00	1.22	1.14	6.88	17.75	5	35.21	0.00	.1926	39.8	3.747
617	88.80	2.30	1.88	9.36	29.32	5	89.28	.01	.4064	18.9	9.482
618	149.10	2.57	2.14	11.71	38.35	5	149.49	.01	.6239	12.3	15.012

SYSTEM	TUBE CM	BP MM	OL GPM	TEMP C	SATC MF	VP MM
2	1.757	749.400	1.070	15.000	70.962	12.800

NO	OG CFH	P1	PD	H IN	H OUT	TYPE	UGM	VOLE	NTU	LTU	VELG
619	1.30	.63	.63	2.93	6.91	1	1.30	0.00	.0621	123.5	.138
620	1.71	.66	.66	3.15	7.82	1	1.71	0.00	.0736	104.3	.182
621	3.23	.77	.76	4.05	10.72	1	3.24	0.00	.1086	70.7	.345
622	35.60	2.49	2.27	7.90	19.59	5	35.70	.01	.2119	36.2	3.800

SYSTEM	TUBE CM	BP MM	OL GPM	TEMP C	SATC MF	VP MM
2	1.757	749.400	2.100	15.000	70.962	12.800

NO	OG CFH	P1	PD	H IN	H OUT	TYPE	UGM	VOLE	NTU	LTU	VELG
623	1.30	1.85	1.91	2.10	4.44	1	1.30	0.00	.0356	215.9	.138
624	2.86	2.05	2.09	2.92	6.58	1	2.96	0.00	.0585	131.2	.305
625	5.50	2.46	2.40	4.10	9.72	1	5.50	.01	.0904A	84.0	.536

COMPUTATION OF NTU

SYSTEM	TUBE CM	BP MM	OL GPM	TEMP C	SATC ML	CYCLO
5	1.757	755.900	1.070	15.000	47.270	.003

RUN	OG CFH	P IN	PD	C IN	C OUT	TYPE	QGM	VCOR	TUN	TUL	VG
626	1.59	.68	5.87	2.50	3.80	1	1.44	.13	.0188	407.4	.153
627	2.62	.76	6.39	3.15	4.80	1	2.42	.16	.0250	306.7	.257
628	5.53	.87	7.34	3.55	5.80	2	5.22	.22	.0355	216.0	.556
629	9.70	.89	7.58	3.45	5.55	3	9.34	.21	.0328	233.6	.694
630	12.92	.98	8.05	3.50	5.70	4	12.48	.22	.0345	222.2	1.328
631	18.12	1.08	9.16	3.75	6.10	5	17.56	.23	.0375	205.7	1.869
632	26.70	1.15	10.60	4.00	6.70	5	25.97	.27	.0437	175.6	2.764
633	38.90	1.36	11.60	4.40	7.80	5	37.60	.33	.0564	136.1	4.002

SYSTEM	TUBE CM	BP MM	OL GPM	TEMP C	SATC ML	CYCLO
5	1.757	756.100	1.070	15.000	47.270	.003

RUN	OG CFH	P IN	PD	C IN	C OUT	TYPE	QGM	VCOR	TUN	TUL	VG
634	4.04	.81	6.58	3.20	5.15	1	3.78	.19	.0301	255.0	.405
635	7.27	.86	7.25	3.25	5.60	3	6.92	.23	.0370	207.5	.737
636	12.74	.98	8.62	3.20	5.35	4	12.32	.21	.0334	229.4	1.311
637	65.10	1.70	14.10	4.65	9.55	5	62.76	.48	.0839	91.5	6.680
638	90.90	2.02	16.80	5.30	11.85	5	87.21	.64	.1167	65.8	9.281
639	135.10	2.63	21.80	6.30	15.55	5	128.34	.90	.1749	43.0	13.659
640	171.20	3.13	24.60	7.10	18.30	5	160.96	1.08	.2207	34.8	17.130

SYSTEM	TUBE CM	BP MM	OL GPM	TEMP C	SATC ML	CYCLO
5	1.757	752.900	.620	15.000	47.270	.00390

RUN	OG CFH	P IN	PD	C IN	C OUT	TYPE	QGM	VCOR	TUN	TUL	VG
641	1.59	.41	3.49	1.70	3.60	1	1.47	.11	.0281	272.8	.156
642	2.53	.43	3.78	2.00	4.30	1	2.38	.13	.0351	218.8	.254
643	5.48	.47	4.06	2.15	5.25	2	5.27	.18	.0489	157.0	.561
644	9.79	.52	4.65	2.40	5.55	3	9.56	.18	.0500	153.4	1.018
645	13.23	.57	4.74	2.30	5.35	4	12.97	.17	.0481	159.6	1.381
646	18.86	.64	5.50	2.35	5.65	4	18.54	.19	.0524	146.4	1.973
647	27.30	.74	6.20	2.50	6.10	5	26.86	.21	.0578	132.9	2.858
648	40.50	.85	7.05	2.70	7.20	5	39.82	.26	.0759	103.8	4.238

SYSTEM	TUBE CM	BP MM	OL GPM	TEMP C	SATC ML	CYCLO
5	1.757	752.900	.620	15.000	47.270	.00390

RUN	OG CFH	P IN	PD	C IN	C OUT	TYPE	QGM	VCOR	TUN	TUL	VG
649	5.09	.45	3.91	1.90	4.55	1	3.82	.15	.0409	187.6	.406
650	7.23	.49	4.69	2.30	5.45	3	7.02	.18	.0499	153.6	.747
651	70.50	1.02	8.70	3.10	9.50	5	69.23	.37	.1098	69.0	7.368
652	92.30	1.19	9.90	3.75	11.45	5	90.36	.44	.1368	56.1	9.619
653	132.70	1.55	12.10	4.20	14.15	5	129.02	.57	.1839	41.7	13.732
654	176.10	1.82	14.90	4.85	16.15	5	170.42	.67	.2220	34.5	18.138

SYSTEM	TUBE CM	BP MM	OL GPM	TEMP C	SATC ML	CYCLO
5	1.757	750.500	2.100	15.000	47.270	.00110

RUN	OG CFH	P IN	PD	C IN	C OUT	TYPE	QGM	VCOR	TUN	TUL	VG
655	1.53	1.58	13.25	3.05	3.65	1	1.48	.11	.0089	856.7	.157
656	2.88	1.64	14.01	3.55	4.40	1	2.65	.16	.0132	580.8	.282
657	5.64	1.80	15.70	4.15	5.25	3	5.30	.21	.0176	436.0	.564
658	9.89	2.03	17.30	4.70	5.85	5	9.40	.22	.0186	412.6	1.001
659	13.64	2.15	18.30	4.90	6.30	5	12.99	.27	.0229	334.4	1.382
660	19.93	2.41	20.60	5.25	7.00	5	18.95	.33	.0291	263.5	2.017
661	27.40	2.52	21.40	5.70	7.85	5	26.05	.41	.0365	210.4	2.773
662	41.10	2.97	25.40	6.70	9.60	5	38.88	.55	.0508	151.1	4.138

SYSTEM	TUBE CM	BP MM	OL GPM	TEMP C	SATC ML	CYCLO
5	1.757	754.500	2.100	15.000	47.270	.00110

RUN	OG CFH	P IN	PD	C IN	C OUT	TYPE	QGM	VCOR	TUN	TUL	VG
663	4.04	1.74	1.72	3.70	4.75	1	3.72	.20	.0164	465.0	.396
664	7.08	1.89	1.83	4.15	5.30	3	6.64	.22	.0182	420.0	.707
665	21.60	2.51	2.47	5.10	6.85	5	20.41	.33	.0287	266.8	2.173
666	63.40	3.60	3.51	7.80	11.80	5	59.04	.77	.0739	103.0	6.283
667	87.80	4.21	4.16	9.20	14.80	5	81.05	1.04	.1062	72.3	8.626
668	135.90	5.62	5.46	11.85	20.05	5	122.61	1.49	.1698	45.2	13.049
669	174.60	6.68	6.33	13.70	25.85	5	154.92	1.82	.2250	34.1	16.477

COMPUTATION OF NTU

SYSTEM	TUBE CM	BP MM	OL GPM	TEMP C	SATC ML	CYCLO
5	1.757	756.200	2.100	30.000	36.070	.00110

RUN	OG CFH	P IN	PD	C IN	C OUT	TYPE	OGM	VCOR	TUN	TUL	VG	
670	4.21	1.19	1.17	4.50	5.85	1	4.06	.27	.0303	252.0	.432	X
671	7.07	1.34	1.29	4.75	5.95	3	7.02	.24	.0269	284.0	.747	
672	21.82	1.89	1.84	5.40	7.50	5	21.85	.42	.0490	156.6	2.320	
673	63.40	2.86	2.82	7.55	12.00	5	62.69	.89	.1158	60.3	6.673	
674	88.60	3.39	3.28	9.35	15.30	5	86.84	1.18	.1694	45.3	9.242	
675	132.30	4.31	4.08	11.10	19.30	5	127.70	1.60	.2601	29.5	13.591	
676	172.80	5.19	4.84	12.45	22.55	5	164.34	1.94	.3529	21.7	17.491	

SYSTEM	TUBE CM	BP MM	OL GPM	TEMP C	SATC ML	CYCLO
5	1.757	756.600	2.100	30.000	36.070	.00110#

RUN	OG CFH	P IN	PD	C IN	C OUT	TYPE	OGM	VCOR	TUN	TUL	VG
677	1.64	1.04	8.79	4.15	4.80	1	1.56	.13	.0139	552.1	.166
678	2.73	1.12	9.44	4.10	4.90	1	2.65	.16	.0172	444.1	.282
679	5.22	1.22	10.62	4.30	5.45	2	5.14	.23	.0254	301.3	.547
680	9.04	1.47	12.54	4.65	6.00	5	9.92	.27	.0303	253.1	1.056
681	13.82	1.64	14.00	5.00	6.65	5	13.80	.33	.0377	203.3	1.469
682	19.87	1.83	15.40	5.45	7.35	5	19.87	.38	.0442	173.4	2.115
683	27.70	2.00	17.00	6.00	8.35	5	27.69	.47	.0562	136.5	2.047
684	41.90	2.33	20.10	6.50	9.80	5	41.74	.66	.0816	94.0	4.443

SYSTEM	TUBE CM	BP MM	OL GPM	TEMP C	SATC ML	CYCLO
5	1.757	753.900	1.070	30.000	36.070	.00280

RUN	OG CFH	P IN	PD	C IN	C OUT	TYPE	OGM	VCOR	TUN	TUL	VG
975	1.59	3.82	3.81	2.60	3.85	1	1.53	.13	.0256	300.0	.162
976	2.58	4.35	4.34	2.60	4.15	1	2.53	.16	.0323	237.4	.269
977	5.37	4.99	5.03	3.05	5.10	1	5.39	.21	.0443	173.0	.573
978	9.74	6.00	5.95	3.25	5.60	3	9.90	.24	.0516	148.7	1.054
979	13.28	6.40	6.30	3.20	5.50	4	13.58	.24	.0503	152.6	1.446
980	18.12	7.02	6.87	3.30	5.85	5	18.58	.27	.0563	136.3	1.977
981	26.40	7.75	7.70	3.45	6.25	5	27.13	.29	.0625	122.7	2.987
982	39.80	9.10	9.00	3.80	7.55	5	40.84	.39	.0860	88.6	4.347

SYSTEM	TUBE CM	BP MM	OL GPM	TEMP C	SATC ML	CYCLO
5	1.757	754.000	1.070	30.000	36.070	.00280

RUN	OG CFH	P IN	PD	C IN	C OUT	TYPE	OGM	VCOR	TUN	TUL	VG
983	22.03	7.40	7.42	2.80	5.55	5	22.61	.29	.0601	127.7	2.406
984	62.30	11.15	10.95	3.75	8.85	5	63.74	.53	.1296	63.6	6.783
685	87.20	13.10	12.80	4.35	10.95	5	88.92	.69	.1637	46.9	9.463
686	134.30	17.30	16.30	5.40	14.35	5	135.79	.92	.2401	31.0	14.452
687	175.30	21.10	19.10	5.05	17.15	5	175.68	1.15	.3199	24.0	18.697

SYSTEM	TUBE CM	BP MM	OL GPM	TEMP C	SATC ML	CYCLO
5	1.757	753.800	.620	30.000	36.070	.00420

RUN	OG CFH	P IN	PD	C IN	C OUT	TYPE	OGM	VCOR	TUN	TUL	VG
688	1.64	2.09	2.06	1.75	3.65	1	1.60	.11	.0384	199.7	.170
689	2.63	2.24	2.26	1.85	4.10	1	2.62	.13	.0465	165.1	.279
690	5.07	2.29	2.29	1.90	4.55	1	5.16	.16	.0557	137.7	.549
691	9.80	3.08	3.01	2.05	5.00	3	10.09	.18	.0629	122.1	1.074
692	13.00	3.48	3.49	2.15	5.50	4	13.41	.20	.0725	105.9	1.427
693	18.70	3.90	3.95	2.35	5.65	5	19.37	.20	.0717	107.0	2.062
694	27.00	4.47	4.35	2.30	6.00	5	28.00	.22	.0810	94.7	2.980
695	40.10	5.22	5.30	2.45	7.05	5	41.60	.28	.1035	74.2	4.427

SYSTEM	TUBE CM	BP MM	OL GPM	TEMP C	SATC ML	CYCLO
5	1.757	752.800	.620	30.000	36.070	.00420

RUN	OG CFH	P IN	PD	C IN	C OUT	TYPE	OGM	VCOR	TUN	TUL	VG
696	6.07	2.47	2.52	2.10	4.75	2	6.21	.16	.0561	136.7	.661
697	9.11	2.97	2.96	2.30	5.25	3	9.38	.18	.0635	120.8	.998
698	63.40	6.35	6.41	2.75	8.60	5	65.80	.36	.1366	56.2	7.005
699	87.70	7.45	7.47	3.15	10.15	5	90.89	.43	.1695	45.3	9.473
700	137.60	9.93	9.48	3.50	12.95	5	141.88	.57	.2427	31.6	15.100
701	176.10	12.40	11.20	4.00	15.25	5	180.49	.68	.3045	25.2	19.210

COMPUTATION OF NTU, EFFECT OF ENTRANCE TYPE

SYSTEM	TUBE CM	BP MM	QL GPM	TEMP C	SATC ML	VP MM
1	1.757	754.000	1.070	15.000	45.470	12.800

RUN	QG CFH	P IN	PD	C IN	C OUT	TYPE	QGMΔ	VCOR	ΔTUN	TUL	VG
703	6.20	1.26	.30	5.75	9.40	3	5.64	.65	.0988	77.7	.600
704	12.29	1.87	.49	6.30	10.75	3	Δ11.65	.79	.1233	62.2	1.240
705	53.40	4.55	1.58	8.00	14.30	5	52.50	1.14	.1866	41.1	5.588
706	6.20	1.10	.24	3.35	6.35	3	5.76	.53	.0758	101.5	.613
707	12.29	1.59	.44	4.00	7.35	3	11.87	.59	.0861	89.1	1.263
708	53.40	4.50	1.30	7.60	13.50	5	52.56	1.06	.1715	44.7	5.595
709	6.20	1.57	.72	5.53	8.70	3	5.72	.56	.0847	90.6	.609
710	12.29	2.37	1.27	4.75	8.60	3	11.76	.68	.1014	75.7	1.251
711	53.40	4.50	1.30	8.85	15.15	5	52.48	1.14	.1913	40.1	5.586
712	6.20	1.29	.39	5.15	9.10	3	5.58	.70	.1056	72.7	.594
713	12.29	1.88	.67	5.90	10.35	3	11.65	.79	.1220	62.9	1.240
714	53.40	4.48	1.77	7.35	13.95	5	52.48	1.20	.1928	39.8	5.586

Runs 703 to 705 inclusive, regular entrance

Runs 706 to 708 inclusive, liquid through run of tee

Runs 709 to 711 inclusive, gas through concentric tube

Runs 712 to 714 inclusive, tee same diameter as tube

COMPUTATION OF NTU FOR VARIOUS ENTRANCE CONCENTRATIONS

SYSTEM	TUBE CM	BP MM	QL GPM	TEMP C	SATC ML	VP MM
1	1.757	764.500	1.070	15.000	45.470	12.800

RUN	QG CFH	P IN	PD	C IN	C OUT	TYPE	QGM	VCOR	TUN	TUL	VG
901	71.30	6.05	4.61	4.00	12.80	5	69.47	1.17	.2376	32.3	7.395
902	71.30	6.05	4.61	3.90	12.70	5	69.47	1.17	.2369	32.4	7.395
903	71.30	6.05	4.61	11.55	18.70	5	69.69	.95	.2356	32.6	7.418
904	71.30	6.05	4.61	11.45	18.55	5	69.70	.94	.2330	32.0	7.419
905	71.30	6.05	4.61	22.90	27.30	5	70.06	.58	.2153	35.6	7.457
906	71.30	6.05	4.61	23.05	27.80	5	70.01	.63	.2364	32.4	7.452
907	71.30	6.05	4.61	32.50	35.40	5	70.26	.39	.2501	30.7	7.478
908	71.30	6.05	4.61	32.60	35.40	5	70.27	.37	.2424	31.6	7.480

COMPUTATION OF NTU

SYSTEM	TUBE CM	BP MM	OL GPM	TEMP C	SATC ML	VP MM
1	1.757	750.300	1.070	45.000	21.420	71.000

RUN	OG CFH	P IN	PD	C IN	C OUT	TYPE	UGM	VCOR	TUN	TUL	VG
715	1.61	.50	.55	2.80	3.65	1	1.79	.18	.0534	143.8	.191
716	2.55	.58	.64	2.95	4.10	1	2.86	.24	.0736	104.2	.304
717	4.52	.72	.74	5.25	4.85	1	5.20	.34	.1060	72.4	.554
718	9.61	1.01	1.02	3.35	5.75	1	11.26	.52	.1646	46.6	1.199
719	11.84	1.09	1.08	3.60	5.80	2	14.04	.48	.1525	50.4	1.495
720	15.02	1.25	1.08	3.70	5.85	3	17.95	.47	.1495	51.3	1.910
721	20.68	1.75	1.75	4.05	6.20	4	24.87	.47	.1531	50.1	2.647
722	30.60	2.30	2.27	4.05	6.45	5	36.92	.52	.1725	44.5	5.030

SYSTEM	TUBE CM	BP MM	OL GPM	TEMP C	SATC ML	VP MM
7	2.504	750.800	2.010	15.000	45.470	12.800

RUN	OG CFH	P IN	PD	C IN	C OUT	TYPE	UGM	VCOR	TUN	TUL	VG
723	2.03	.35	.34	2.75	3.55	1	1.91	.26	.0194	594.2	.095
724	3.52	.37	.36	2.95	5.05	1	3.25	.34	.0257	298.2	.170
725	5.32	.39	.37	4.00	5.35	1	4.99	.44	.0341	224.8	.261
726	8.78	.38	.30	6.50	8.25	1	8.47	.58	.0475	161.5	.443
727	14.98	.44	.47	10.65	12.60	2	14.67	.55	.0598	128.2	.769
728	21.32	.55	.60	11.35	13.55	2	21.57	.73	.0695	110.8	1.124
729	35.60	.73	.74	11.50	13.90	5	35.59	.77	.0728	105.3	1.700
730	53.00	1.06	.99	11.60	14.10	5	53.32	.84	.0795	96.4	2.794

SYSTEM	TUBE CM	BP MM	OL GPM	TEMP C	SATC ML	VP MM
7	2.504	752.300	1.150	15.000	45.470	12.800

RUN	OG CFH	P IN	PD	C IN	C OUT	TYPE	UGM	VCOR	TUN	TUL	VG
731	1.63	.05	.11	4.25	5.15	1	1.49	.16	.0227	557.5	.078
732	2.72	.06	.13	4.45	5.40	2	2.63	.17	.0241	517.0	.136
733	5.11	.07	.15	5.20	6.45	2	4.99	.23	.0325	256.1	.261
734	8.08	.12	.17	5.25	6.45	3	8.95	.22	.0312	245.8	.469
735	14.67	.24	.27	5.00	6.25	5	14.75	.23	.0325	257.4	.773
736	22.44	.65	.75	4.95	6.15	4	22.69	.22	.0539	248.0	1.189
737	36.70	1.20	1.45	4.80	6.45	5	37.13	.35	.0426	187.1	1.046
738	60.00	1.80	1.80	5.00	7.40	5	60.66	.45	.0628	122.2	3.170
739	114.70	2.40	2.20	6.55	11.40	5	115.71	.92	.1308	56.1	6.264
740	181.70	3.10	2.70	7.85	13.55	5	183.34	1.89	.1688	45.5	9.608

SYSTEM	TUBE CM	BP MM	OL GPM	TEMP C	SATC ML	VP MM
7	2.504	753.100	3.950	15.000	45.470	12.800

RUN	OG CFH	P IN	PD	C IN	C OUT	TYPE	UGM	VCOR	TUN	TUL	VG
741	1.63	.90	.97	4.20	4.65	1	1.37	.29	.0112	681.0	.071
742	2.78	.94	1.00	4.70	5.30	1	2.44	.38	.0152	504.1	.128
743	5.11	.99	1.06	6.35	7.25	1	4.62	.58	.0259	320.7	.242
744	10.02	1.17	1.23	11.00	12.10	1	9.49	.71	.0334	229.3	.497
745	19.86	1.49	1.49	14.15	15.70	1	19.22	1.01	.0525	146.1	1.007
746	39.40	2.35	2.11	12.30	14.40	3	38.64	1.37	.0674	115.0	2.025
747	67.40	4.12	3.85	14.65	17.20	5	66.58	1.67	.0867	86.5	3.487
748	111.20	6.50	4.05	15.25	18.95	5	109.16	2.37	.1286	59.7	5.720

SYSTEM	TUBE CM	BP MM	OL GPM	TEMP C	SATC ML	VP MM
7	2.504	749.400	5.950	15.000	45.470	12.800

RUN	OG CFH	P IN	PD	C IN	C OUT	TYPE	UGM	VCOR	TUN	TUL	VG
749	12.68	1.22	1.25	11.85	13.25	1	11.85	.01	.0442	173.5	.421
750	31.10	1.93	1.78	11.95	13.90	5	30.50	1.28	.0622	123.3	1.598
751	57.20	3.41	2.29	12.00	14.45	5	57.15	1.91	.0905	152.6	2.095 X
752	113.80	5.95	3.52	15.30	19.00	5	112.38	2.46	.1359	57.3	5.869
753	139.40	8.10	3.78	16.05	20.20	5	136.79	2.75	.1537	49.0	7.168
754	170.30	8.60	4.18	16.75	21.65	5	167.00	3.28	.1889	40.6	8.751

SYSTEM	TUBE CM	BP MM	OL GPM	TEMP C	SATC ML	VP MM
7	2.504	755.500	2.010	15.000	45.470	12.800

RUN	OG CFH	P IN	PD	C IN	C OUT	TYPE	UGM	VCOR	TUN	TUL	VG
755	40.10	.89	.88	8.10	10.65	5	39.80	.85	.0720	105.8	2.090
756	70.00	1.45	1.26	8.80	11.95	5	69.96	1.05	.0921	83.3	3.466
757	116.70	1.08	1.55	9.30	13.70	5	116.72	1.48	.1329	57.7	6.116
758	146.20	2.22	1.85	9.45	14.70	5	146.25	1.79	.1616	47.5	7.664
759	180.10	2.64	2.05	10.10	16.15	5	180.05	2.08	.1921	39.0	9.435

COMPUTATION OF NTU

SYSTEM	TUBE CM	BP MM	OL GPM	TEMP C	SATC ML	VP MM
7	2.504	755.900	1.130	15.000	45.470	12.800

RUN	OG	CFH	P IN	PD	C IN	C OUT	TYPE	QGM	VCOR	TUN	TUL	VG
760	1.71	-.12	.11	2.95	3.80	1	1.58	.15	.0207	371.0	.082	
761	3.42	.04	.12	3.00	4.95	2	3.28	.19	.0256	299.4	.172	
762	7.81	.12	.16	3.25	4.45	3	7.68	.25	.0343	223.4	.402	
763	95.10	1.30	1.00	5.05	8.80	5	95.70	.70	.0996	77.1	4.010	
764	146.20	2.20	2.15	6.30	11.85	5	147.00	1.06	.1563	49.1	7.703	
765	181.80	2.90	2.70	6.75	12.90	5	182.62	1.18	.1766	43.4	9.570	

SYSTEM	TUBE CM	BP MM	OL GPM	TEMP C	SATC ML	VP MM
5	1.228	755.600	.520	15.000	45.470	12.800

RUN	OG	CFH	P IN	PD	C IN	C OUT	TYPE	QGM	VCOR	TUN	TUL	VG
766	1.43	1.31	1.14	2.95	7.10	1	1.09	.36	.1050	73.1	.257	
767	2.21	1.36	1.27	3.10	9.10	1	1.71	.52	.1563	49.1	.373	
768	3.68	1.43	1.64	3.05	11.65	1	3.04	.69	.2103	36.5	.603	
769	5.48	2.26	2.25	3.05	14.70	1	4.66	.88	.2795	27.4	1.017	
770	8.20	2.35	2.68	4.25	19.90	3	7.72	.59	.1800	42.6	1.682	
771	11.98	2.93	2.77	4.40	10.85	4	11.54	.57	.1744	44.0	2.515	
772	19.84	3.95	3.05	5.25	12.95	5	19.34	.69	.2167	35.4	4.214	
773	33.50	5.95	5.57	6.50	17.90	5	32.64	1.05	.3484	22.0	7.115	

SYSTEM	TUBE CM	BP MM	OL GPM	TEMP C	SATC ML	VP MM
6	1.228	752.600	.520	15.000	45.470	12.800

RUN	OG	CFH	P IN	PD	C IN	C OUT	TYPE	QGM	VCOR	TUN	TUL	VG
774	6.76	2.46	2.37	4.60	12.55	3	6.15	.71	.2224	34.5	1.341	
775	65.50	10.15	7.55	8.80	25.20	5	63.62	1.64	.5975	12.8	13.862	
776	112.10	15.30	12.00	12.65	33.20	5	106.93	2.37	.0982	7.6	23.301	
777	150.00	19.50	17.60	17.00	38.20	6	144.13	2.93	1.3677	5.6	31.405	
778	194.00	27.50	24.60	21.70	40.70	7	184.94	2.77	1.5526	4.0	40.100	

SYSTEM	TUBE CM	BP MM	OL GPM	TEMP C	SATC ML	VP MM
5	1.228	753.300	.293	15.000	45.470	12.800

RUN	OG	CFH	P IN	PD	C IN	C OUT	TYPE	QGM	VCOR	TUN	TUL	VG
779	1.56	.16	.60	2.90	9.00	1	1.28	.30	.1505	48.1	.283	
780	2.07	.32	.74	3.45	10.75	1	1.74	.36	.1969	39.0	.380	
781	3.58	.50	.84	3.85	13.05	2	3.17	.47	.2579	29.7	.692	
782	5.49	.60	.95	3.85	12.90	3	5.14	.46	.2511	30.5	1.119	
783	8.34	.80	1.10	3.90	11.35	5	8.12	.37	.2036	37.7	1.771	
784	11.80	1.05	1.32	4.00	10.70	3	11.69	.33	.1815	42.3	2.547	
785	19.11	1.85	2.15	5.05	13.15	5	19.03	.41	.2302	33.3	4.147	
786	31.10	2.75	2.65	5.90	17.65	5	30.94	.62	.3620	21.1	6.743	

SYSTEM	TUBE CM	BP MM	OL GPM	TEMP C	SATC ML	VP MM
5	1.228	751.600	.293	15.000	45.470	12.800

RUN	OG	CFH	P IN	PD	C IN	C OUT	TYPE	QGM	VCOR	TUN	TUL	VG
787	62.80	3.95	5.65	7.90	24.85	5	62.80	.93	.5919	12.0	13.685	
788	109.30	7.55	6.55	12.80	35.55	5	108.56	1.37	1.0474	7.3	23.655	
789	149.10	12.50	10.50	18.45	42.90	6	146.39	1.82	1.6690	4.6	31.898	
790	190.30	18.00	15.60	24.85	42.90	7	185.01	1.99	2.2241	3.4	40.312	

SYSTEM	TUBE CM	BP MM	OL GPM	TEMP C	SATC ML	VP MM
6	1.228	751.600	1.020	15.000	45.470	12.800

RUN	OG	CFH	P IN	PD	C IN	C OUT	TYPE	QGM	VCOR	TUN	TUL	VG
791	1.36	5.40	5.19	2.85	5.50	1	.93	.44	.0657	116.0	.203	
792	1.80	3.96	5.55	3.15	6.45	1	1.26	.56	.0830	91.5	.275	
793	3.68	4.82	4.58	4.20	9.55	1	2.80	.92	.1418	54.1	.610	
794	5.17	5.63	5.15	5.30	11.80	1	4.09	1.13	.1802	42.6	.891	
795	8.39	6.35	6.23	6.15	13.15	3	7.24	1.22	.2001	38.3	1.578	
796	11.71	7.00	6.15	6.35	11.40	3	10.92	.86	.1405	54.6	2.380	
797	19.83	10.10	8.40	7.15	13.40	5	18.70	1.11	.1857	41.3	4.074	
798	31.50	15.40	10.95	8.60	17.40	5	29.67	1.55	.2722	28.2	6.465	

SYSTEM	TUBE CM	BP MM	OL GPM	TEMP C	SATC ML	VP MM
6	1.228	751.100	1.020	15.000	45.470	12.800

RUN	OG	CFH	P IN	PD	C IN	C OUT	TYPE	QGM	VCOR	TUN	TUL	VG
799	63.90	20.20	16.90	11.05	28.15	5	59.23	3.22	.6478	11.8	12.007	
800	91.30	25.80	22.40	14.10	34.55	5	83.61	4.65	1.0239	7.5	18.218	
801	123.90	33.40	27.40	17.50	39.85	6	109.00	5.59	1.3569	5.5	23.751	

LIQ	TUBE	QL GPM	DIFF	S TENS	VISC	VELL
1	1.757	.620	1.465	73.530	1.140	.529

NO	J	OGM	NTU	LTU	VELG	FACTOR	CORR Y
45	1	1.07	.0571	134.40	.114	.9998	.0367
46	1	4.29	.0950	80.80	.457	.9998	.0936
49	3	18.02	.1170	65.60	1.918	.9998△	.2862
112	1	1.08	.0525	146.20	.143	.9998	.0352
113	1	2.22	.0900	85.30	.294	.9998	.0740
114	2	5.48	.1216	63.10	.727	.9998	.1527
115	3	10.08	.1378	55.70	1.355	.9998	.2566
116	3	15.06	.1527	57.10	1.994	.9998	.3347
117	3	20.04	.1283	59.80	2.655	.9998	.4064
193	1	1.12	.0498	154.00	.119	.9998	.0322
194	1	2.86	.0950	80.80	.304	.9998	.0791
195	1	5.11	.1150	66.70	.544	.9998	.1234
196	1	7.76	.1268	59.60	.826	.9998	.1745
197	2C	10.55	.1288	59.60	1.123	.9998	.2127
198	3	12.35	.1284	59.80	1.314	.9998△	.2366
199	3	16.00	.1166	65.80	1.703	.9998	.2602
200	4	19.00	.1093	70.20	2.023	.9998	.2789

LIQ	TUBE	QL GPM	DIFF	S TENS	VISC	VELL
1	1.757	1.070	1.465	73.530	1.140	.913

NO	J	OGM	NTU	LTU	VELG	FACTOR	CORR Y
163	4	18.31	.1220	62.90	1.949	.9998	.3491
164	4	22.15	.1282	59.90	2.358	.9998	.4193
169	1	1.13	.0385	199.40	.120	.9998	.0397
170	1	2.73	.0641	119.70	.291	.9998	.0771
171	1	8.33	.1190	64.50	.886	.9998	.2140
172	2	10.95	.1314	58.40	1.166	.9998	.2731
173	3	13.27	.1275	60.20	1.413	.9998	.2965
174	3	15.93	.1271	60.40	1.696	.9998	.3315‡
178	1	1.85	.0490	156.70	.197	.9998	.0544
179	1	3.25	.0746	102.90	.346	.9998	.0939
180	1	5.89	.0976	78.60	.627	.9998	.1503
181	1	9.26	.1277	60.10	.986	.9998	.2425
182	3	12.29	.1332	57.60	1.308	.9998	.2958
183	3	15.57	.1227	62.60	1.657	.9998	.3153
260	1	4.19	.0836	91.80	.446	.9998	.1136
261	1	6.22	.1155	66.40	.662	.9998	.1819
262	2	9.28	.1283	59.80	.988	.9998	.2439
263	4	20.85	.1023	75.00	2.219	.9998	.3203
284	1	1.58	.0585	131.10	.168	.9998	.0632
285	1	3.78	.0791	97.10	.403	.9998	.1041
286	1	8.63	.1343	57.10	.918	.9998	.2459
287	3	16.87	.1125	66.20	1.796	.9998	.3047
288	4	22.14	.1067	71.90	2.357	.9998△	.3488
293	1	2.52	.0595	128.90	.269	.9998	.0703
294	1	6.32	.1034	74.20	.672	.9998	.1639
295	3	16.61	.1078	71.20	1.768	.9998	.2890
296	5	25.99	.1235	62.10	2.766	.9998	.4543
300	1	1.83	.0371	206.70	.194	.9998	.0410
301	1	4.21	.0777	98.70	.448	.9998	.1057
302	2	9.24	.1228	62.50	.983	.9998	.2328
303	3	12.83	.1265	60.70	1.366	.9998	.2882
304	4	21.50	.1048	75.30	2.268	.9998	.3354

LIQ	TUBE	QL GPM	DIFF	S TENS	VISC	VELL
1	1.757	1.500	1.465	73.530	1.140	1.280‡

NO	J	OGM	NTU	LTU	VELG	FACTOR	CORR Y
74	1	1.10	.0299	256.90	.146	.9998	.0426
75	1	1.72	.0448	171.20	.227	.9998	.0675
77	1	5.32	.0847	90.60	.705	.9998	.1681
78	1	8.40	.1136	67.50	1.113	.9998	.2718
79	1	11.44	.1307	58.70	1.515	.9998	.3653
80	1	15.06	.1220	62.90	1.996	.9998	.3996
81	3	18.63	.1120	68.50	2.468	.9998	.4197
90	1	3.18	.0581	132.00	.421	.9998	.0988
91	1	4.34	.0702	109.40	.574	.9998	.1301
92	3	18.70	.1183	64.90	2.476	.9998	.4443
141	1	1.42	.0336	228.30	.188	.9998	.0493
142	1	2.48	.0550	139.50	.328	.9998	.0884
143	1	7.25	.1024	74.90	.960	.9998	.2293
144	1	10.28	.1277	60.10	1.362	.9998	.3373
145	1	14.34	.1394	55.10	1.900	.9998	.4432
149	1	2.05	.0425	180.60	.218	.9998	.0636
150	1	3.59	.0613	125.20	.362	.9998	.1018
151	3	19.54	.1181	65.00	2.080	.9998	.3968
156	1	5.15	.0785	97.70	.548	.9998	.1435
157	1	12.06	.1345	57.00	1.284	.9998	△.3448
158	3	17.12	.1160	60.20	1.822	.9998	.3598
162	4	21.27	.1145	67.00	2.264	.9998	.4057

CORRELATING VARIABLE FOR BUBBLE-PLUG FLOW

LIQ	TUBE	QL GPM	DIFF	S TENS	VISC	VELL
1	1.757	2.100	1.465	73.530	1.140	1.792

NO	J	QGM	NTU	LTU	VELG	FACTOR	CORR Y
59	3	25.82	.1336	57.40	2.748	.9998	.6065
125	1	1.13	.0232	330.60	.150	.9998	.0450
126	1	2.48	.0365	210.10	.329	.9998	.0774
127	1	14.61	.1109	69.20	1.856	.9998	.4045
130	1	1.64	.0291	263.50	.217	.9998	.0584
133	1	13.84	.1074	71.50	1.853	.9998	.3893
134	3	18.48	.1117	66.70	2.448	.9998	.4735
135	1	11.02	.1024	75.00	1.460	.9998	.3530
136	1	1.40	.0252	304.40	.186	.9998	.0496
137	1	8.14	.0788	97.40	1.079	.9998	.2262
138	3	16.77	.1056	72.70	2.222	.9998	.4238
139	3	22.56	.1194	64.30	2.988	.9998	.5707

LIQ	TUBE	QL GPM	DIFF	S TENS	VISC	VELL
1	1.757	3.000	1.465	73.530	1.140	2.560#

NO	J	QGM	NTU	LTU	VELG	FACTOR	CORR Y
210	1	2.38	.0231	331.20	.254	.9998	.0650
211	1	4.97	.0411	186.70	.529	.9998	.1269
212	1	8.65	.0604	127.10	.921	.9998	.2102
213	1	14.07	.0815	94.10	1.498	.9998	.3307
214	3	21.77	.0940	81.60	2.318	.9998	.4585
219	1	1.66	.0217	352.50	.177	.9998	.0594
221	1	10.41	.0659	116.50	1.108	.9998	.2417
222	3	16.96	.0893	86.00	1.805	.9998	.3898
228	10	4.67	.0371	206.60	.497	.9998	.1134
229	1	8.17	.0527	145.60	.870	.9998	.1807
230	1	12.34	.0749	102.50	1.314	.9998	.2901
231	5	26.23	.0998	76.90	2.792	.9998	.5341

LIQ	TUBE	QL GPM	DIFF	S TENS	VISC	VELL
1	1.757	4.200	1.465	73.530	1.140	3.585

NO	J	QGM	NTU	LTU	VELG	FACTOR	CORR Y
269	1	5.13	.0271	282.60	.546	.9998	.1119
270	1	11.61	.0521	147.30	1.236	.9998	.2511
271	5	21.58	.0764	100.50	2.297	.9998	.4493
276	1	18.22	.0559	137.20	1.939	.9998	.3587

| 99 | | -8.09425 | | -72.99438 | | 16.81291 | | 19.32515 | -.66970 | .82700 |

LIQ	TUBE	QL GPM	DIFF	SƆTENS	VISC	VELL
1	1.757	1.070	1.072	75.100	1.505	.913

NO	J	QGM	NTU	LTU	VELG	FACTOR	CORRₐY
236	1	3.92	.0658	116.60	.417	1.1124	.0973
237	1	7.36	.1022	75.10	.783	1.1124	.1928
238	3	11.55	.1054	72.80	1.229	1.1124	.2511
239	5	22.90	.0915	83.90	2.437	1.1124	.3410

LIQ	TUBE	QL GPM	DIFF	S TENS	VISC	VELL
1	1.757	1.070	2.019	71.200	.800	.913

NO	J	QGM	NTU	LTU	VELG	FACTOR	CORR Y
244	1	4.64	.1031	74.40	.494	.9094	.1319
245	1	8.62	.1366	56.20	.918	.9094ₐ	.2275
246	3	13.44	.1395	55.00	1.430	.9094	.2973
247	5	25.48	.1392	55.10	2.712	.9094	.4589

LIQ	TUBE	QL GPM	DIFF	S TENS	VISC	VELL
1	1.757	1.070	3.080	68.800	.599	.913

NO	J	QGM	NTU	LTU	VELG	FACTOR	CORR Y
252	1	5.42	.0890	86.20	.577	.7800	.1034
253	1	9.79	.1448	53.00	1.042	.7800ₐ	.2208
254	3	14.89	.1318	58.20	1.585	Δ.7800Δ	.2568
255	5	27.58	.1268	60.50	2.936	.7800ₐ	.3807
715	1	1.79	.0534	143.80	.191	.7800	.0460
716	1	2.86	.0736	104.20	.304	.7800	.0698
717	1	5.20	.1060	72.40	.554	.7800ₐ	.1213
718	1	11.26	.1646	46.60	1.199	.7800	.2712
719	2	14.04	.1523	50.40	1.495	.7800	.2861
720	3	17.05	.1495	51.30	1.910	.7800	.3292
721	4	24.87	.1531	50.10	2.647	.7800	.4252

LIQ	TUBE	QL GPM	DIFF	SATENS	VISC	VELL
2	1.757	.620	3.690	73.530	1.140	.529

NO	J	QGM	NTU	LTU	VELG	FACTOR	CORR Y
597	1	1.30	.0975	78.70	.138	.6299	.0409
598	1	1.67	.1205	65.70	.178	.6299	.0536
599	1	2.67	.1428	53.70	.284	.6299	.0731
600	2	4.58	.1719	44.60	.487	.6299	.1100
601	2	7.43	.1655	46.40	.790	.6299	.1375
602	3	10.96	.1558	49.20	1.166	.6299	.1663
603	3	16.07	.1600	48.60	1.710	.6299	.2257
604	1	1.31	.0956	80.30	.139	.6299	.0402
605	1	2.22	.1244	61.70	.236	.6299	.0599
606	2	5.96	.1650	47.10	.634	.6299	.1194
607	3	10.40	.1672	45.90	1.107	.6299	.1723
608	3	19.90	.1621	47.30	2.118	.6299	.2705
609	4	27.27	.1910	40.20	2.903	.6299	.4129
612	2	4.39	.1564	49.70	.466	.6299	.1002
613	2	8.83	.1591	48.20	.939	.6299	.1471
614	3	13.97	.1500	51.10	1.487	.6299	.1905
615	4	24.25	.1615	47.50	2.581	.6299	.3164

LIQ	TUBE	QL GPM	DIFF	S TENS	VISC	VELL
2	1.757	1.070	3.690	73.530	1.140	.915

NO	J	QGM	NTU	LTU	VELG	FACTOR	CORR AY
507	1	6.26	.1620	47.40	.666	.6299	.1611
508	3	14.47	.1962	39.10	1.541	.6299	.3053
509	4	21.96	.1849	41.50	2.338	.6299	.3787
514	1	1.31	.0463	165.70	.140	.6299	.0307
515	1	2.07	.0632	121.30	.221	.6299	.0451
516	1	5.49	.1494	51.30	.585	.6299	.1410
517	2	10.12	.2076	36.90	1.077	.6299	.2603
518	2	11.44	.2169	35.40	1.217	.6299	.2911
519	4	19.38	.2028	37.80	2.062	.6299	.3801
520	5	26.79	.2096	36.60	2.852	.6299	.4972
523	1	1.66	.0563	136.20	.177	.6299	.0386
524	1	3.78	.1180	65.10	.402	.6299	.0977
525	1	9.81	.1977	38.80	1.045	.6299	.2639
526	3	13.66	.1910	40.20	1.454	.6299	.2848
527	3	15.70	.1866	41.10	1.671	.6299	.3038
528	5	25.85	.1802	42.60	2.539	.6299	.3919
533	1	1.29	.0547	140.20	.137	.6299	.0361
534	1	1.61	.0624	123.10	.171	.6299	.0426
535	1	2.83	.0801	95.80	.301	.6299	.0612
536	1	7.36	.1768	43.40	.783	.6299	.1889
537	2	11.92	.2019	38.00	1.269	.6299	.2775
538	3	18.43	.1796	42.70	1.962	.6299	.3253
539	5	22.41	.1972	38.90	2.385	.6299	.4197
619	1	1.30	.0621	123.50	.138	.6299	.0411
620	1	1.71	.0736	104.30	.182	.6299	.0507
621	1	3.24	.1066	70.70	.345	.6299	.0865

LIQ	TUBE	QL GPM	DIFF	S TENS	VISC	VELL
2	1.757	2.100	3.690	73.530	1.140	1.792

NO	J	QGM	NTU	LTU	VELG	FACTOR	CORR Y
558	1	4.12	.0774	99.20	.439	.6299	.1068
559	1	7.03	.1098	69.90	.749	.6299	.1758
560	1	11.96	.1267	60.60	1.273	.6299	.2446
561	3	15.01	.1317	58.30	1.598	.6299	.2813
562	3	18.72	.1282	59.90	1.993	.6299	.3057
563	5	24.81	.1585	48.60	2.641	.6299	.4427
567	1	1.29	.0325	236.30	.138	.6299	.0395
568	1	1.89	.0446	172.00	.202	.6299	.0565
569	1	2.43	.0516	148.60	.259	.6299	.0666
570	1	4.12	.0802	95.70	.439	.6299	.1127
571	1	7.03	.1142	67.20	.749	.6299	.1820
572	1	11.96	.1456	52.70	1.273	.6299	.2812
573	3	15.01	.1502	51.10	1.598	.6299	.3208
574	3	18.72	.1464	52.40	1.993	.6299	.3491
575	5	24.81	.1524	50.30	2.641	.6299	.4256
579	1	1.66	.0427	179.60	.177	.6299	.0529
580	1	3.30	.0556	138.00	.352	.6299	.0751
581	1	7.06	.1001	76.70	.751	.6299	.1604
582	3	13.92	.1356	56.60	1.482	.6299	.2747
583	3	20.91	.1489	51.50	2.225	.6299	.3768
589	1	2.00	.0453	169.20	.212	.6299	.0572
590	1	2.99	.0699	109.80	.318	.6299	.0929
591	1	10.06	.1415	54.20	1.071	.6299	.2552
592	3	17.85	.1554	49.40	1.900	.6299	.3615
623	1	1.30	.0356	215.80	.138	.6299	.0453
624	1	2.86	.0585	131.20	.305	.6299	.0773
625	1	5.50	.0908	84.90	.586	.6299	.1354

LIQ TUBE QL GPM DIFF S TENS VISC VELL
4 1.757 .620 .285 47.900 13.900 .529

NO	J	QGM	NTU	LTU	VELG	FACTOR	CORR AY
688	1	1.60	.0384	199.70	.170	1.9789	.0531
689	1	2.62	.0465	165.10	.279	1.9789	.0743
690	1	5.16	.0557	137.70	.549	1.9789	.1188
691	3	10.09	.0629	122.10	1.074	1.9789	.1995
692	4	15.41	.0725	105.90	1.427	1.9789	.2808
693	5	19.37	.0717	107.00	2.062	1.9789	.3676
694	5	28.00	.0810	94.70	2.980	1.9789	Δ.5625
696	2	6.21	.0561	136.70	.661	1.9789	.1321
697	3	9.38	.0635	120.80	.998	1.9789	.1919

LIQ TUBE QL GPM DIFF S TENS VISC VELL
4 1.757 1.070 .285 47.900 13.900 .913

NO	J	QGM	NTU	LTU	VELG	FACTOR	CORR Y
975	1	1.53	.0256	300.00	.162	1.9789	.0544
976	1	2.53	.0323	237.40	.269	1.9789	.0755
977	1	5.39	.0443	175.00	.573	1.9789	.1303
978	3	9.90	.0516	148.70	1.054	1.9789	.2008
979	4	13.58	.0503	152.60	1.446	1.9789	.2348
980	5	18.58	.0563	136.30	1.977	1.9789	.3220
981	5	27.13	.0625	122.70	2.887	1.9789	.4700
983	5	22.61	.0601	127.70	2.406	1.9789	.3947

LIQ TUBE QL GPM DIFF S TENS VISC VELL
4 1.757 2.100 .285 47.900 13.900 1.792

NO	J	QGM	NTU	LTU	VELG	FACTOR	CORR Y
671	3	7.02	.0269	284.90	.747	1.9789	.1351
672	5	21.80	.0490	156.60	2.320	1.9789	.3987
677	1	1.56	.0139	552.10	.166	1.9789	.0538
678	1	2.65	.0172	444.10	.282	1.9789	.0706
679	2	5.14	.0254	301.30	.547	1.9789	.1176
680	5	9.92	.0313	253.10	1.056	1.9789	.1708
681	5	13.80	.0377	203.30	1.060	1.9789	.2433
682	5	19.87	.0442	173.40	2.115	1.9789	.3417
683	5	27.69	.0562	136.50	2.947	1.9789	.5271

96 -13.00644 -78.44414 19.18323 24.55369 -.70882 .79937

LIQ TUBE QL GPM DIFF S TENS VISC VELL
5 1.757 .620 .142 49.300 26.500 .529

NO	J	QGM	NTU	LTU	VELG	FACTOR	CORR Y
641	1	1.47	.0281	272.80	.156	2.5247	.0486
642	1	2.38	.0351	218.80	.254	2.5247	.0694
643	2	5.27	.0489	157.00	.561	2.5247	.1346
644	3	9.56	.0500	153.40	1.018	2.5247	.1953
645	4	12.97	.0481	159.60	1.381	2.5247	.2319
646	4	18.54	.0524	146.40	1.973	2.5247	.3310
647	5	26.86	.0578	132.90	2.858	2.5247	.4943
649	1	3.82	.0409	187.60	.406	2.5247	.0965
650	3	7.02	.0499	153.60	.747	2.5247	.1607

LIQ TUBE QL GPM DIFF S TENS VISC VELL
5 1.757 1.070 .142 49.300 26.500 .913

NO	J	QGM	NTU	LTU	VELG	FACTOR	CORR Y
626	1	1.44	.0188	407.40	.153	2.5247	.0506
627	1	2.42	.0250	306.70	.257	2.5247	.0738
628	2	5.22	.0355	216.00	.556	2.5247	.1317
629	3	9.34	.0328	233.60	.994	2.5247	.1579
630	4	12.48	.0345	222.20	1.328	2.5247	.1952
631	5	17.56	.0373	205.70	1.869	2.5247	.2620
632	5	25.97	.0437	175.60	2.764	2.5247	.4057
634	1	3.78	.0301	255.00	.403	2.5247	.1000
635	3	6.92	.0370	207.50	.737	2.5247	.1541
636	4	12.32	.0334	229.40	1.311	2.5247	.1875

LIQ TUBE QL GPM DIFF S TENS VISC VELL
5 1.757 2.100 .142 49.300 26.500 1.792

NO	J	QGM	NTU	LTU	VELG	FACTOR	CORR Y	Δ
655	1	1.48	.0089	856.70	.157	2.5247	.0438	
656	1	2.65	.0132	580.80	.282	2.5247	.0691	
657	3	5.30	.0176	436.00	.564	2.5247	.1047*	
658	5	9.40	.0186	412.60	1.001	2.5247	.1311	
659	5	12.98	.0229	334.40	1.382	2.5247	.1835	
660	5	18.95	.0291	263.50	2.017	2.5247	.2798	
661	5	26.05	.0365	210.40	2.773	2.5247	.4207	
663	1	3.72	.0164	465.90	.396	2.5247	.0906	
664	3	6.64	.0182	420.00	.707	2.5247	.1148	
665	5	20.41	.0287	266.80	2.173	2.5247	.2873	

CORRELATING VARIABLE FOR BUBBLE-PLUG FLOW

LIQ	TUBE	OL GPM	DIFF	S TENS	VISC	VELL
6	1.228	.293	1.465	73.530	1.140	.512

NO	J	QGM	NTU	LTU	VELG	FACTOR	CORR AY
779	1	1.28	.1595	48.10	.280	.4884	.0616
780	1	1.74	.1969	39.00	.380	.4884	.0857
781	2	3.17	.2579	29.70	.692	.4884	.1516
782	3	5.13	.2511	30.50	1.119	.4884	.2000
783	3	8.12	.2036	37.70	1.771	.4884	.2270
784	3	11.69	.1815	42.30	2.547	.4884	.2711

LIQ	TUBE	OL GPM	DIFF	S TENS	VISC	VELL
6	1.228	.520	1.465	73.530	1.140	.908

NO	J	QGM	NTU	LTU	VELG	FACTOR	CORR YA
766	1	1.09	.1050	75.10	.237	.4884	.0587
767	1	1.71	.1563	49.10	.373	.4884	.0978
768	1	3.04	.2103	36.50	.663	.4884	.1614
769	1	4.66	.2795	27.40	1.017	.4884Δ	.2628
770	3	7.72	.1800	42.60	1.662	.4884	.2277
771	4	11.54	.1744	44.00	2.515	.4884 Δ	.2916
774	3	6.15	.2224	34.50	1.341	.4884	.2443

LIQ	TUBE	OL GPM	DIFF	S TENS	VISC	VELL
6	1.228	1.020	1.465	73.530	1.140	1.782

NO	J	QGM	NTU	LTU	VELG	FACTOR	CORR Y
791	1	.93	.0657	116.90	.203	.4884	.0637
792	1	1.26	.0830	92.50	.275	.4884	.0834
793	1	2.80	.1418	54.10	.610	.4884	.1656
794	1	4.09	.1802	42.60	.891	.4884	.2352
795	3	7.24	.2001	38.30	1.578	.4884	.3284
796	3	10.92	.1405	54.60	2.380	.4884	.2856

LIQ	TUBE	OL GPM	DIFF	S TENS	VISC	VELL
7	2.504	1.130	1.465	73.530	1.140	.474

NO	J	QGM	NTU	LTU	VELG	FACTOR	CORR Y
731	1	1.49	.0227	337.50	.078	2.0307	.0254
732	2	2.60	.0241	317.90	.136	2.0307	.0298
733	2	4.99	.0325	236.10	.261	2.0307Δ	.0485
734	3	8.95	.0312	245.80	.469	2.0307	.0598
735	3	14.75	.0323	237.40	.773	2.0307	.0818
736	4	22.69	.0309	248.00Δ	1.189	2.0307	.1044
737	5	37.13	.0426	180.10	1.946	2.0307	.2094
760	1	1.58	.0207	371.00	.082	2.0307Δ	.0234
761	2	3.28	.0256	299.40	.172	2.0307	.0336
762	3	7.68	.0343	223.40	.402	2.0307	.0610

LIQ	TUBE	OL GPM	DIFF	S TENS	VISC	VELL
7	2.504	2.010	1.465	73.530	1.140	.844

NO	J	QGM	NTU	LTU	VELG	FACTOR	CORR YA
723	1	1.81	.0194	394.00	.095	2.0307	.0370
724	1	3.25	.0257	298.20	.170	2.0307	.0529
725	1	4.99	.0341	224.80	.261	2.0307	.0765
726	1	8.40	.0475	161.50	.440	2.0307Δ	.1239
727	2	14.67	.0598	128.20	.769	2.0307	.1959
728	2	21.07	.0693	110.80	1.104	2.0307	.2742
729	3	33.59	.0728	105.30	1.760	2.0307	.3850
730	5	53.32	.0796	96.40	2.794	2.0307	.5881
755	3	39.89	.0726	105.80	2.090	2.0307	.4326

LIQ	TUBE	OL GPM	DIFF	S TENS	VISC	VELL
7	2.504	3.950	1.465	73.530	1.140	1.660

NO	J	QGM	NTU	LTU	VELG	FACTOR	CORR Y
741	1	1.37	.0112	681.90	.071	2.0307	.0393
742	1	2.44	.0152	504.10	.128	2.0307	.0551
743	1	4.62	.0239	320.70	.242	2.0307	.0923
744	1	9.49	.0334	229.30	.497	2.0307	.1463
745	1	19.22	.0525	146.10	1.007	2.0307	.2843
746	3	38.64	.0674	113.90	2.025	2.0307	.5043
749	1	11.85	.0442	173.50	.621	2.0307Δ	.2047
750	3	30.50	.0622	123.30	1.598	2.0307	.4115

| | 75 | -14.60868 | -65.47905 | 17.01018 | 23.24763 | -.72875 | .74081 |

LIQ	TUBE	OL	GPM	DIFF	S TENS	VISC	VELL
1	1.757	.620	1.465	73.530	1.140	.529	

NO	J	OGM	NTU	LTU	VELG	FACTOR	CORR	Y
41	5	132.74	.4023	19.00	14.128	1.0000		.3838
42	5	103.24	.3414	22.40	10.989	1.0000		.3152
43	5	73.04	.2508	30.60	7.774	1.0000A		.2489
44	5	37.02	.1491	51.50	3.941	1.0000		.1547
50	4	28.23	.1386	55.40	3.005	1.0000		.1356
51	5	47.13	.1953	39.30	5.017	1.0000		.1769
52	5	60.62	.2239	34.30	6.452	1.0000A		.2111
117	3	20.04	.1283	59.80	2.055	1.0000		.1250
118	5	30.64	.1523	50.40	4.059	1.0000		.1573
123	5	144.02	.4109	18.60	19.076	1.0000		.4950
124	5	168.76	.4921	15.60	22.353	1.0000		.5687
200	4	19.00	.1093	70.20	2.023	1.0000		.1116
202	5	42.22	.1557	49.30	4.494	1.0000A		.1671
203	5	53.90	.4071	41.00	5.766	1.0000		.1953
204	5	72.20	.2397	32.00	7.685	1.0000		.2389
205	5	96.03	.2861	26.80	10.221	1.0000		.2959
206	5	135.03	.3596	21.30	14.160	1.0000		.3845
207	5	174.78	.4651	16.50	18.603	1.0000A		.4844
208	5	194.33	.5405	14.20	20.664	1.0000		.5312

LIQ	TUBE	OL	GPM	DIFF	S TENS	VISC	VELL
1	1.757	1.070	1.465	73.530	1.140	.913	

NO	J	OGM	NTU	LTU	VELG	FACTOR	CORR	Y
164	4	22.15	.1262	59.90	2.358	1.0000		.1250
165	5	30.99	.1514	50.70	3.298	1.0000		.1503
166	5	65.47	.2853	26.90	9.397	1.0000		.3003
167	5	136.05	.4029	19.00	14.481	1.0000		.4511
168	5	195.15	.5985	12.80	20.771	1.0000		.6204
175	5	54.72	.2120	30.20	5.825	1.0000		.2183
176	5	160.63	.4742	16.20	17.735	1.0000A		.5367
177	5	197.28	.5518	13.90	20.998	1.0000		.6265
263	4	20.85	.1023	75.00	2.219	1.0000A		.1212
264	5	41.67	.1519	50.50	4.435	1.0000		.1809
265	5	64.33	.2417	31.70	6.847	1.0000		.2458
266	5	95.89	.3058	25.10	10.206	1.0000		.3361
267	5	122.53	.3575	21.40	13.042	1.0000A		.4124
288	4	22.14	.1067	71.90	2.357	1.0000		.1250
289	5	34.33	.1433	53.50	3.654	1.0000		.1599
290	5	61.62	.2365	32.40	6.558	1.0000		.2380
291	5	112.96	.3609	21.20	12.023	1.0000		.3802
292	5	118.27	.3846	19.90	12.588	1.0000		.4042
296	5	25.99	.1235	62.10	2.766	1.0000A		.1361
297	5	38.09	.1540	49.80	4.150	1.0000		.1732
298	5	51.75	.2029	37.80	5.508	1.0000A		.2097
304	4	21.50	.1048	73.30	2.288	1.0000		.1231
305	5	31.95	.1279	60.00	3.401	1.0000		.1530
306	5	53.59	.1933	39.70	5.704	1.0000		.2150

LIQ	TUBE	OL	GPM	DIFF	S TENS	VISC	VELL
1	1.757	1.500	1.465	73.530	1.140	1.280	

NO	J	OGM	NTU	LTU	VELG	FACTOR	CORR	Y
81	3	18.63	.1120	68.50	2.468	1.0000		.1278
82	5	28.14	.1543	57.20	3.728	1.0000		.1676
83	5	36.07	.1426	53.80	4.778	1.0000		.1997
92	3	18.70	.1183	64.90	2.476	1.0000		.1281
146	4	24.58	.1316	58.30	3.255	1.0000		.1523
147	5	39.37	.1637	46.90	5.214	1.0000		.2153
148	5	67.80	.2715	28.20	8.981	1.0000		.3305
151	3	19.54	.1181	65.00	2.680	1.0000		.1158
152	5	54.11	.2053	37.40	5.760	1.0000		.2383
153	5	105.29	.3735	20.50	11.207	1.0000		.3996
154	5	147.77	.5468	14.00	15.728	1.0000A		.5406
155	6	185.24	.7147	10.70	19.716	1.0000		.6647
159	5	119.70	.4035	19.00	12.741	1.0000		.4476
160	5	161.33	.5294	14.50	17.172	1.0000		.5855
161	6	191.09	.6233	12.30	20.339	1.0000		.6841
162	4	21.27	.1145	67.00	2.264	1.0000		.1215

LIQ	TUBE	OL	GPM	DIFF	S TENS	VISC	VELL
1	1.757	2.100	1.465	73.530	1.140	1.792	

NO	J	OGM	NTU	LTU	VELG	FACTOR	CORR	Y
59	3	25.82	.1336	57.40	2.748	1.0000		.1279
60	5	35.20	.1542	49.80	3.747	1.0000		.1649
61	5	44.93	.2027	37.80	4.782	1.0000		.2052
62	5	65.54	.2792	27.50	6.976	1.0000		.2844
63	5	88.72	.4201	16.20	9.444	1.0000		.3757
64	6	141.08	.6621	11.60	15.016	1.0000		.5820
65	6	115.56	.4984	15.40	12.300	1.0000A		.4815
66	5	97.35	.4392	17.40	10.362	1.0000A		.4097
67	5	88.74	.4056	18.90	9.445	1.0000		.3758
129	6	182.33	.8747	8.70	24.151	1.0000		.9217
134	3	18.48	.1117	68.70	2.448	1.0000A		.1168
138	3	16.77	.1056	72.70	2.222	1.0000		.1084
139	3	22.56	.1194	64.30	2.988	1.0000		.1368

| 72 | | 20.4396 | 21.4218 | 81 | | 8.026 | 8.3198 | .011826 | 1.000396 |

LIQ TUBE OL GPM DIFF	S TENS	VISC	VELL
3 1.757 .610 2.950	23.400	1.360	.520

NO	J	QGM	NTU	LTU	VELG	FACTOR	CORRAY
441	5	.24.78	.1236	62.10	2.638	.9011	.1404
442	5	51.83	.2057	37.30	5.516	.9011	.2119
443	5	98.33	.3722	20.60	10.465	.9011	.3349
444	6	180.03	.5466	14.00	19.160	.9011	.5509
475	5	19.97	.1215	63.10	2.120	.9011	.1277
476	5	34.97	.1690	45.40	3.722	.9011	.1673
477	5	61.43	.2474	31.00	6.538	.9011	.2373
478	6	117.24	.3889	19.70	12.478	.9011	.3849

LIQ TUBE OL GPM DIFF	S TENS	VISC	VELL
3 1.757 1.070 2.950	23.400	1.360	.913

NO	J	QGM	NTU	LTU	VELG	FACTOR	CORR Y
356	5	24.87	.1026	74.80	2.647	1.0524	.1254
358	5	58.21	.2077	36.90	6.195	1.0524	.2161
359	5	105.79	.3437	22.30	11.259	1.0524	.3456
381	5	25.85	.1338	57.30	2.752	1.0524△	.1281
382	5	42.40	.1621	47.30	4.513	1.0524	.1731
390	5	24.79	.1282	59.90	2.639	1.0524	.1252
390	5	24.72	.1331	57.60	2.631	1.0524	.1250
391	5	36.44	.1639	46.80	3.878	1.0524	.1569
391	5	36.32	.1705	45.00	3.866	1.0524	.1566
392	5	51.14	.2414	31.80	5.443	1.0524	.1969
393	5	86.14	.2942	26.10	9.168	1.0524	.2921
393	5	85.77	.3148	24.40	9.129	1.0524	.2911
394	5	142.46	.4523	16.90	15.162	1.0524	.4454
394	5	142.95	.4249	18.00	15.214	1.0524	.4467
395	6	190.60	.4996	15.30	20.292	1.0524	.5765
395	6	190.46	.5176	14.80	20.276	1.0524	.5760
398	4	19.00	.0921	83.30	2.022	1.0524	.1095
399	5	24.64	.1042	73.60	2.623	1.0524	.1248
399	5	24.46	.1142	67.20	2.603	1.0524	.1243
400	5	39.02	.1522	50.40	4.153	1.0524△	.1639
400	5	38.87	.1590	48.30	4.137	1.0524	.1635
401	5	89.91	.2812	27.30	9.569	1.0524△	.3024
401	5	89.92	.2787	27.50	9.570	1.0524△	.3024
402	6	184.20	.5435	14.10	19.604	1.0524	.5589
402	6	183.48	.5981	12.80	19.528	1.0524	.5572
431	5	23.28	.1212	63.30	2.478	1.0524	.1211
432	5	37.49	.1702	45.10	3.991	1.0524	.1598
433	5	79.41	.2896	26.50	8.451	1.0524	.2738
434	5	147.82	.4522	16.90	15.732	1.0524	.4599
435	5	179.86	.5590	13.70	19.142	1.0524	.5471
485	5	29.88	.1194	64.30	3.180	1.0524	.1391
486	5	59.82	.2063	37.20	6.367	1.0524	.2205
487	5	115.23	.3688	20.80	12.264	1.0524	.3713
488	6	182.90	.5378	14.20	19.465	1.0524	.5554

LIQ TUBE OL GPM DIFF	S TENS	VISC	VELL
3 1.757 2.100 2.950	23.400	1.360	1.792

NO	J	QGM	NTU	LTU	VELG	FACTOR	CORRAY
408	5	30.81	.1051	73.10	3.279	1.1210	.1301
408	5	30.22	.1225	62.60	3.216	1.1210△	.1280
409	5	78.30	.2850	26.90	8.333	1.1210△	.2970
409	5	77.54	.3155	24.30	8.253	1.1210△	.2943
410	6	169.91	.6117	12.50	18.083	1.1210△	.6189
410	6	169.05	.6360	12.00	17.991	1.1210	.6158
415	3	23.71	.0994	77.20	2.524	1.1210	.1052
415	3	24.30	.0837	91.70	2.586	1.1210	.1072
416	5	46.73	.1757	43.70	4.974	1.1210△	.1860
416	5	47.57	.1493	51.40	5.062	1.1210	.1890
417	6	138.82	.4897	15.60	14.774	1.1210	△.5096
417	6	139.46	.4642	16.50	14.843	1.1210△	.5119
422	3	22.39	.1086	70.70	2.383	1.1210	.1005
423	5	31.74	.1385	55.40	3.378	1.1210	.1334
424	5	68.95	.3073	24.90	7.358	1.1210	.2641
425	5	139.74	.6498	11.80	14.872	1.1210△	.5129
426	6	174.64	.7082	10.80	18.586	1.1210	.6355
493	3	24.25	.0865	88.70	2.581	1.1210	.1072
494	5	43.28	.1403	54.70	4.606	1.1210	.1739
495	5	65.53	.2434	31.50	6.974	1.1210△	.2521
496	6	105.54	.4044	18.90	11.233	1.1210△	.3927
497	6	168.67	.7025	10.90	17.952	1.1210△	.6146

BT	23.7379	24.599195	9.515	9.7112	.017163	.977715

LIO	TUBE	OL	GPM	DIFF	S TENS	VISC	VELL
1	1.757	1.070	1.072	75.100		1.505	.913

NO	J	QGM	NTU	LTU	VELG	FACTOR	CORR	Y
239	5	22.90	.0915	83.90	2.437	1.1038		.1138
240	5	43.28	.1360	55.60	4.607	1.1038		.1667
241	5	82.73	.2365	32.40	8.806	1.1038		.2690
242	5	116.52	.3217	23.80	12.402	1.1038		.3567
243	5	156.31	.3971	19.30	16.637	1.1038		.4599

LIO	TUBE	OL	GPM	DIFF	S TENS	VISC	VELL
1	1.757	1.070	2.019	71.200		.800	.913

NO	J	QGM	NTU	LTU	VELG	FACTOR	CORR	Y
247	5	25.48	.1392	55.10	2.712	.9038		.1503
248	5	49.10	.2043	37.60	5.226	.9038		.2251
249	5	94.68	.3509	21.80	10.077	.9038		.3695
250	5	152.52	.4446	17.30	16.165	.9038 A		.4848
251	5	178.01	.5645	15.60	18.946	.9038		.6335

LIO	TUBE	OL	GPM	DIFF	S TENS	VISC	VELL
1	1.757	1.070	3.080	68.800		.599	.913

NO	J	QGM	NTU	LTU	VELG	FACTOR	CORR	Y	A
255	5	27.56	.1268	60.50	2.936	.7937		.1807	
256	5	54.10	.2185	35.10	5.759	.7937 A		.2768	
257	5	102.70	.3837	20.00	10.931	.7937		.4517	
258	5	146.75	.4926	15.50	15.620	.7937		.6106	
259	5	196.36	.6651	11.50	20.900	.7937		.7896	
721	4	24.87	.1531	50.10	2.647	.7937		.1709	
722	5	30.92	.1723	44.50	3.930	.7937		.2144	

PREDICTION OF NTU BY SLUG CORRELATION

LIO	TUBE	OL	GPM	DIFF	S TENS	VISC	VELL
2	1.757	.620	3.690	75.530		1.140	.529

NO	J	QGM	NTU	LTU	VELG	FACTOR	CORR	AY
608	3	19.90	.1621	47.30	2.118	.7078		.1664
609	4	27.27	.1910	40.20	2.903	.7078		.1913
610	5	44.98	.2309	33.30	4.786	.7078		.2512
611	5	70.11	.3490	22.00	7.463	.7078		.3362
615	4	24.25	.1615	47.50	2.581	.7078		.1814
616	5	35.21	.1926	39.80	3.747	.7078		.2182
617	5	89.08	.4064	18.90	9.482	.7078		.4003
818	5	149.49	.6239	12.30	15.912	.7078		.6046

LIO	TUBE	OL	GPM	DIFF	S TENS	VISC	VELL
2	1.757	1.070	3.690	75.530		1.140	.913

NO	J	QGM	NTU	LTU	VELG	FACTOR	CORR	Y
509	4	21.96	.1849	41.50	2.358	.7530		.1699
510	5	39.25	.2588	29.60	4.178	.7530		.2356
519	4	19.38	.2028	37.80	2.062	.7530		.1600
520	5	26.79	.2096	36.60	2.852	.7530 A		.1882
521	5	43.99	.2793	27.50	4.682	.7530		.2536
528	5	23.85	.1802	42.60	2.539	.7530		.1770
529	5	48.96	.2675	28.70	5.211	.7530 A		.2725
530	5	70.01	.3673	20.90	7.452	.7530 A		.3526
531	5	157.96	.6605	11.60	16.813	.7530		.6870
532	5	224.68	.8221	9.30	23.914	.7530		.9407
539	5	22.41	.1972	38.90	2.385	.7530 A		.1715
540	5	30.65	.2051	37.40	3.262	.7530		.2029
541	5	66.23	.3444	22.30	7.049	.7530		.3382
542	5	96.09	.4521	16.90	10.227	.7530		.4517
543	5	131.90	.5455	14.00	14.039	.7530		.5879
544	5	197.63	.7057	10.90	21.036	.7530		.8379
622	5	35.70	.2119	36.20	3.800	.7530		.2221

LIO	TUBE	OL	GPM	DIFF	S TENS	VISC	VELL
2	1.757	2.100	3.690	75.530		1.140	1.792

NO	J	QGM	NTU	LTU	VELG	FACTOR	CORR	AY
563	5	24.81	.1585	48.40	2.641	.8367		.1558
564	5	31.99	.1898	40.40	3.405	.8367		.1846
565	5	42.35	.2127	36.10	4.508 A	.8367		.2334
566	5	63.92	.3250	23.60	6.803	.8367		.3350
575	5	24.81	.1524	50.30	2.641	.8367		.1508
576	5	31.99	.1716	44.70	3.405	.8367		.1846
577	5	42.35	.2115	36.30	4.508	.8367		.2334
578	5	63.92	.3277	23.40	6.803	.8367		.3350
583	3	20.91	.1469	51.50	2.225	.8367		.1324
584	5	29.72	.1924	39.90	3.163	.8367		.1739
585	5	49.07	.2701	28.40	5.223	.8367		.2651
586	5	77.86	.4178	18.30	8.288	.8367		.4007
587	5	122.47	.6017	12.70	13.035	.8367		.6107
588	6	170.58	.7264	10.50	18.794	.8367		.8655
593	5	39.23	.2127	36.10	4.176	.8367		.2188
594	5	79.76	.3936	19.50	8.489	.8367		.4096
595	5	124.07	.5889	13.00	13.302	.8367		.6225
596	5	173.26	.8110	9.40	18.442	.8367		.8499

PREDICTION OF NTU BY SLUG CORRELATION

LIQ	TUBE	QL GPM	DIFF	S TENS	VISC	VELL
4	1.757	.620	.285	47.900	13.900	.529

NO	J	QGM	NTU	LTU	VELG	FACTOR	CORR Y
693	5	19.37	.0717	107.00	2.062	1.5871	.0656
694	5	28.00	.0810	94.70	2.980	1.5871	.0786
695	5	41.60	.1035	74.20	4.427	1.5871	.0991
698	5	65.80	.1366	56.20	7.005	1.5871	.1356
699	5	90.89	.1695	45.30	9.673	1.5871	.1735
700	5	141.88	.2427	31.60	15.100	1.5871	.2504
701	5	180.49	.3043	25.20	19.210	1.5871	.3086

LIQ	TUBE	QL GPM	DIFF	S TENS	VISC	VELL
4	1.757	2.100	.285	47.900	13.900	1.792

NO	J	QGM	NTU	LTU	VELG	FACTOR	CORRAY
981	5	27.13	.0625	122.70	2.887	2.2284	.0519
982	5	40.84	.0866	68.60	4.347	2.2284	.0762
983	5	22.61	.0601	127.70	2.406	2.2284	.0440
984	5	63.74	.1206	63.60	6.783	2.2284	.1167
685	5	88.92	.1637	46.90	9.463	2.2284	.1612
686	5	135.79	.2401	31.90	14.452	2.2284	.2440
687	5	175.68	.3199	24.00	18.697	2.2284	.3146

LIQ	TUBE	QL GPM	DIFF	S TENS	VISC	VELL
4	1.757	1.070	.285	47.900	13.900	.913

NO	J	QGM	NTU	LTU	VELG	FACTOR	CORR Y
672	5	21.80	.0490	156.60	2.320	1.9548	.0565
673	5	62.69	.1158	66.30	6.673	1.9548	.1165
674	5	86.84	.1694	45.30	9.242	1.9548	.1518
675	5	127.70	.2601	29.50	13.591	1.9548	.2117
676	5	164.34	.3529	21.70	17.491	1.9548	.2653
662	5	19.87	.0442	173.40	2.115	1.9548	.0537
663	5	27.69	.0562	136.50	2.947	1.9548	.0652
664	5	41.70	.0816	90.70	4.443	1.9548	.0858

65	17.8161	16.085096	7.218	7.5253	-.023178	1.094661

LIQ	TUBE	QL GPM	DIFF	S TENS	VISC	VELL
5	1.757	.620	.142	49.300	26.500	.529

NO	J	QGM	NTU	LTU	VELG	FACTOR	CORR YA
647	5	26.86	.0578	132.90	2.858	1.9398	.0604
648	5	39.82	.0739	103.85	4.238	1.9398	.0764
651	5	69.23	.1098	69.90	7.368	1.9398	.1127
652	5	90.38	.1368	56.10	9.619	1.9398	.1367
653	5	129.02	.1839	41.70	13.732	1.9398	.1864
654	5	170.42	.2226	34.50	18.138	1.9398A	.2375

LIQ	TUBE	QL GPM	DIFF	S TENS	VISC	VELL
5	1.757	1.070	.142	49.300	26.500	.913

NO	J	QGM	NTU	LTU	VELG	FACTOR	CORRAY
632	5	25.97	.0437	175.60	2.764	2.4490	.0472
633	5	37.60	.0564	136.10	4.002	2.4490A	.0668
637	5	62.76	.0859	91.50	6.680	2.4490	.0902
638	5	87.21	.1167	65.80	9.281	2.4490A	.1188
639	5	128.34	.1749	43.90	13.659	2.4490	.1669
640	5	160.96	.2207	34.80	17.130	2.4490	.2050

LIQ	TUBE	QL GPM	DIFF	S TENS	VISC	VELL
5	1.757	2.100	.142	49.300	26.500	1.792

NO	J	QGM	NTU	LTU	VELG	FACTOR	CORR Y
660	5	18.95	.0291	265.50	2.017	2.8125	.0268
661	5	26.05	.0365	210.40	2.773	2.8125	.0367
662	5	38.88	.0508	151.10	4.138	2.8125	.0547
665	5	20.41	.0287	266.80	2.173	2.8125	.0288
666	5	59.04	.0739	103.90	6.283	2.8125	.0829
667	5	81.05	.1062	72.30	8.626	2.8125	.1138
668	5	122.61	.1698	45.20	13.049	2.8125	.1720
669	5	154.82	.2250	34.10	16.477	2.8125	.2171

PREDICTION OF NTU BY SLUG CORRELATION

LTO TUBE	OL GPM DIFF	S TENS VISC	VELL
6 1.228	.293 1.465	73.53C 1.140	.512

NO	J	OGM	NTU	LTU	VELG	FACTOR	CORRAY
784	3	11.69	.1815	42.30	2.547Δ	.6232	.2057
785	5	19.03	.2302	33.30	4.147	.6232	.2629
786	5	30.04	.3626	21.10	6.743	.6232	.3557
787	5	62.80	.5919	12.90	13.685	.6232	.6940
788	5	108.56	1.0474	7.30	23.655	.6232Δ	.9805
789	6	146.39	1.6690	4.60	31.898	.6232	1.2553
790	7	185.01	2.2241	3.40	40.312	.6232	1.5563

LTO TUBE	OL GPM DIFF	S TENS VISC	VELL
6 1.228	.520 1.465	73.53C 1.140	.908#

NO	J	OGM	NTU	LTU	VELG	FACTOR	CORRAY
771	4	11.54	.1744	44.00	2.515	.6833	.1955
772	5	19.34	.2167	35.40	4.214	.6833	.2623
773	5	32.64	.3464	22.00	7.113	.6833Δ	.3762
775	5	63.62	.5975	12.80	13.862	.6833	.6414
776	5	106.93	.9982	7.60	23.301	.6833	1.0123
777	6	144.13	1.3677	5.60	31.405	.6833	1.3307
778	7	184.04	1.5506	4.90	40.100	.6833	1.6724

LIO TUBE	OL GPM DIFF	S TENS VISC	VELL
6 1.228	1.020 1.465	73.53C 1.140	1.782

NO	J	OGM	NTU	LTU	VELG	FACTOR	CORRAYΔ
796	3	10.02	.1465	54.60	2.380	.7210	.1644
797	5	18.70	.1857	41.30	4.074	.7210	.2510
798	5	29.67	.2722	28.20	6.465	.7210Δ	.3734
799	5	59.23	.6478	11.80	12.907	.7210	.7031
800	5	83.61	1.0209	7.50	18.218	.7210	.9749
801	6	109.00	1.3569	5.60	23.751	.7210	1.2580

LTO TUBE	OL GPM DIFF	S TENS VISC	VELL
7 2.504	1.130 1.465	73.53C 1.140	.474

NO	J	OGM	NTU	LTU	VELG	FACTOR	CORR Y
738	5	60.66	.0628	122.20	3.179	1.5962	.0797
739	5	115.71	.1368	56.10	6.064	1.5962	.1193
740	5	183.34	.1688	45.50	9.608	1.5962	.1678
763	5	93.70	.0996	77.10	4.910	1.5962	.1034
764	5	147.00	.1563	49.10	7.703	1.5962Δ	.1417
765	5	182.62	.1766	43.40	9.570	1.5962	.1673

LTO TUBE	OL GPM DIFF	S TENS VISC	VELL
7 2.504	2.010 1.465	73.53C 1.140	.844

NO	J	OGM	NTU	LTU	VELG	FACTOR	CORR Y
730	5	55.32	.0796	96.40	2.794	1.4573	.0886
755	3	39.89	.0726	105.80	2.090	1.4573	.0762
756	5	69.96	.0921	83.30	3.666	1.4573	.1044
757	5	116.72	.1329	57.70	6.116	1.4573	.1483
758	5	146.25	.1614	47.50	7.664	1.4573	.1760
759	5	180.05	.1921	39.90	9.435	1.4573	.2078

LIO TUBE	OL GPM DIFF	S TENS VISC	VELL
7 2.504	3.950 1.465	73.53C 1.140	1.660#

NO	J	OGM	NTU	LTU	VELG	FACTOR	CORRAY
746	3	30.64	.0674	115.90	2.025	1.3818	.0725
747	5	60.54	.0887	86.50	3.487	1.3818	.1161
748	5	109.16	.1286	59.70	5.720	1.3818	.1674
752	5	112.58	.1559	57.30	5.889	1.3818	.1718
753	5	136.79	.1537	49.90	7.168	1.3818Δ	.2046
754	5	167.00	.1889	40.60	8.751	1.3818	.2453

58	19.6781	19.205037	19.308	17.1956	.844286	.845422